Ministry for Primary Industries
Manatū Ahu Matua

Characterisation and a length-based assessment model for scampi (*Metanephrops challengeri*) at the Auckland Islands (SCI 6A)

New Zealand Fisheries Assessment Report 2015/21.

I.D. Tuck

ISSN 1179-5352 (online)
ISBN 978-0-477-10582-8 (online)

March 2015

New Zealand Government

Growing and Protecting New Zealand

Requests for further copies should be directed to:

Publications Logistics Officer
Ministry for Primary Industries
PO Box 2526
WELLINGTON 6140

Email: brand@mpi.govt.nz
Telephone: 0800 00 83 33
Facsimile: 04-894 0300

This publication is also available on the Ministry for Primary Industries websites at:
http://www.mpi.govt.nz/news-resources/publications.aspx
http://fs.fish.govt.nz go to Document library/Research reports

TABLE OF CONTENTS

EXECUTIVE SUMMARY

Tuck, I.D. (2015). Characterisation and a length-based assessment model for scampi (*Metanephrops challengeri*) at the Auckland Islands (SCI 6A).

***New Zealand Fisheries Assessment Report 2015/21.* 160 p.**

A stock assessment of the Auckland Islands (SCI 6A) scampi stock has been undertaken through MPI project DEE201002SCIC. This work has further developed an existing model for this stock, developed within a previous MPI project. Progress was made, but the assessment was not accepted by the SFAWG.

A fishery characterisation was undertaken, and a CPUE index was estimated for the stock, incorporating spatial and temporal components in the fishery. The previous model for this stock incorporated considerable spatial structure, but following preliminary investigations, the SFAWG recommended developing only a single area model for these stocks, and fitting an annual CPUE index, along with photographic and trawl survey indices. Sensitivity to natural mortality, and estimation of catchability as free or nuisance parameters were investigated, with models taken to MCMC with M fixed at 0.2, 0.25 and 0.3. Models with catchability estimated as free parameters showed evidence of lack of convergence, and were not accepted. Models with catchability estimated as nuisance parameters showed no evidence of lack of convergence, and provided similar estimates of SSB_0 and stock status to the free parameter models, but the use of nuisance parameters was not considered acceptable.

Although not accepted, the Working Group felt that the assessments were able to provide some information, and indicated that there did not appear to be any cause for concern over the SCI 6A stock, with $SSB_{current}$ over 50% SSB_0.

1. INTRODUCTION

This report undertakes a fishery characterisation for the Auckland Islands (SCI 6A) scampi stock, and applies the previously described Bayesian, length-based, two-sex population model to this stock. Previous characterisations of scampi stocks are described by Tuck (2009). The first attempt at developing a length-based population model for any scampi stock was conducted for SCI 1 (Cryer et al. 2005) and implemented using the general-purpose stock assessment program CASAL v2.06 (September 2004). This model for SCI 1 was developed further and the same model structure was also applied to SCI 2 in a later project (Tuck & Dunn 2006). The model was first applied to the SCI 6A stock in 2011, although this assessment was not accepted (Tuck & Dunn 2012). The current study used CASAL v 2.22 (Bull et al. 2008) with a slightly modified selectivity option. Developments in the model implementation and structure have been largely based on suggestions raised at the MFish funded Scampi Assessment Workshop (Tuck & Dunn 2009), and subsequently at Shellfish Fisheries Assessment Working Group (SFAWG) meetings. Assessments for SCI 1 and SCI 2 using this model were accepted in 2011 and 2013 (Tuck & Dunn 2012, Tuck 2014).

We describe the available data and how they were used, the parameterisation of the model, and model fits and sensitivity. This report fulfils Ministry of Fisheries project DEE201002SCIC "*Stock assessment of scampi*", undertaking an assessment of SCI 6A. The objective of this project was to conduct a stock assessment, including estimating yield for SCI 6A in 2013–14.

1.1 The Auckland Islands (SCI 6A) scampi fishery

Scampi is fished all around New Zealand, in nine fishery management areas (Figure 1). The SCI 6A fishery is one of New Zealand's four main scampi fisheries (the others being SCI 1, SCI 2 and SCI 3), and over the last 5 years (2008–09 to 2012–13) has contributed an average of 184 tonnes annually, having declined from the previous 5 years (2003–04 to 2007–08 average 296 tonnes). The TACC for SCI 6A is 306 tonnes, and the total TACC for all management areas is 1191 tonnes.

The spatial distribution of the targeted scampi fishing within SCI 6A is focussed to the east of the Auckland Islands in water depths from 350 – 550 m. (Figure 2). This fishery extends slightly deeper than other scampi fisheries around New Zealand. The scampi surveys conducted in the area have focussed on the main area of the fishery, and survey strata coverage is illustrated in Figure 2.

The history of scampi management in New Zealand has been complex, and subject to legal scrutiny (Carter 2003). The first reported domestic catches of scampi were in the 1987–88 fishing year, with special section 63 and section 64 permits for investigative fishing and the use of small mesh trawl nets. Interpretation of the requirements for fishing under the Fisheries Act 1983 varied between regional offices of the Ministry of Fisheries, but the fishery expanded rapidly, and by the start of the 1990–91 fishing year, 14 commercial fishing permits had been granted, and 39 applications for special permits had been received.

The Ministry recognised that it needed to control the rapid expansion of the fishery, to prevent overfishing, and adopted a national approach, with a species specific prohibition on the taking of scampi imposed on 1st October 1990 under section 65 of the Fisheries Act 1983, with rules and criteria established for granting exemptions to the prohibition. These criteria included recognition of previous access to the fishery, or a demonstration of a commitment to the fishery.

Prior to the 1991–92 fishing year, there were no limits on scampi catches for any area. In the 1991–92 fishing year, Individual Quotas (IQs) were introduced for SCI 1 and SCI & 2 (allocated on the basis of the permit holder's catch in 1990–91), with competitive catch limits introduced for all other areas. The IQs were maintained for SCI 1 & 2 in 1992–93, and introduced for SCI 4 & 6A (allocated on the

basis of the permit holder's catch in 1991–92), with competitive catch limits maintained for other areas. This management system (with IQs for SCI 1, 2, 4 & 6A, and competitive limits for other stocks) was maintained with the introduction of Individual Catch Entitlement (ICE) regulations in 1999, and continued until the Court of Appeal ruled that the scampi ICE regulations were unlawful in October 2001, after which all scampi stocks were managed under competitive catch limits. Scampi was introduced into the QMS on 1st October 2004 with a Total Allowable Commercial Catch of 306 tonnes for SCI 6A, and this limit has been unchanged to date.

Coincident with the introduction of scampi to the QMS, management area boundaries were revised for SCI 3 and SCI 4, SCI 6A and SCI 6B (Figure 3), on the basis of examination of patterns in catch distribution and composition (Cryer 2000). This changed the SCI 6A area from a "bubble" encompassing the area within 50 nautical miles of the Auckland Islands to a larger box which included all the scampi fishing activity in the area.

Previous fishery characterisations have been undertaken for this area within Cryer & Coburn (2000) and Tuck (2009).

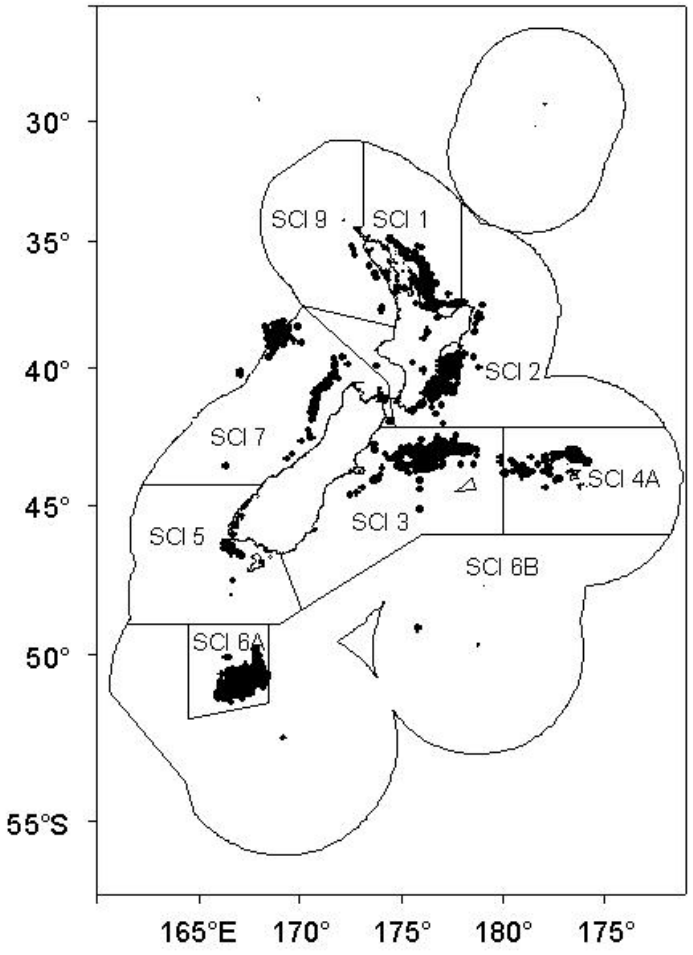

Figure 1: Spatial distribution of the scampi fishery since 1988–89. Each dot shows the midpoint of one or more tows recorded on TCEPR with scampi as the target species.

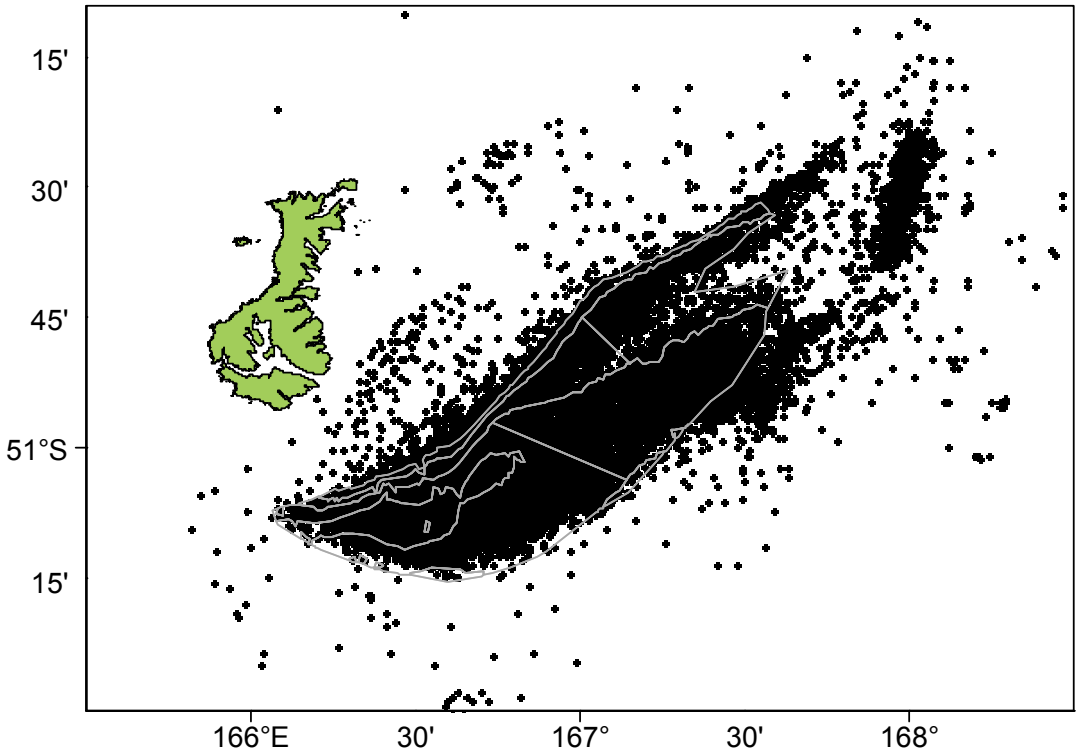

Figure 2: Spatial distribution of the scampi fishery within management area SCI 6A since 1988–89. Each dot shows the midpoint of one or more tows recorded on TCEPR with scampi as the target species. The boundaries of the scampi survey strata are shown in grey.

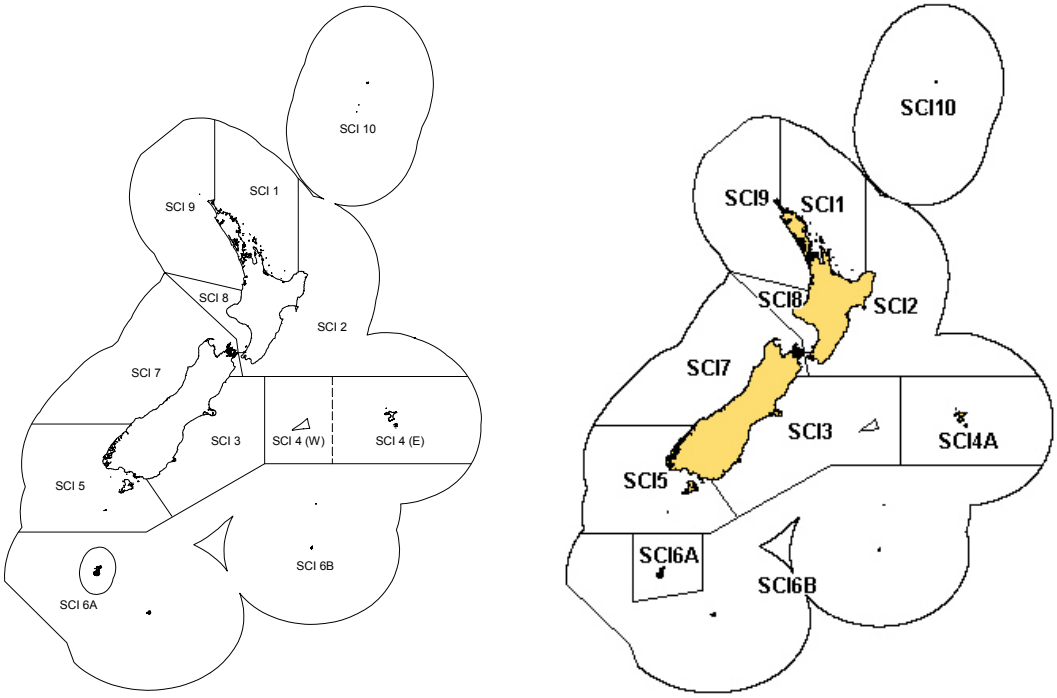

Figure 3: Left - Scampi fishery management areas, prior to 2004–05 fishing year. Right - Scampi fishery management areas, as revised at the start of the 2004–05 fishing year, when the boundaries between SCI 3 and SCI 4A, and SCI 6A and SCI 6B were changed.

2. FISHERY CHARACTERISATION AND DATA

2.1 Commercial catch and effort data

Scampi fishers have consistently reported catches on the Trawl Catch, Effort, and Processing Returns (TCEPR) form since its introduction in 1989–90, providing a very valuable record of catch and effort on a tow by tow basis.

Data were extracted from the MPI TCEPR database, requesting all tows where scampi (SCI) was the nominated target species, or was reported in the catch. Errors in TCEPR records are reducing in frequency, but do occur, and the raw records were groomed in the following manner. For each record, the reported data were used to estimate the duration of the trawl shot, the distance between the start and finish locations, and the mid point between the start and finish locations. Tows with zero scampi catch were excluded. All tows with zero hours tow duration recorded (but some scampi catch) were reset to the median tow duration for the trip. All tows with a tow distance greater than 100 km were reset to the median of the midpoint of tows on the same day, adjacent days, or the trip, depending on available data. The SCI 6A data were then extracted from this full data set on the basis of latitude and longitude. All analysis was conducted on the basis of the current management area boundaries.

Subsequent analyses were conducted on this "groomed" version of the data set (27 804 records), representing over 95% of all scampi landings from SCI 6A. This data set is considered to be the most appropriate to investigate patterns in the fishery, given that it represents the targeted scampi fishery, and latitude and longitude data are available for spatial aspects of the analysis. Previous characterisations have used a slightly different grooming approach (to that discussed above), details of which are provided in Tuck (2009). Comparisons of unstandardized CPUE data for the earlier and revised grooming approaches have previously been examined (Tuck 2014). The revised grooming slightly reduces the estimated CPUE prior to 2003 (due to rounding of the haul duration data), but the medians of the annual values appear identical after this.

Total annual landings for the fishery, and the percentage by the target scampi fishery, are presented in Table 1, and the distribution of fishing activity within the SCI 6A area over time is presented in Figure 4 and Figure 5. The area over which the assessment model is applied is defined as the survey strata (350–550 m depth range in the main area of the fishery) (Figure 2), and over 99% of the targeted scampi catch has been reported from this area in all years (Table 1). The fishery initially developed in the shallower and western areas of the grounds, closest to the Auckland Islands, but covered the full extent of the core area by the late 1990s, and has consistently been fished since this time, with smaller isolated patches (to the east) fished until 2004. These more easterly patches were outside the SCI 6A management area at the time (see Figure 3), and as such were subject to different catch constraints. The core (modelled) area has accounted for over 97% of scampi targeted catch in all years. A boxplot of the unstandardized CPUE (Figure 6) shows that catch rates initially declined from very high values in the early 1990s, fluctuated without trend until the late 2000s, but have remained at the lower end of the observed range in recent years.

The breakdown of catch by survey depth strata and fishing year is presented in Figure 7. As evident from the spatial pattern (Figure 4), catches were focussed in the shallower areas in the initial years of the fishery, but since the mid 1990s, the middle depth bands (400–450m and 450–500m) have dominated. No more than 3% of catches have come from outside the 350–550m depth range in any one year, and less than 1% in all years since 1993–94.

Monthly patterns of effort and catch are presented for SCI 6A in Figure 8 and Figure 9. Up until 1999–2000, fishing was focussed between January and May, although there was activity throughout the year. The fishery was managed with competitive catch limits between 2001–02 and 2003–04, and during this period, effort and catches were focussed in the first few months of the fishing year. Since the introduction of scampi into the QMS (2004–05), effort has avoided January and February (and

December in more recent years), the period during which there is a high incidence of post moult (soft shell) animals, but been relatively evenly distributed through the rest of the year.

Table 1: Reported commercial landings (tonnes) from the 1986–87 to 2012–13 fishing years for SCI 6A, catch estimated from scampi target fishery, and estimated catch from modelled area (survey strata).

	Landings (MHR)	Target catch (TCEPR)	% SCI target	Estimated catch (modelled area)	% catch (modelled area)
1990–91	2	1.90	95%	1.90	100.00%
1991–92	325	324.49	100%	315.35	97.19%
1992–93	279	253.84	91%	247.55	97.52%
1993–94	303	269.43	89%	266.00	98.73%
1994–95	239	217.45	91%	216.96	99.78%
1995–96	270	226.52	84%	225.63	99.60%
1996–97	275	276.15	100%	275.06	99.60%
1997–98	279	298.27	107%	297.71	99.81%
1998–99	325	309.71	95%	308.26	99.53%
1999–00	328	311.22	95%	310.94	99.91%
2000–01	264	283.39	107%	282.94	99.84%
2001–02	272	249.36	92%	248.88	99.81%
2002–03	255	249.31	98%	248.79	99.79%
2003–04	311	285.83	92%	285.47	99.87%
2004–05	295	280.82	95%	280.82	100.00%
2005–06	286	273.43	96%	272.29	99.58%
2006–07	302	288.34	95%	287.79	99.81%
2007–08	287	274.71	96%	274.31	99.86%
2008–09	264	249.63	95%	248.60	99.59%
2009–10	144	136.99	95%	136.73	99.81%
2010–11	198	185.03	93%	184.56	99.75%
2011–12	166	158.72	96%	157.80	99.42%
2012–13	146	137.04	94%	136.61	99.68%

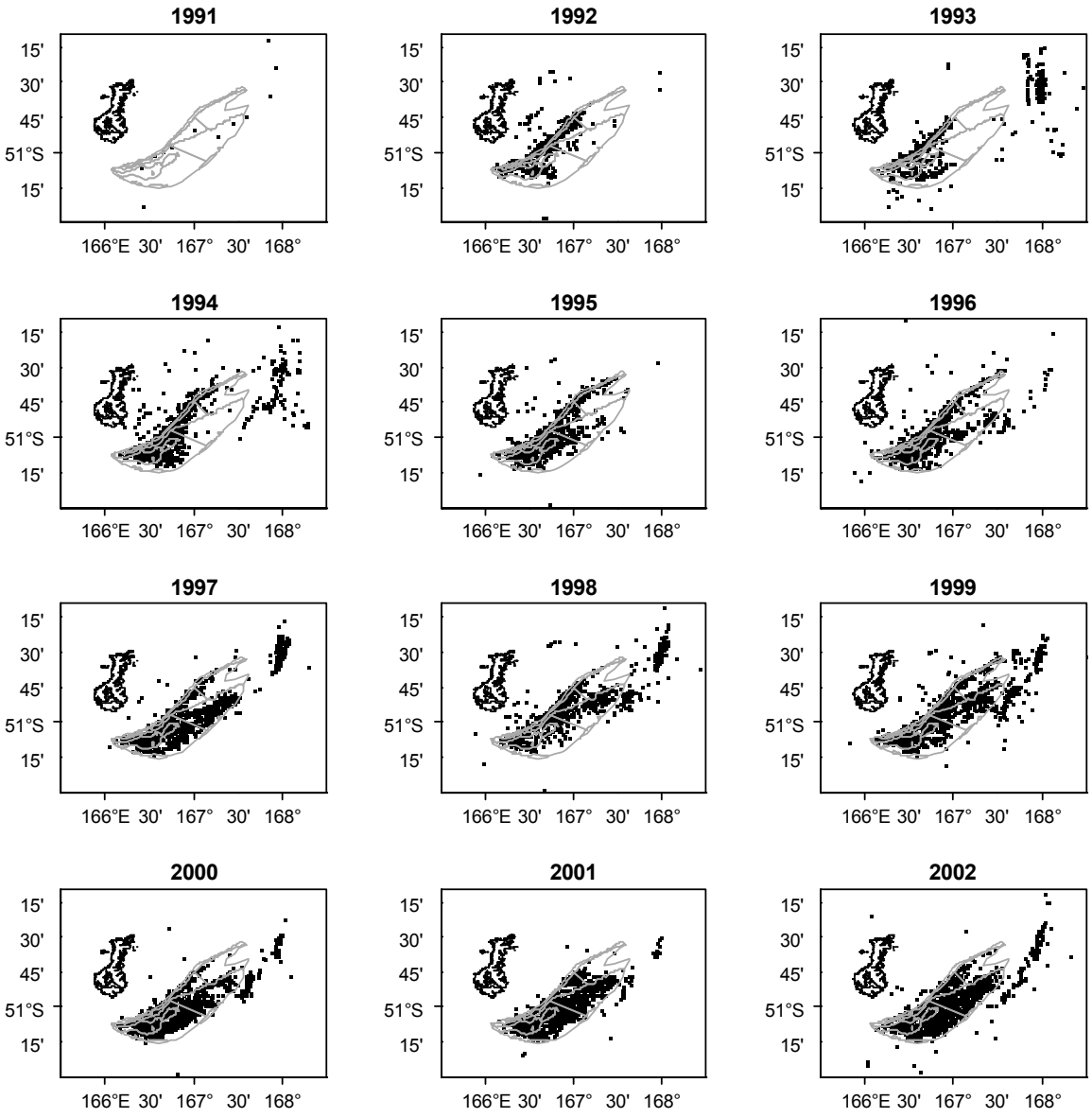

Figure 4: Spatial distribution of the main area of the SCI 6A scampi trawl fishery from 1990–91 to 2001–02. Each dot represents the midpoint of one or more tows reported on TCEPR. The general area covered by the plots is indicated within Figure 5.

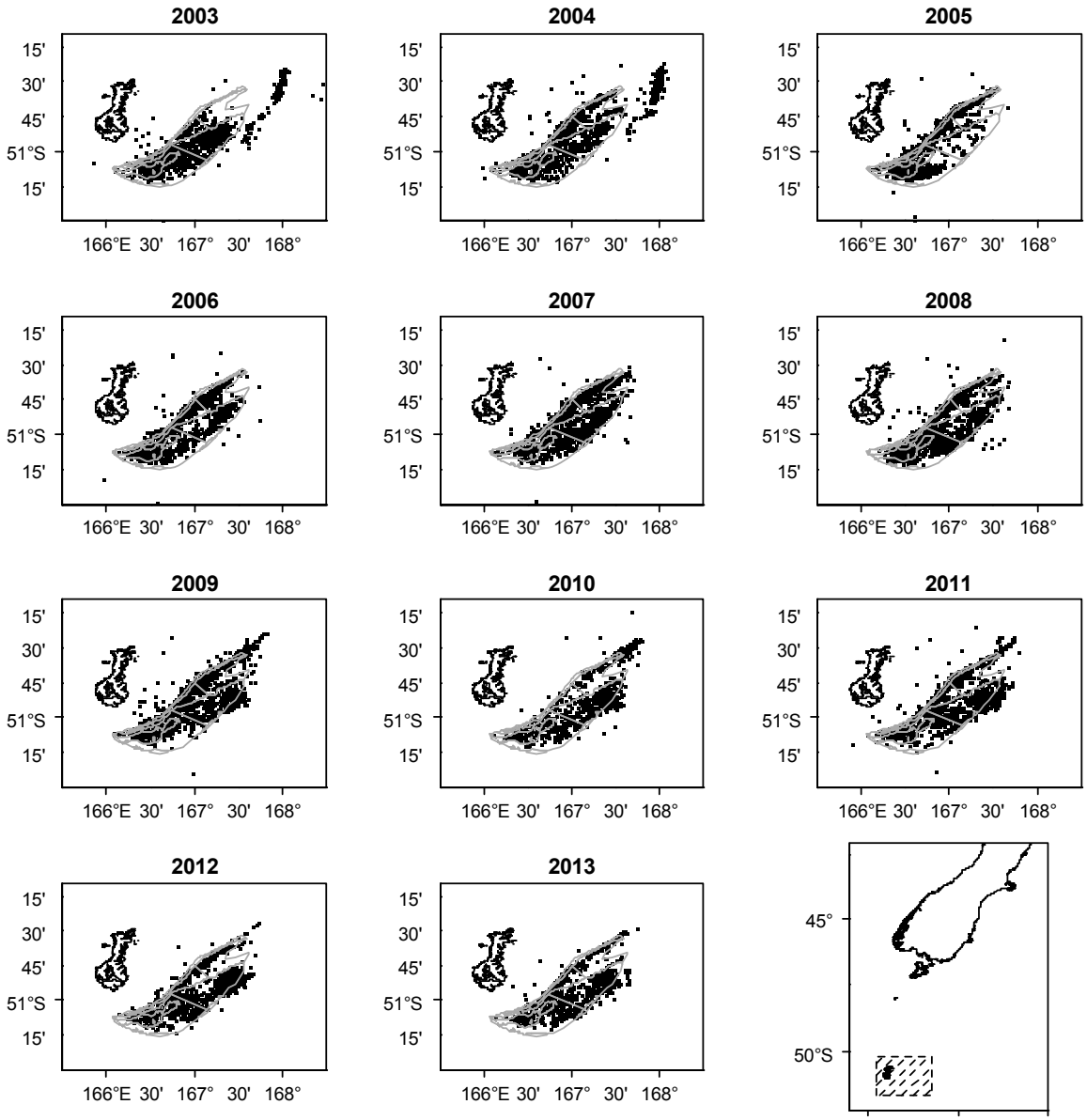

Figure 5: Spatial distribution of the main area of the SCI 6A scampi trawl fishery from 2002-03 to 2012-13. Each dot represents the midpoint of one or more tows reported on TCEPR. The general area covered by the plots is indicated by the shaded box in bottom right plot.

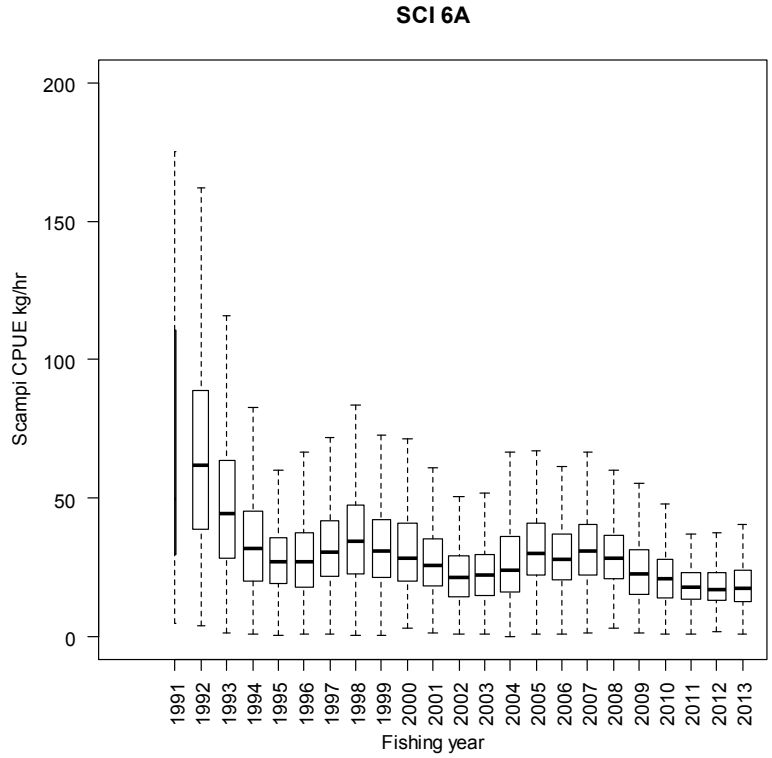

Figure 6: Boxplot (with outliers removed) of individual observations from TCEPR of unstandardized catch rate (catch (kg) divided by tow effort (hours)) with tows of zero scampi catch excluded, by fishing year for the SCI 6A fishery. Box width proportional to square root of number of observations.

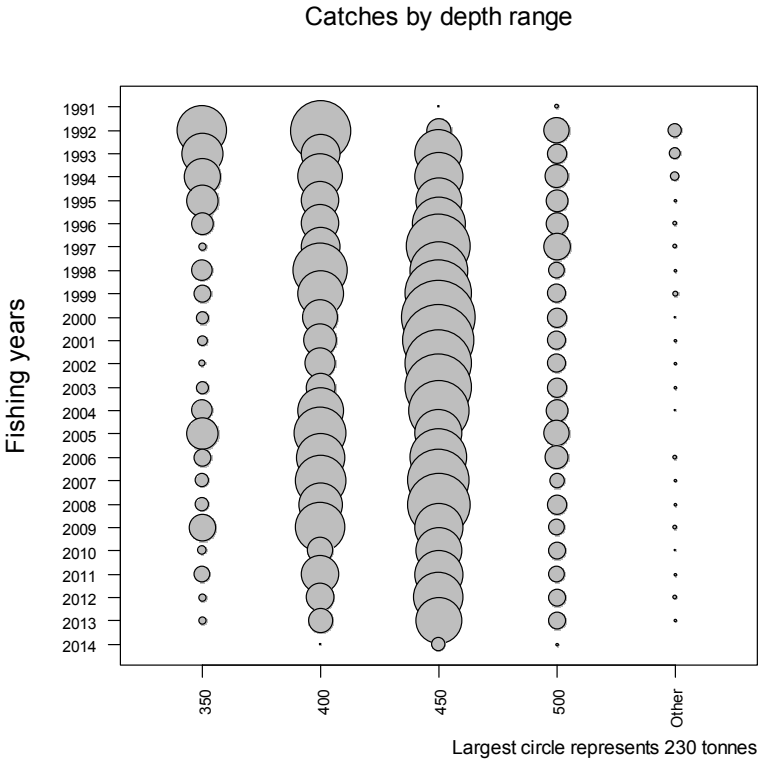

Figure 7: Annual catch breakdown by survey depth strata (and outside modelled area, 'Other') and fishing year for SCI 6A. Data only extracted to end November 2013 (2013–14 fishing year). Label '350' on x-axis indicates the 350–400 m stratum, etc.

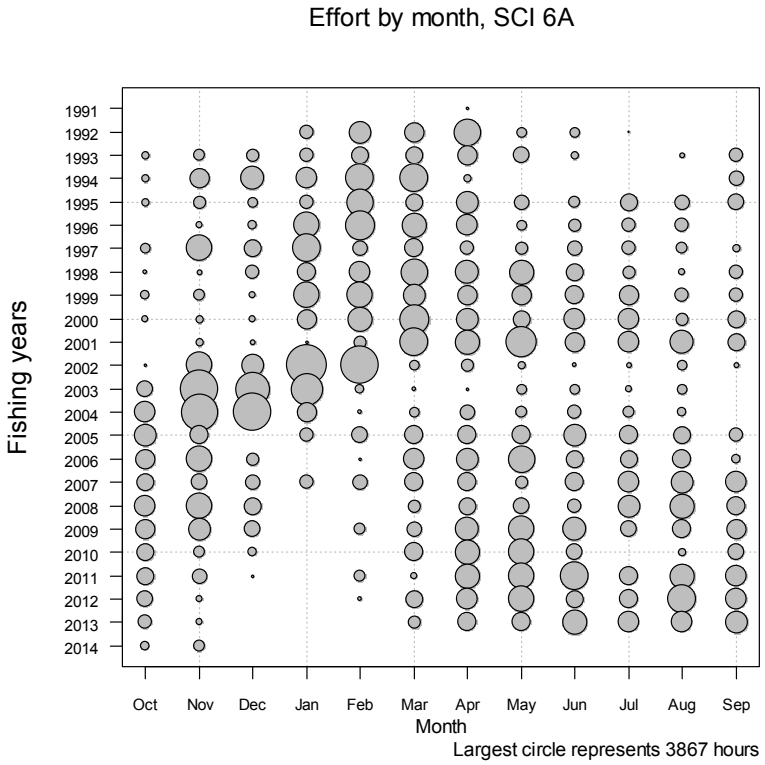

Figure 8: Monthly pattern of fishing effort in the scampi targeted fishery by fishing year for the core (modelled) area of SCI 6A. Data only extracted to end November 2013 (2013–14 fishing year).

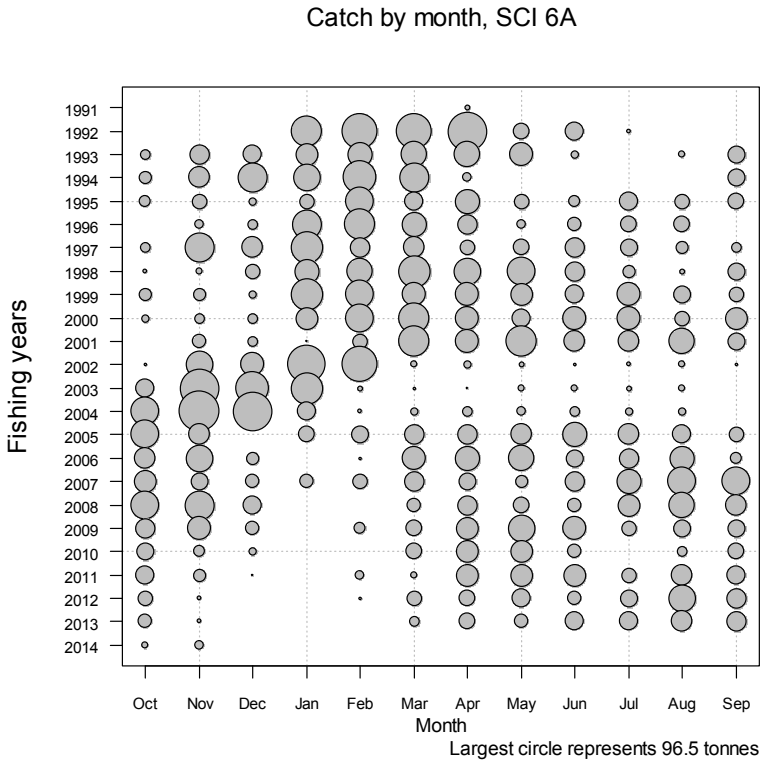

Figure 9: Monthly pattern of scampi catches in the scampi targeted fishery by fishing year for the core (modelled) area of SCI 6A. Data only extracted to end November 2013 (2013–14 fishing year).

2.2 Seasonal patterns in scampi biology

Previous development of the length based model for scampi has shown that determination of appropriate time steps for the model is important in fitting to length and sex ratio data in particular (Tuck & Dunn 2006, 2009, 2012). Scampi inhabit burrows, and are not available to trawling when within a burrow. Catchability varies between the sexes on a seasonal basis in relation to moulting and reproductive behaviour, which leads to seasonal changes in the sex ratio of catches.

Current knowledge of the timing of scampi biological processes in SCI 6A are summarised in Table 2 (revised from Tuck 2010, Tuck & Dunn 2012). From patterns in the proportion of soft (post moult) animals (Figure 10), ovigerous females (Figure 11), and egg stage observed from commercial sampling (Figure 12), mature female moulting appears to start in September and be focussed around October and November, just after the hatching period (July – August). The timing of hatching can only be confirmed from one observation from aquarium studies, occurring in late August (Wear 1976). Mating occurs after the females have moulted, while the shell is still soft, and new eggs are spawned onto the pleopods in December – January. The main male moulting is completed between December and March.

The combination of different biological processes for males and females leads to different relative availabilities of the two sexes through the year, resulting in the pattern of sex ratio (displayed as proportion males) shown in Figure 13. This figure has been plotted on a half monthly basis, as some months appear to include a clear shift in sex ratio. Males are markedly less abundant than females in catches between December and March (male catches being reduced during their moulting period), the ratio of the sexes in the catches is roughly equal between April and June, and also in November, with males dominating from July to October.

On the basis of our understanding of the timing of biological processes for scampi in this area, and the seasonal pattern in sex ratio, we have defined the modelled year as running from mid-November, with three time steps, mid-November to mid-April (when females dominate in catches), mid-April to June (when the sex ratio is about equal), and July to mid-November (when males dominate in catches).

Table 2: Summary of scampi biological processes for SCI 6A. Revised from Tuck (2010) and Tuck & Dunn (2012).

	Jan	Feb	Mar	Apr	May	Jun	Jul	Aug	Sep	Oct	Nov	Dec
Male moult	X	X	X									X
Female moult									X	X	X	
Mating										X	X	
Eggs spawn	X											X
Eggs hatch								X	X			

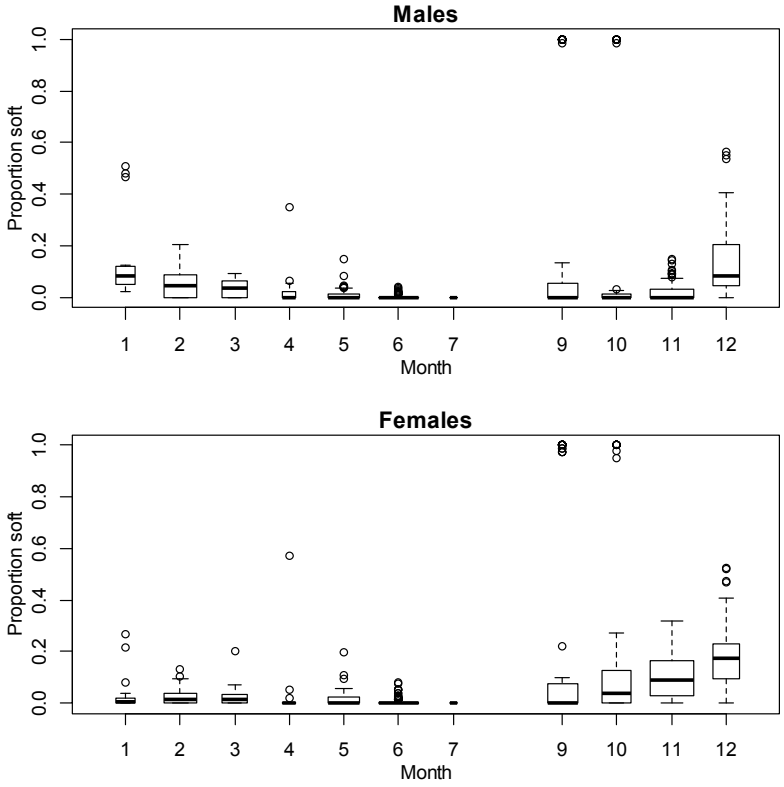

Figure 10: Boxplots of proportions of soft animals (post moult) by sex and month, as recorded by observers. Box widths proportional to square root of number of observations for that month. No samples available from August.

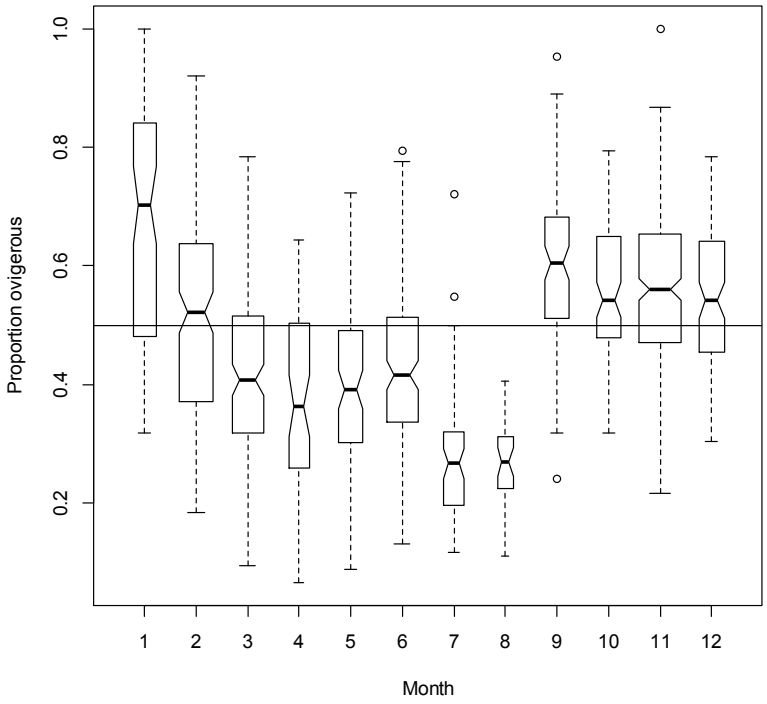

Figure 11: Boxplots of proportions of ovigerous females by month, as recorded by observers. Box widths proportional to square root of number of observations for that month.

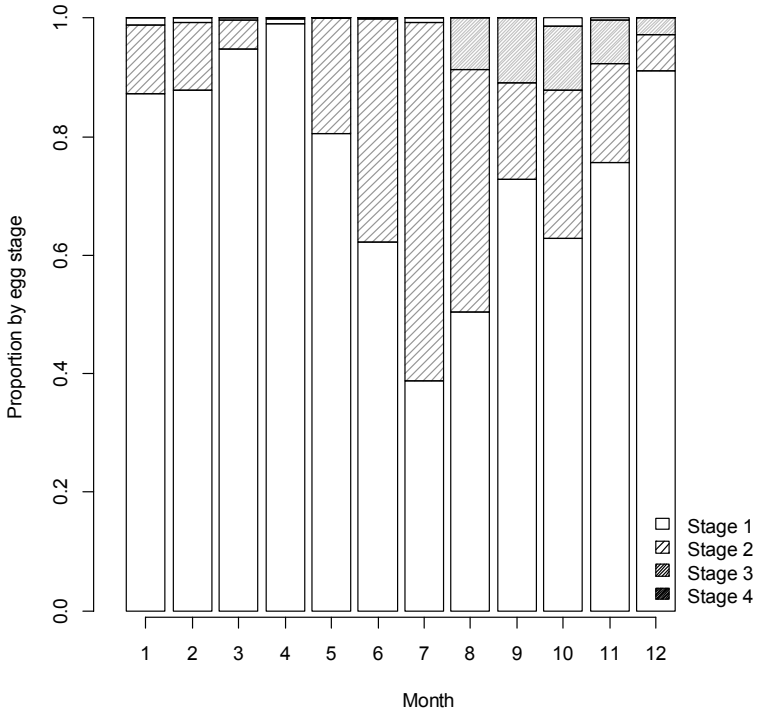

Figure 12: Barplots of the proportion of ovigerous females by egg stage and month, from observer sampling in SCI 6A.

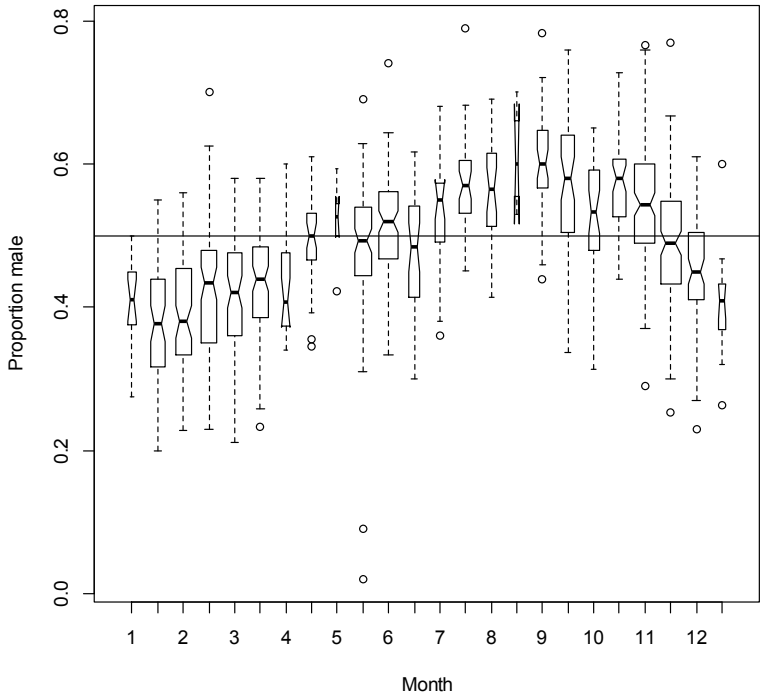

Figure 13: Boxplots of proportion of males in catches by half month from observer sampling in the SCI 6A fishery. Box widths proportional to square root of number of observations for that half month.

2.3 Standardised CPUE indices

2.3.1 Core vessels

A plot of vessel activity (number of scampi targeted tows recorded) over time is presented for SCI 6A in Figure 14. Eight vessels were active through most of the first decade of the fishery, but some of these dropped out of the fishery after 2003–04 (vessels C, F, H, M and O continuing to be active in most years), and a new vessel (R) being introduced at around this time.

Figure 15 (upper plot) shows the proportion of the total catch (over the history of the fishery) in relation to the number of years the vessels contributing that catch have been active in the fishery, and on the basis of this, a cut off of 10 years of activity has been selected to identify ten core vessels. Over the full history of the fishery, these vessels contribute over 92% of the scampi catches by scampi targeted fishing. The lower plot of Figure 15 shows the proportion of catch accounted for in each year by vessels active for over 10 years. Similar analyses in previous characterisations (e.g., Tuck 2014) have also examined a 5 year vessel activity cutoff, but for SCI 6A, this results in the same vessels being selected. Other than the 1991–92 to 1993–94 and 2002–03 to 2003–04 periods, the core vessels (active for over 10 years) have accounted for over 90% of targeted scampi catches in each year, and often over 99%.

The pattern of activity for the selected core vessels is shown in Figure 16. Vessels C, F, H, J, and M have been active throughout the history of the fishery (albeit with some gaps for some vessels), while vessels D, E, and G were only active to about 2002–03, vessel O has been active since 1997–98, and vessel R has been active since 2002–03.

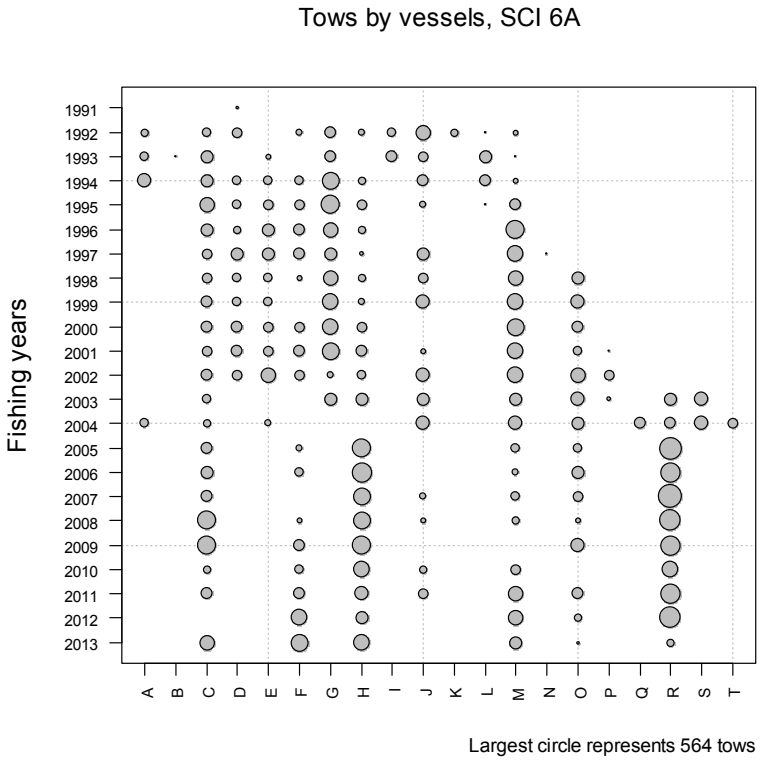

Figure 14: Pattern of fishing activity by vessel and fishing year for SCI 6A. The area of the circles is proportional to the number of tows recorded.

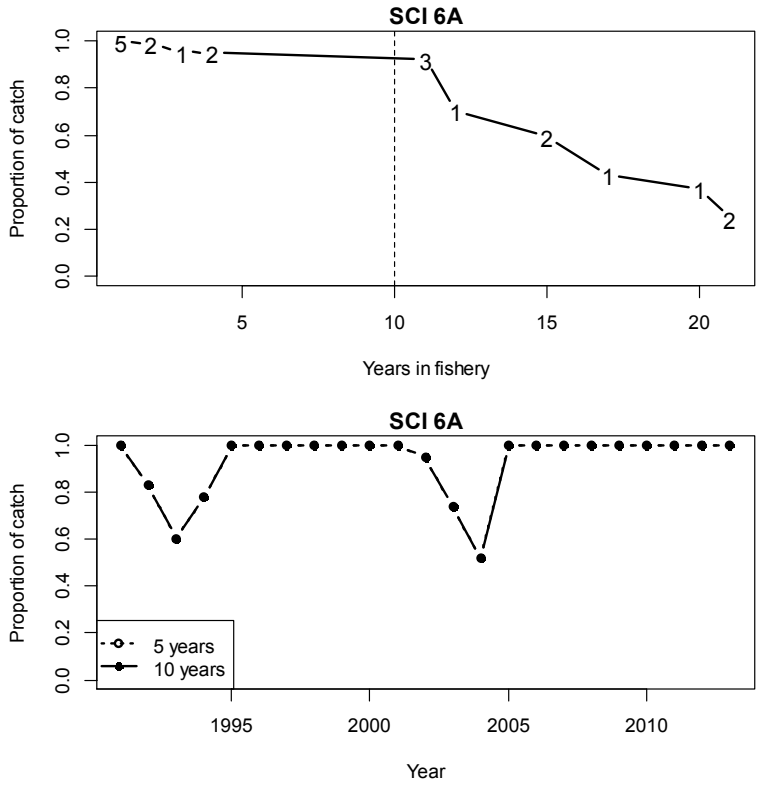

Figure 15: Catch breakdown by vessel. Upper plot - Proportion of total scampi catch (all years) plotted against the number of years the vessels reporting that catch have been active in the fishery. Numbers indicate number of vessels active for that duration. Vertical dotted line represents cut off for core vessels. Lower plot – Proportion of annual catch reported by vessels active in the fishery for 5 and 10 years.

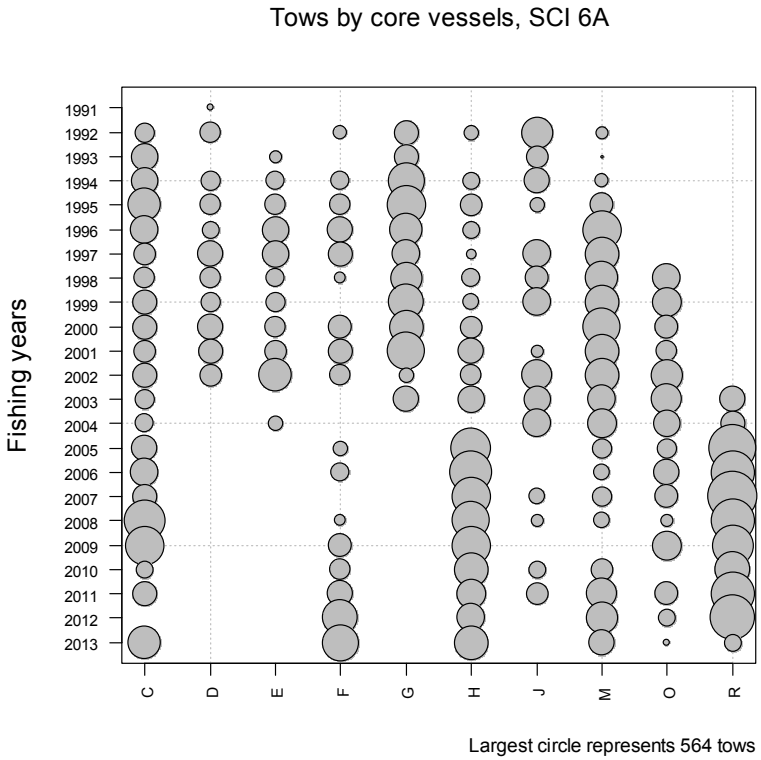

Figure 16: Core vessel pattern of fishing activity by vessel and fishing year for SCI 6A. The area of the circles is proportional to the number of tows recorded.

2.3.2 Calculation of indices

Within the previous preliminary assessment of SCI 6A, separate abundance indices were fitted for different survey strata and time steps (Tuck & Dunn 2012), but more recently the SFAWG has suggested a simplification of the model structure. Therefore, an initial model was examined allowing for the potential of model year*time_step*depth_band interactions. Scampi catch of core vessels was modelled using a year index (forced), model time step, vessel, time of day, state of moon, depth, fishing duration and trawl gear parameters.

The time of day of each tow was calculated in relation to nautical dawn and dusk (time when the sun is 12 degrees below the horizon in the morning and evening), as calculated by the *crepescule* function of the *maptools* package in R. Individual tows were characterised on the basis of whether they included dawn (shot before dawn, hauled after dawn and before dusk), day (shot after dawn, hauled before dusk), dusk (shot before dusk, hauled after dusk and before dawn) or night (shot after dusk and hauled before dawn). Longer tows including more than one period (i.e. shot before dusk and hauled after dawn were excluded from this part of the analysis (excluding 97 records from a total of over 27 800 for SCI 6A).

Individual hauls were also categorised in terms of moon state, on the assumption that tidal current strength at the sea floor will be related to the lunar cycle. Tows were categorised by their date in relation to the lunar cycle, as Full moon (more than 26 days since full moon, or less than 3 days since full moon), Waning (4 – 11 days since full moon), New moon (12 – 18 days since full moon), and Waxing (19 – 26 days since full moon).

Core vessels were selected as described above, by examining the scampi fleet's activity over the history of the fishery, and selecting vessels that had consistently contributed over a number of years, and together, had contributed a significant proportion of the overall catches over the whole fishery, and in each year.

Within the core vessels identified, three have changed gear configuration (twin rig to triple rig) in recent years, and two have changed engine power over the history of the fishery. Engine power was fitted within the model as a third order polynomial, and gear configuration as a two level factor (twin or triple rig). Gear configuration for a particular vessel and date was determined on the basis of information provided by the fishing industry as to when vessels changed from twin to triple, and all tows after this date are defined as triple rig. It is acknowledged that vessels may change configuration within a trip depending on gear damage or fishing conditions, but it is unclear how reliably this has been recorded on TCEPR forms in the past (as effort width). Preliminary examination of the data for the core vessels suggested that the values recorded were generally realistic, and following some minor grooming, "effort width" was also included as a term (third order polynomial) as a term in the model.

In addition, examination of the data for SCI 3 (Tuck 2013) identified a distinct shift in trawl duration between 2002–03 and 2006–07 (from about 5 hours to 7 hours). This shift (in SCI 3) was fleet-wide, and associated with a modification to the top of the trawl to reduce the bycatch (John Finlayson, Sanford Ltd. pers comm.), enabling vessels to fish for longer on each tow. Boxplots of tow duration over time have been examined for each of the core vessels identified for SCI 6A (Figure 17), and rather than the relatively rapid shift in trawl duration recorded by the same vessels in SCI 3 (Figure 18), within SCI 6A, the increase in haul duration appears to have been more gradual, starting in the early 1990s, and stabilising at about 7 hours by the late 1990s or early 2000s. This is a very similar pattern to that observed for SCI 1 and SCI 2 (Tuck 2014). Once the bycatch modification to the gear was introduced by a vessel (around 2004–05), it was used in all fisheries, but it does not appear to have had an effect on tow duration in SCI 6A (or SCI 1 and SCI 2). For each vessel, the timing of the gear modification was estimated from examination of tow durations in SCI 3, and fitted as a two level factor in the model.

Catch indices were derived using generalised linear modelling (GLM) procedures (Vignaux 1994, Francis 1999), using the statistical software package R. The response variable in the GLM was the natural logarithm of scampi catch. The fishing-year (combined with any time step or depth strata for the index) was entered as a categorical covariate (explanatory) term on the right-hand side of the model. Standardised CPUE abundance indices (canonical) were derived from the exponential of the fishing-year covariate terms as described in Francis (1999).

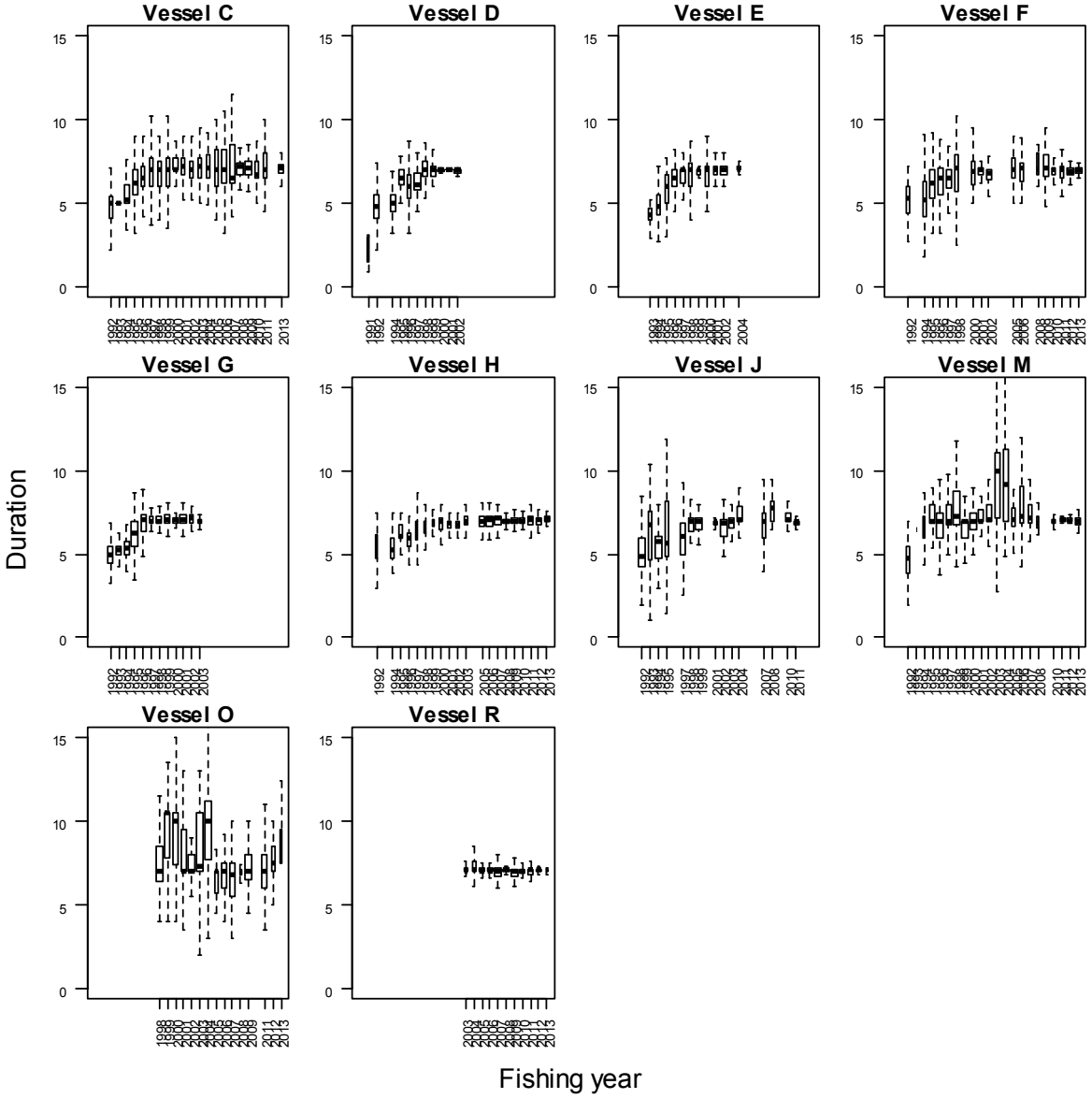

Figure 17: Boxplots of tow duration (hours) for scampi targeted fishing in SCI 6A for the ten core vessels identified. Box widths proportional to square root of number of observations.

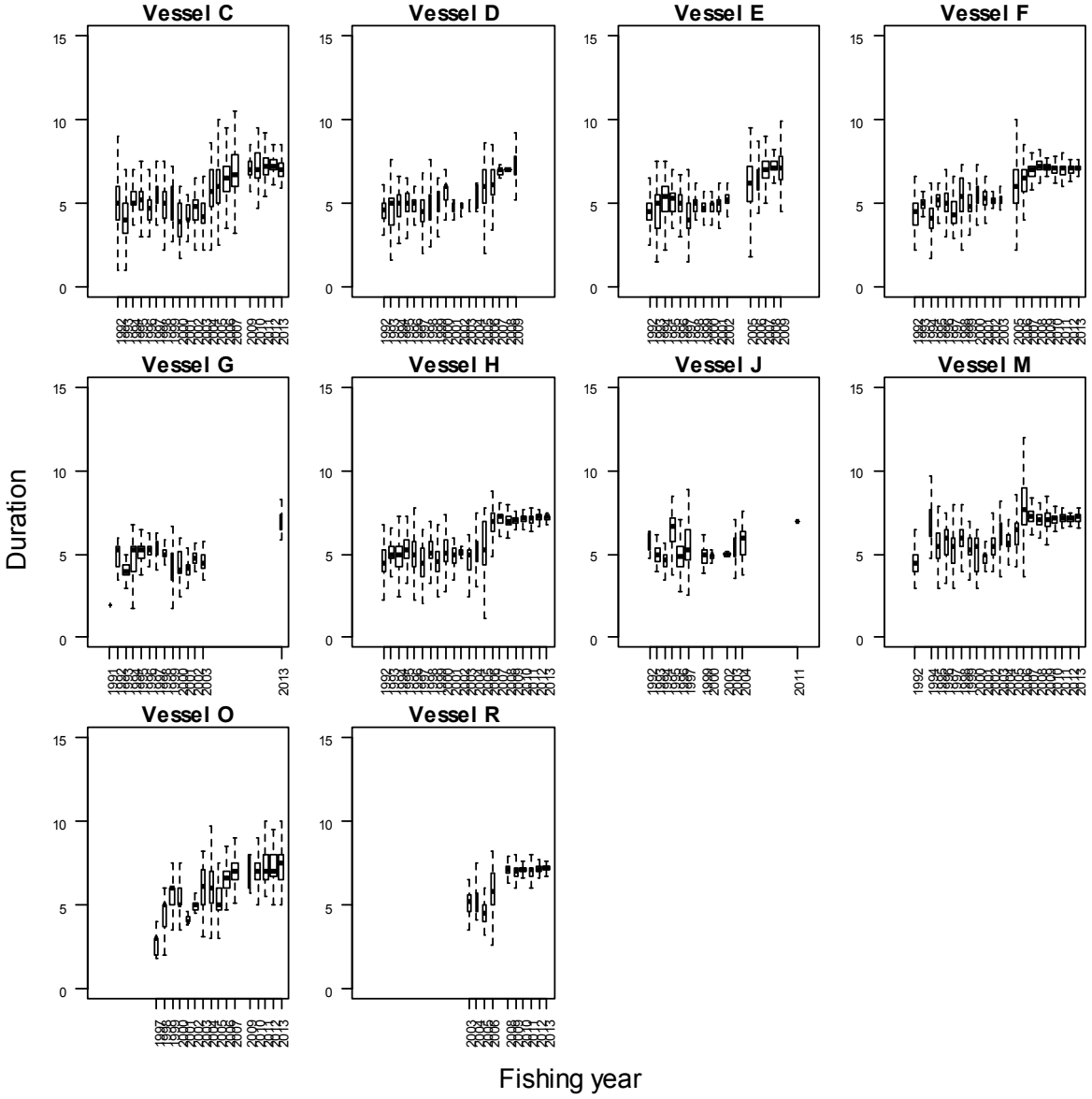

Figure 18: Boxplots of tow duration (hours) for scampi targeted fishery in SCI 3 for the ten core vessels identified for SCI 6A. Box widths proportional to square root of number of observations.

In order to accommodate a non-linear relationship with the response variable (log catch), the continuous variables (effort, engine power, gear width) were "offered" to the GLMs as third order polynomials. Vessel, depth (binned into the 50 m survey strata), time of day, state of tide, twin or triple rig and bycatch modification were "offered" to the GLMs as factors. Some effects (e.g., gear width) were represented by more than one term, and the model was allowed to select which (if any) were retained. A forward fitting, stepwise, multiple-regression algorithm was used to fit GLMs to groomed catch, effort and characterisation data. The stepwise algorithm generates a final regression model iteratively and uses a simple model with a single predictor variable, fishing year, as the initial or base model. The reduction in residual deviance relative to the null deviance is calculated for each additional term added to the base model. The term that results in the greatest reduction in residual deviance is added to the base model if this results in an improvement in residual deviance of more than 1%. The algorithm repeats this process, updating the model, until no new terms can be added. Diagnostic plots for the final models are presented in Appendix 1 (Bentley et al. 2012).

2.3.3 Final CPUE index

Stepwise regression analysis of the dataset with the full model to estimate the CPUE indices for SCI 6A resulted in an initial model with model year, fishing duration, time of day, vessel, model step, and a second order interaction between model year and model step retained (Table 3). The model explained 34% of the variation in the data. Depth was not retained within the model, either as a separate term, or as part of an interaction, suggesting that it does not contribute much to explaining the deviance in the model.

Table 3: Analysis of deviance table for initial standardisation model selected by stepwise regression for SCI 6A.

	Df	Deviance explained	Additional deviance explained (%)
NULL			
model_year	22	1285.87	14.45
poly(fishing_duration, 3)	3	654.71	7.36
TOD	3	488.17	5.49
vessel	9	241.19	2.71
model_step	2	149.08	1.68
model_year:model_step	41	230.26	2.59

A second model was examined without the option of interactions, which explained 32% of the variation in the data. Predicted CPUE (for vessel M with a 7 hour fishing duration) from the models with and without model_year:time_step interactions did not suggest that exclusion of the interaction term would have a big influence on the assessment model outputs (Figure 19), and the WG agreed to use the standardised CPUE from the model excluding interactions.

A further investigation into different error distributions (comparing log normal, gamma and Weibull) identified that the gamma distribution provided a slight improvement in the distribution of residuals (Figure 20), although the overall index was not sensitive to the choice of error distribution used (Figure 21). The Working Group proposed that the index calculated with the gamma distribution be fitted within the assessment model (Figure 22, Table 4). Diagnostic plots for this model are presented in Appendix 1.

Table 4: Analysis of deviance table for initial standardisation model selected by stepwise regression for SCI 6A.

	Df	Deviance explained	Additional deviance explained (%)	Overall influence (%)*
NULL				
model_year	22	1450.11	18.08	
poly(fishing_duration, 3)	3	429.47	5.35	7.48
TOD	3	445.34	5.55	4.15
vessel	9	208.32	2.60	3.23
model_step	2	102.63	1.28	2.06

*- Overall influence as in table 1 of Bentley et al. (2012)

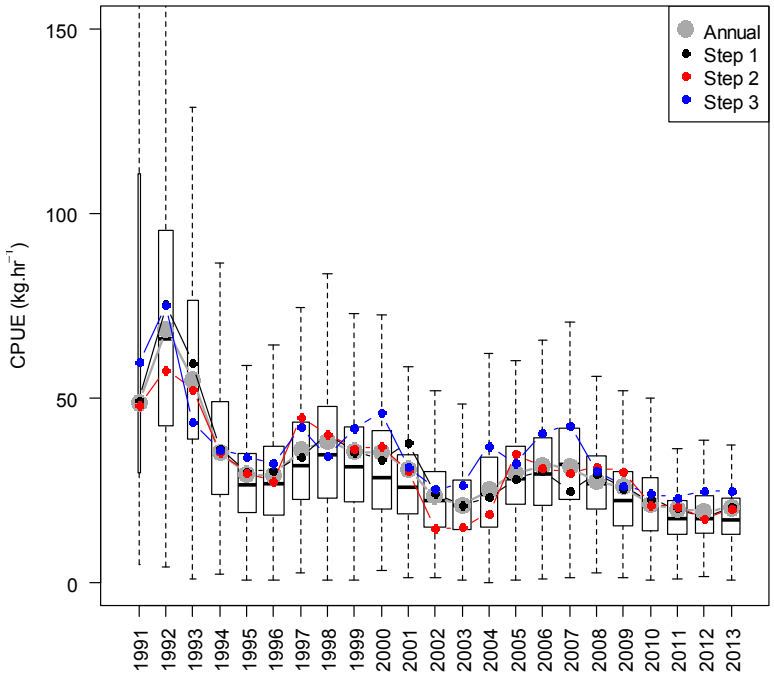

Figure 19: Predicted CPUE (for vessel M, with 7 hour tows) from the model with and without the model_year:time_step interaction. Box plots show unstandardized CPUE for each year. Box widths proportional to square root of number of observations.

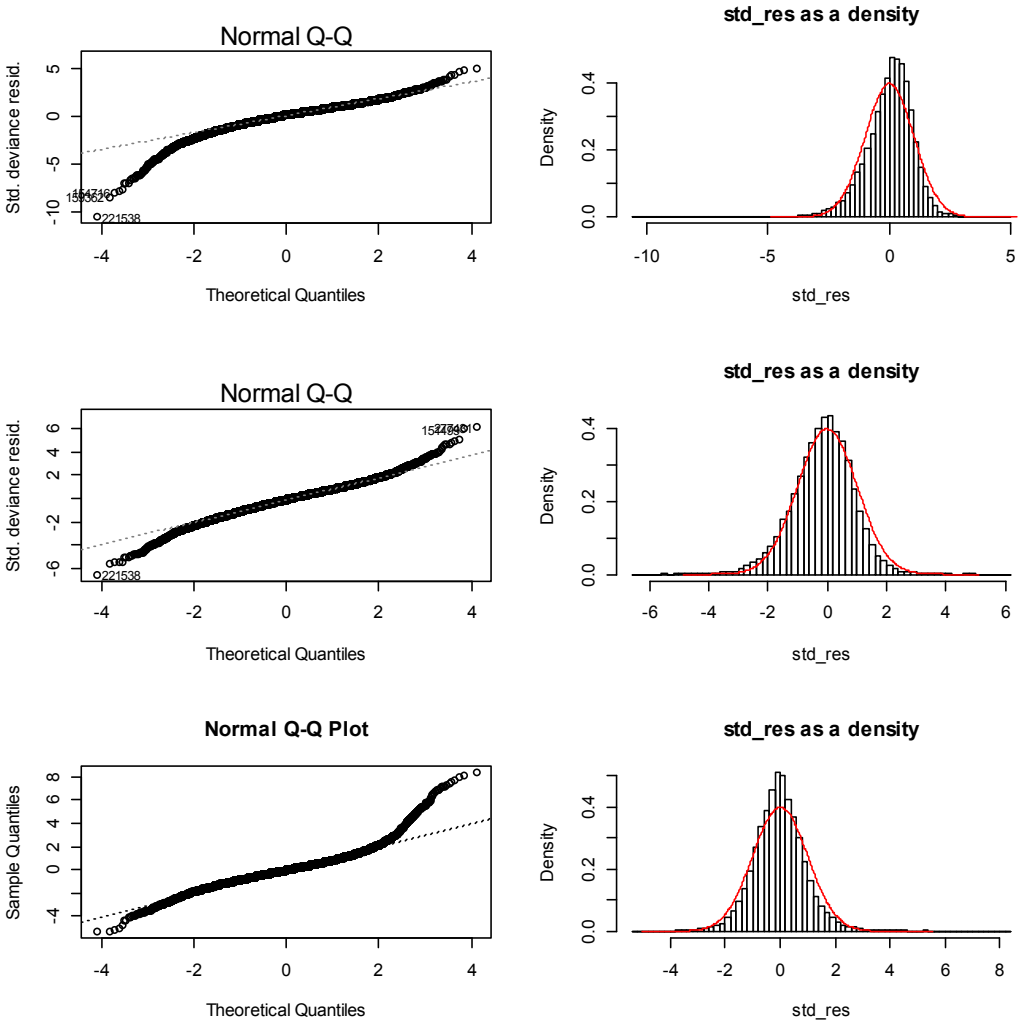

Figure 20: Plots of the distributions of standardised residuals for standardised CPUE models with log normal (top panel), gamma (middle panel), and Weibull (bottom panel) error distributions.

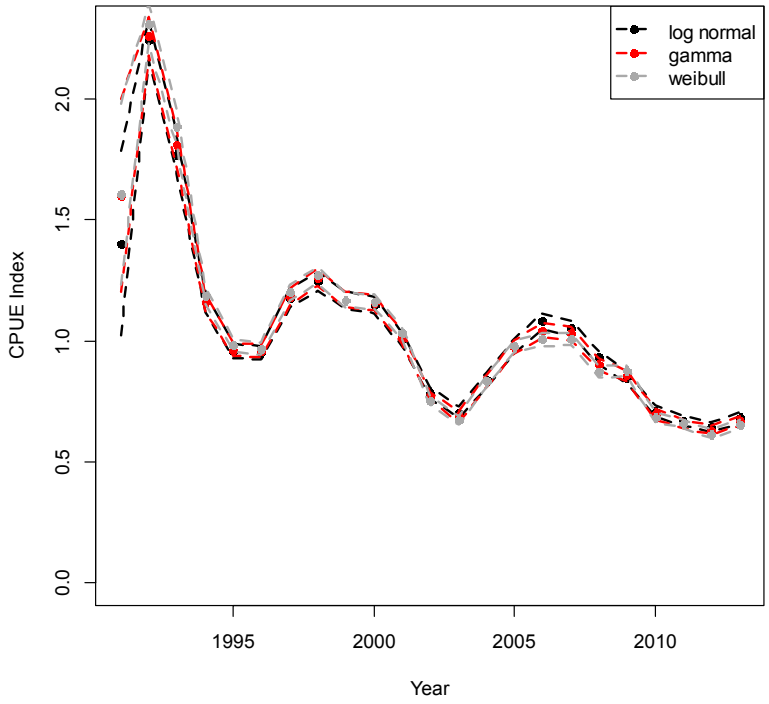

Figure 21: Standardised CPUE indices from final model structure with log normal, gamma and Weibull error distributions.

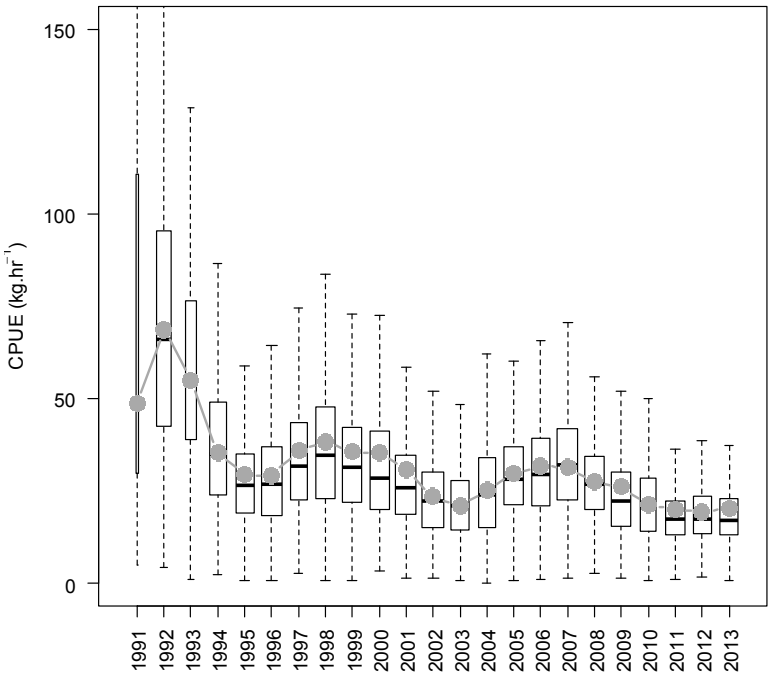

Figure 22: Annual standardised CPUE index from final model, and boxplots of unstandardized CPUE. Box widths proportional to square root of number of observations.

3. MODEL STRUCTURE

3.1 Seasonal and spatial structure, and the model partition

The model partitions scampi by sex, and length class. Growth between length classes is determined by sex-specific, length-based growth parameters. Individuals enter the partition by recruitment and are removed by natural mortality and fishing mortality. The model's annual cycle is based on the fishing year and is divided into the three time-steps described above (on basis of Table 2). The choice of three time steps was based on current understanding of scampi biology and sex ratio in catches. Note that model references to "year" within this report refer to the modelled or fishing year, and are labelled as the most recent calendar year, e.g. the fishing year 1998–99 is referred to as "1999" throughout. Previous models for SCI 6A have included spatial structure (Tuck & Dunn 2012), but following the characterisation and preliminary model investigation, the SFAWG recommended a single area model for the assessment.

The model uses capped logistic length based selectivity curves for commercial fishing and research trawl surveys, but allowed to vary with sex and time step (where necessary). While the sex ratio data suggest that the relative catchability of the sexes varies through the year (hence the model time structure adopted), there is no reason to suggest that assuming equal availability, selectivity at size would be different between the sexes. Therefore the two sex selectivity implementation developed within CASAL for previous scampi assessments (Tuck & Dunn 2012) was applied. This allows the L_{50} (size at which 50% of individuals are retained) and a_{95} (size at which 95% of individuals are retained) selectivity parameters to be estimated as single values shared by both sexes in a particular time step, but allows for different availability between the sexes through estimation of different a_{max} (maximum level of selectivity) values for each sex. The change in the depth distribution of the fishery in the early years (Figure 7), and the implication for selectivity (since mean size is larger in shallower areas) were allowed for using a shift parameter in the selectivity, related to the median depth of fishing in each year. Photographic survey abundance indices are not sex specific, and a double normal length based selectivity curve is applied, to allow for reduced availability of males (which grow to a larger size than females) at the time of the survey, related to moulting.

3.2 Biological inputs

3.2.1 Growth

Scampi growth has been investigated through field tagging exercises in SCI 6A in 2007, 2008, 2009 and 2013 (Tuck et al. 2007, Tuck et al. 2009a, Tuck et al. 2009b, Tuck et al. 2015), with recaptures reported by the fishing industry. Growth data are fitted within the model. The tag recapture data for each release event have been split into year-time step combinations, and the numbers of recaptures per event are tabulated in Table 5.

Table 5: Numbers of scampi recaptured by release and recapture time step (SCI 6A). Releases and recaptures labelled by fishing year – time step.

Release/ Recapture	2007-1	2007-2	2007-3	2008-1	2008-2	2008-3	2009-1	2009-2	2009-3	2010-2	2013-1	2013-2	2013-3
2007-1	26	42	81	4	6	6	0	1	1	0			
2008-1				47	30	76	18	23	14	0			
2009-1							51	136	78	1			
2013-1											42	85	25

For the various combinations of release and recapture, the length increment is plotted by sex against initial length for the 2007 release in Figure 23, for the 2008 and 2009 release in Figure 24, and for the 2009 and 2013 release in Figure 25. Growth for both sexes is thought to occur in time step 1.

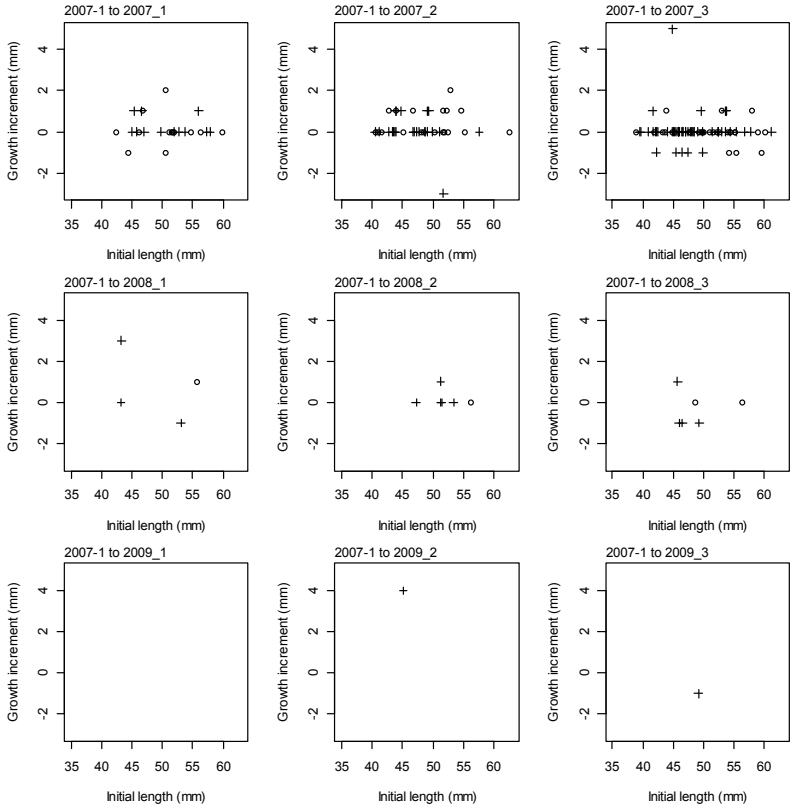

Figure 23: Plot of initial length against growth increment by combination of release and recapture time steps for 2007 releases. Males represented by hollow symbols, females represented by crosses.

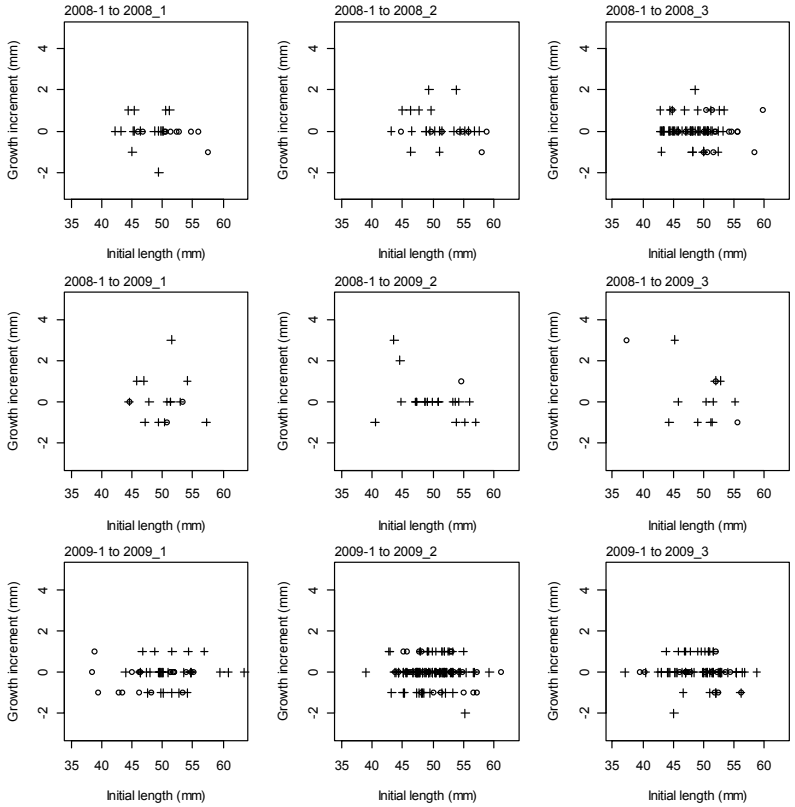

Figure 24: Plot of initial length against growth increment by combination of release and recapture time steps for 2008 and 2009 releases. Males represented by hollow symbols, females represented by crosses.

Given the overall size distribution of scampi from SCI 6A, with animals reaching larger sizes (compared to the other areas examined), it would be anticipated that the growth increment at size would be greater than in SCI 1 and SCI 2, and more comparable with SCI 3.

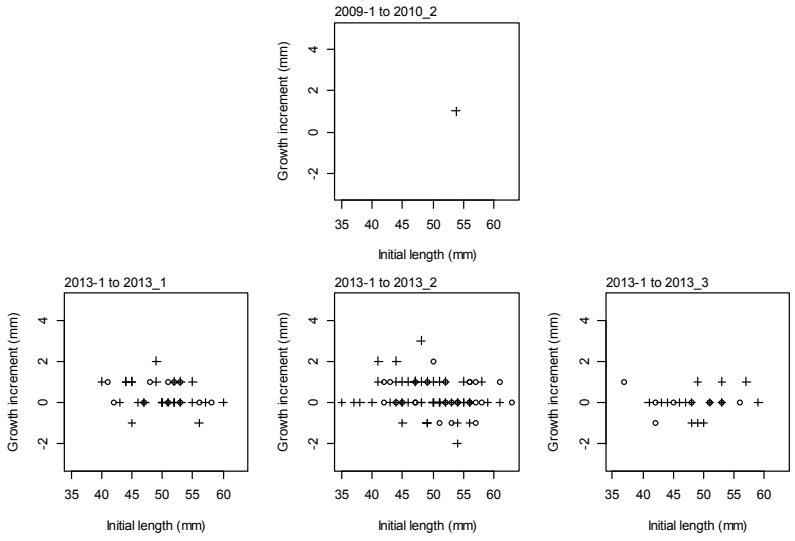

Figure 25: Plot of initial length against growth increment by combination of release and recapture time steps for 2009 (recaptured in 2010) and 2013 releases. Males represented by hollow symbols, females represented by crosses.

3.2.2 Maturity

Female maturity can be estimated from gonad staging or the presence of eggs on the pleopods. Gonad stages are recorded from research survey catches (although only on scampi not tagged and released), while the presence and development stage of eggs on pleopods are recorded from research survey and observer sampling. No data are available for the maturity of male scampi, so their maturity ogive was assumed to be identical to that of females, although studies on *N. norvegicus* have suggested that male maturity may occur at a larger size (although possibly the same age) than females (Tuck et al. 2000). Maturity is not considered to be a part of the model partition, but proportions mature were fitted within the model based on a logistic ogive with a binomial likelihood (Bull et al. 2008). Analysis of the proportion mature data, modelled as a function of length within a GLM framework, with a quasi distribution of errors and a logit link (McCullagh & Nelder 1989),

$$P.mature = a + b * Length$$

which equates to the logistic model. The model was weighted by the number measured at each length. After obtaining estimates for the parameters *a* and *b*, the length at which 50% are mature (L_{50}) was calculated from:

$$L_{50} = -\frac{a}{b}$$

with selection range (SR) calculated from:

$$SR = \frac{(2.\ln(3))}{b}$$

Ovary stage at length data are presented in Figure 26. The L_{50} estimate for the SCI 6A data was 37.0 mm, with a selection range a_{25} to a_{75} of 5.8 mm.

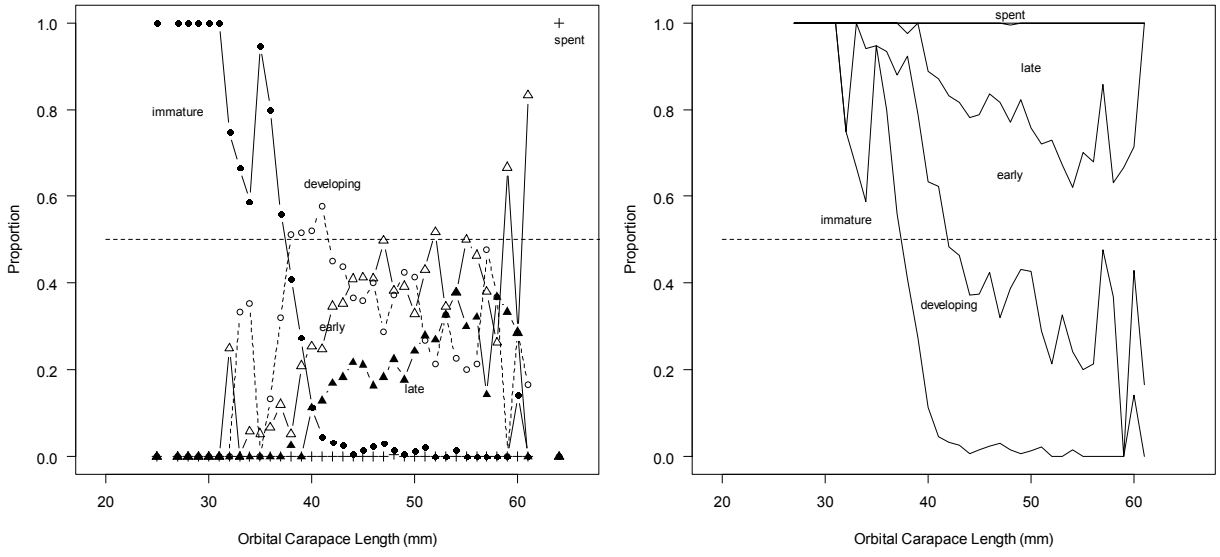

Figure 26: Proportions of female scampi having various developmental stages of internal ovaries. Left panel shows proportions of each stage separately, right panel shows combined proportions. Aggregated data from research voyages in SCI 6A, all conducted in February/March.

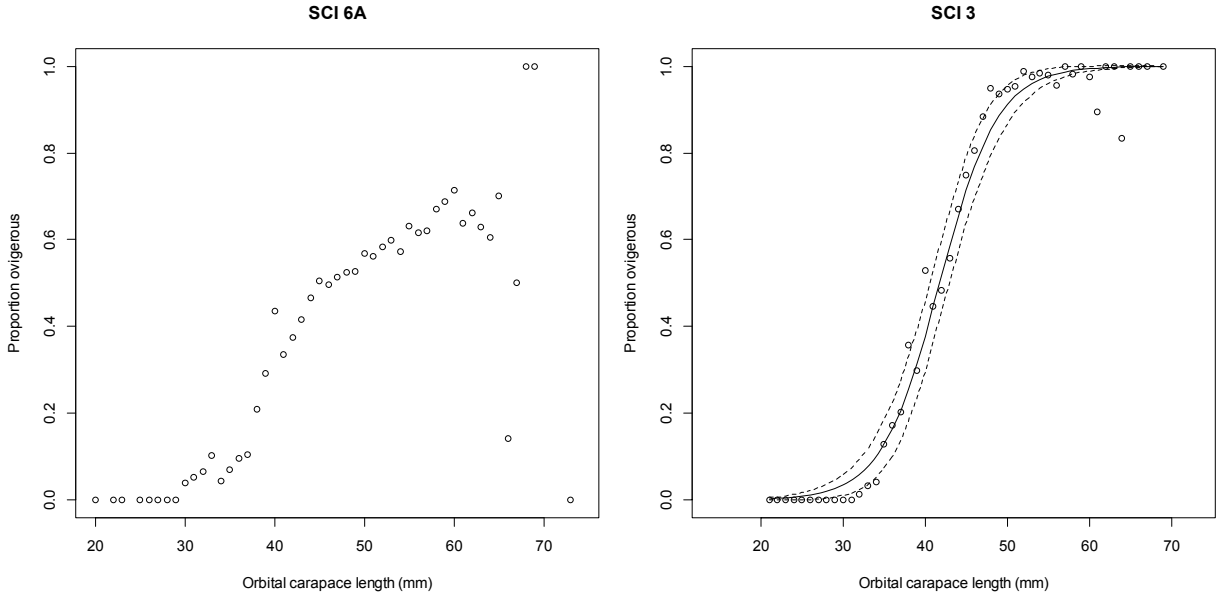

Figure 27: Left: Proportions of female scampi carrying eggs (ovigerous) at length, from observer sampling in January to March in SCI 6A, just after the spawning period. Right: Equivalent figure for SCI 3 for comparison. Solid line represents logistic curve fitted to the data (L_{50} 41.8 mm and selection range 7.8 mm). Dashed line represents plus or minus one Standard Error.

3.2.3 Natural mortality

The instantaneous rate of natural mortality, M, has not been estimated directly for any scampi species, but estimates have been made (0.2 – 0.25) based on the estimate of the K parameter from a von Bertalanffy growth curve (Cryer & Stotter 1999) using a correlative method (Pauly 1980, Charnov et al. 1983). Morizur (1982) used length distributions from 'quasi-unexploited' *Nephrops* stocks to obtain estimates for annual *M* of 0.2–0.3. The values most commonly assumed for assessment of *Nephrops* stocks in the Atlantic is 0.3 for males and immature females, and 0.2 for mature females (assumed less vulnerable to predation during the ovigerous period) (Bell et al. 2006). For New Zealand scampi, M has previously been fixed at 0.2 (Tuck & Dunn 2012), or both 0.2 and 0.3 (Tuck 2014). Within the current assessment, an attempt was made to estimate M within the model, but sensitivities were also examined with M fixed at 0.2, 0.25 and 0.3.

3.3 Catch data

Data for the model were collated over the spatial and temporal strata as defined in the model structure. Catches in the modelled area represent over 96% of scampi catches from SCI 6A. Details of catches by fishing year and time step, are provided in Table 6.

Table 6: Catch (t) breakdown by fishing year and time step for SCI 6A.

Fishing year	Step 1	Step 2	Step 3
1988	0.0	0.0	0.0
1989	0.0	0.0	0.0
1990	0.0	0.0	0.0
1991	2.0	0.0	0.0
1992	230.5	93.2	13.6
1993	180.1	63.2	50.1
1994	256.3	0.2	37.5
1995	121.1	43.4	56.8
1996	201.9	28.6	77.8
1997	155.4	47.5	34.8
1998	155.5	93.9	46.0
1999	167.0	74.2	76.4
2000	160.4	75.4	82.1
2001	85.9	100.7	94.8
2002	242.8	5.9	80.2
2003	168.2	6.8	119.4
2004	168.6	20.4	79.0
2005	75.4	82.4	116.4
2006	83.4	82.6	111.5
2007	76.9	49.3	207.0
2008	78.7	37.4	144.6
2009	59.5	103.0	78.7
2010	44.1	53.3	53.0
2011	24.7	79.3	79.2
2012	21.0	44.6	98.4
2013	11.1	48.5	81.0

3.4 CPUE indices

The annual CPUE indices estimated within the standardisation (Figure 22) were fitted within the model as abundance indices. There has been considerable discussion on whether CPUE is proportional to abundance for scampi (Tuck 2009), with rapid increases in both CPUE and trawl survey catch rates for a number of stocks in the early to mid 1990s (and changes in sex ratio in trawl survey catches) initially being considered related to changes in catchability. Later analysis (Tuck & Dunn 2009) suggested that the observed changes in sex ratio were related to slight changes in the survey timing in relation to the moult cycle. Similar patterns in CPUE are observed over the same period for rock lobster (Starr 2009, Starr et al. 2009), and scampi in SCI 3 (Tuck 2013), which may suggest broad scale environmental drivers influencing crustacean recruitment. The CPUE patterns for SCI 1 are mirrored by trawl survey catch rates, suggesting that they do not reflect fisher learning. While not considered appropriate for use as an index in the model (Tuck 2013), a scampi abundance index generated from the middle depths (*R.V. Tangaroa*) trawl survey shows a very similar temporal pattern to the standardised CPUE indices for SCI 3, also supporting the suggestion that the increases in scampi catch rate observed during the 1990s reflect scampi abundance rather than fisher learning.

The standardised CPUE index was fitted using the approach of Clark & Hare (2006), as recommended by Francis (2011). This approach fits lowess smoothers with different degrees of smoothing (Figure 28), and uses the residuals from each fit to estimate the CV. From visual examination of the fits, the Working Group determined that a CV of 0.15 was appropriate for the CPUE, but that sensitivity to larger CVs should also be examined.

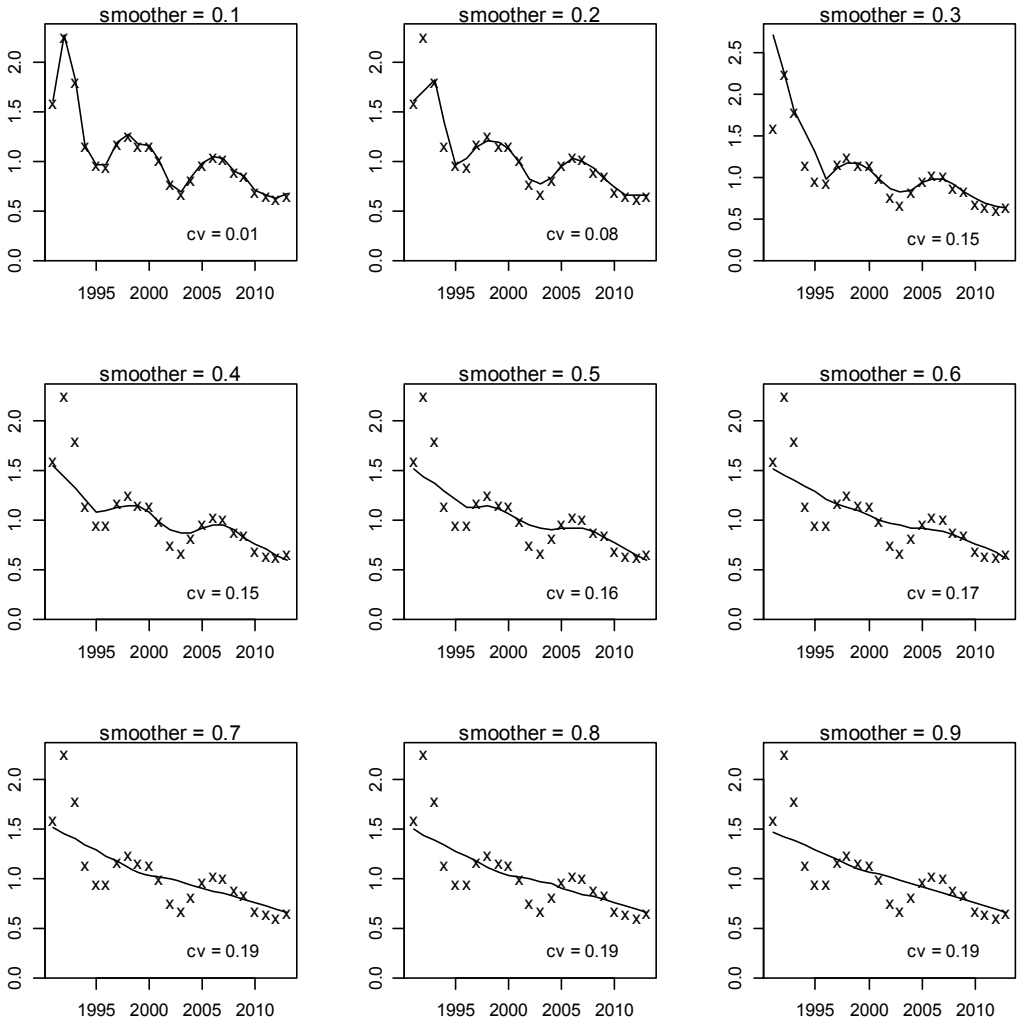

Figure 28: Fits of lowess smoothers to the standardised CPUE index.

3.5 Research survey indices

Trawl surveys were conducted annually from the *F.V. San Tongariro* in SCI 6A between 2007 and 2009, with a fourth survey in 2013. Each of these surveys was conducted (in conjunction with a photographic survey) between February and April.

3.5.1 Photographic surveys

Photographic surveys of SCI 6A have been conducted in 2007–09 and 2013 (Tuck et al. 2007, Tuck et al. 2009a, Tuck et al. 2009b, Tuck et al. 2015). The surveys provide two indices of scampi abundance, one based on major burrow openings, and one based on visible scampi. Both indices are subject to uncertainty, either from burrow detection and occupancy rates (for burrow based indices) or emergence patterns (for visible scampi based indices). The burrow index has been used to date within assessments for SCI 1, SCI 2 and SCI 3 (Tuck & Dunn 2012, Tuck 2013), but in SCI 6A scampi appear to spend less time in burrows (Tuck et al. 2007), and the visible scampi index has been used (Tuck & Dunn 2012). Survey estimates are provided in Table 7. Details of the estimation of the catchability priors are provided in Section 3.7.

Table 7: Time series of photographic survey visible scampi abundance (millions) and CV for SCI 6A.

Survey	Abundance	CV
2007	38.2	0.107
2008	31.7	0.103
2009	21.1	0.146
2013	17.5	0.202

3.5.2 Trawl surveys

Stratified random trawl surveys of scampi in SCI 6A, 350–550 m depth, were conducted in 2007–2009 and 2013, in conjunction with photographic surveys. Surveys have been conducted by the same vessel, using the same trawl, but a gear loss just before the 2009 survey meant that slightly different trawl doors were used for that survey, with the catch rates scaled appropriately to account for this (Tuck et al. 2009a). Survey estimates are provided in Table 8. Details of the estimation of the catchability priors are provided in Section 3.7.

Table 8: Time series of trawl survey scampi biomss (tonnes) and CV for SCI 6A.

Survey	Biomass	CV
2007	1 073.5	0.18
2008	1 229.2	0.18
2009	821.6	0.09
2013	1 258.0	0.09

3.6 Length distributions

3.6.1 Commercial catch length distributions

Ministry for Primary Industries observers have collected scampi length frequency data from scampi targeted fishing on commercial vessels in SCI 6A since 1991–92. The numbers of tows for which length data are available are presented by fishing year in Table 9.

The Working Group expressed concern that there may be depth related spatial structure in the length composition (larger scampi in shallower water), and that this should be taken account of within the analysis. Patterns in the sex ratio and mean size from the scampi observer length frequency data were examined using multivariate tree regression (using the R package *mvpart*). Data were analysed for each year separately at the observed tow level, with response variables regressed on the explanatory variables half month and depth bin. Pruning was conducted to give the tree with the smallest cross-validated relative error. Details of the splits identified for each year are provided in Appendix 2. Depth splits were identified in the data from eleven years, with 450 m identified on six occasions. Splits at 400 m and 500 m were only identified three times each. The temporal splits identified were consistent with those already proposed for the model structure (Table 2).

On the basis of both the mean size and sex ratio (proportion males) within catches, it was considered appropriate to stratify the length sampling by depth, with separate strata for 350–450m, and 450–550m (combined).

The Working Group also expressed interest in any potential "observer effect" in the data. Fifty observer trips have been conducted targeting scampi in SCI 6A, with a unique observer id available for 49 of these (one trip had no observer id recorded). These 49 trips were conducted by 36 different observers, with 28 observers only completing one trip, 6 observers completing 2 trips and 3 observers completing 3 trips. Given the lack of replicate trips for most observers, any observer effect would be

confounded with other trip variables. Of the 49 trips, 21 were the first scampi trip for that observer, the other all having completed at least one scampi trip in another fishery before their first in SCI 6A.

Boxplots of scampi mean size per tow for each trip (Figure 29) show that the median size per tow has generally varied between about 44 mm and 55 mm, although the median size on trip 10242 was about 39 mm. Half of the scampi targeted observer trips appear to be "first" scampi trips for observers, and in general these first trips do not stand out from the others, but trip 10242 is clearly somewhat different, and may suggest that the observer was not following measurement protocols correctly. Data from this trip were excluded from further analysis.

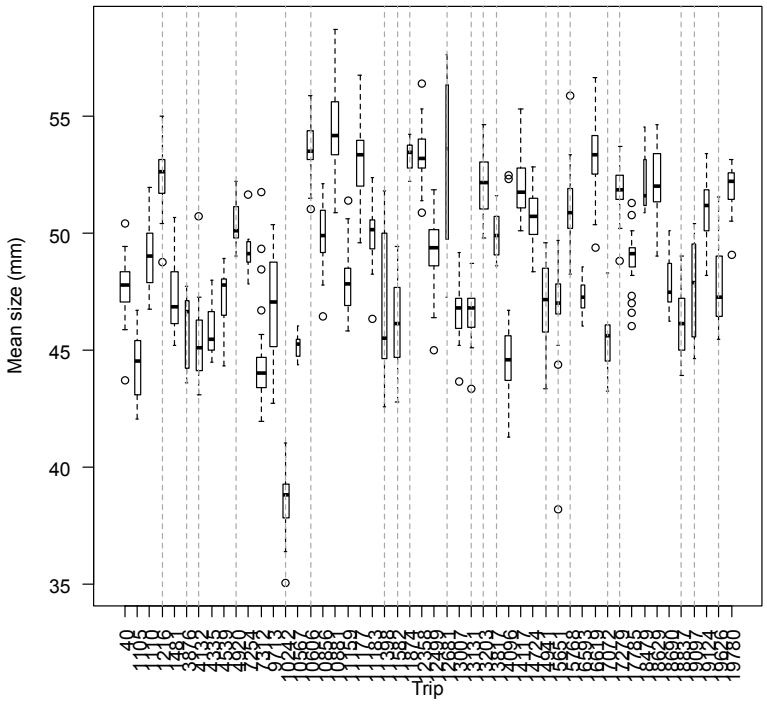

Figure 29: Boxplots of scampi mean size per tow by observer trip, with those trips which were the first scampi targeted trips for the observer concerned identified by a grey dashed line. Trips are not plotted in chronological order.

On the basis of the observer sampling within the two depth bands (350–450m and 450–550m) and the three time steps within each fishing year (Table 9), the proportion of scampi catch represented by the observer sampling (having at least one observer sample from that depth in that time step) has been examined (Table 10). This ranged from 25% (1998, time step 3) to 100%, with 29 of the 36 observed year_step combinations having over 90% of the catches represented by sampling. The Working Group considered that 90% representation was an appropriate cut-off for inclusion in the assessment model, with the other data being excluded. For the year_step combinations retained, proportional length distributions (and associated CVs) were calculated using CALA (Francis & Bian 2011), using the approaches previously implemented in NIWA's *Catch-at-Age* software (Bull & Dunn 2002). Plots of the proportional length distribution are shown by year by time step in Figure 30 to Figure 34.

Table 9: Numbers of scampi observer length frequency samples from SCI 6A, by model year, time step and combined depth band.

	Step			Step 1		Step 2		Step 3	
Model year	1	2	3	350–450	450–550	350–450	450–550	350–450	450–550
1991	0	0	0	0	0	0	0	0	0
1992	81	0	0	78	1	0	0	0	0
1993	69+	0	13	49	19	0	0	9	4
1994	88	0	35	34	54	0	0	7	28
1995	20	0	0	5	15	0	0	0	0
1996	32	0	19	13	19	0	0	0	19
1997	24	24	58	5	19	0	24	1	57
1998	87	6	1	65	22	0	6	1	0
1999	0	0	21	0	0	0	0	2	19
2000	24	0	0	1	23	0	0	0	0
2001	0	36	11	0	0	0	36	0	11
2002	14	0	55	0	14	0	0	38	17
2003	39	0	57	10	29	0	0	26	31
2004	7	0	0	1	6	0	0	0	0
2005	0	0	24*	0	0	0	0	2	22*
2006	17*	0	0	1*	16*	0	0	0	0
2007	34	0	13	29	5	0	0	0	13
2008	13	12	25	2	11	8	4	6	19
2009	14	0	0	2	12	0	0	0	0
2010	0	30	0	0	0	4	26	0	0
2011	43	27	59	16	27	17	10	1	58
2012	0	31	0	0	0	20	11	0	0
2013	0	89	0	0	0	8	81	0	0

+ - 35 tows in 1993_1 measured scampi to the centimetre, rather than millimetre, and these have been excluded from further analysis

* - exclusion of observer trip 10242 removes 8 samples from time step 3 in 2005 (all from the 450–550 m depth range, and all 17 samples from time step 1 in 2006.

Table 10: Estimated scampi catch (tonnes) in the modelled area by model year and time step, and the percentage of catch represented by the observer sampling.

	Estimated catch			% represented by sampling		
Model year	Step 1	Step 2	Step 3	Step 1	Step 2	Step 3
1991	2.00	0.00	0.00			
1992	206.85	90.09	12.13	100.00		
1993	162.80	60.02	46.76	100.00		100.00
1994	259.23	0.17	39.00	100.00		100.00
1995	130.24	46.51	61.35	100.00		
1996	172.60	24.03	72.39	100.00		80.33
1997	179.38	54.61	39.83	100.00	70.45	100.00
1998	147.32	89.24	41.94	100.00	61.58	25.51
1999	169.50	75.66	78.13			100.00
2000	165.21	77.78	84.70	100.00		
2001	81.10	94.96	87.33		84.06	92.96
2002	197.43	4.80	69.36	83.84		100.00
2003	148.98	6.04	99.50	100.00		100.00
2004	193.08	23.37	94.10	100.00		
2005	81.03	88.56	125.41			100.00*
2006	85.48	84.52	114.77	100.00*		
2007	69.68	44.15	187.65	100.00		65.86
2008	86.65	41.03	158.23	100.00	100.00	100.00
2009	65.12	112.44	85.59	100.00		
2010	42.38	51.23	50.39		100.00	
2011	26.60	85.02	85.54	100.00	100.00	100.00
2012	20.56	45.18	99.55		100.00	
2013	11.16	50.20	84.04		100.00	

* - exclusion of observer trip 10242 does not affect sample coverage for time step 3 in 2005 (because another trip also provides coverage), but removes all samples from time step 1 in 2006.

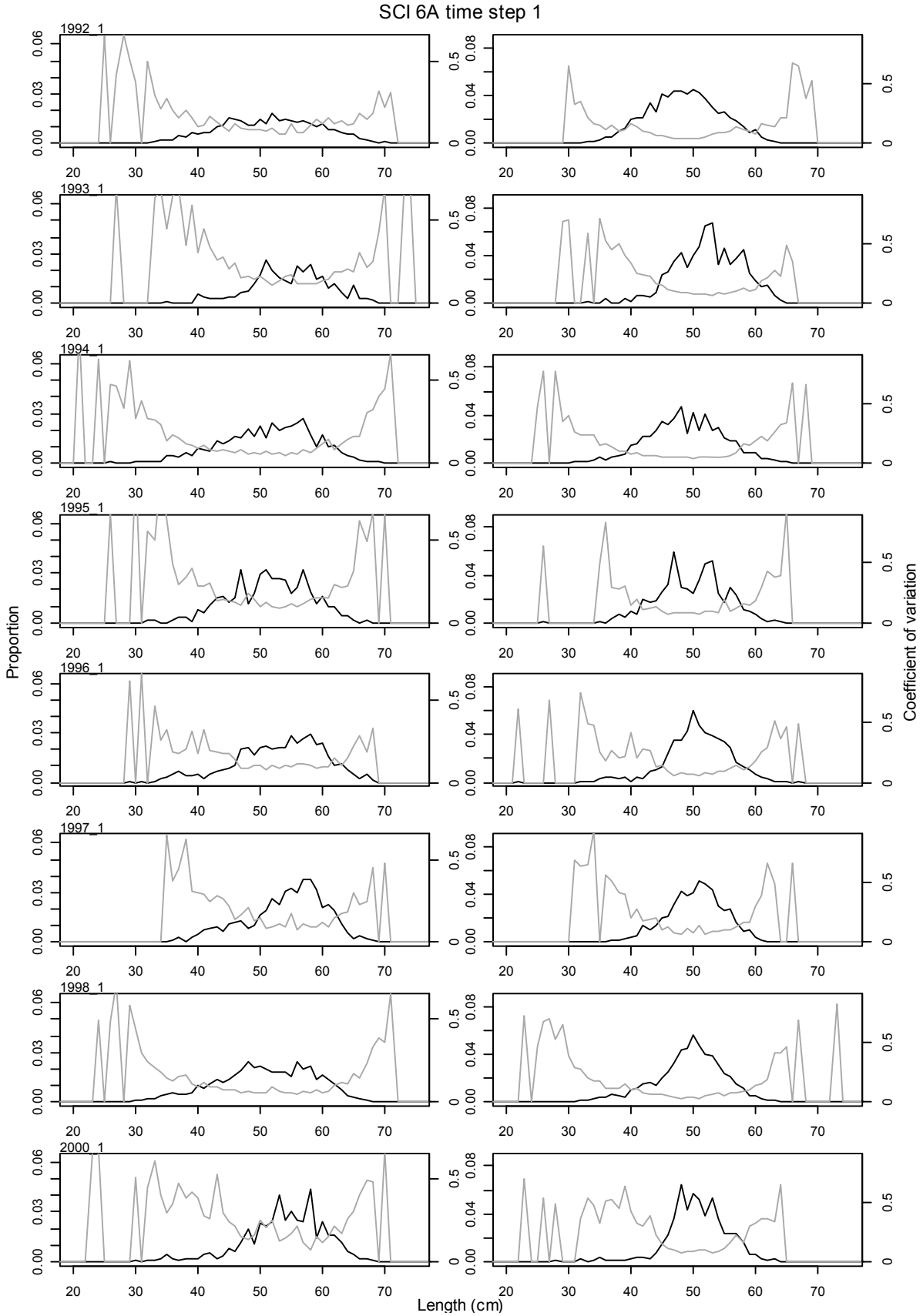

Figure 30: Proportional length frequencies (black line) and CVs (grey line) for commercial catches by model year and time step 1 for SCI 6A. Males plotted on left, females on right.

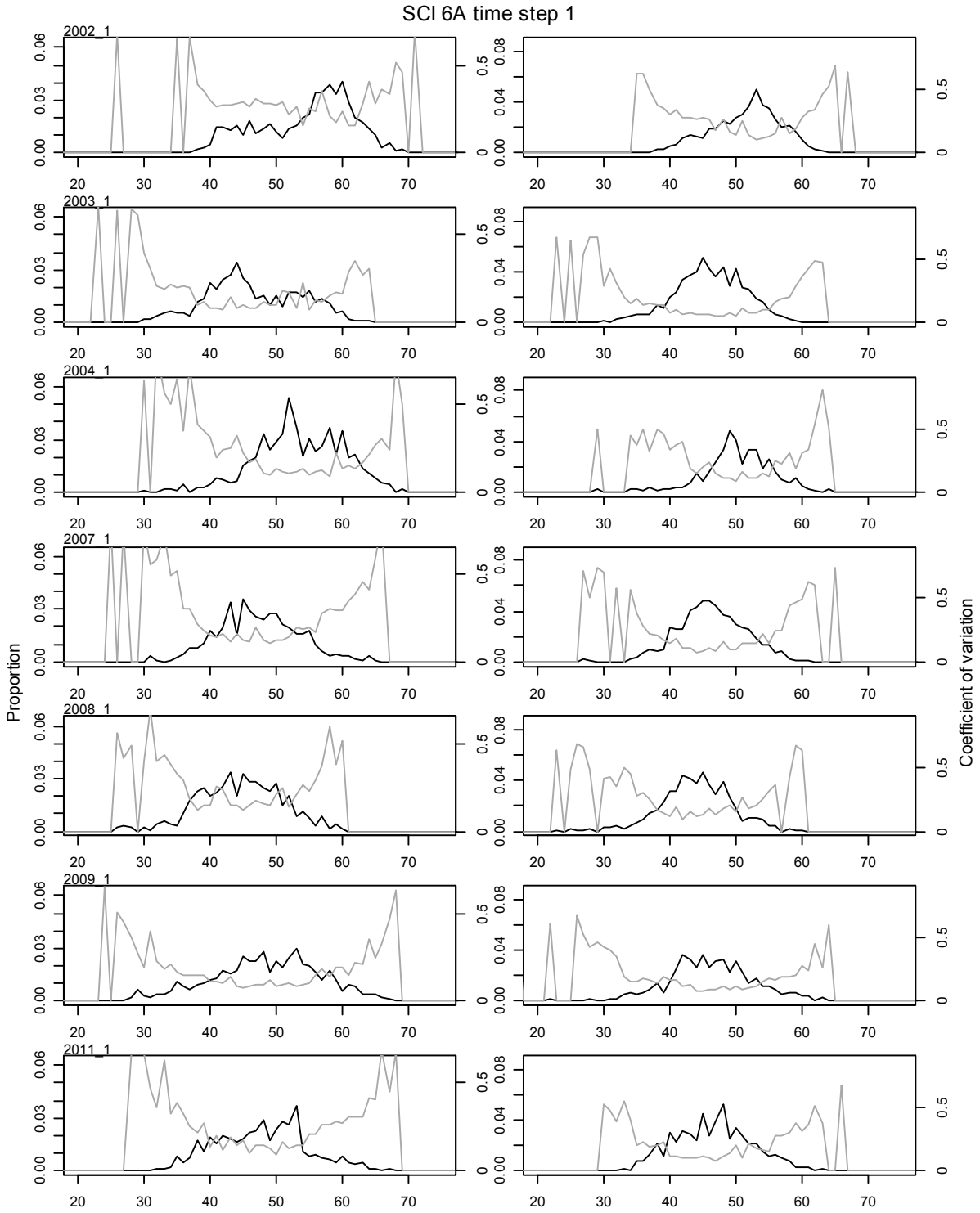

Figure 31: Proportional length frequencies (black line) and CVs (grey line) for commercial catches by model year and time step 1 (continued) for SCI 6A. Males plotted on left, females on right.

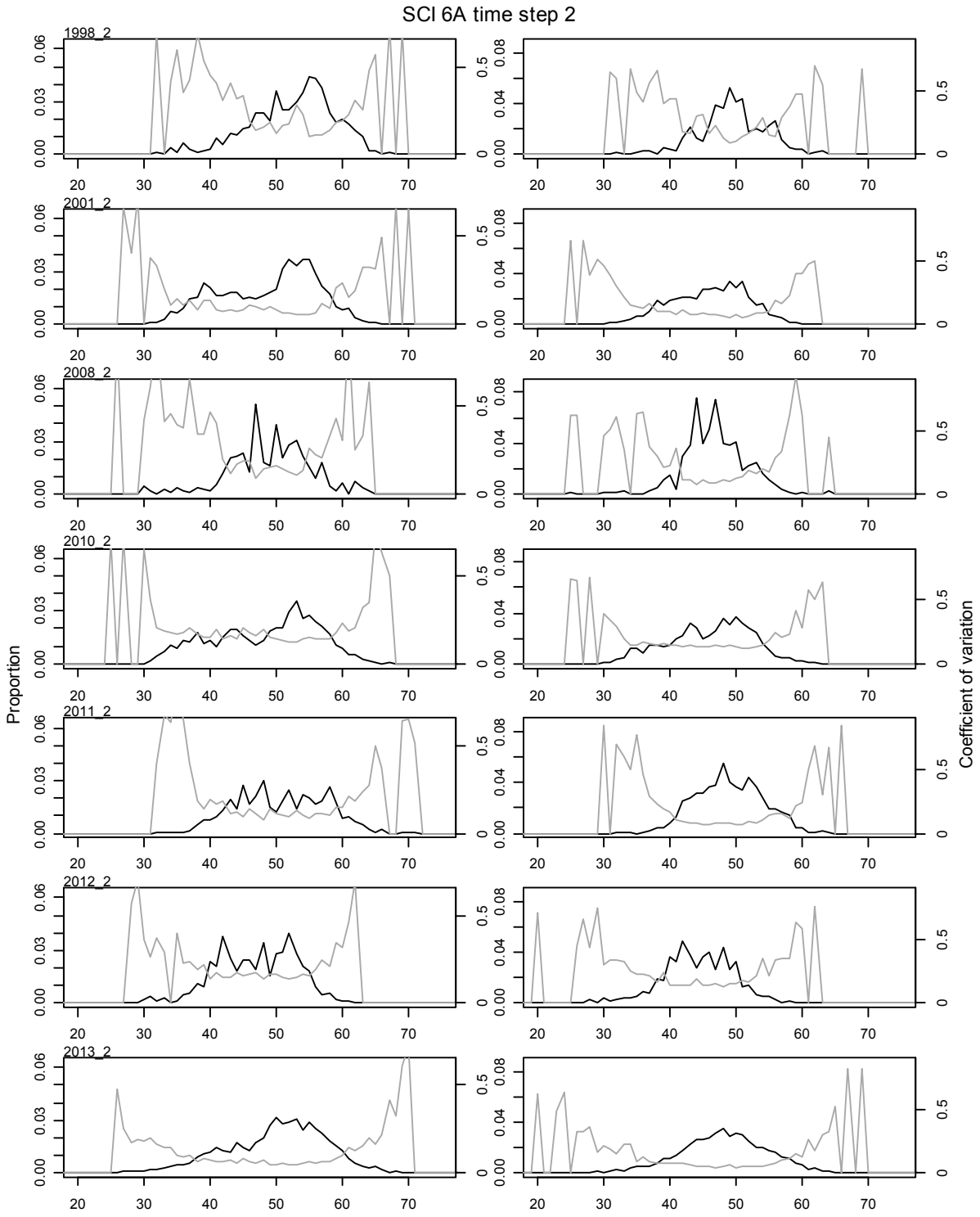

Figure 32: Proportional length frequencies (black line) and CVs (grey line) for commercial catches by model year and time step 2 for SCI 6A. Males plotted on left, females on right.

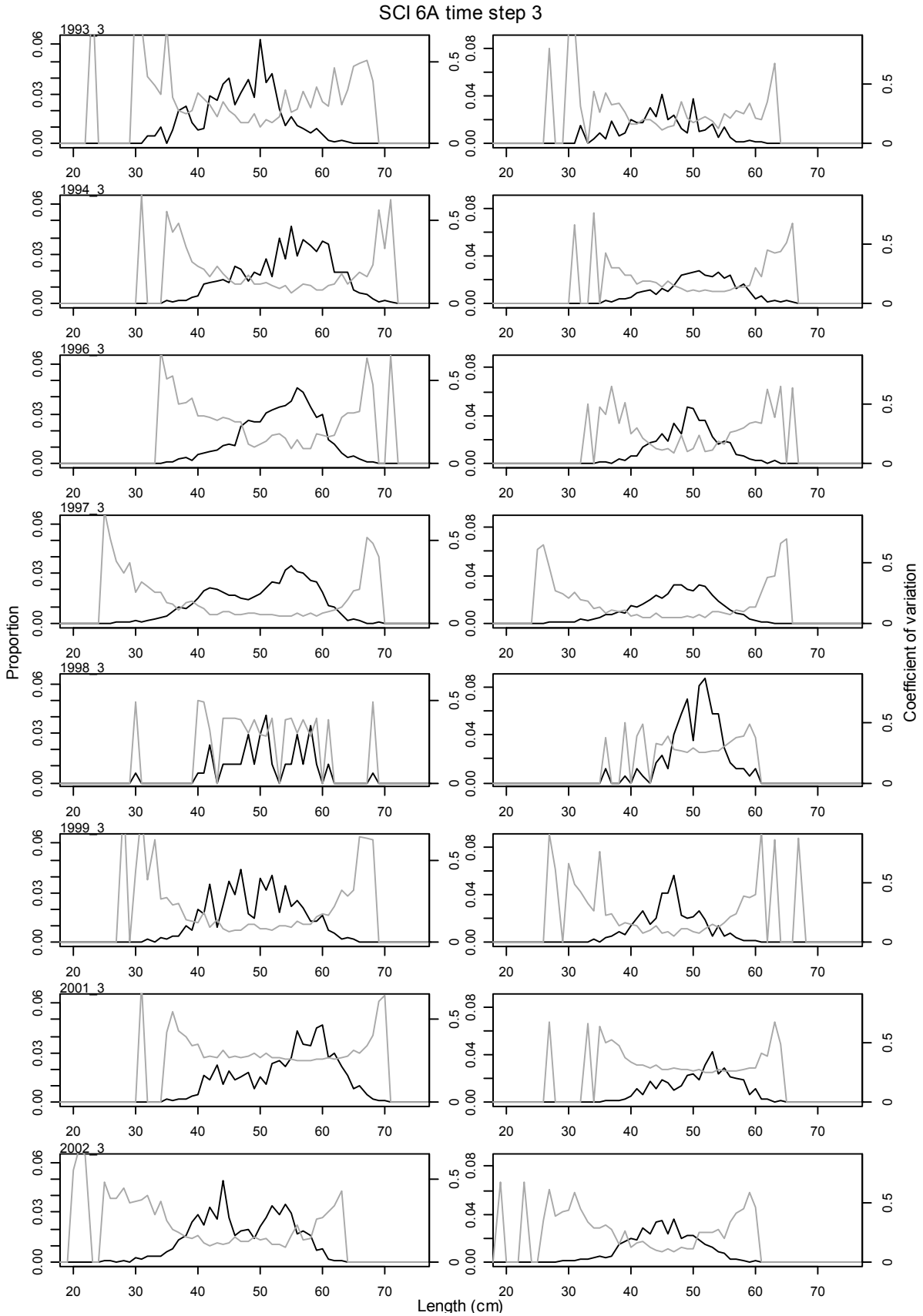

Figure 33: Proportional length frequencies (black line) and CVs (grey line) for commercial catches by model year and time step 3 for SCI 6A. Males plotted on left, females on right.

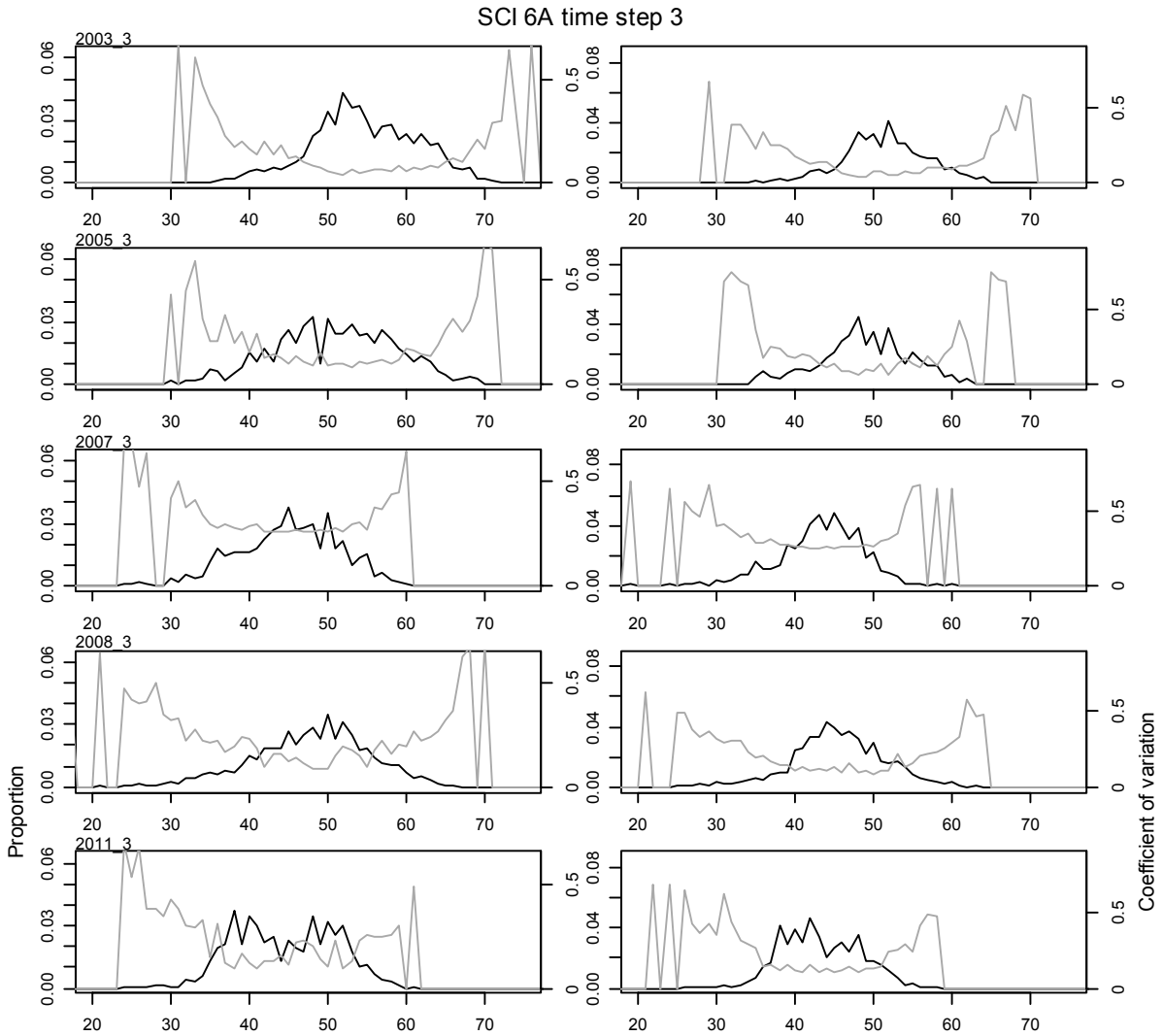

Figure 34: Proportional length frequencies (black line) and CVs (grey line) for commercial catches by model year and time step 3 (continued) for SCI 6A. Males plotted on left, females on right.

3.6.2 Trawl survey length distributions

Length frequency samples from research trawling have been taken by scientific staff on all surveys (Table 8). Estimates of the length frequency distributions (with associated CVs) were derived using the NIWA CALA software (Francis & Bian 2011), using 1 mm OCL (Orbital Carapace Length) length classes by sex, and are presented in Figure 35.

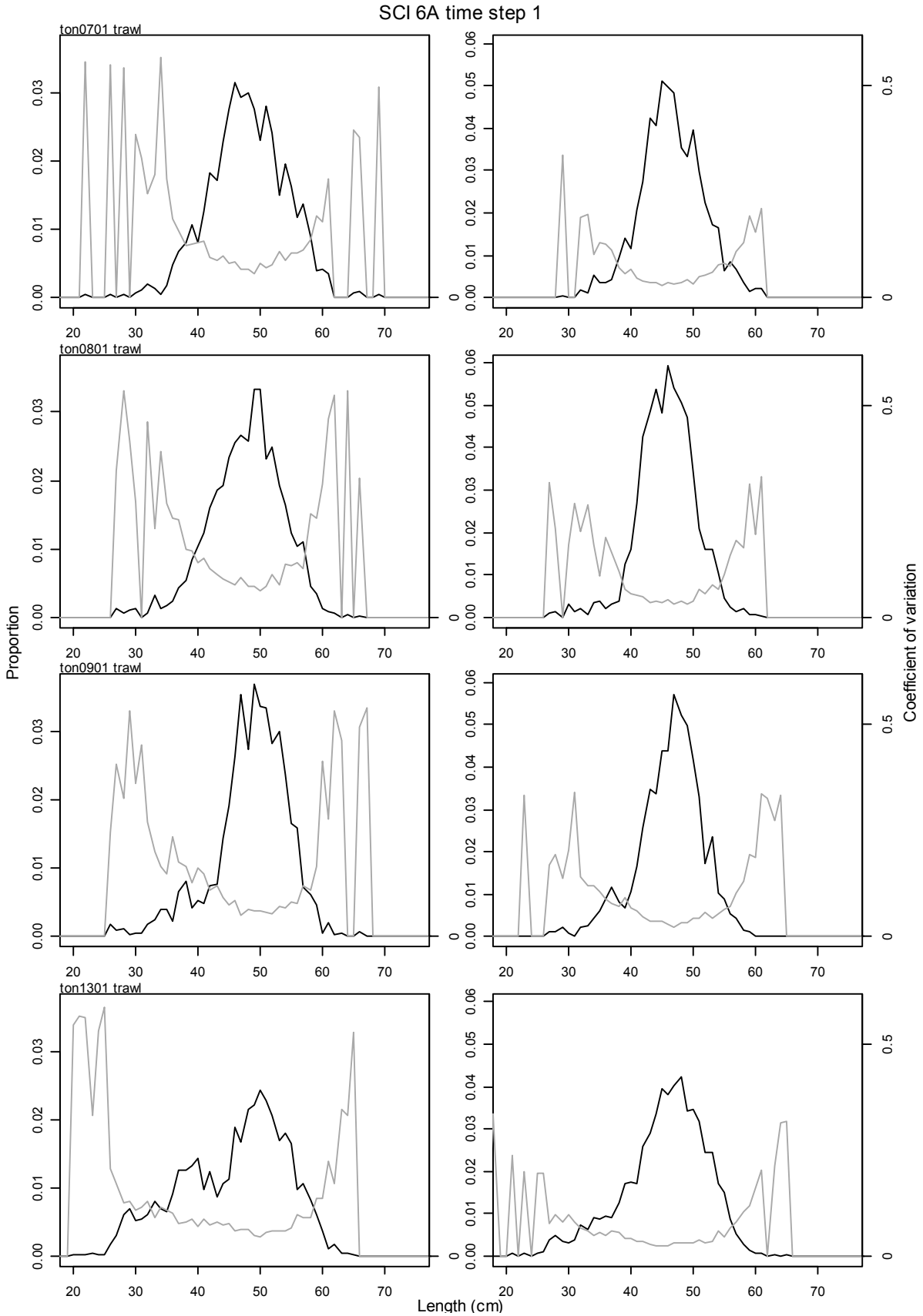

Figure 35: Proportional length frequencies (black line) and CVs (grey line) for research survey catches by model year for SCI 6A. Males plotted on left, females on right.

3.6.3 Photo survey length distributions

Length frequency distributions were estimated for the relative photographic abundance series, by measuring the abdomen width of those visible animals, and converting abdomen width to orbital carapace length. Abdomen width is a measure considered to be less affected by foreshortening, when scampi are not orientated perpendicular to the plane of the camera, which is typically the case when they sit in the entrances to their burrows.

As with other scampi (Tuck et al. 2000), the relationship between abdomen width and carapace length changes for *Metanephrops* females at maturity, with a wider abdomen providing more space to carry eggs on the pleopods (Figure 36).

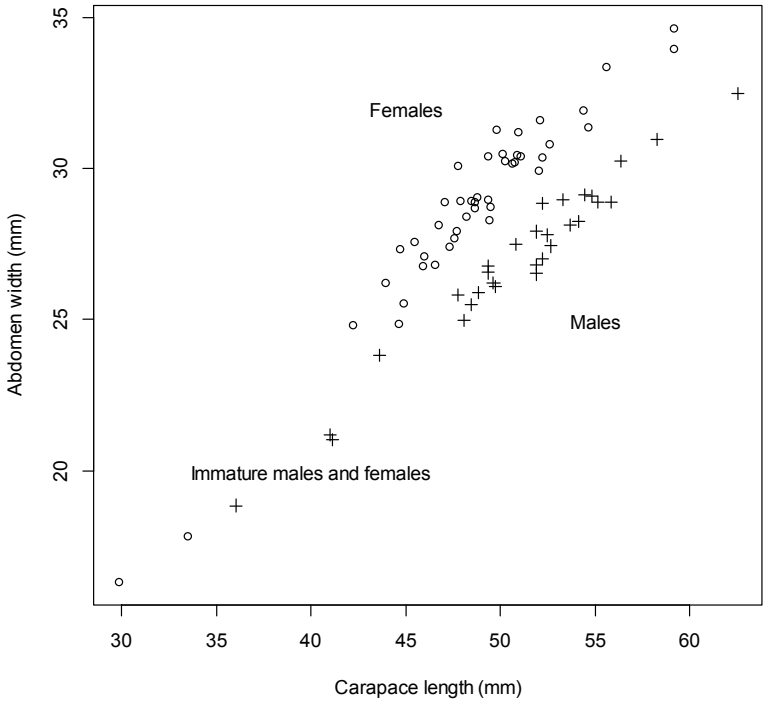

Figure 36: Relationship between abdomen width and carapace length for scampi in SCI 6A.

It is not possible to confidently determine scampi sex from the survey photographs, but the pattern in sex ratio in relation to length appears quite consistent between surveys (Figure 37). Using the data from the trawl surveys on the proportions by sex at length, and the relationship between carapace length and abdomen width for males (and immature females), maturing females, and mature females (Figure 38), the proportion of males by abdomen width increment can be estimated (Figure 39).

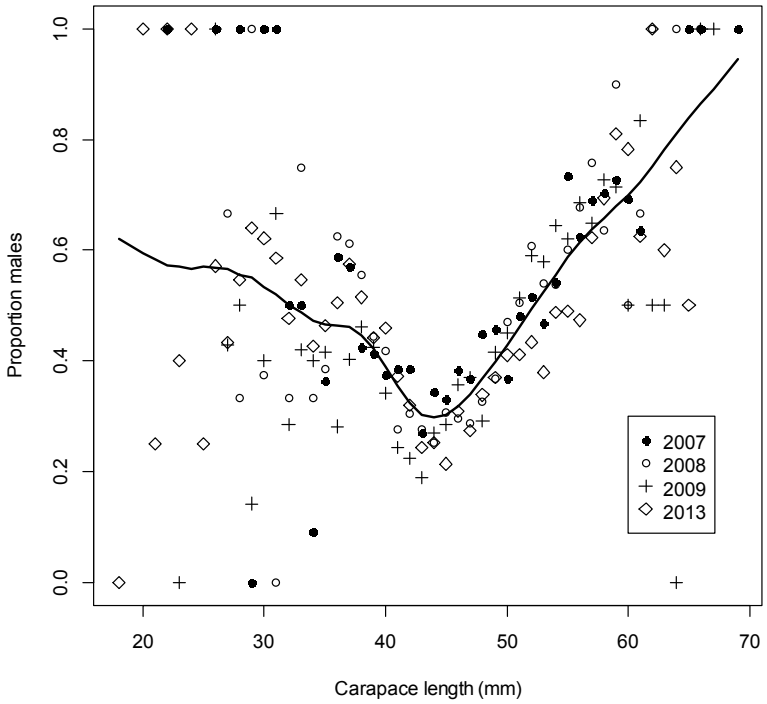

Figure 37: Plot of proportion of males in trawl survey catches against carapace length for each of the SCI 6A surveys, with an overall (lowess) smoother fitted through the data.

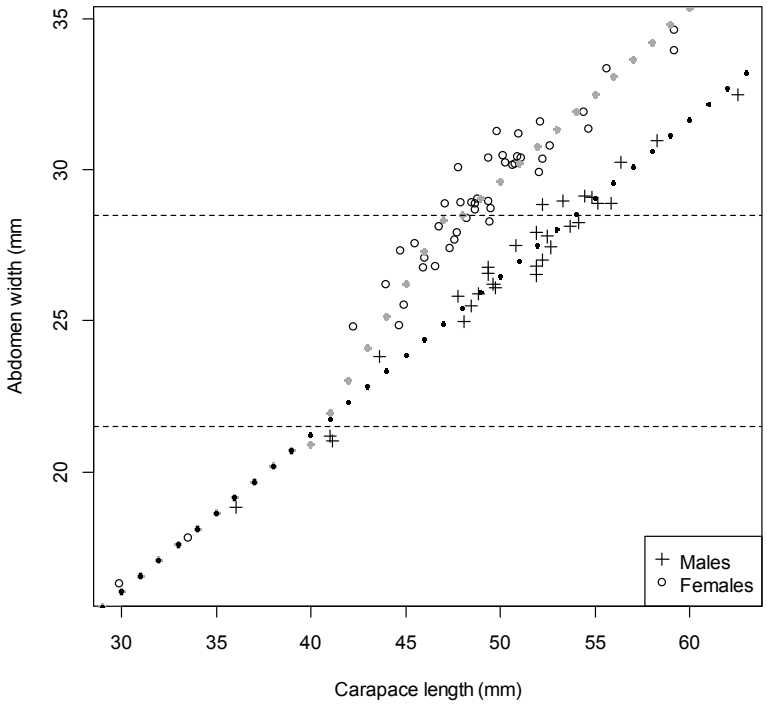

Figure 38: Relationship between abdomen width and carapace length for scampi in SCI 6A, with regression fits shown for different population components. Solid black symbols represent male regression. Solid grey symbols represent female regressions, with horizontal dashed lines representing transition range between immature and mature regressions.

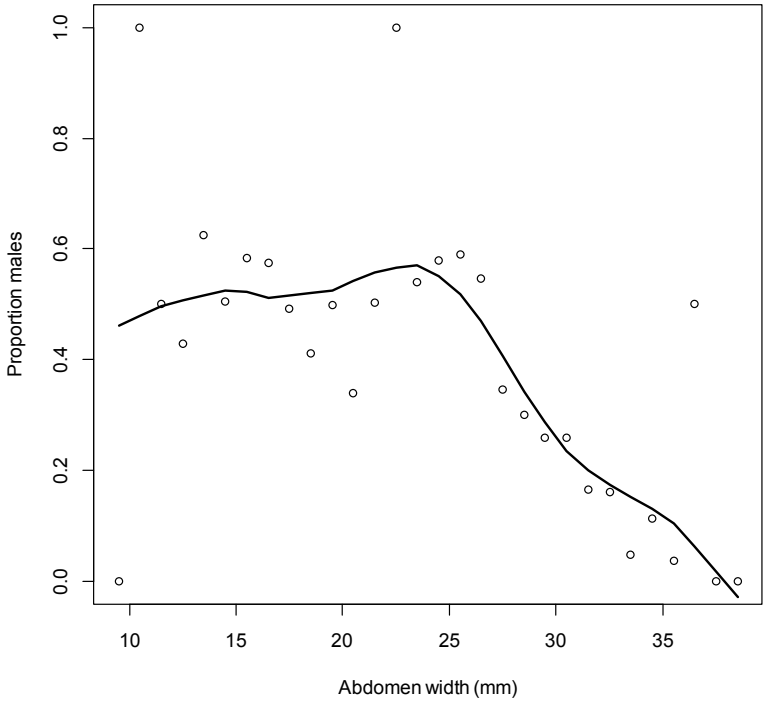

Figure 39: Overall plot of proportion of males in trawl survey catches against abdomen width for SCI 6A surveys, with an overall (lowess) smoother fitted through the data.

Each abdomen width measurement from each photographic survey was assigned a sex (on the basis of the probability observed in the trawl survey data (Figure 39), and then converted to a carapace length using the sex and abdomen width appropriate, abdomen width ~ carapace length relationship (Figure 38). To estimate the CVs at length for each year, we used a bootstrap procedure, resampling with replacement from the original observations. Compared with the length frequency distributions from trawl catches, this procedure gave very large CVs, but we think this is realistic given the uncertainties involved in generating a length frequency distribution from photographs, and converting from abdomen width to carapace length. Estimates of the length frequency distributions (with associated CVs) for visible scampi are presented in Figure 40.

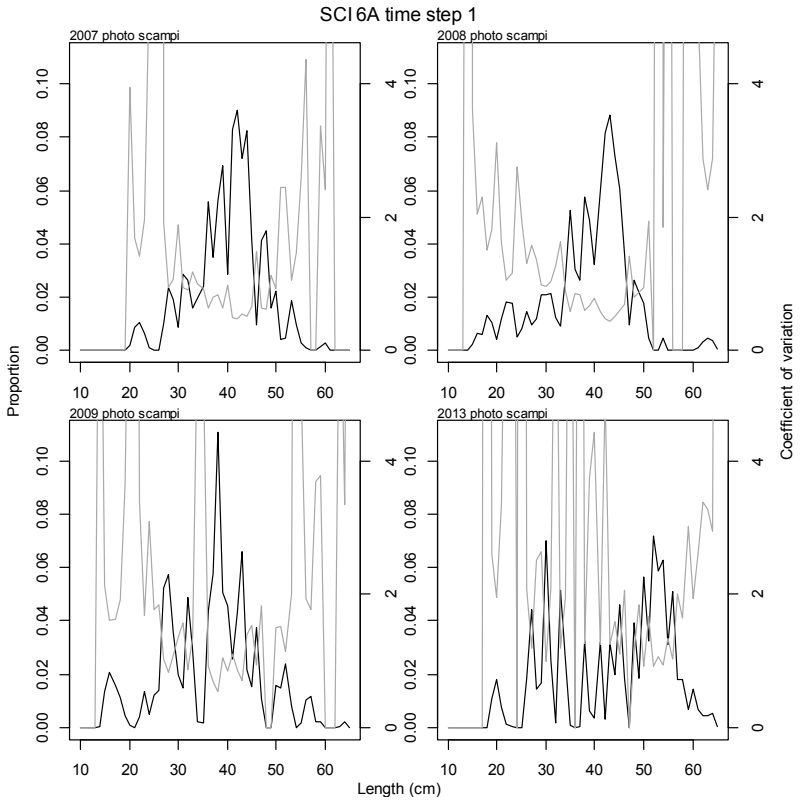

Figure 40: Proportional length frequencies (black line) and CVs (grey line) for photo survey observations of visible scampi by model year for SCI 6A.

3.7 Model assumptions and priors

Maximum Posterior Density (MPD) fits were found within CASAL using a quasi-Newton optimiser and the BETADIFF automatic differentiation package (Bull et al. 2008). Fitting was done inside the model except for the weighting of the abundance and length frequency data. For the length frequency data, observation-error CVs were estimated using CALA, converted to equivalent observation-error multinomial Ns, and used within the model. The appropriate multinomial Ns to account for both observation and process error were then calculated from the model residuals (method TA1.8), and these final Ns were used in all models reported (Francis 2011). This generally resulted in small Ns for the commercial length frequency data in particular, and therefore relatively low weighting within the model. For the CPUE indices, the approach proposed by Clark & Hare (2006), and recommended by Francis (2011) was applied, estimating the appropriate CV by fitting a smoother to the index. Process error for trawl and photo survey indices were estimated within the model. CASAL was also used to run Monte-Carlo Markov Chains (MCMC) on the base models. MPD output was analysed using the extract and plot utilities in the CASAL library running under the general analytical package R.

The initial model was based on that described previously (Tuck & Dunn 2009, 2012, Tuck 2014). The model inputs include catch data, abundance indices (CPUE, trawl and photo surveys) and associated length frequency distributions. The parameters estimated by the base model include SSB0 and R0, and time series of SSB and year class strength, selectivity parameters for commercial and research trawling, and the photo survey, and associated catchability coefficients. To reduce the number of fitted parameters, the catchability coefficients (q's) for commercial fishing, research trawling, and photographic surveys have previously been assumed to be "nuisance" rather than free parameters. At the request of the Working Group, models were also run with the qs as free parameters. The only informative priors used in the initial model were for q-Photo, q-Trawl, and the YCS vector (which constrains the variability of recruitment).

3.7.1 Scampi catchability

Previous priors for scampi catchability have been largely based on information on *Nephrops* emergence and occupancy rates from European studies conducted in far shallower waters than Metanephrops populations inhabit (Tuck & Dunn 2012), but the acoustic tagging study conducted at the Mernoo Bank in October 2010 offered an opportunity to estimate priors for occupancy and emergence from New Zealand data (Tuck 2013). Acoustic tagging was repeated successfully within the SCI 1 and SCI 2 surveys in 2012, and was also conducted within the SCI 6A survey in 2013 (although less successfully). The data collected within these studies have been used to estimate catchability priors (Tuck et al. 2015).

Acoustic tags were fitted to scampi, and released with a moored hydrophone which recorded tag detections, when animals were emerged from burrows. Data were recorded over a period of up to 21 days (Tuck et al. 2015). Some tag detections showed distinct cyclical patterns (12.6 hour cycle), but most animals showed no clear patterns, and the proportion of scampi detectable over the duration of the studies varied from 40 to 86% (2.5th to 97.5th percentile of range), with a median detection of 66%. On the basis of shallow water trials with the acoustic tags, and scampi observations, it is assumed that these detections include scampi in burrow entrances and scampi walking free on the seabed (all of which would be visible to the photographic survey). Estimates of the density of major burrow openings, all visible scampi and scampi out of burrows are available from the surveys conducted in March / April 2013 (at the time of the emergence study). An estimate of scampi density is provided by dividing the density of visible scampi by emergence.

Priors for three q terms have been estimated (Table 11). The best estimate for each q term is based on the median estimate of emergence, while the upper and lower estimates are based on the 2.5th and 97.5th percentiles of the distribution of emergence values. The 2.5th, median and 97.5th percentiles of the estimated scampi density distribution are calculated by dividing the density of visible scampi by the emergence. This estimated density is used to calculate the priors.

3.7.2 Priors for qs

q-Photo

This is the proportion of the scampi population represented by the count of major burrow openings. The best estimate is 3.721 (major burrow openings divided by estimated scampi density). Upper and lower estimates are taken as the 2.5th and 97.5th percentiles of the distribution.

q-Trawl

This is the proportion of the scampi population represented by the trawl survey catches. The best estimate is 0.36 (scampi out of burrows divided by estimated scampi density). Upper and lower estimates are taken as the 2.5th and 97.5th percentiles of the distribution.

q-Scampi

This is the proportion of the scampi population represented by the count of visible scampi. The best estimate is 0.66 (scampi out of burrows divided by estimated scampi density). Upper and lower estimates are taken as the 2.5th and 97.5th percentiles of the distribution.

3.7.3 Estimation of prior distributions

The bounds and best estimate were assumed to represent the 2.5th, 50th and 97.5th percentiles of the prior distribution. These values were fitted within a binomial GLM (probit link) to estimate the slope and intercept of the cfd, which in turn were used to estimate the mean and standard deviation of the lognormal distribution of the prior. The distributions of the priors are presented in Figure 41. The distributions of the priors are somewhat different to those used in the SCI 1 assessment (Tuck 2014),

reflecting the lower proportion of the SCI 6A scampi population that appear to be associated with burrows than in other areas (Tuck et al. 2015).

Table 11: Component factors for estimation of priors for q-Scampi, q-Photo, and q-Trawl.

	SCI 6A			Source
	lower	best	upper	
Major opening	0.039	0.039	0.039	Survey
Visible scampi	0.007	0.007	0.007	Survey
Scampi "out"	0.004	0.004	0.004	Survey
Scampi as % of openings		18%		Visible/openings
% of scampi "out"		55%		Out/visible
Emergence	40%	66%	86%	Acoustic tags
Est. scampi density	0.017	0.010	0.008	Visible/emergence
Est. occupancy	44%	27%	21%	Est. den./major
q_Trawl	0.220	0.363	0.474	Out/Est. den.
q_scampi	0.400	0.660	0.860	Vis/Est. den.
q_photo	2.255	3.721	4.848	Major/Est. den.

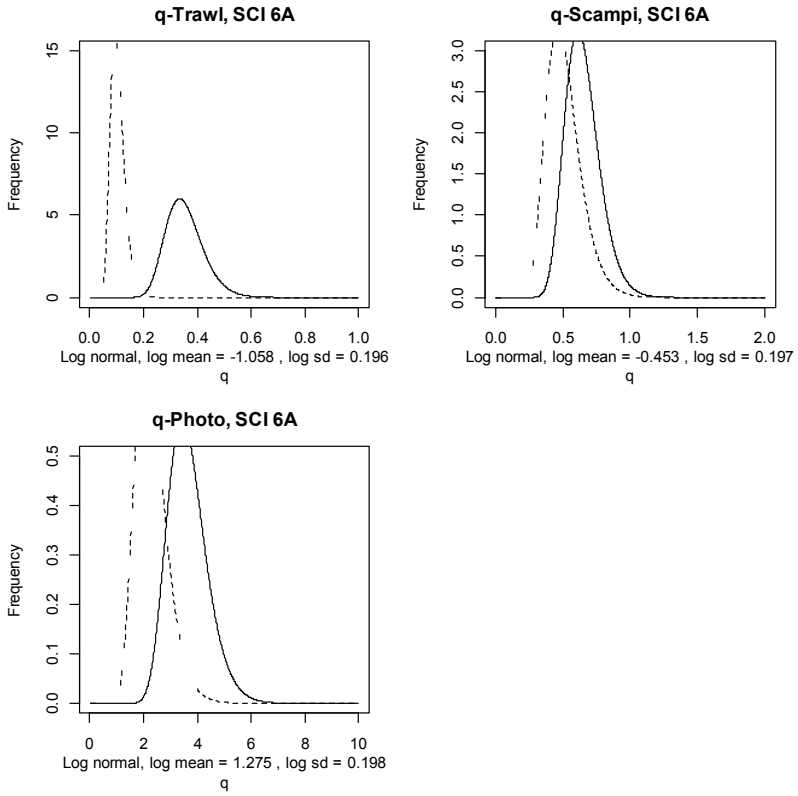

Figure 41: Estimated distribution of *q-Trawl*, *q-Scampi* and *q-Photo* for SCI 6A. Dashed lines represent prior distributions used in SCI 1 assessment for comparison (Tuck 2014).

3.7.4 Recruitment

Few data are available on scampi recruitment. Relative year class strengths were fixed at 1 for the two most recent years, and were assumed to average 1.0 over all other years. In the initial model development (Cryer et al. 2005) lognormal priors on relative year class strengths were assumed, with mean 1.0 and CV of 0.2, and the sensitivity of year class strength (YCS) variation was examined in further developments (Tuck & Dunn 2006). More recent model investigations, particularly those

fitting the CPUE indices, suggest that the constraint on variability in YCS may be too severe, and the SFAWG suggested increasing the CV (Tuck & Dunn 2012). In the current implementation, lognormal priors on relative year class strengths were assumed, with mean 1.0 and CV of 1.0. The relationship between stock size and recruitment for scampi is unknown, and a Beverton Holt relationship with a steepness of 0.8 has been assumed. New Zealand scampi have very low fecundity (Wear 1976, Fenaughty 1989) (in the order of tens to hundreds of eggs carried by each female), so very successful recruitment is probably not plausible at low abundance. Recruitment enters the model partition as a year class, with a normally distributed OCL of mean 10 mm and CV of 0.4.

4. ASSESSMENT MODEL RESULTS

4.1 Initial models

As described in Section 3.1, a single area model was applied, with an annual CPUE index, and photo and trawl survey indices. Preliminary models did not suggest that the model was sensitive to the CV for the CPUE index, and so all models were run with CPUE CV fixed at 0.15. M was estimated within the model, but given the difficulties in obtaining values that were considered to be realistic in previous assessments, sensitivity to M was also examined using values of 0.2, 0.25 and 0.3. The sensitivity of the model to estimating catchability terms as free parameters was also examined. Details of differences between models examined within sensitivity analyses are presented in Table 12. Key parameter and quantity estimates from the MPD fits for the models described in Table 13, and stock and recruitment trajectories for some models (those with catchability estimated as free parameters, and N_0.25) are presented in Figure 42.

Table 12: General details of models examined within sensitivity analyses for SCI 6A.

Model	M	Catchability
F_0.2	0.2	Free
F_0.25	0.25	Free
F_0.3	0.3	Free
F_est	estimated	Free
N_0.2	0.2	Nuisance
N_0.25	0.25	Nuisance
N_0.3	0.3	Nuisance
N_est	estimated	Nuisance

There was little difference between models in terms of fits to observed data. All the models showed an increase in biomass at the start of the series, with a fluctuating decline over time, with the SSB_{2013} just over 50% SSB_0 (Figure 42). With M fixed at 0.2, the magnitude of the fluctuations in the SSB were smaller, and recruitment peaks were estimated one year earlier (because growth was estimated to be slower). For the models where M was not fixed, it was estimated at 0.35 (F_est) and 0.31 (N_est). The models with the catchabilities estimated as nuisance parameters tended to estimate slightly higher SSB than the free parameter models, with the difference particularly apparent in the peak in biomass in the late 1980s (Figure 42, only N_0.25 shown, but other nuisance models showing a similar pattern). Across the eight models examined, estimates of SSB_0 varied from 5707 to 6884 tonnes, and although stock trajectories varied between models over the history of the fishery (Figure 42), the estimates of SSB_{2013}/SSB_0 were very consistent (between 50 and 55% SSB_0). Patterns in YCS were very similar between the models, with all models estimating large recruitments in the mid 1980s, early 1990s, and early 2000s.

Table 13: Estimated key parameters and quantities from MPD fits for SCI 6A sensitivity model runs.

		F_0.2	F_0.25	F_0.3	F_est	N_0.2	N_0.25	N_0.3	N_est
M		0.2	0.25	0.3	0.35	0.2	0.25	0.3	0.31
CPUE-Commercialq		0.0004	0.0005	0.0005	0.0007	0.0003	0.0003	0.0004	0.0004
TrawlSurveyq		0.35	0.36	0.36	0.37	0.34	0.33	0.34	0.35
PhotoSurvey_animals_q		0.38	0.39	0.37	0.35	0.41	0.38	0.36	0.36
initialization.B0		6181	5761	5859	5707	5972	6884	5985	5882
TrawlSurvey.cv_p_error		0.22	0.24	0.27	0.28	0.25	0.27	0.27	0.28
PhotoSurvey.cv_p_error		0.15	0.12	0.00	0.00	0.00	0.00	0.00	0.00
maturity_props.all	a50	36.69	36.69	36.69	36.69	36.69	36.69	36.69	36.69
	a to 95	7.16	7.16	7.15	7.15	7.16	7.16	7.16	7.16
selectivity.shift_a		0.06	0.06	0.05	0.04	0.06	0.06	0.04	0.04
selectivity[Fishing_1]	a50	46.33	49.36	50.41	52.13	44.87	44.81	47.44	48.40
	a to 95	12.37	14.53	14.49	14.44	12.21	12.02	13.02	13.30
	amax M	0.72	0.74	0.75	0.78	0.72	0.75	0.76	0.77
	amax F	1.00	1.00	1.00	1.00	1.00	1.00	1.00	1.00
selectivity[Fishing_2]	a50	42.35	43.03	44.14	46.72	40.28	40.85	43.58	44.52
	a to 95	12.25	12.76	12.92	13.59	11.09	11.34	12.50	12.84
	amax M	1.00	1.05	1.08	1.12	0.99	1.02	1.05	1.07
	amax F	1.00	1.00	1.00	1.00	1.00	1.00	1.00	1.00
selectivity[Fishing_3]	a50	47.11	49.31	51.09	53.69	45.20	46.87	51.00	52.27
	a to 95	14.20	14.96	15.06	15.10	13.34	14.58	15.82	15.99
	amax M	1.40	1.43	1.45	1.48	1.37	1.40	1.43	1.45
	amax F	1.00	1.00	1.00	1.00	1.00	1.00	1.00	1.00
selectivity[TrawlSurvey]	a50	40.31	40.62	41.38	42.62	39.22	39.78	41.13	41.61
	a to 95	12.30	12.63	12.91	12.86	12.47	13.10	13.04	13.05
	amax M	0.78	0.82	0.84	0.88	0.75	0.76	0.81	0.83
	amax F	1.00	1.00	1.00	1.00	1.00	1.00	1.00	1.00
selectivity[Scampi_out]	a1	38.41	38.70	39.12	40.28	37.99	38.27	38.71	39.04
	aL	16.04	19.47	19.44	18.14	18.98	21.74	19.41	18.62
	aR	16.06	16.59	16.42	17.51	15.08	14.61	15.78	16.15
growth[1].g_male	g20	8.29	9.51	9.77	9.80	8.98	10.12	10.13	10.03
	g45	1.20	1.38	1.49	1.59	1.26	1.43	1.53	1.54
growth[1].g_female	g20	9.54	11.57	12.22	12.64	10.09	11.83	12.36	12.43
	g45	0.00	0.00	0.00	0.00	0.00	0.00	0.00	0.00
growth[1].minsigma_male		3.82	4.27	4.47	4.55	3.92	4.34	4.49	4.51

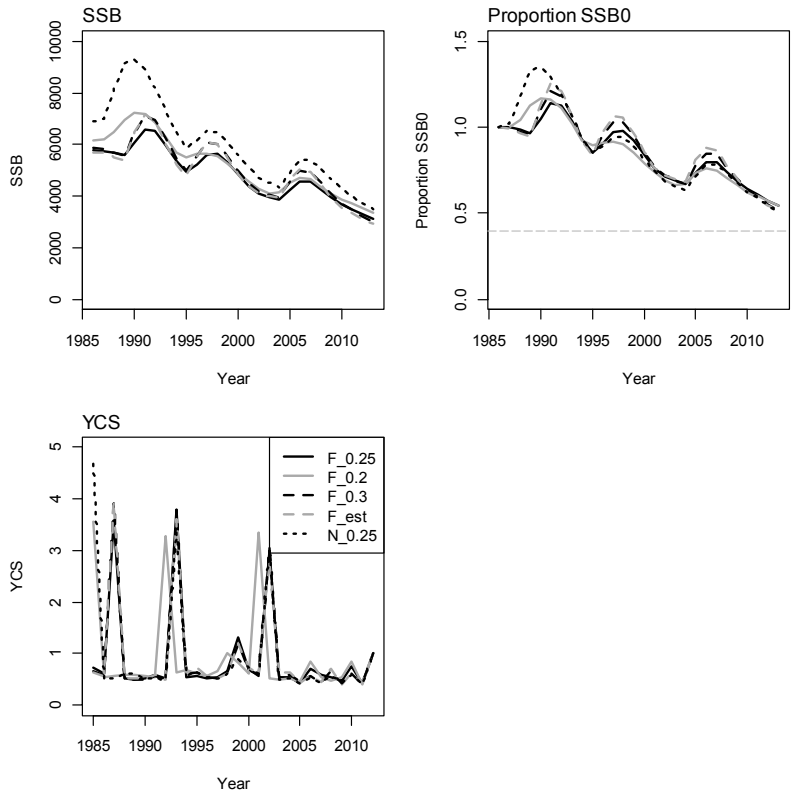

Figure 42: Plots of SSB, SSB as a proportion of SSB_0, and year class strength (YCS) for MPD fits to the SCI 6A sensitivity model runs.

4.2 Base models

On the basis of presentation of the sensitivity runs to the SFAWG, models with M fixed at 0.2, 0.25 and 0.3, with catchability estimated as a free parameter, were examined further. The model with M fixed at 0.25 with catchability estimated as a nuisance parameter was also examined for comparison. Various model output plots and diagnostics are presented as an Appendix for each model.

Model outputs and MCMC diagnostics were very similar for each of the three models with catchability estimated as a free parameter, and the Working Group concluded that the MCMCs provided sufficient evidence of lack of convergence to be unacceptable for management. Therefore, only the catchability free and catchability nuisance parameter models for M = 0.25 are presented in detail below, with the other models examined (F_0.2 and F_0.3) presented as Appendices 3 and 5, respectively.

4.2.1 M fixed at 0.25, free catchability (F_0.25)

The outputs and diagnostics for the F_0.25 model (M = 0.25, free catchability) are presented in Appendix 4. The estimated SSB_0 was 5761 t, with SSB_{2013} 3127 t, 54% of SSB_0. Fits to the abundance indices and normalised residuals (A4. 1), show that the model fitted the observed fluctuations in CPUE since the mid 1990s reasonably well, but simply estimated a steady decline in recent years for the trawl and photographic surveys, and did not match the observed pattern as well. SSB is estimated to have fluctuated around a declining trend over the time series (A4. 2). Strong year class strengths were estimated in 1987, 1993 and 2002, with periods of low recruitment between these peaks. Estimated selectivity curves (A4. 3) matched observed changes in sex ratio between time steps, with males less available to trawling during time step 1, and more available in time step 3. MPD estimates of trawl and photo survey catchability were within the prior distribution (A4. 4). Fits to the observer length frequencies were variable (A4. 5 – A4. 7), with the data weighting giving observer length

frequency samples low effective sample size (A4. 8 – A4. 10), while fits to the trawl survey length frequencies were generally better (A4. 13), and effective sample size larger (A4. 15). Sample sizes for photo survey length frequencies were low, with high CVs, but the model estimated the overall shape of the length distribution reasonably well (A4. 18).

The likelihood profile when B_0 is fixed shows a minimum at just under 6000 t (A4. 19), although it is relatively flat in this region of the curve, and some fits failed to converge. The various data sets do not provide any consistent signal, and none are particularly informative, other than suggesting that the SSB_0 is greater than about 4000 t, except the CPUE index, which prefers a smaller SSB_0.

MCMC runs

Three independent MCMC chains were started a random step away from the MPD for the model, and run for 3 million simulations, with every two thousandth sample saved, giving a set of 1500 samples, from which the first 500 were excluded as a burn in. The three chains were examined for evidence of lack of convergence (A4. 20 – A4. 21), and concatenated and systematically thinned to produce a 3000 sample chain for projections. While there was considerable evidence that the individual chains had not converged (A4. 20), the distributions for SSB_0, SSB_{2013} and SSB_{2013}/SSB_0 were reasonably similar (A4. 21). Posterior distributions of trawl and photo survey catchability were within the prior distribution (A4. 22), with the MPD estimates also located within the posterior distributions. The posterior trajectory of SSB (Figure 43) suggests a fluctuating decline from about 1991 to 2013, with more stable periods or slight increases in SSB within this period. The median estimate of current status (SSB_{2013}/SSB_0) is 56%, with 0% probability that SSB_{2013} is below 40% SSB_0.

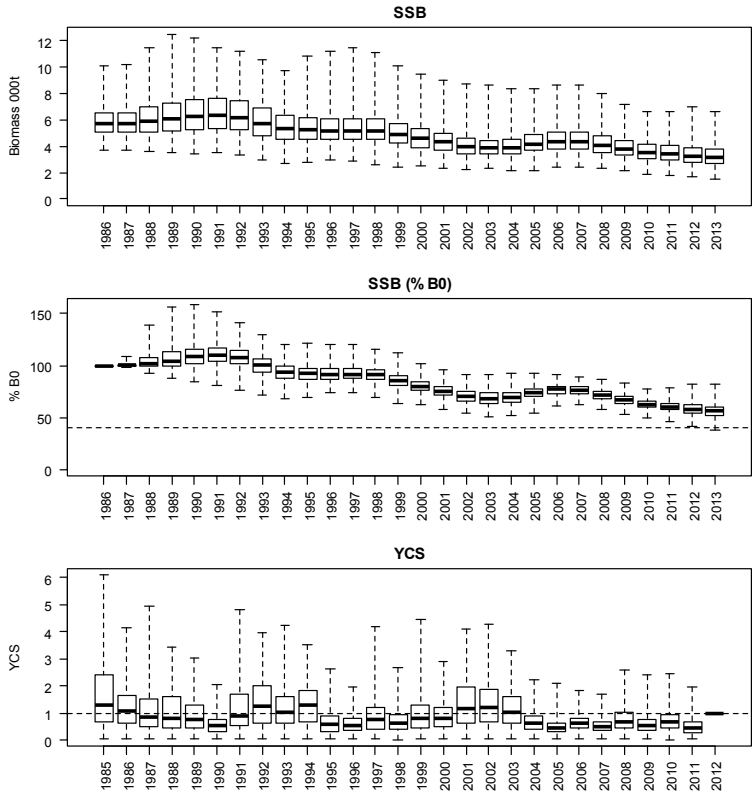

Figure 43: Posterior trajectory of SSB, SSB_{2013}/B_0 and YCS for model F_0.25.

4.2.2 M fixed at 0.25, nuisance catchability (N_0.25)

The outputs and diagnostics for the N_0.25 model (M = 0.25, nuisance catchability) are presented in Appendix 6. The estimated SSB_0 was 6884 t, with SSB_{2013} 3513 t, 51% of SSB_0. Fits to the abundance

indices and normalised residuals (A6. 1), show that the model fitted the observed fluctuations in CPUE slightly better than the F_0.25 model, but as with the other model, simply estimated a steady decline in recent years for the trawl (in particular) and photographic surveys, and did not match the observed pattern as well. SSB is estimated to have fluctuated around a declining trend over the time series (A6. 2). Strong year class strengths were estimated in 1985, 1993 and 2002, with periods of low recruitment between these peaks. Estimated selectivity curves (A6. 3) matched observed changes in sex ratio between time steps, with males less available to trawling during time step 1, and more available in time step 3. MPD estimates of trawl and photo survey catchability were within the prior distribution (A6. 4). As with the F_0.25 model, fits to the observer length frequencies were variable (A6. 5 – A6. 7), with the data weighting giving observer length frequency samples low effective sample size (A6. 8 – A6. 10), while fits to the trawl survey length frequencies were better (A6. 13), and effective sample size larger (A6. 15). Sample sizes for photo survey length frequencies were low, with high CVs, but the model estimated the overall shape of the length distribution reasonably well (A6. 18).

The likelihood profile when B_0 is fixed shows a minimum at just under 7000 t (A6. 19), although the overall likelihood is relatively flat in this region of the curve. The various data sets appear slightly more consistent than the F_0.25 model, but none are particularly informative, other than suggesting that the SSB_0 is greater than about 4000 t, except the CPUE index, which prefers a smaller SSB_0.

MCMC runs

Three independent MCMC chains were started a random step away from the MPD for the model, and run for 3 million simulations, with every two thousandth sample saved, giving a set of 1500 samples, from which the first 500 were excluded as a burn in. The three chains were examined for evidence of lack of convergence (A6. 20 – A6. 21), and concatenated and systematically thinned to produce a 3000 sample chain for projections. The individual chains appeared to be reasonably consistent (A6. 20), and the distributions for SSB_0, SSB_{2013} and SSB_{2013}/SSB_0 were very similar (A6. 21), providing no evidence for lack of convergence. Posterior distributions of trawl and photo survey catchability were within the prior distribution (A6. 22), with the MPD estimates also located within the posterior distributions. The posterior trajectory of SSB (Figure 44) suggests a fluctuating decline from about 1991 to 2013, with more stable periods or slight increases in SSB within this period. The median estimate of current status (SSB_{2013}/SSB_0) is 56%, with 0% probability that SSB_{2013} is below 40% SSB_0.

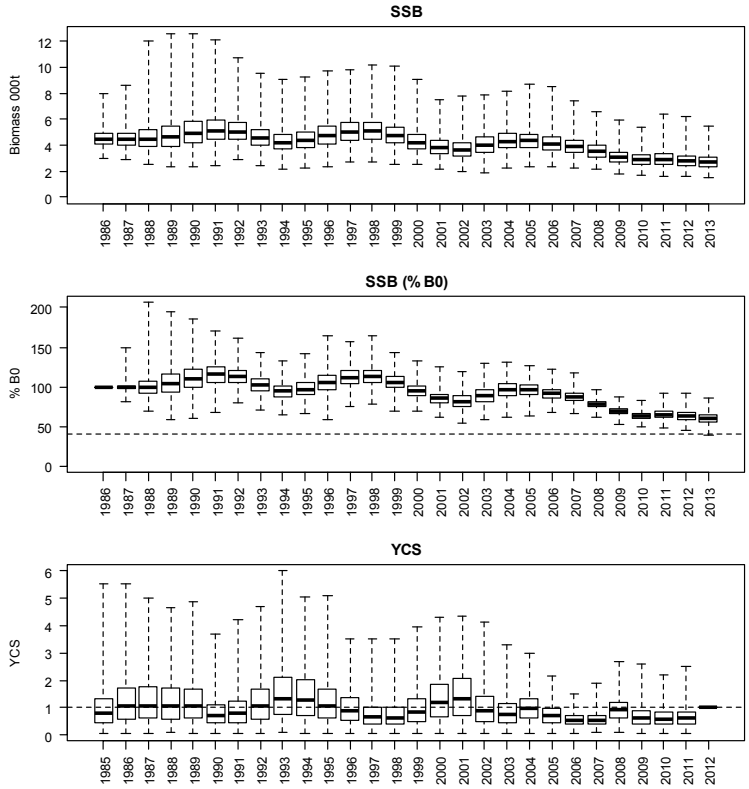

Figure 44: Posterior trajectory of SSB, SSB_{2013}/B_0 and YCS for model N_0.25.

4.3 Projections

Given the evidence of lack of convergence in the models with catchability as free parameters, these models were considered unacceptable for management. The Working Group did not consider the use of catchability as nuisance parameters to be appropriate, and so those models were considered unacceptable for management. However, given the relative consistency between the models in terms of stock trajectory, and estimated level of depletion, it was considered informative to examine the stock projections.

The assessments reported SSB_0 and $SSB_{current}$ and used the ratio of current and projected SSB to SSB_0 as preferred indicators. Projections were conducted up to 2019 on the basis of a range of catch scenarios (between current landings and current TACC of 306 t) (Table 14). Projections have been conducted by randomly resampling year class strengths from the last decade estimated within the model (2002 – 2011). The probability of exceeding the default Harvest Strategy Standard target and limit reference points are reported (Table 15).

For all models examined, future catches up to the TACC (306 tonnes) are predicted to reduce the SSB relative to SSB_{2013}, but remain above 40% SSB_0 (the most pessimistic prediction giving a 70% probability of SSB exceeding 40% SSB_0 by 2019). Projected stock trajectories are shown for models F_0.25 and N_0.25 in Figure 45 and Figure 46, respectively.

Table 14: Results from MCMC runs showing B_0, B_{curr}, B_{2017} and B_{2019} estimates at varying catch levels for SCI 6A.

	Model	F_0.2	F_0.25	F_0.3	N_0.25
	M	0.2	0.25	0.3	0.25
	B_0	5502	5678	5391	6113
	B_{curr}	3508	3149	3264	3410
	B_{curr}/B_0	0.64	0.56	0.61	0.56
160 tonnes (current landings)	B_{2017}/B_0	0.59	0.57	0.55	0.56
	B_{2017}/B_{curr}	0.93	0.91	0.90	0.89
	B_{2019}/B_0	0.58	0.57	0.56	0.55
	B_{2019}/B_{curr}	0.91	0.91	0.92	0.89
200 tonnes	B_{2017}/B_0	0.57	0.55	0.53	0.54
	B_{2017}/B_{curr}	0.90	0.88	0.87	0.87
	B_{2019}/B_0	0.56	0.54	0.54	0.53
	B_{2019}/B_{curr}	0.87	0.87	0.88	0.85
250 tonnes	B_{2017}/B_0	0.55	0.53	0.51	0.52
	B_{2017}/B_{curr}	0.86	0.85	0.84	0.83
	B_{2019}/B_0	0.52	0.51	0.51	0.5
	B_{2019}/B_{curr}	0.82	0.82	0.83	0.81
306 tonnes (TACC)	B_{2017}/B_0	0.52	0.50	0.49	0.5
	B_{2017}/B_{curr}	0.82	0.81	0.80	0.79
	B_{2019}/B_0	0.48	0.48	0.48	0.47
	B_{2019}/B_{curr}	0.75	0.76	0.78	0.75

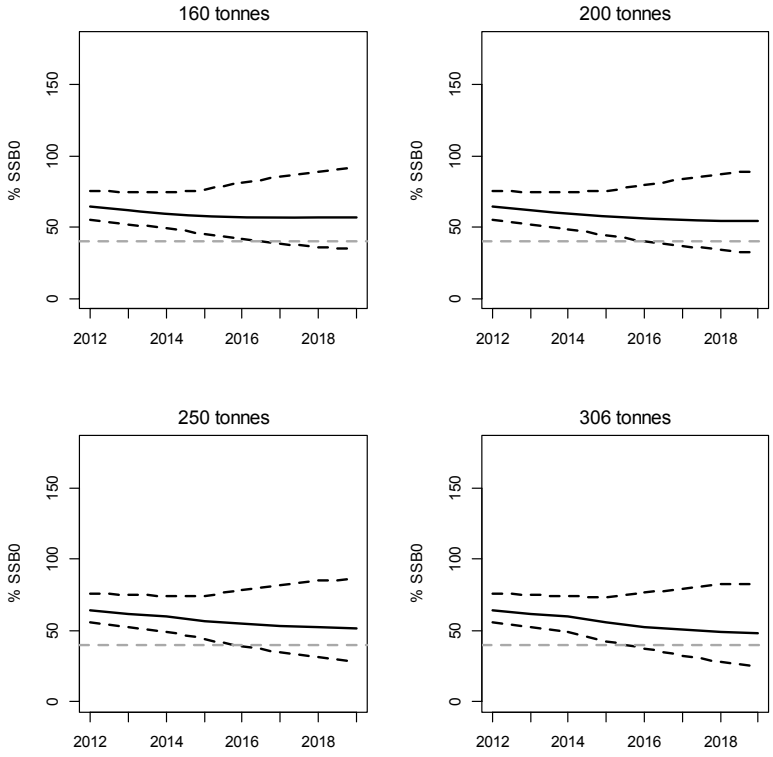

Figure 45: Projected stock trajectory (as a % of SSB_0) for SCI 6A from model F_0.25 for different constant future catches. Solid black line represents median of projections, while dashed black lines represent 2.5th and 97.5th quantiles. Horizontal dashed grey line represents 40% SSB_0.

Table 15: Results from MCMC runs for SCI 6A, showing probabilities of projected spawning stock biomass exceeding the default Harvest Strategy Standard target and limit reference points.

	160 tonnes (current landings)	200 tonnes	250 tonnes	306 tonnes (TACC)
F_0.2				
2017				
P(SSB<10% B0)	0.000	0.000	0.000	0.000
P(SSB<20% B0)	0.000	0.000	0.000	0.000
P(SSB>40% B0)	0.994	0.985	0.968	0.929
P(B2017 < B2013)	0.730	0.800	0.860	0.920
2019				
P(SSB<10% B0)	0.000	0.000	0.000	0.000
P(SSB<20% B0)	0.000	0.000	0.001	0.003
P(SSB>40% B0)	0.968	0.940	0.872	0.773
P(B2019 < B2013)	0.690	0.760	0.850	0.910
F_0.25				
2017				
P(SSB<10% B0)	0.000	0.000	0.000	0.000
P(SSB<20% B0)	0.000	0.000	0.000	0.000
P(SSB>40% B0)	0.962	0.938	0.902	0.847
P(B2017 < B2013)	0.710	0.770	0.810	0.860
2019				
P(SSB<10% B0)	0.000	0.000	0.000	0.000
P(SSB<20% B0)	0.000	0.000	0.001	0.007
P(SSB>40% B0)	0.920	0.876	0.810	0.717
P(B2019 < B2013)	0.660	0.710	0.780	0.850
F_0.25				
2017				
P(SSB<10% B0)	0.000	0.000	0.000	0.000
P(SSB<20% B0)	0.000	0.000	0.000	0.001
P(SSB>40% B0)	0.933	0.900	0.846	0.776
P(B2017 < B2013)	0.690	0.730	0.780	0.830
2019				
P(SSB<10% B0)	0.000	0.000	0.000	0.000
P(SSB<20% B0)	0.000	0.001	0.004	0.011
P(SSB>40% B0)	0.886	0.839	0.772	0.691
P(B2019 < B2013)	0.620	0.670	0.730	0.800
F_0.25				
2017				
P(SSB<10% B0)	0.000	0.000	0.000	0.000
P(SSB<20% B0)	0.000	0.000	0.000	0.000
P(SSB>40% B0)	0.965	0.944	0.904	0.839
P(B2017 < B2013)	0.730	0.770	0.820	0.850
2019				
P(SSB<10% B0)	0.000	0.000	0.000	0.000
P(SSB<20% B0)	0.000	0.000	0.001	0.004
P(SSB>40% B0)	0.907	0.860	0.792	0.705
P(B2019 < B2013)	0.680	0.720	0.780	0.830

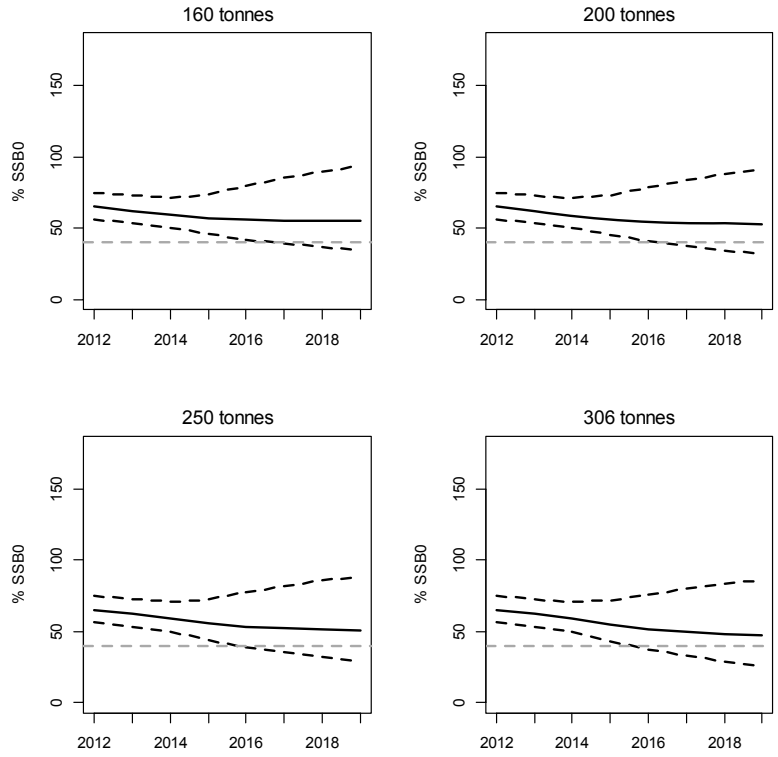

Figure 46: Projected stock trajectory (as a % of SSB_0) for SCI 6A from model N_0.25 for different constant future catches. Solid black line represents median of projections, while dashed black lines represent 2.5th and 97.5th quantiles. Horizontal dashed grey line represents 40% SSB_0.

4.4 Nuisance catchability

Previous accepted scampi assessment models have estimated catchability as a nuisance parameter (Tuck & Dunn 2012, Tuck 2014), and the decision by the Working Group to consider nuisance catchability as unacceptable is a new development.

When treating *q*s as nuisance parameters, for each set of values of the free parameters, the model uses the values of the *q*s which minimise the objective function (Bull et al. 2008). These optimal *q*s are calculated algebraically. If one of the *q*s falls outside the bounds specified by the user, it is set equal to the closest bound. This approach reduces the size of the parameter vector and hence should improve the performance of the estimation method, and is the default in CASAL. Simulations suggest that the use of nuisance *q*s may underestimate B_0 when estimated over a small number of years, but the methods converge for high numbers of years (Walters & Ludwig 1994). Within the scampi assessment model, the CPUE time series would be considered a high number of years.

Examining the previously accepted assessment for SCI 2 in 2013 (Tuck 2014) the use of nuisance *q*s improves the stability of the MCMC chains (compare Figure 47 with free *q*s to Figure 49 with nuisance *q*s), although there appears to be little difference between the models in terms of the SSB_{2012}/SSB_0 (Figure 48 compared to Figure 50). The MCMC traces with nuisance *q*s are clearly very consistent (Figure 49 and Figure 50). The traces with free *q*s are reasonably consistent, but clearly more variable.

A similar pattern was observed with the current assessment for SCI 6A, although the MCMC traces for the model with free *q*s show more evidence of lack of convergence (A4. 20). It is unclear why the model with free *q*s did not appear to converge. A preliminary examination of correlations between key parameters was conducted. The strongest correlations observed with the catchabilities were

between SSB0 and *q-trawl* (-0.6), and between SSB0 and *q-photo* (-0.5) (Figure 51), *q-CPUE* and L_{50} for commercial selectivity in time step 1 (Figure 52, 0.8), and *q-photo* and female growth increment at 20 mm carapace length (Figure 53, 0.6). It is unclear whether these correlations would cause problems with performance of the estimation, but this will be considered in future assessments.

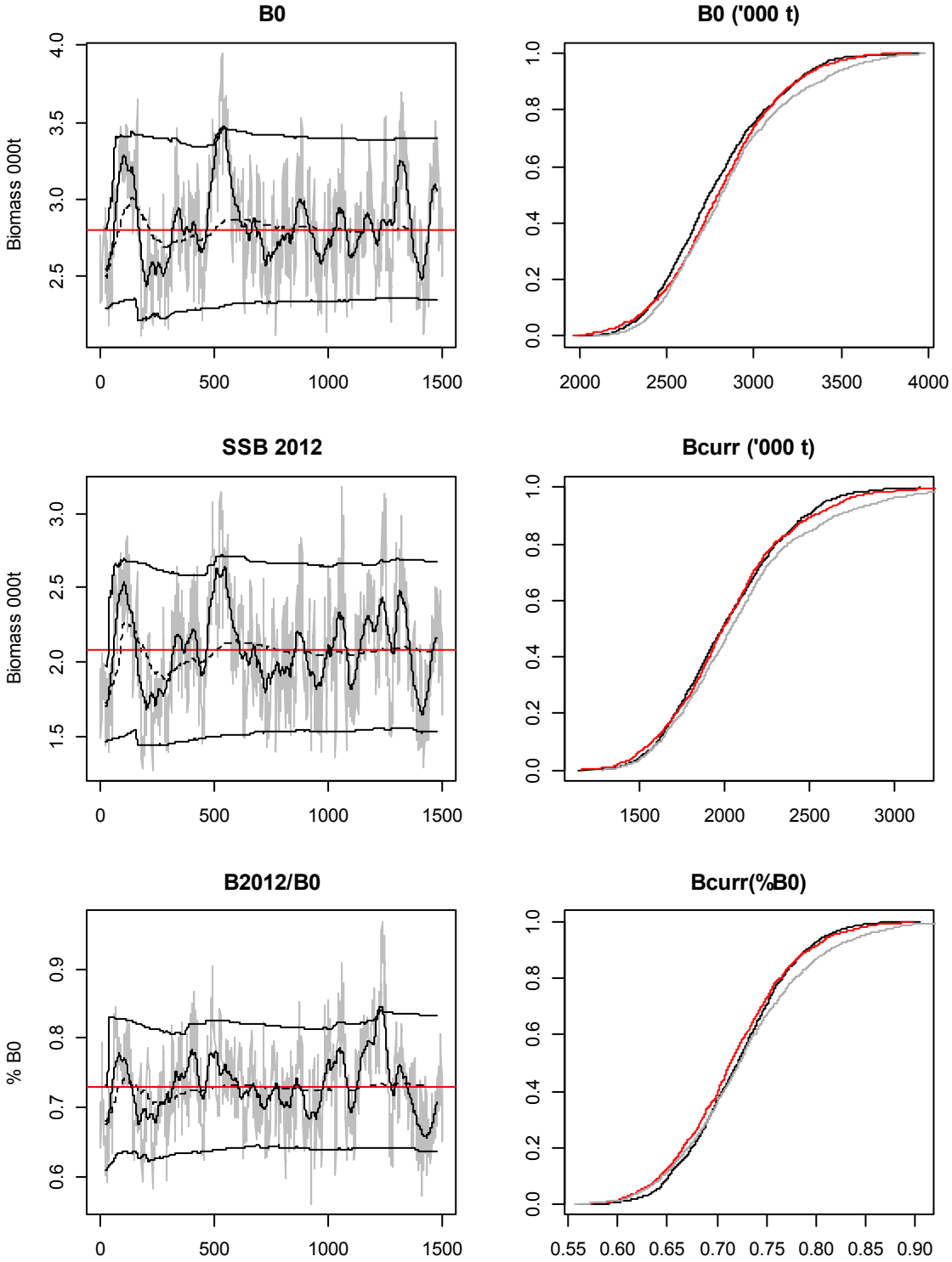

Figure 47: MCMC traces for B_0, SSB_{2012}, and SSB_{2012}/B_0 terms for the revised Base3 model (*q*s as free parameters) for SCI 2 (trace – grey line, cumulative moving median –dashed black line, moving average and cumulative moving 2.5%, 97.5% quantiles – solid black lines, overall median – solid red line, left plots), along with cumulative frequency distributions for three independent MCMC chains (shown as red, grey and black lines, right plots).

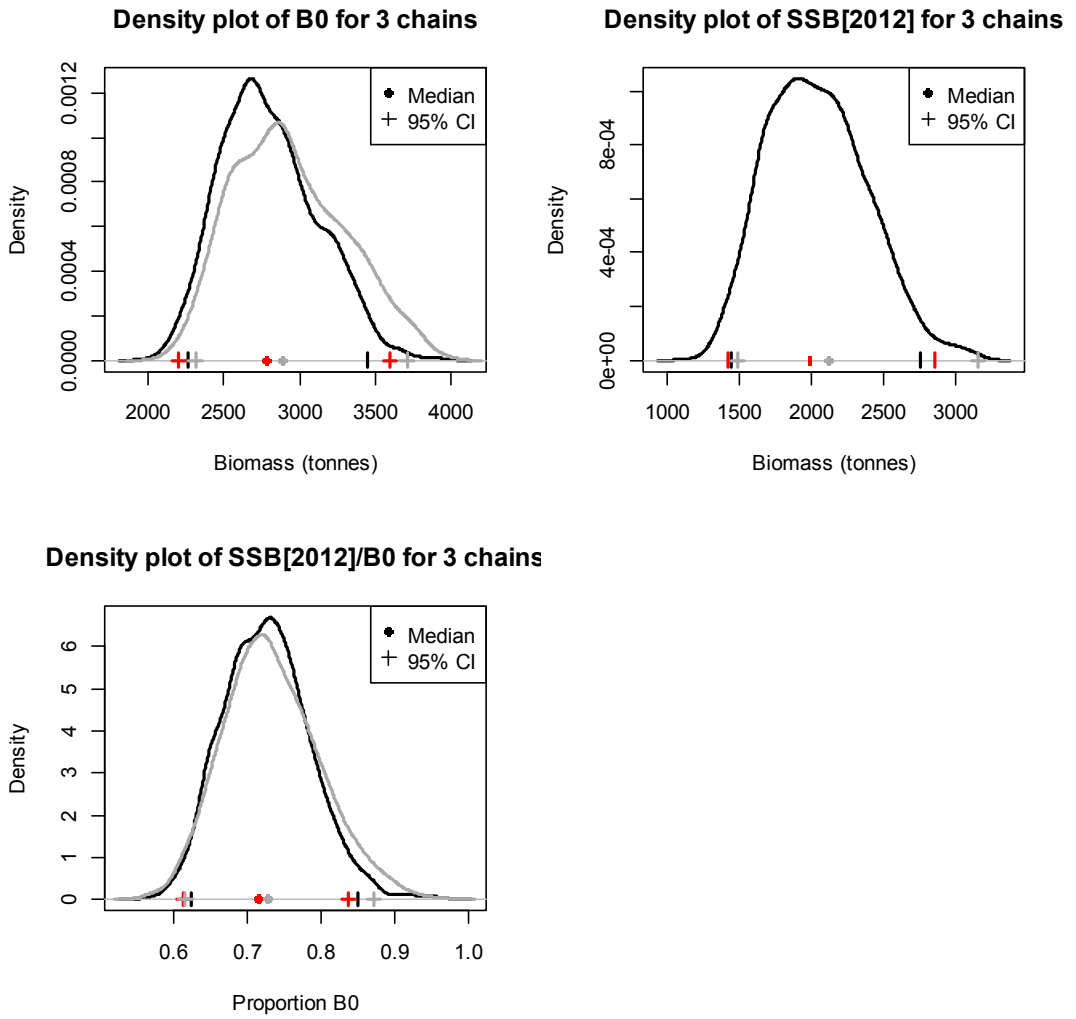

Figure 48: Density plots for B_0, SSB_{2012}, and SSB_{2012}/B_0 terms for the revised Base3 model (*q*s as free parameters) for SCI 2 for three independent MCMC chains, with median and 95% confidence intervals.

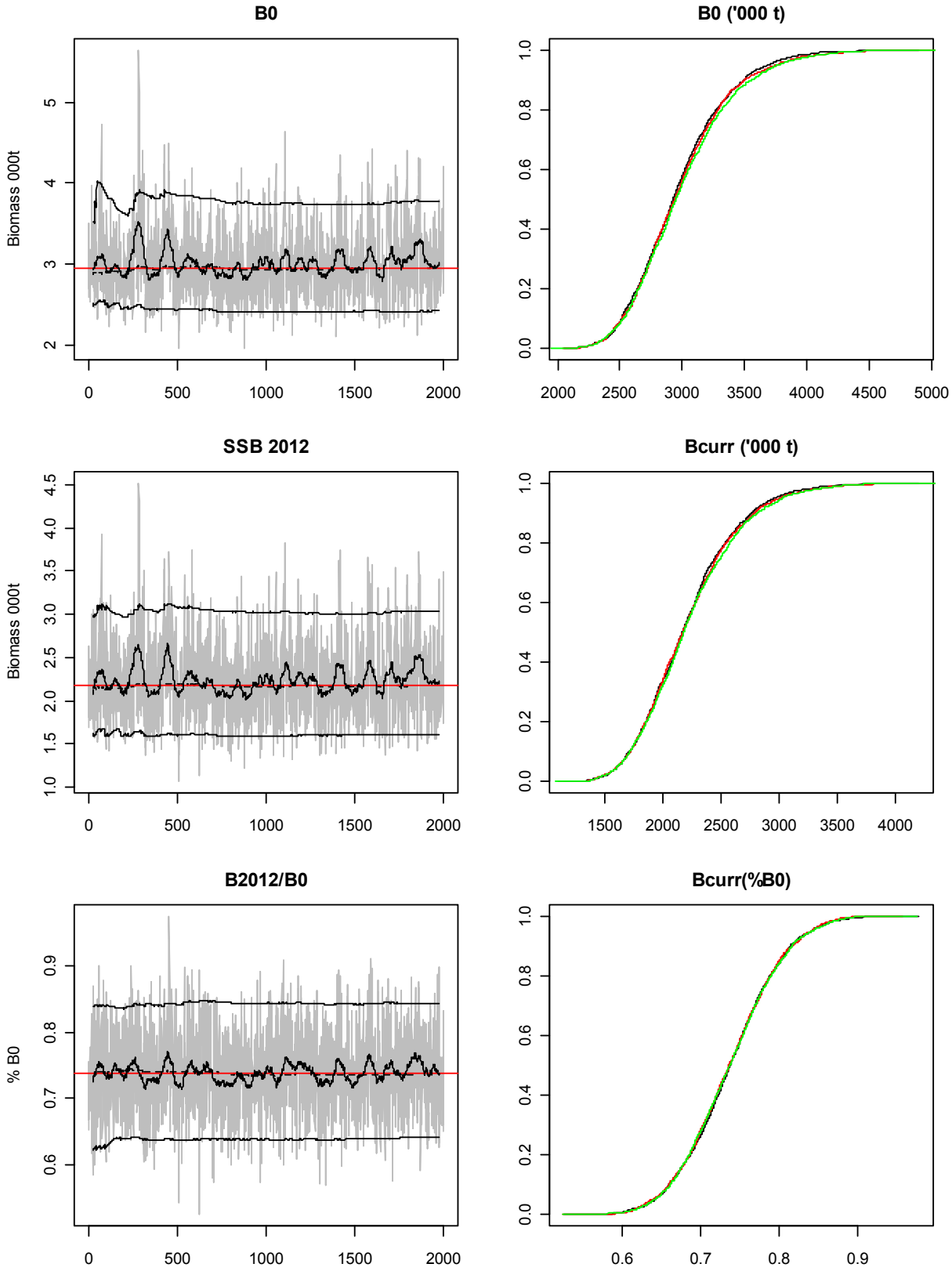

Figure 49: MCMC traces for B_0, SSB_{2012}, and SSB_{2012}/B_0 terms for the original Base3 model (*q*s as nuisance parameters) for SCI 2 (trace – grey line, cumulative moving median –dashed black line, moving average and cumulative moving 2.5%, 97.5% quantiles – solid black lines, overall median – solid red line, left plots), along with cumulative frequency distributions for three independent MCMC chains (shown as red, green and black lines, right plots) (from Tuck 2014).

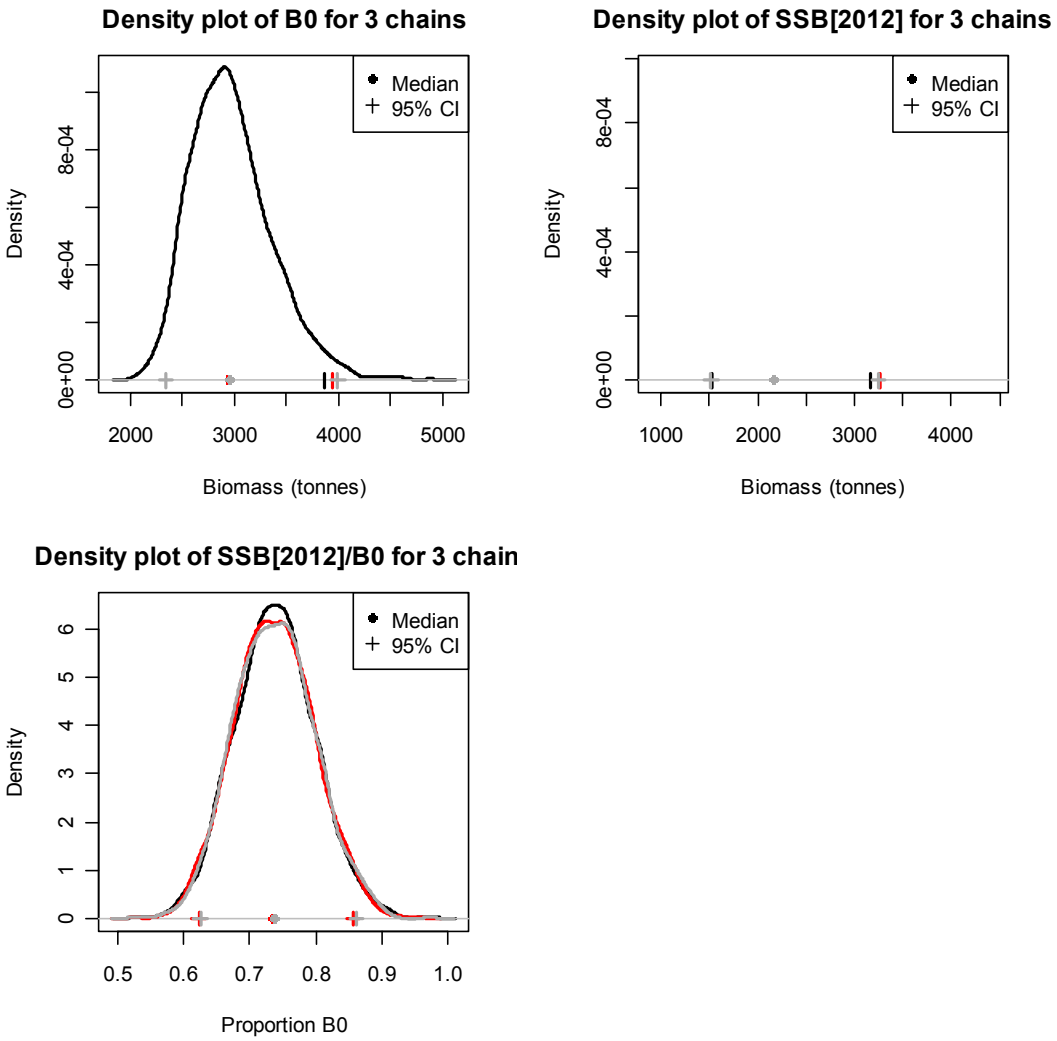

Figure 50: Density plots for B_0, SSB_{2012}, and SSB_{2012}/B_0 terms for the original Base3 model (*q*s as nuisance parameters) for SCI 2 for three independent MCMC chains, with median and 95% confidence intervals (Tuck 2014).

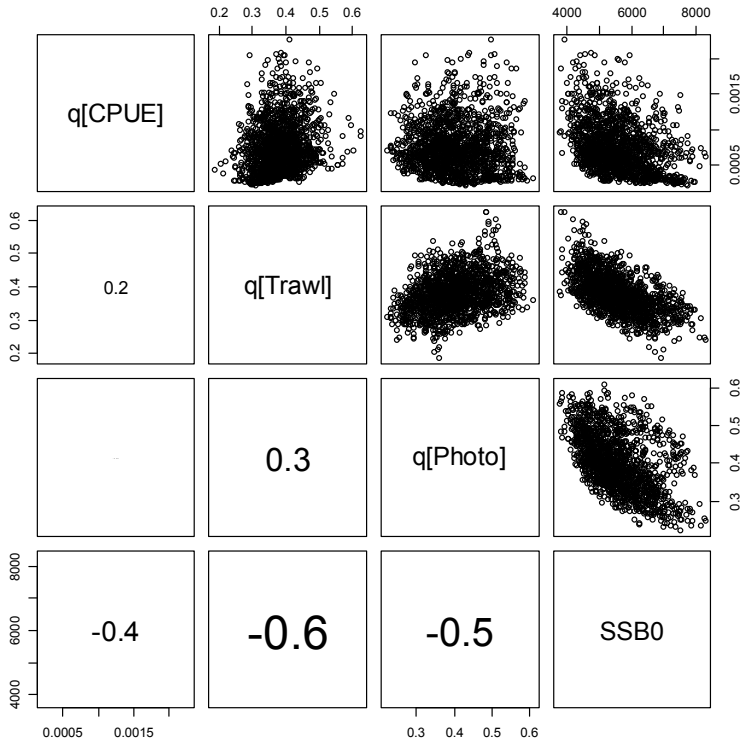

Figure 51: Pairwise scatter plots of *q*s and SSB_0 for model F_0.25 (upper right), with Pearson correlation coefficients (lower left).

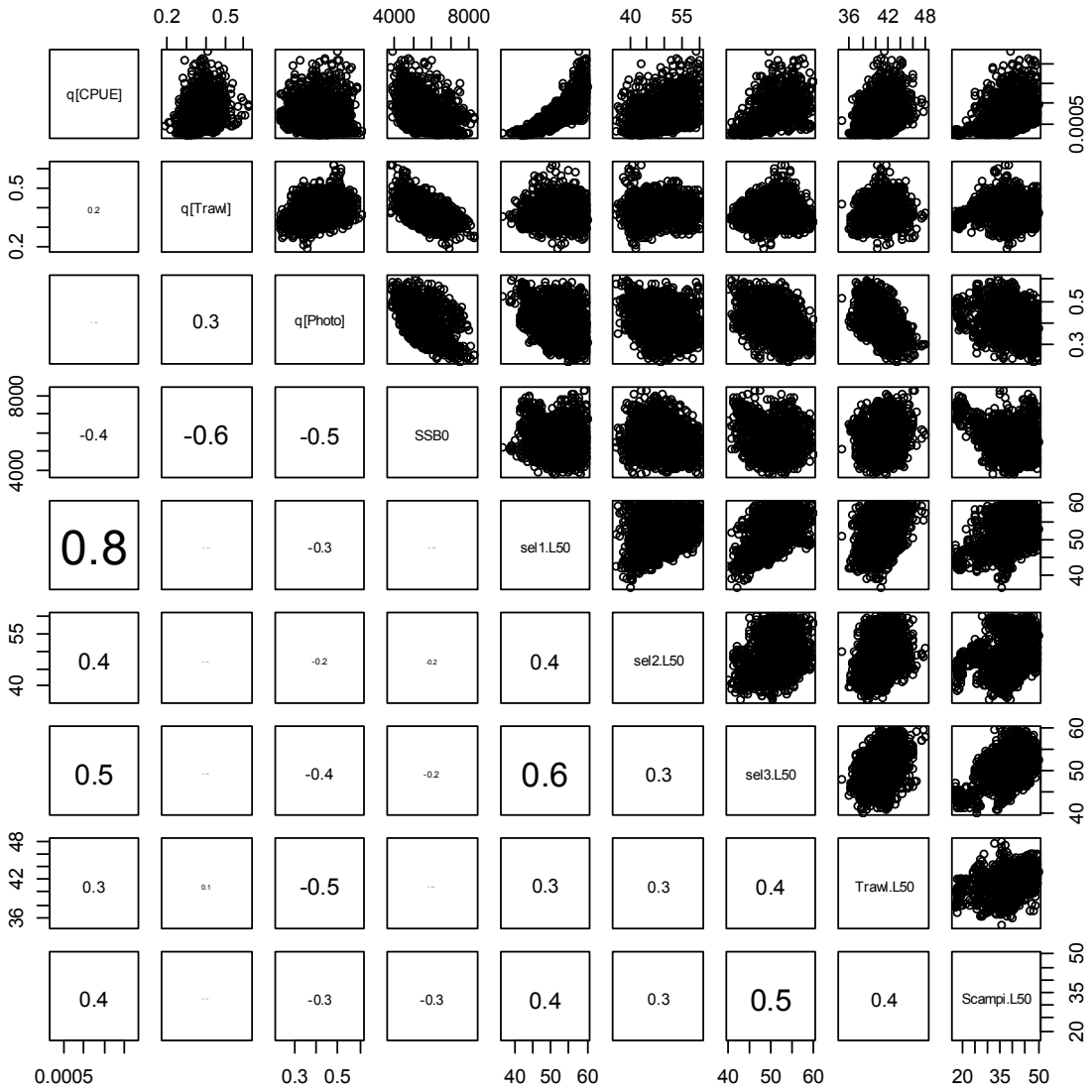

Figure 52: Pairwise scatter plots of *q*s, SSB_0 and selectivity L_{50}s for model F_0.25 (upper right), with Pearson correlation coefficients (lower left).

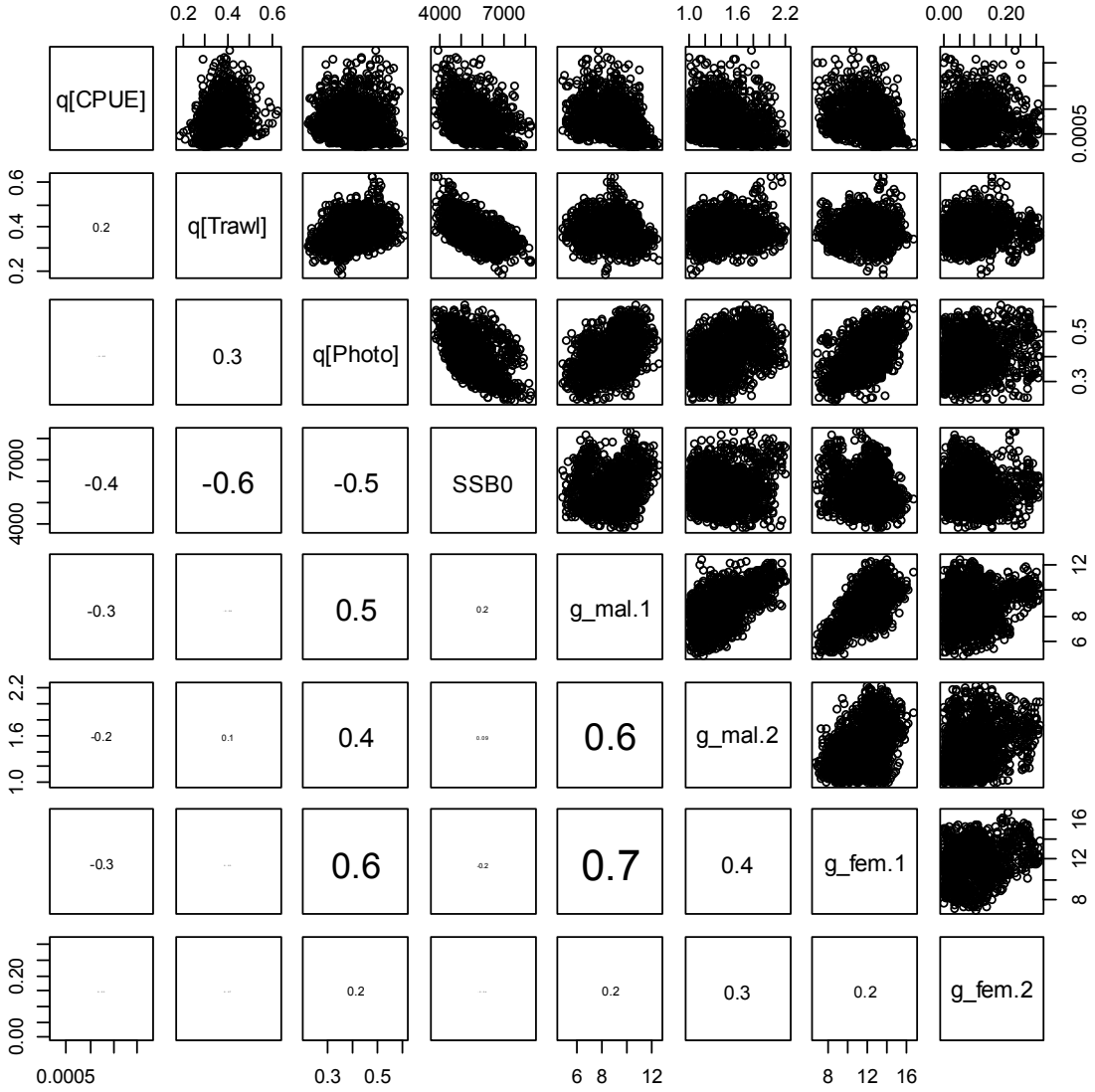

Figure 53: Pairwise scatter plots of *q*s, SSB_0 and growth parameters for model F_0.25 (upper right), with Pearson correlation coefficients (lower left).

4.5 Grade composition data

There is very little evidence of year class modes within the observer (Figure 30 to Figure 34) or trawl survey (Figure 35) length frequency data. The catch composition data (particularly the observer data) has relatively little weight in the model. There was therefore concern that the model had few data from which to estimate year class strengths, and was simply estimating strong year classes where they were required to match increases in CPUE.

While not currently used within the model, additional data are available, in the form of daily catch records by processor grade (Hartill & Tuck 2010, Tuck & Bian 2012). These data have been provided by the scampi fishing industry, and report the daily weight of scampi packaged in each of five whole animal, two tail categories, and the mealed component. In future iterations of the scampi assessment model we aim to include this data, but there are currently a number of logistical difficulties preventing this. A preliminary analysis of the data was conducted, modelling the proportion (by weight) that small scampi (meal, grade 5, and tailed categories) contribute to daily catches against year, time step

and vessel, with a binomial distribution of errors. The model estimated high contributions of small scampi in 1994 and 2005 (Figure 54), which would be consistent with good YCS in 1993 and 2003 (allowing for growth to fishable size), supporting the recruitment pattern estimated by the model.

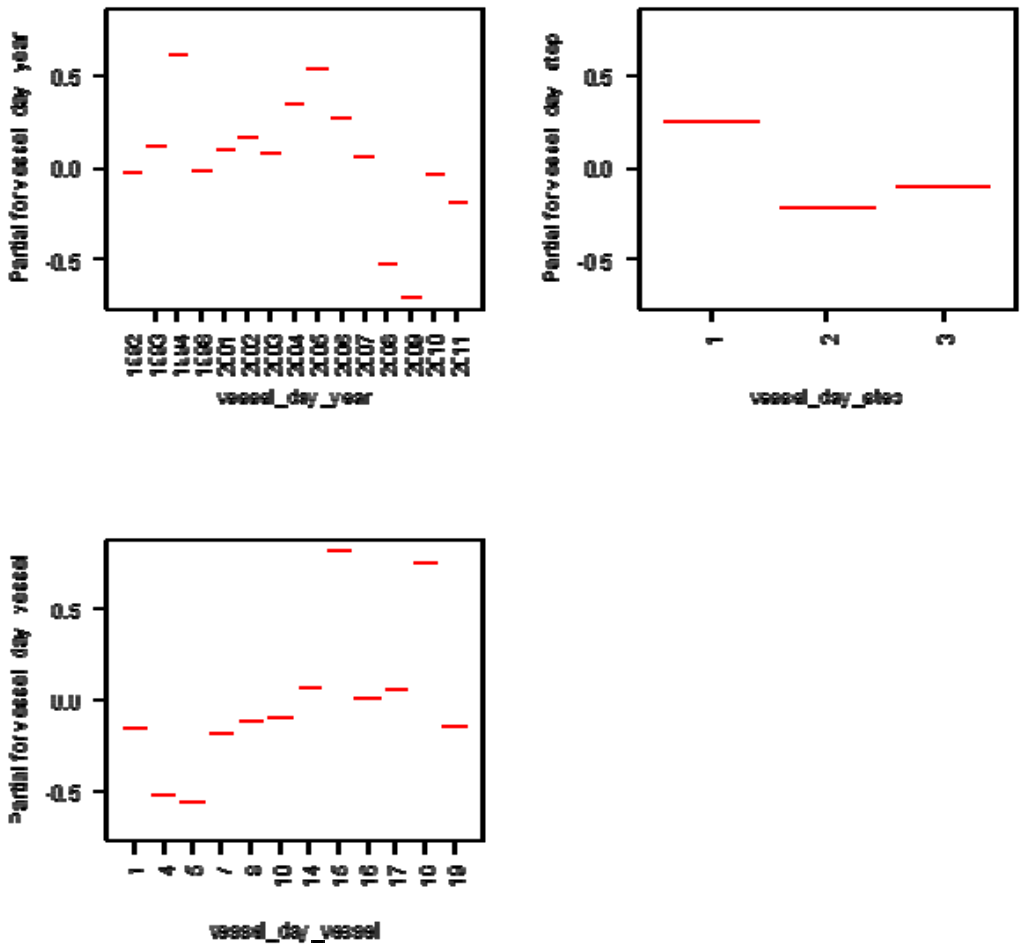

Figure 54: Termplot for model examining the proportion of the catch weight made up by small scampi, showing the effect of year time step and vessel on the proportion of small scampi in the catch, having taken into account (partialled out) the other terms.

5. DISCUSSION

An assessment of the SCI 6A stock was last attempted in 2011 (Tuck & Dunn 2012), and the current study has developed the model further. The assessment was not accepted, but progress has been made, and the current model does not provide any cause for concern over the current state of the stock.

The previous model for SCI 6A included spatial structure, based on survey strata (Tuck & Dunn 2012), but following the characterisation and progress made in assessments for other stocks (Tuck 2014), the SFAWG recommended a single area model for the assessment. Base models were developed, with M fixed at 0.2, 0.25 and 0.3, and also investigating sensitivity to estimating catchabilities as free or nuisance parameters. A single annual standardised CPUE index was calculated, and along with trawl survey and photo survey data were fitted as abundance indices, with associated length frequency distributions. Projections were conducted up to 2019 on the basis of a range of catch scenarios.

MCMC diagnostics appeared very sensitive to the choice of estimating catchabilities as free or nuisance parameters, and while the model using nuisance parameters appeared to converge, the Working Group did not consider this appropriate, and the models using free parameters did not appear to have converged, and were not accepted. Both catchability parameter approaches provided similar estimates of SSB_0 and stock status, suggesting SSB_{2013} is between 50 and 60% SSB_0. Projections out to 2019 suggested SSB would remain above 40% SSB_0 with future catches up to the TACC (the most pessimistic prediction giving a 70% probability of SSB exceeding 40% SSB_0 by 2019).

6. ACKNOWLEDGEMENTS

This work was funded by the Ministry for Primary Industries under project DEE201002SCIC, and builds on a series of scampi assessment projects funded by the Ministry. I thank the many NIWA and Ministry of Fisheries staff who measured scampi over the years, and the members of the NIWA scampi image reading team. Development of the model structure benefitted greatly from comments by David Middleton and Paul Breen in particular, along with other members of the Shellfish Fisheries Assessment Working Group. Malcolm Haddon also provided very useful comments. This report was reviewed by Peter Horn (NIWA, Wellington).

7. REFERENCES

Bell, M.C.; Redant, F.; Tuck, I.D. (2006). *Nephrops* species. *In*: Phillips, B. (ed.). Lobsters: biology, management, aquaculture and fisheries, pp. 412–461. Blackwell Publishing, Oxford.

Bentley, N.; Kendrick, T.H.; Starr, P.J.; Breen, P.A. (2012). Influence plots and metrics: tools for better understanding fisheries catch-per-unit-effort standardisations. *ICES Journal of Marine Science 69*: 84–88.

Bull, B.; Dunn, A. (2002). Catch-at-age: User manual v 1.06.2002/09/12. *NIWA Internal Report 114*.

Bull, B.; Francis, R.I.C.C.; Dunn, A.; McKenzie, A.; Gilbert, D.J.; Smith, M.H.; Bian, R. (2008). CASAL (C++ algorithmic stock assessment laboratory). *NIWA Technical Report No. 130*.

Carter, D. (2003). Inquiry into the administration and management of the scampi fishery. Report to the Primary Production Committee. 226 p.

Charnov, E.L.; Berrigan, D.; Shine, R. (1983). The M/*k* ratio is the same for fish and reptiles. *American Naturalist 142*: 707–711.

Clark, W.G.; Hare, S.R. (2006). Assessment and management of Pacific halibut: data, methods, and policy. International Pacific Halibut Commission Scientific Report 83. 111 p.

Cryer, M. (2000). A consideration of current management areas for scampi in QMAs 3, 4, 6A and 6B. Final Research Report for Ministry of Fisheries Project MOF1999-04K. 52 p. (Unpublished report held by MPI, Wellington)

Cryer, M.; Coburn, R. (2000). Scampi stock assessment for 1999. *New Zealand Fisheries Assessment Report 2000/7*.

Cryer, M.; Dunn, A.; Hartill, B. (2005). Length-based population model for scampi (*Metanephrops challengeri*) in the Bay of Plenty (QMA 1). *New Zealand Fisheries Assessment Report 2005/27*: 55 p.

Cryer, M.; Stotter, D.R. (1999). Movement and growth rates of scampi inferred from tagging, Alderman Islands, western Bay of Plenty. *NIWA Technical Report No. 49*.

Fenaughty, C. (1989). Reproduction in *Metanephrops challengeri*. Unpublished Report MAF Fisheries, Wellington. 46 p. (Unpublished report held by MPI, Wellington)

Francis, R.I.C.C. (1999). The impact of correlations in standardised CPUE indices. New Zealand Fisheries Assessment Research Document 99/42. 30 p. (Unpublished report held by NIWA library, Wellington.)

Francis, R.I.C.C. (2011). Data weighting in statistical fisheries stock assessment models. *Canadian Journal Fisheries and Aquatic Science 68*: 1124–1138.

Francis, R.I.C.C.; Bian, R. (2011). Catch-at-length and -age (CALA) User Manual. 83 p. (NIWA Unpublished Report)

Hartill, B.; Tuck, I.D. (2010). Potential utility of scampi processor grade data as a source of length frequency data. Final Research Report for Ministry of Fisheries Project SCI2007-03. 27 p. (Unpublished report held by MFish, Wellington)

McCullagh, P.; Nelder, J.A. (1989). Generalised Linear Models. 2nd Ed. Chapman and Hall, London. 511 p

Morizur, Y. (1982). Estimation de la mortalité pour quelques stocks de langoustine, *Nephrops norvegicus*. *ICES CM 1982/K:10*.

Pauly, D. (1980). On the interrelationships between natural mortality, growth parameters, and mean environmental temperature in 175 fish stocks. *Journal du Conseil International pour l'Exloration du Mer 39*: 175–192.

Starr, P.J. (2009). Rock lobster catch and effort data: summaries and CPUE standardisations, 1979–80 to 2007–08. *New Zealand Fisheries Assessment Report 2009/38*: 73 p.

Starr, P.J.; Breen, P.A.; Kendrick, T.H.; Haist, V. (2009). Model and data used for the 2008 stock assessment of rock lobsters (*Jasus edwardsii*) in CRA 3. *New Zealand Fisheries Assessment Report 2009/22*: 62 p.

Tuck, I.D. (2009). Characterisation of scampi fisheries and the examination of catch at length and spatial distribution of scampi in SCI 1, 2, 3, 4A and 6A. *New Zealand Fisheries Assessment Report 2009/27*: 102 p.

Tuck, I.D. (2010) Scampi burrow occupancy, burrow emergence and catchability. *Final Research Report for Ministry of Fisheries research project 2010/13.* 58 p.

Tuck, I.D. (2013). Characterisation and length-based population model for scampi (*Metanephrops challengeri*) on the Mernoo Bank (SCI 3). *New Zealand Fisheries Assessment Report 2013/24*: 165 p.

Tuck, I.D. (2014). Characterisation and length-based population model for scampi (*Metanephrops challengeri*) in the Bay of Plenty (SCI 1) and Hawke Bay/Wairaraoa (SCI 2). *New Zealand Fisheries Assessment Report 2014/33*: 172 p.

Tuck, I.D.; Atkinson, R.J.A.; Chapman, C.J. (2000). Population biology of the Norway lobster, *Nephrops norvegicus* (L.) in the Firth of Clyde, Scotland. II. Fecundity and size at onset of maturity. *ICES Journal of Marine Science 57*: 1222–1237.

Tuck, I.D.; Bian, R. (2012). Utility of grade based sampling for scampi. Final Research Report for Ministry of Fisheries research project SCI200804. 66 p. (Unpublished report held by MPI, Wellington.)

Tuck, I.D.; Dunn, A. (2006). Length based population model for scampi (*Metanephrops challengeri*) in the Bay of Plenty (SCI 1) and Wairarapa / Hawke Bay (SCI 2). Final Research Report for Ministry of Fisheries research project SCI2005-01. 93 p. (Unpublished report held by MFish, Wellington.)

Tuck, I.D.; Dunn, A. (2009). Length-based population model for scampi (*Metanephrops challengeri*) in the Bay of Plenty (SCI 1) and Wairarapa / Hawke Bay (SCI 2). Final Research Report for Ministry of Fisheries research projects SCI2006-01 & SCI2008-03W. 30 p. (Unpublished report held by MPI, Wellington.)

Tuck, I.D.; Dunn, A. (2012). Length-based population model for scampi (*Metanephrops challengeri*) in the Bay of Plenty (SCI 1), Wairarapa / Hawke Bay (SCI 2) and Auckland Islands (SCI 6A). *New Zealand Fisheries Assessment Report 2012/1*: 125 p.

Tuck, I.D.; Hartill, B.; Parkinson, D.; Drury, J.; Smith, M.; Armiger, H. (2009a). Estimating the abundance of scampi - Relative abundance of scampi, *Metanephrops challengeri*, from a photographic survey in SCI 6A (2009). Final Research Report for Ministry of Fisheries research project SCI2008-01. 26 p. (Unpublished report held by MPI, Wellington.)

Tuck, I.D.; Hartill, B.; Parkinson, D.; Harper, S.; Drury, J.; Smith, M.; Armiger, H. (2009b). Estimating the abundance of scampi - Relative abundance of scampi, *Metanephrops challengeri*, from a photographic survey in SCI 1 and SCI 6A (2008). Final Research Report for Ministry of Fisheries research project SCI2007-02. 37 p. (Unpublished report held by MPI, Wellington.)

Tuck, I.D.; Parkinson, D.; Armiger, H.; Smith, M.; Miller, A.; Rush, N.; Spong, K. (2015). Estimating the abundance of scampi in SCI 6A (Auckland Islands) in 2013. *New Zealand Fisheries Assessment Report 2015/10*: 52 p.

Tuck, I.D.; Parkinson, D.; Hartill, B.; Drury, J.; Smith, M.; Armiger, H. (2007). Estimating the abundance of scampi - relative abundance of scampi, *Metanephrops challengeri*, from a photographic survey in SCI 6A (2007). Final Research Report for Ministry of Fisheries research project SCI2006-02. 29 p. (Unpublished report held by MPI, Wellington.)

Vignaux, M. (1994). Catch per unit effort (CPUE) analysis of west coast South Island and Cook Strait spawning hoki fisheries, 1987–93. New Zealand Fisheries Assessment Research Document 94/11. 29 p. (Unpublished report held by NIWA library, Wellington.)

Walters, C.; Ludwig, D. (1994). Calculation of Bayes posterior probability distributions for key population parameters. *Canadian Journal of Fisheries and Aquatic Science 51*: 713–722.

Wear, R.G. (1976). Studies on the larval development of *Metanephrops challengeri* (Balss, 1914) (Decapoda, Nephropidae). *Crustaceana 30*: 113–122.

APPENDIX 1. CPUE standardisation diagnostics

Annual CPUE index

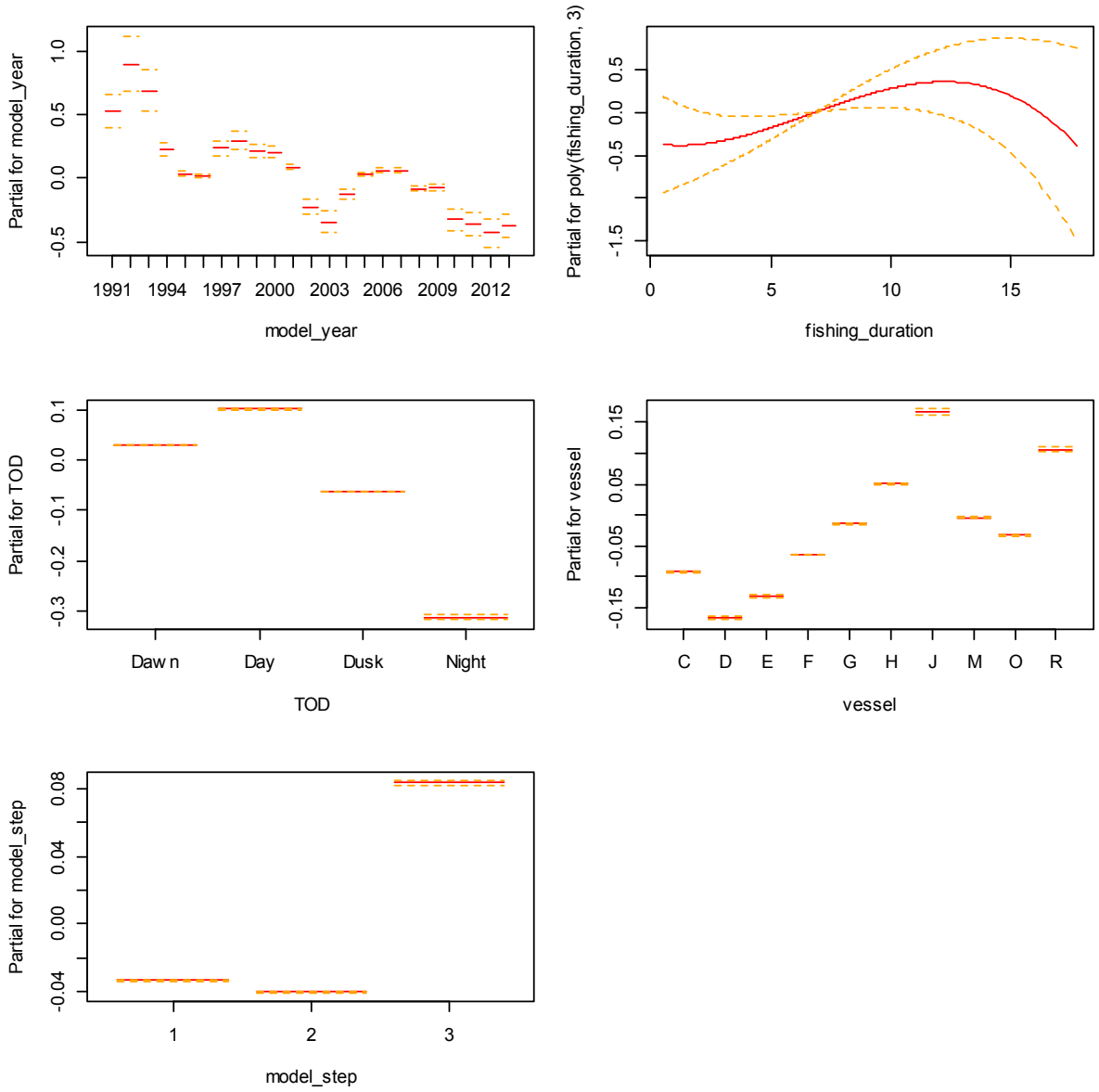

A1. 1: Termplot for final SCI 6A CPUE standardisation model (Table 4).

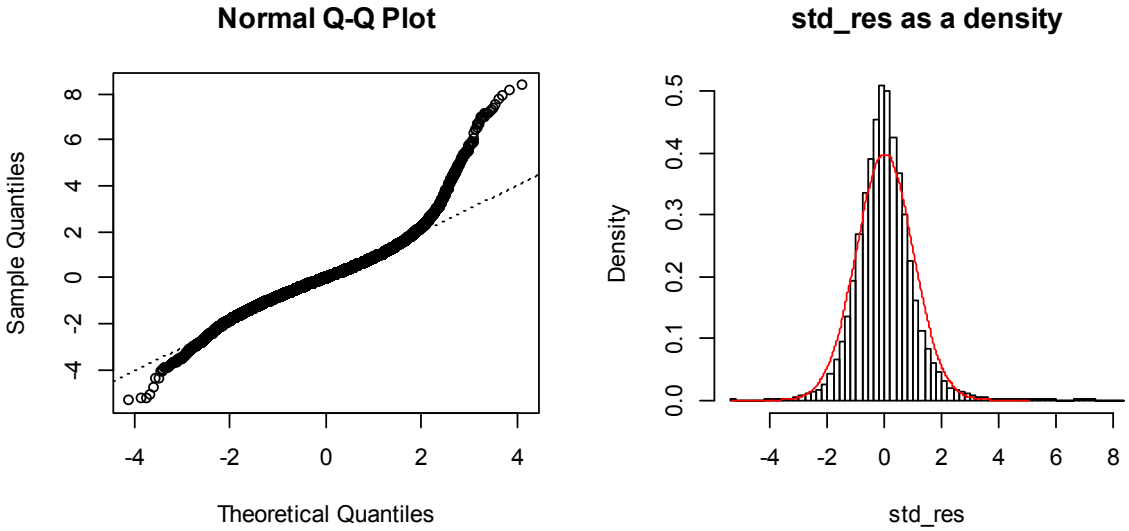

A1. 2: Diagnostic plots for final SCI 6A CPUE standardisation model (Table 4).

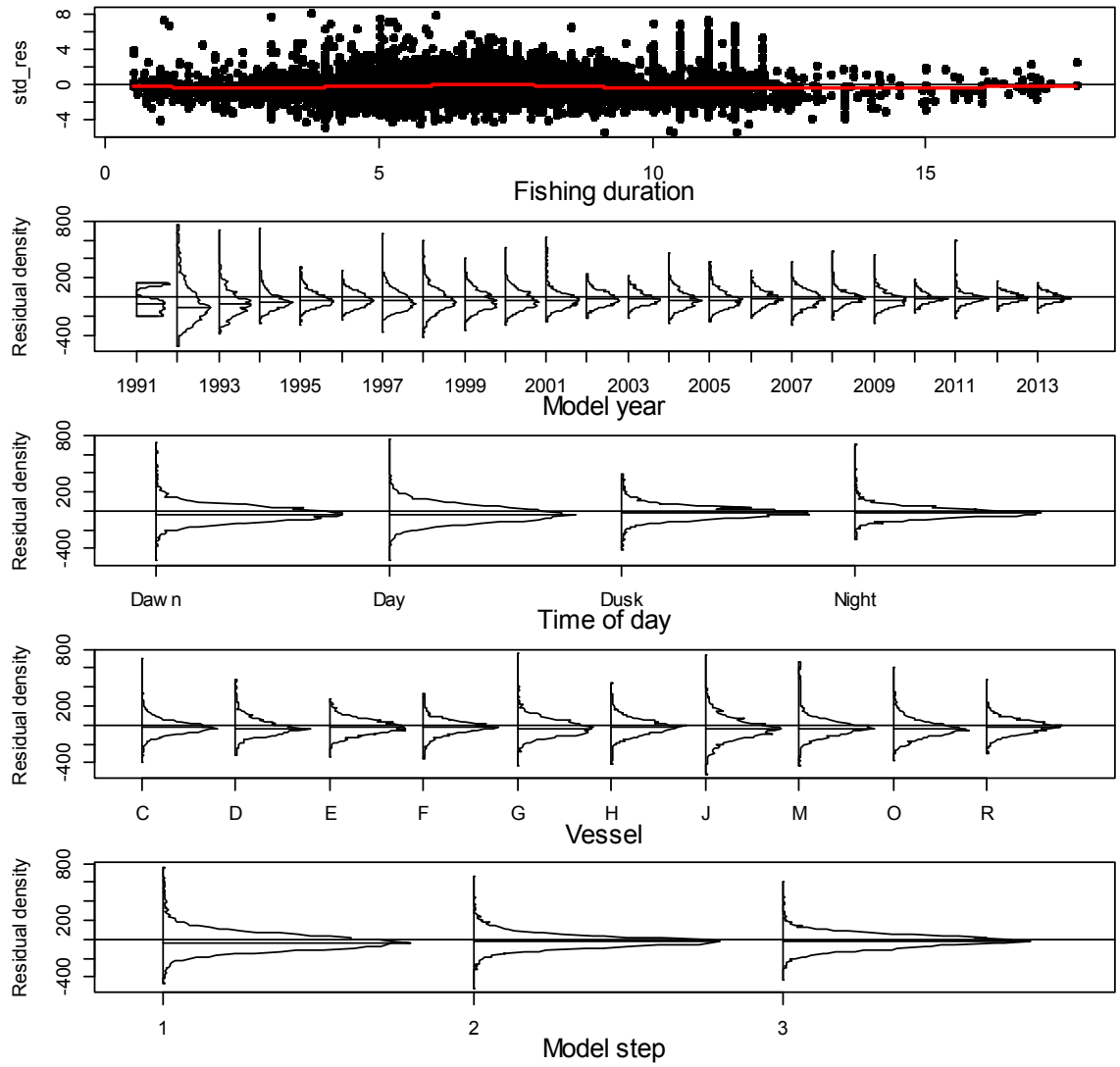

A1. 3: Distributions of residuals for final SCI 6A CPUE standardisation model (Table 4).

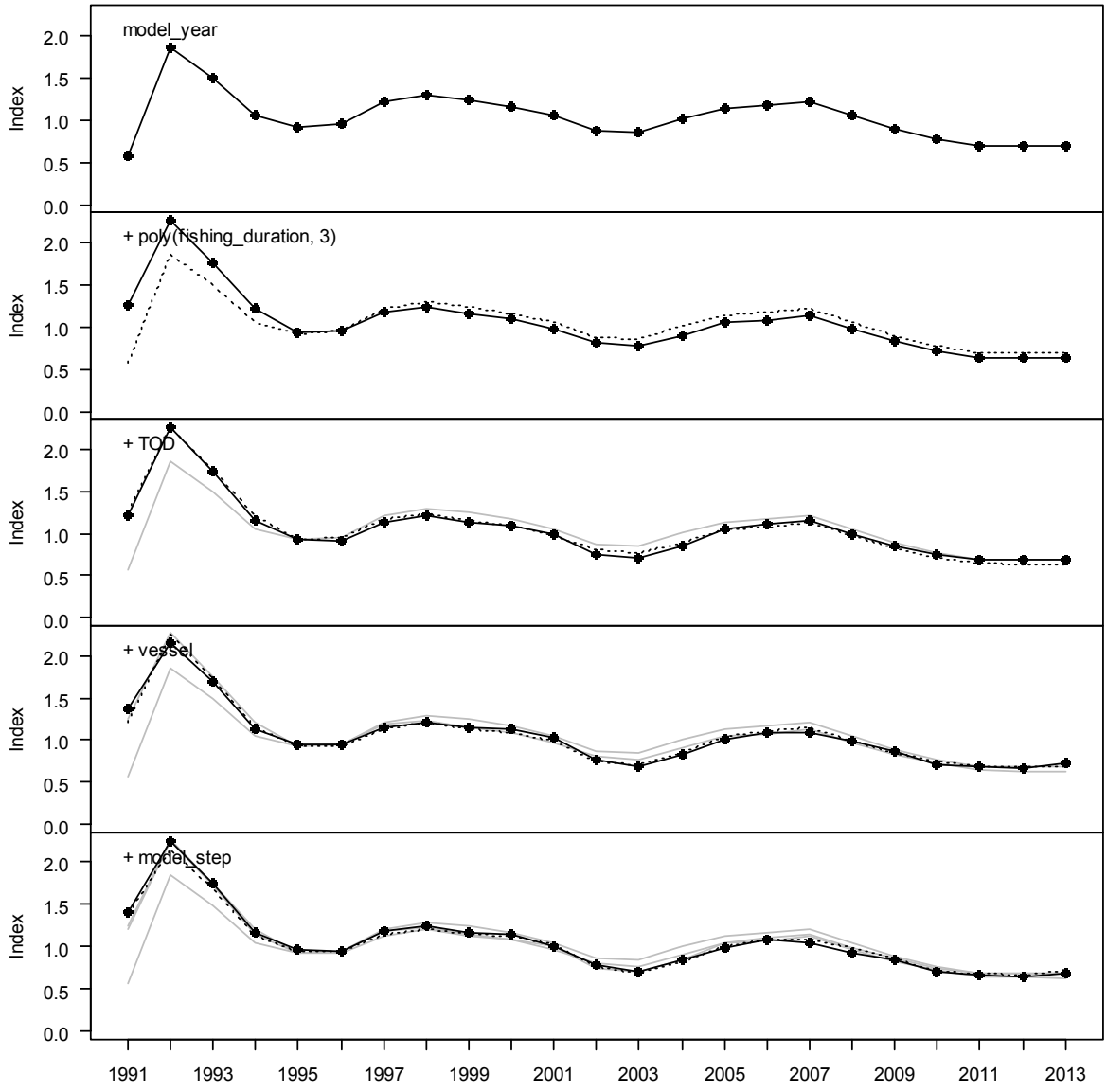

A1. 4: Step influence plot for final SCI 6A CPUE standardisation model (Table 4).

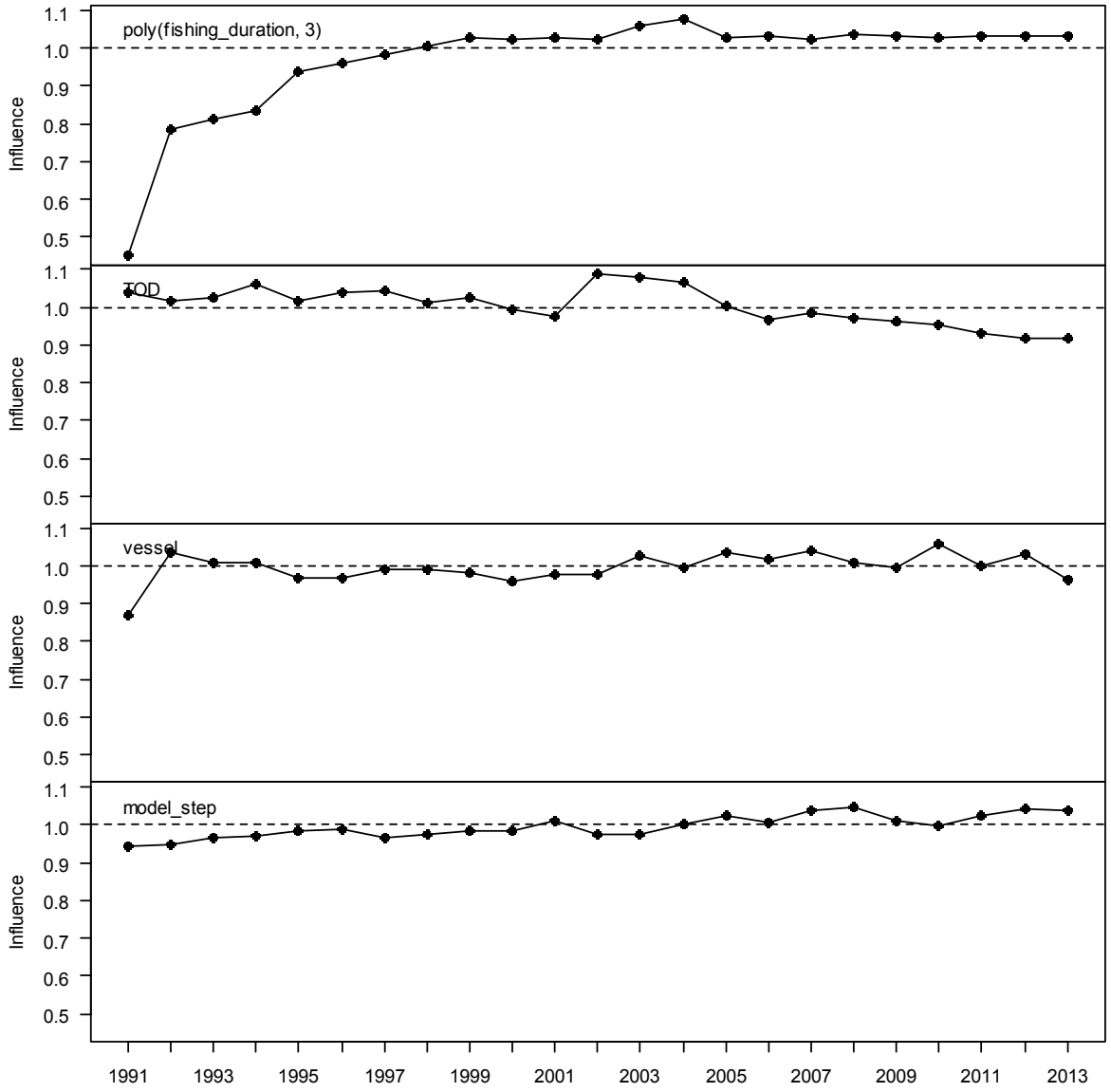

A1. 5: Year influence plots for each explanatory variable for final SCI 6A CPUE standardisation model (Table 4).

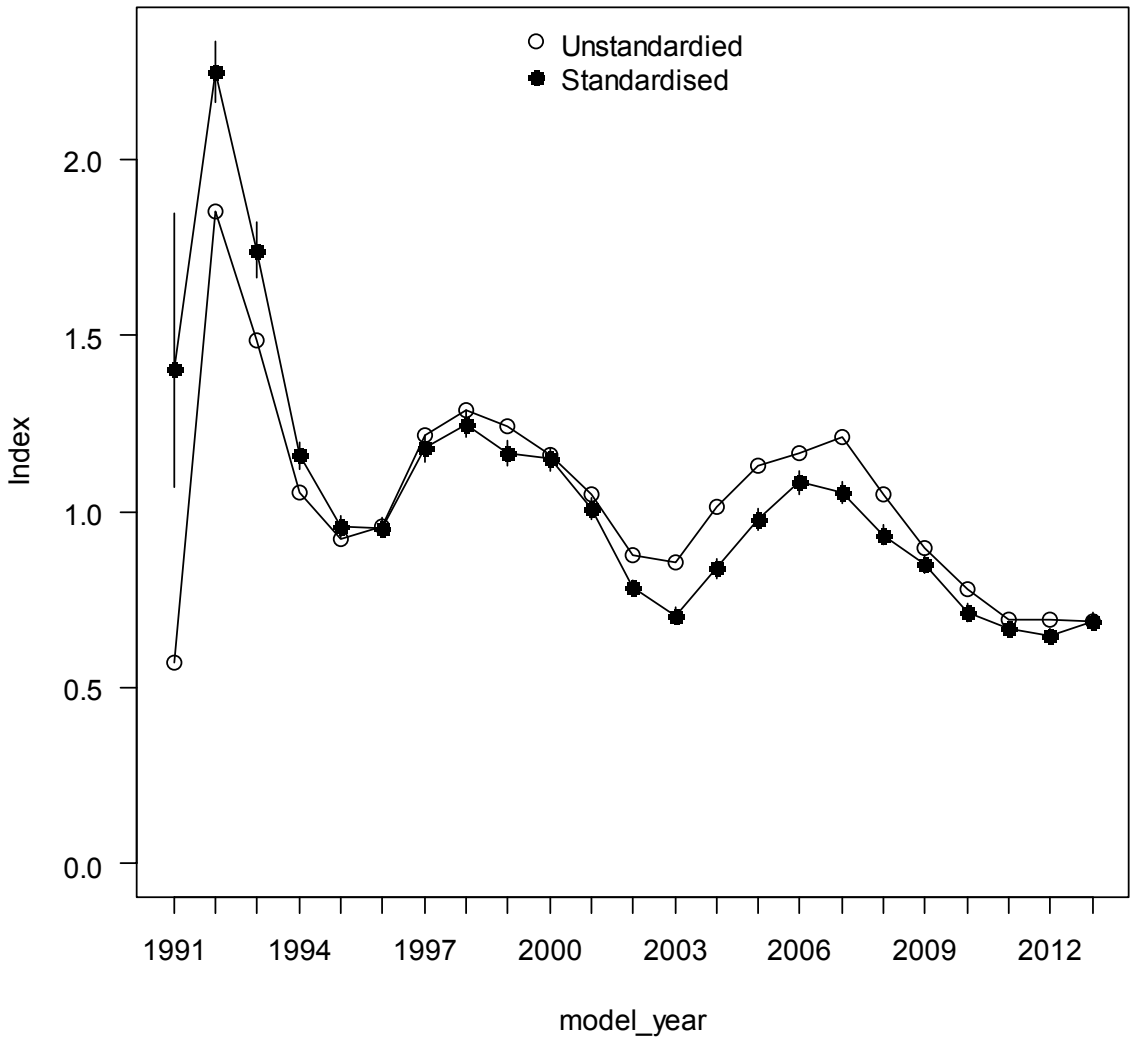

A1. 6: Plot of standardised and unstandardized CPUE indices for SCI 6A.

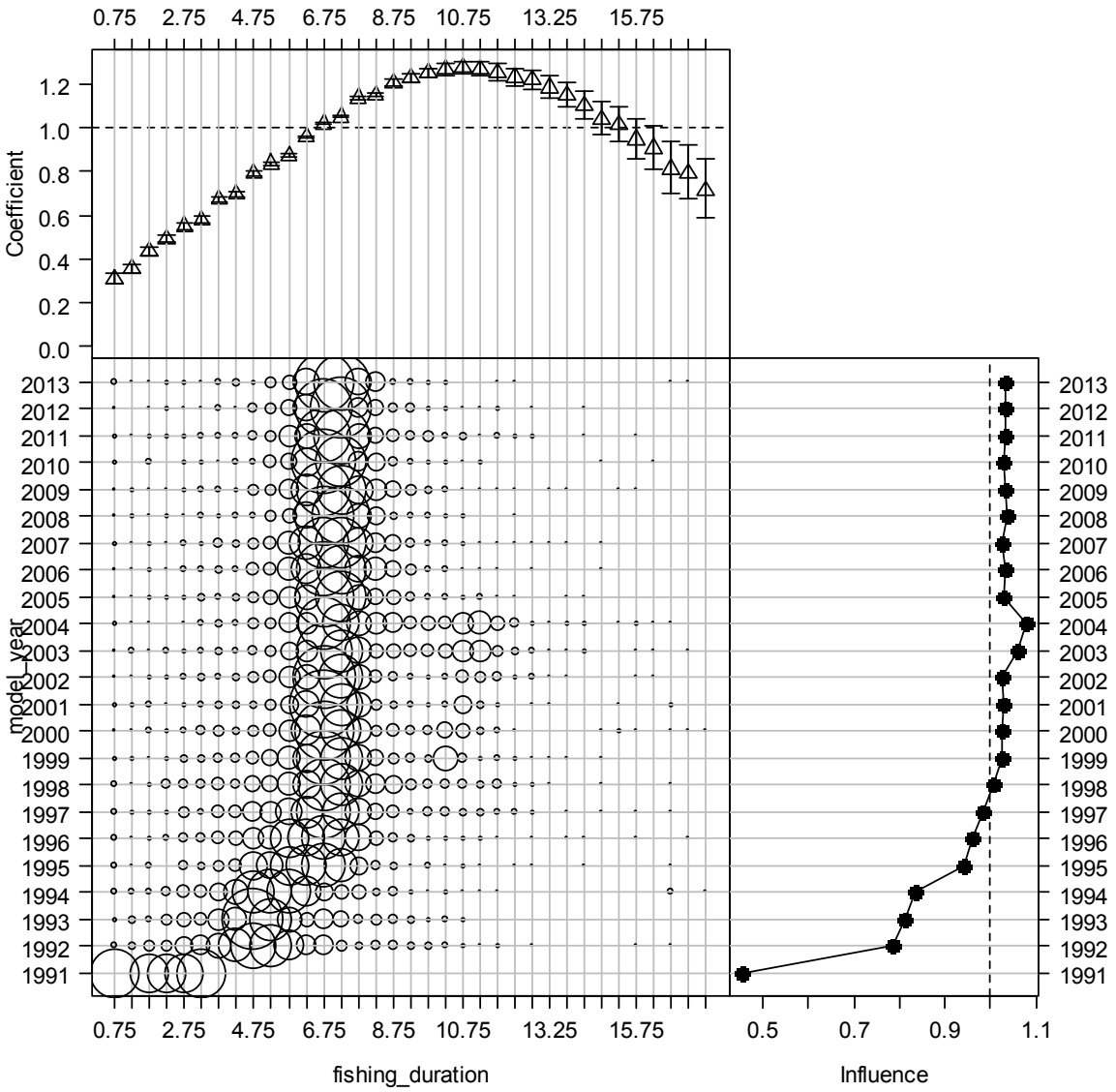

A1. 7: Coefficient-distribution influence plot for effort for final SCI 6A CPUE standardisation model (Table 4).

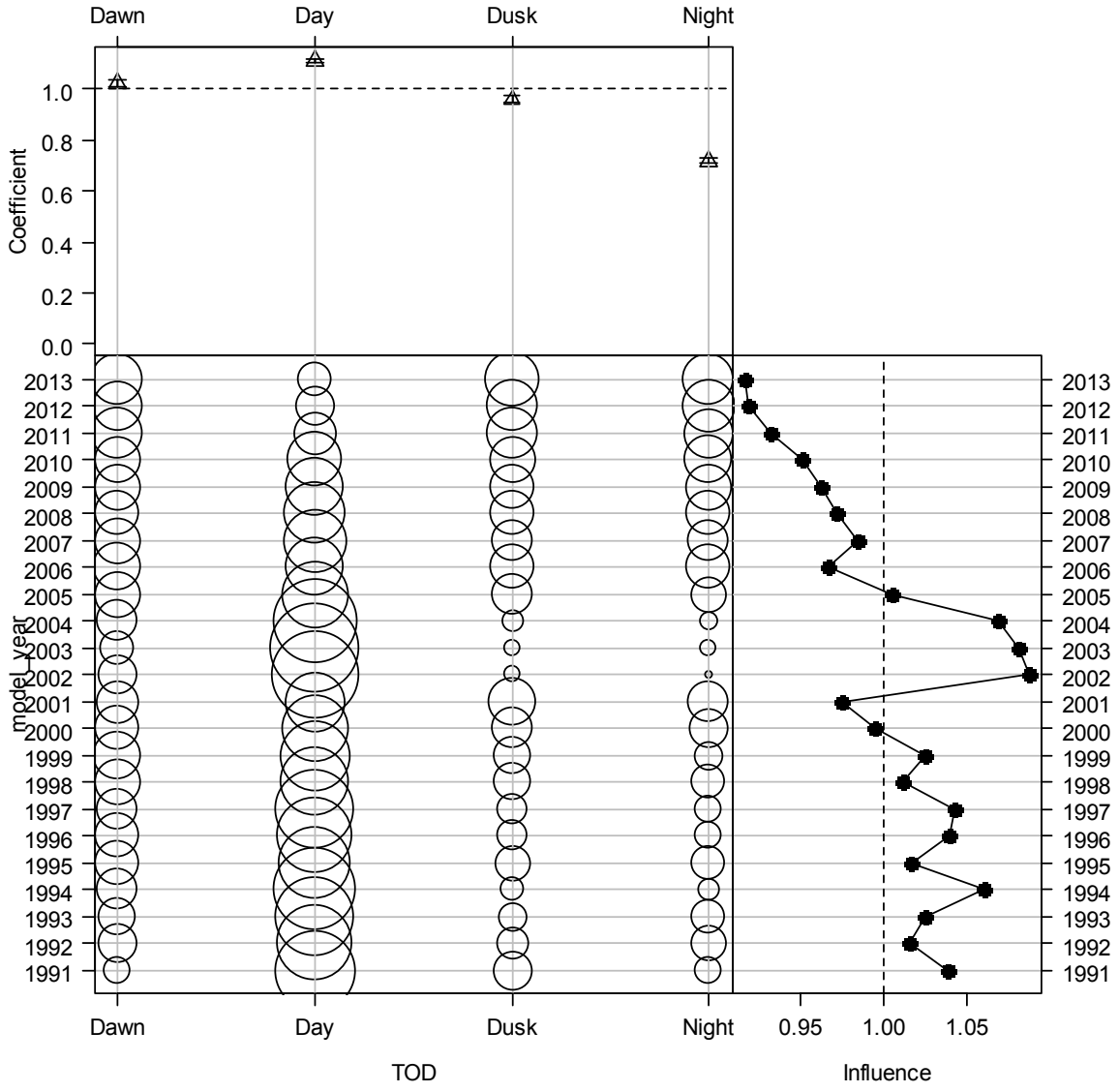

A1. 8: Coefficient-distribution influence plot for time of day for final SCI 6A CPUE standardisation model (Table 4).

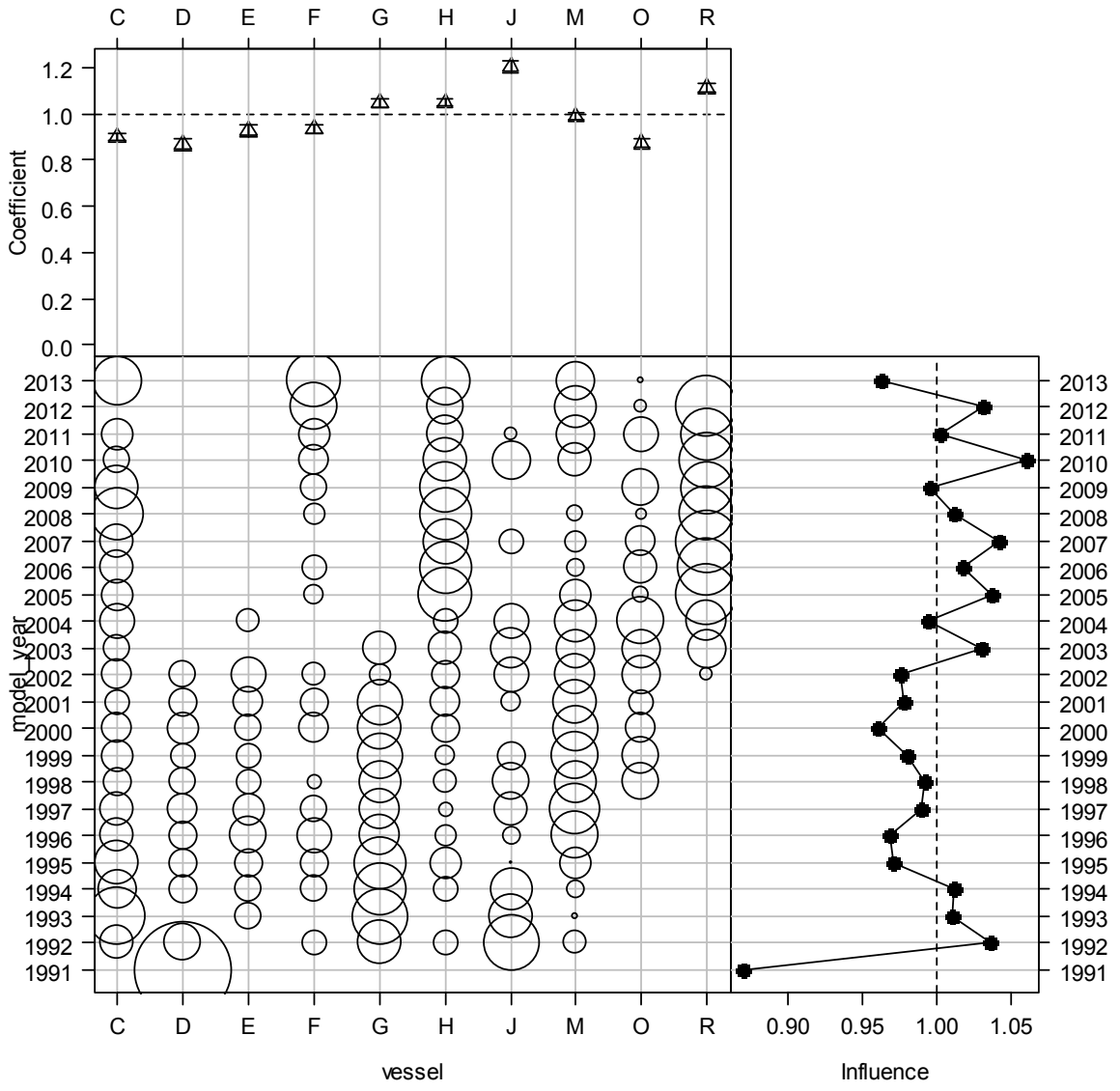

A1. 9: Coefficient-distribution influence plot for vessel for final SCI 6A CPUE standardisation model (Table 4).

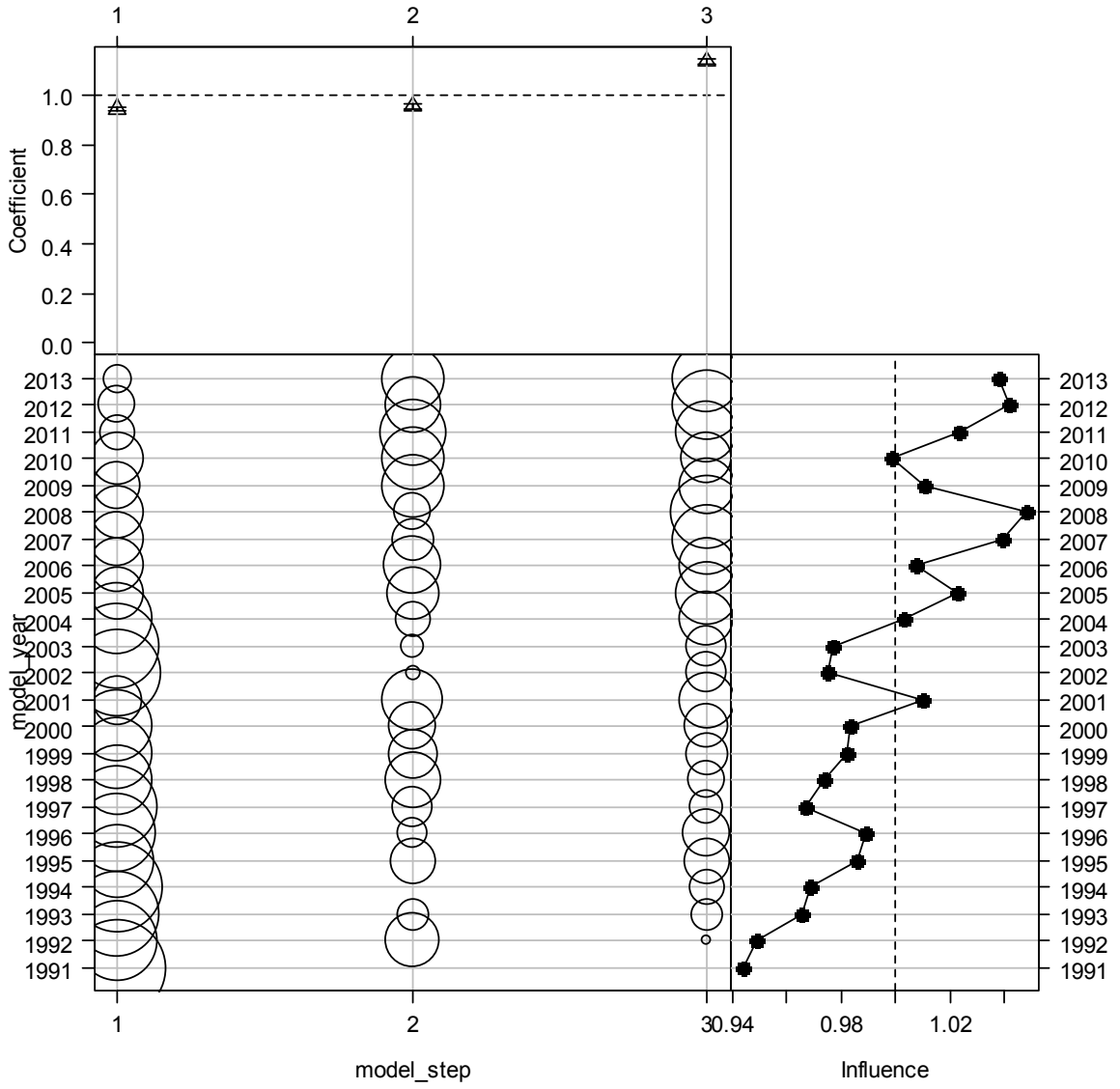

A1. 10: Coefficient-distribution influence plot for timestep for final SCI 6A CPUE standardisation model (Table 4).

APPENDIX 2. Analysis of length composition data

Summary of Multivariate tree regression of mean size and proportion males in scampi observer length frequencies.

A2. 1: Depth and month splits identified by multivariate tree regression of observer length frequency data (Section 3.6.1).

Year	Depth split (m)	Month split
1992	400	2.75
1993	400, 450	11.25, 1.5
1994		10.5, 6.25, 3.25
1995	400	
1996		7
1997		9.75
1998	450	
1999		9.25
2000		3.25
2001		8.75
2002		11.25
2003	450	11.25, 5.75
2004		
2005	500	10.75
2006		11.75
2007		7.5, 2.25
2008	450	
2009	500	
2010	500	
2011		7.5, 3
2012	450	5.25, 5.75
2013	450	

Trawl survey length frequency

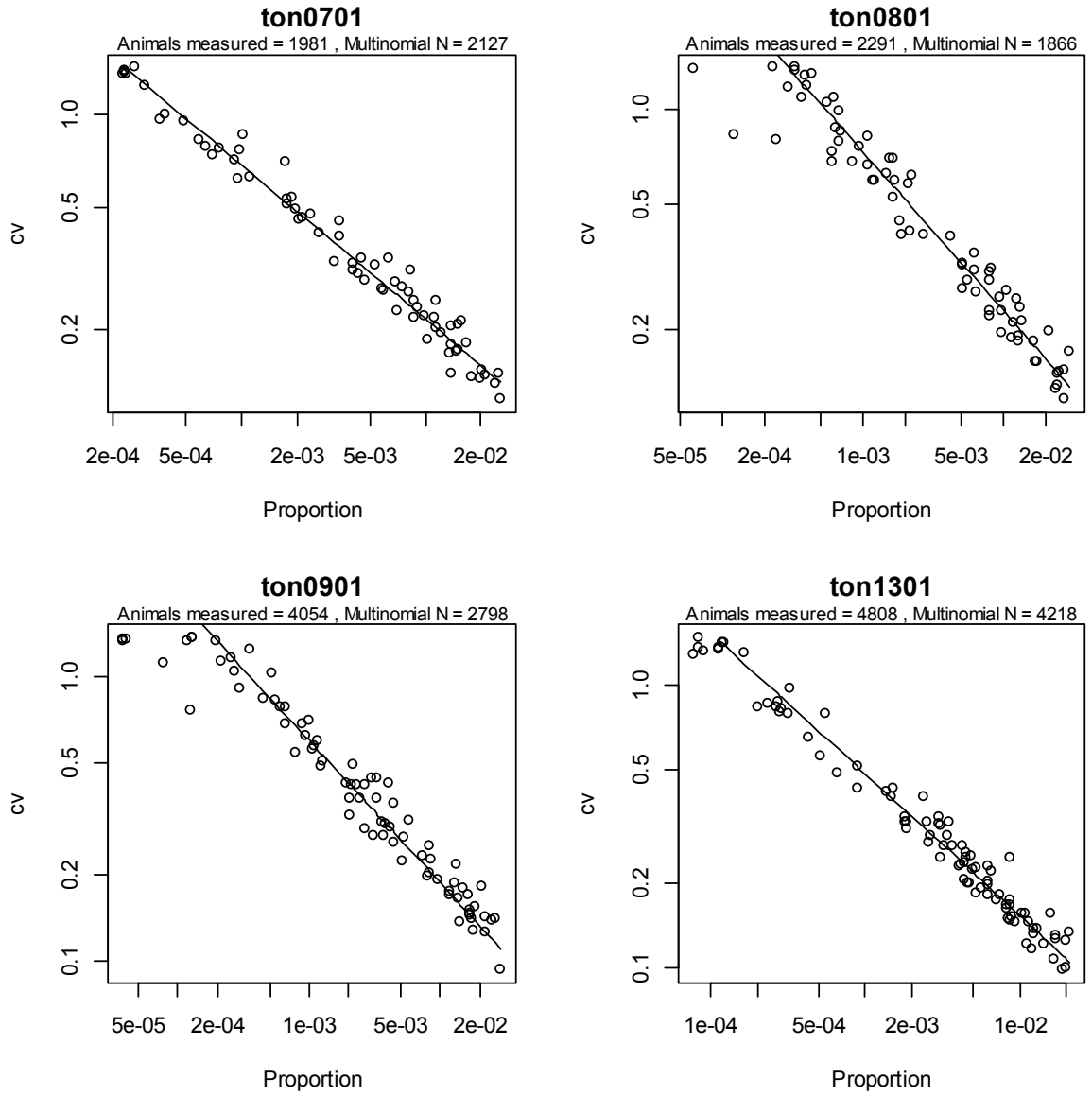

A2. 2: Observation-error CVs for the trawl survey proportions-at-length data sets. Each point represents a proportion at a specific length and sex for a given year. The diagonal line, which is the same in each panel, is added to aid comparison between panels; it shows the relationship between proportion and CV that would hold with simple multinomial sampling with sample size 500.

Observer length frequency

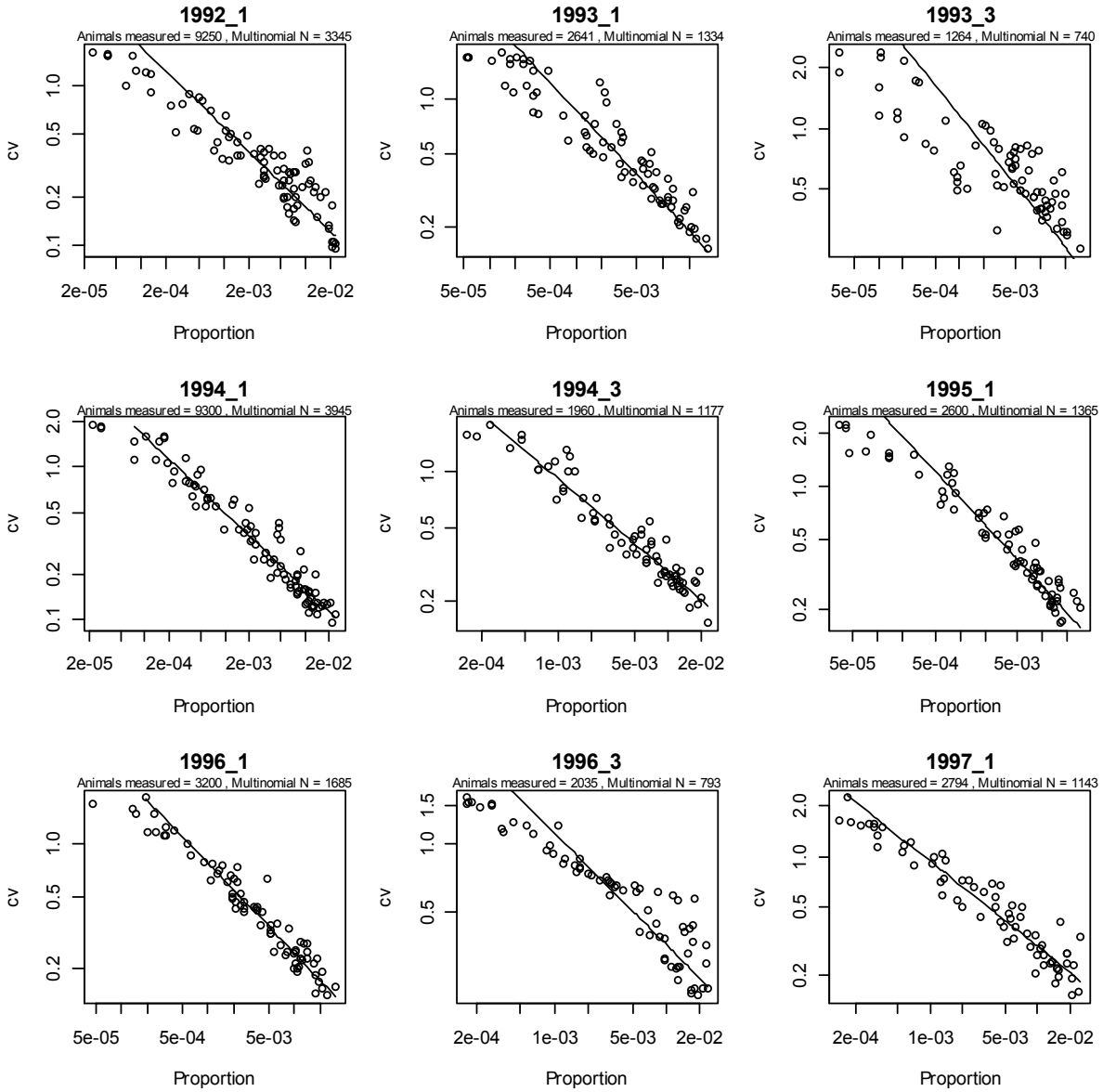

A2. 3: Observation-error CVs for the observer proportions-at-length data sets. Each point represents a proportion at a specific length and sex for a given year. The diagonal line, which is the same in each panel, is added to aid comparison between panels; it shows the relationship between proportion and CV that would hold with simple multinomial sampling with sample size 500.

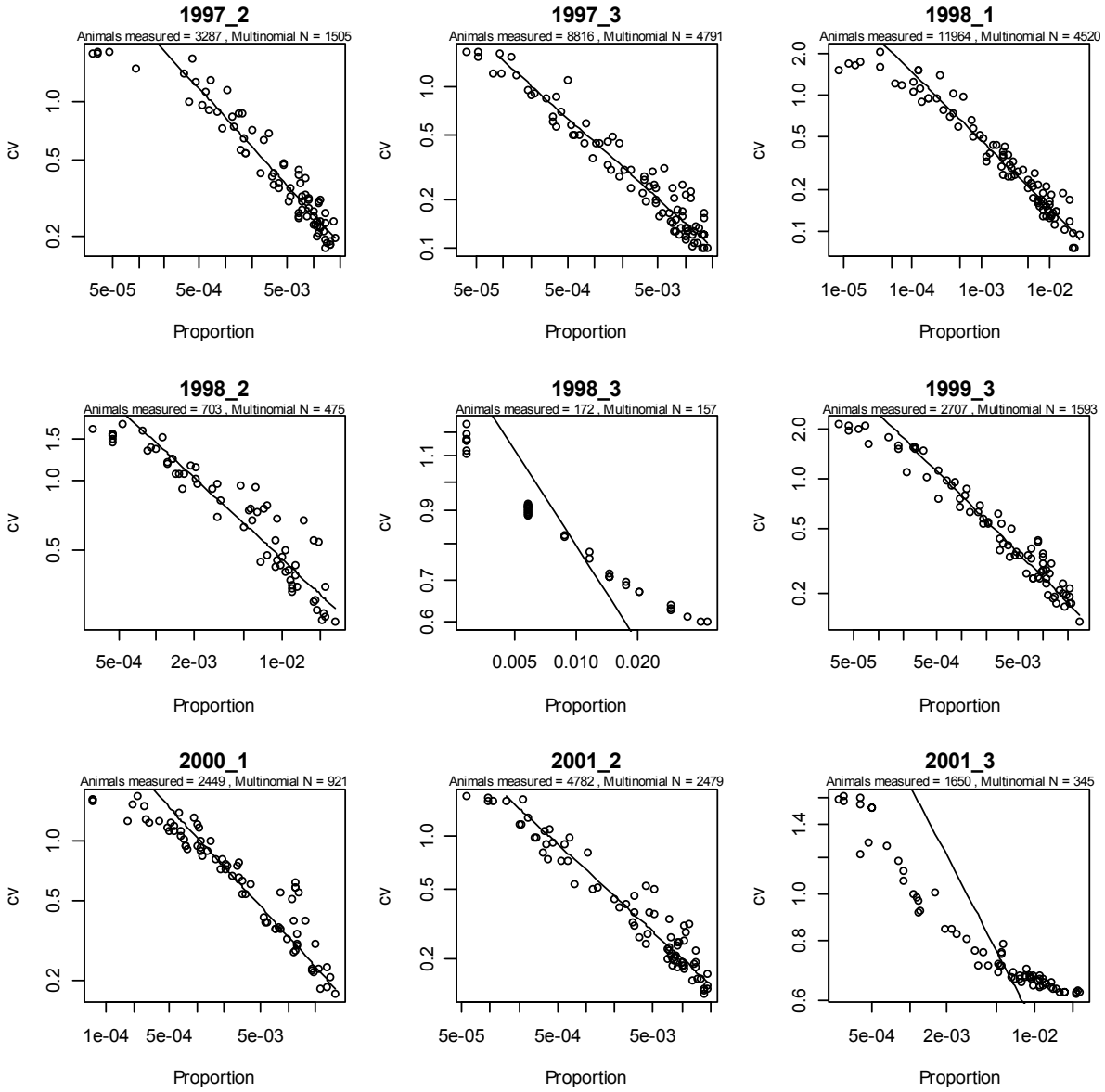

A2. 4: Observation-error CVs for the observer proportions-at-length data sets. Each point represents a proportion at a specific length and sex for a given year. The diagonal line, which is the same in each panel, is added to aid comparison between panels; it shows the relationship between proportion and CV that would hold with simple multinomial sampling with sample size 500.

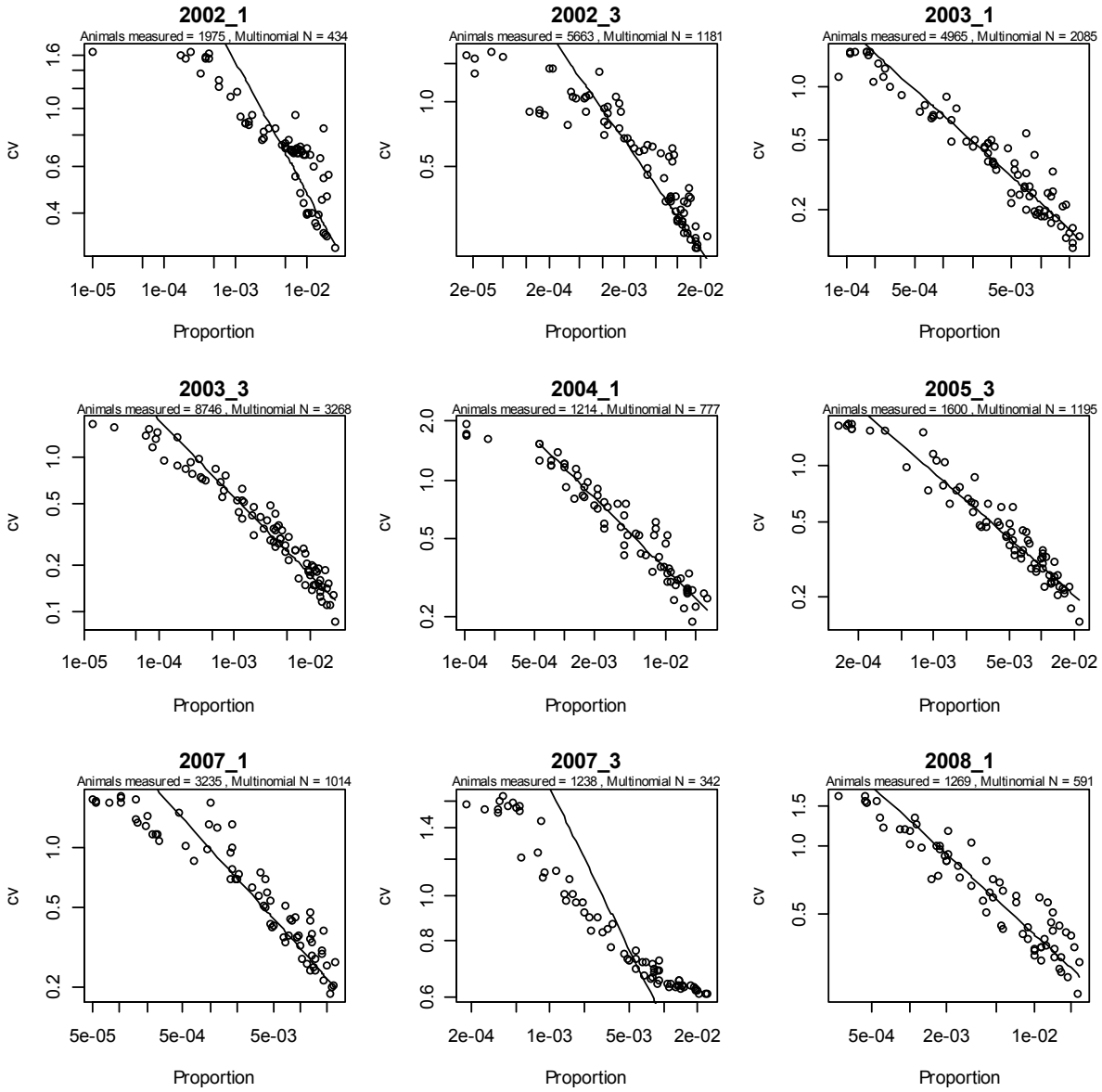

A2. 5: Observation-error CVs for the observer proportions-at-length data sets. Each point represents a proportion at a specific length and sex for a given year. The diagonal line, which is the same in each panel, is added to aid comparison between panels; it shows the relationship between proportion and CV that would hold with simple multinomial sampling with sample size 500.

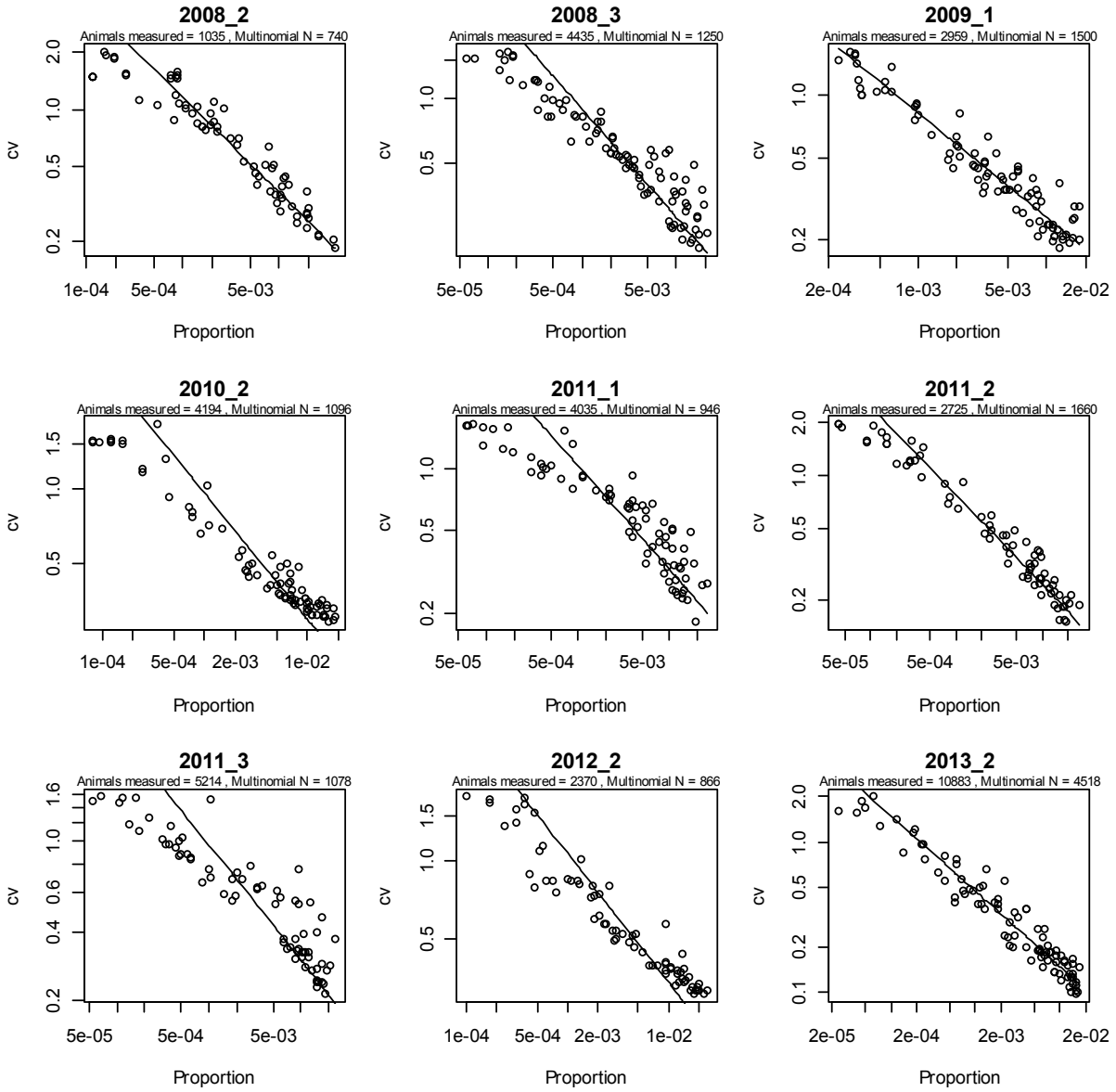

A2. 6: Observation-error CVs for the observer proportions-at-length data sets. Each point represents a proportion at a specific length and sex for a given year. The diagonal line, which is the same in each panel, is added to aid comparison between panels; it shows the relationship between proportion and CV that would hold with simple multinomial sampling with sample size 500.

Photo survey

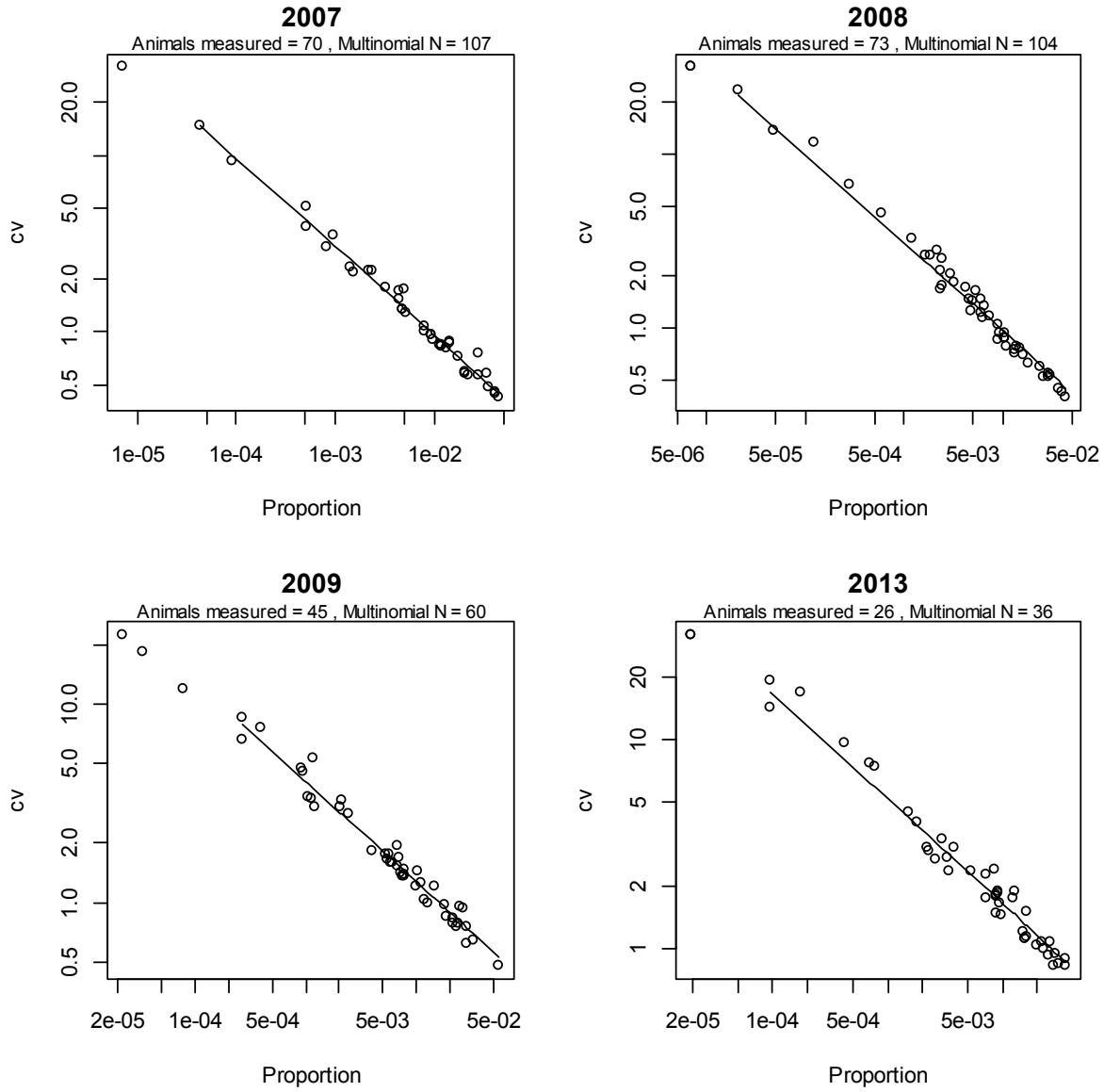

A2. 7: Observation-error CVs for the photo survey proportions-at-length data sets. Each point represents a proportion at a specific length and sex for a given year. The diagonal line, which is the same in each panel, is added to aid comparison between panels; it shows the relationship between proportion and CV that would hold with simple multinomial sampling with sample size 500.

APPENDIX 3. MODEL F_0.2

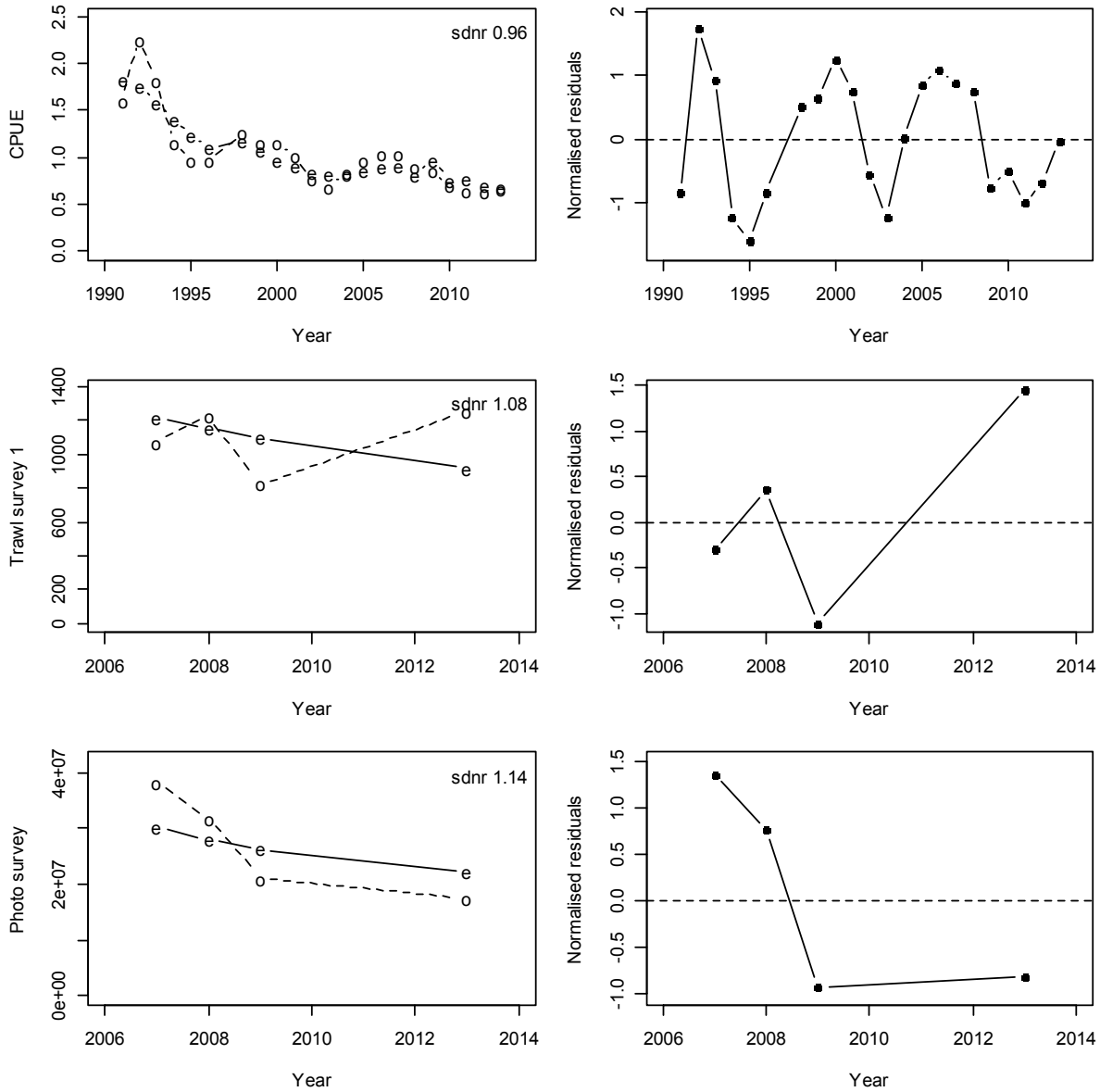

A3. 1: Fits to abundance indices (left column) and normalised residuals (right column) for standardised CPUE index (top row) trawl survey biomass index covering whole area (second row), trawl survey biomass index covering limited area (third row) and photo survey abundance index (fourth row) for SCI 6A F_0.20.

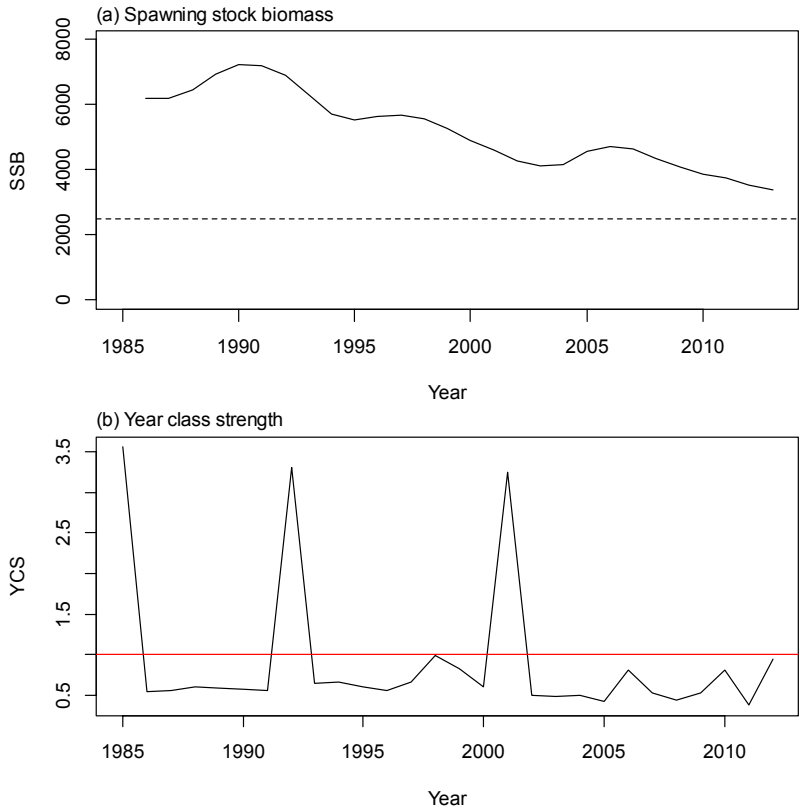

A3. 2: Spawning stock biomass trajectory (upper plot), year class strength (lower plot) for SCI 6A F_0.20.

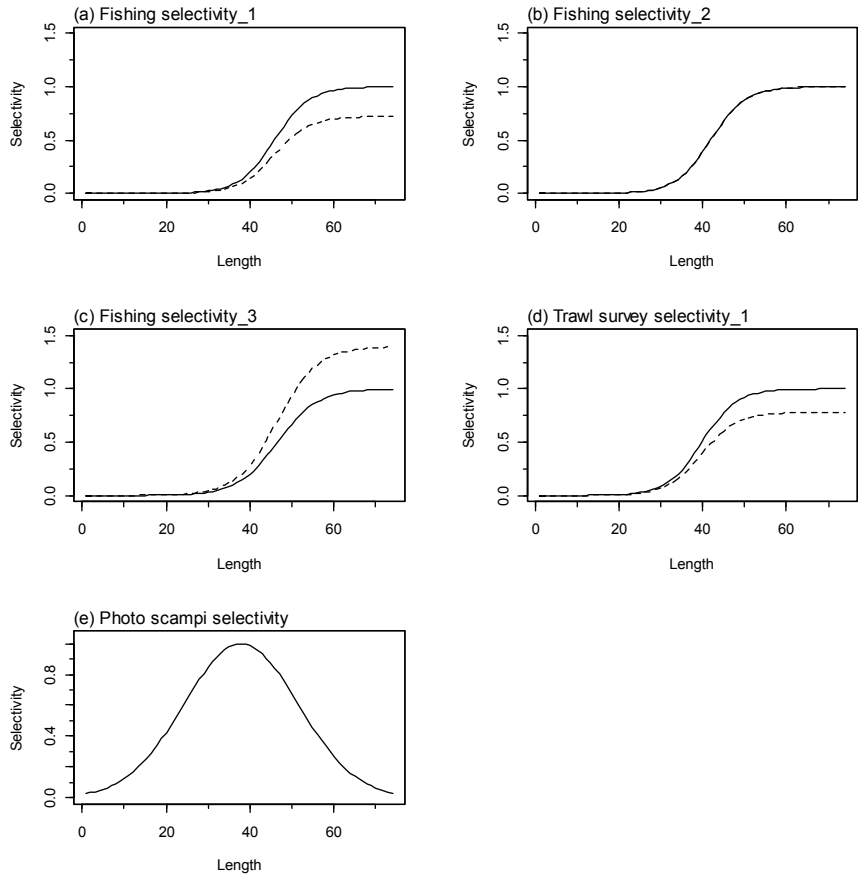

A3. 3: Fishery and survey selectivity curves. Solid line – females, dotted line – males. The scampi photo index is not sexed, and a single selectivity applies.

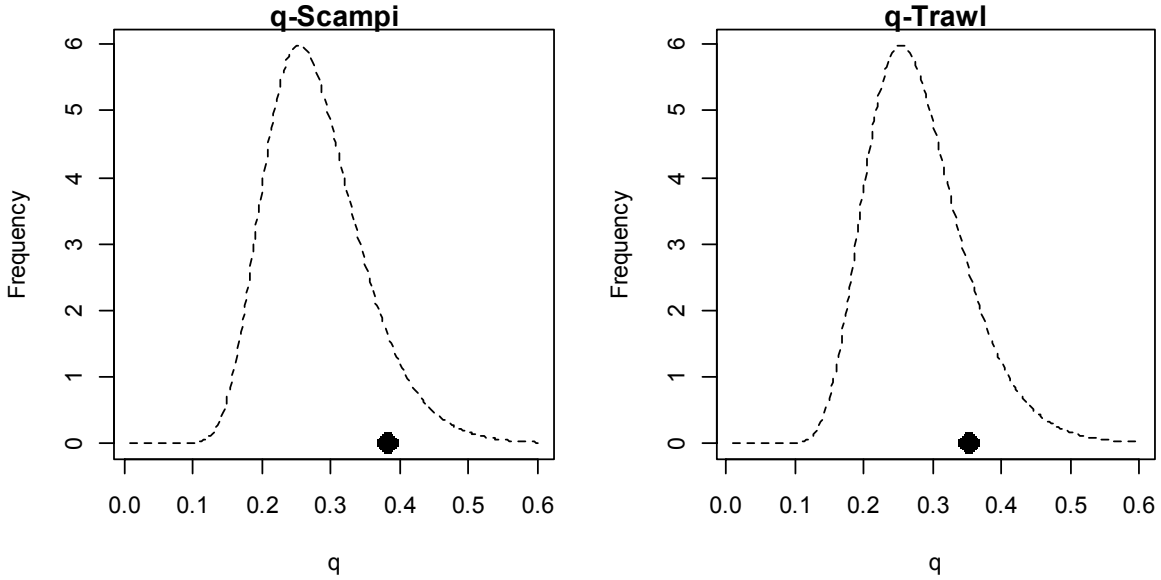

A3. 4: Catchability estimates from MPD model run, plotted in relation to prior distribution.

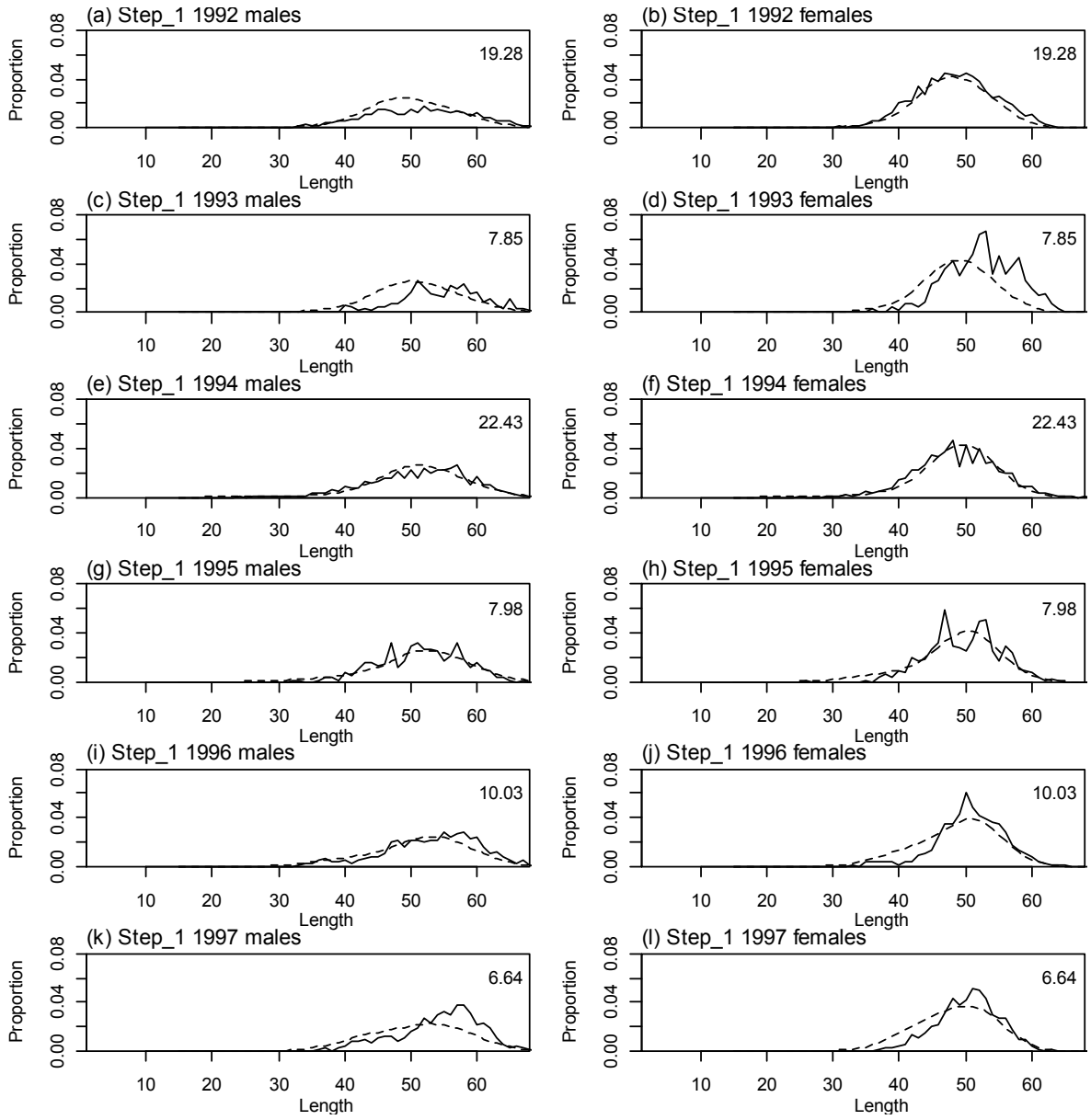

A3. 5: Observed (solid line) and fitted (dashed line) length frequency distributions for observer samples, time step 1.

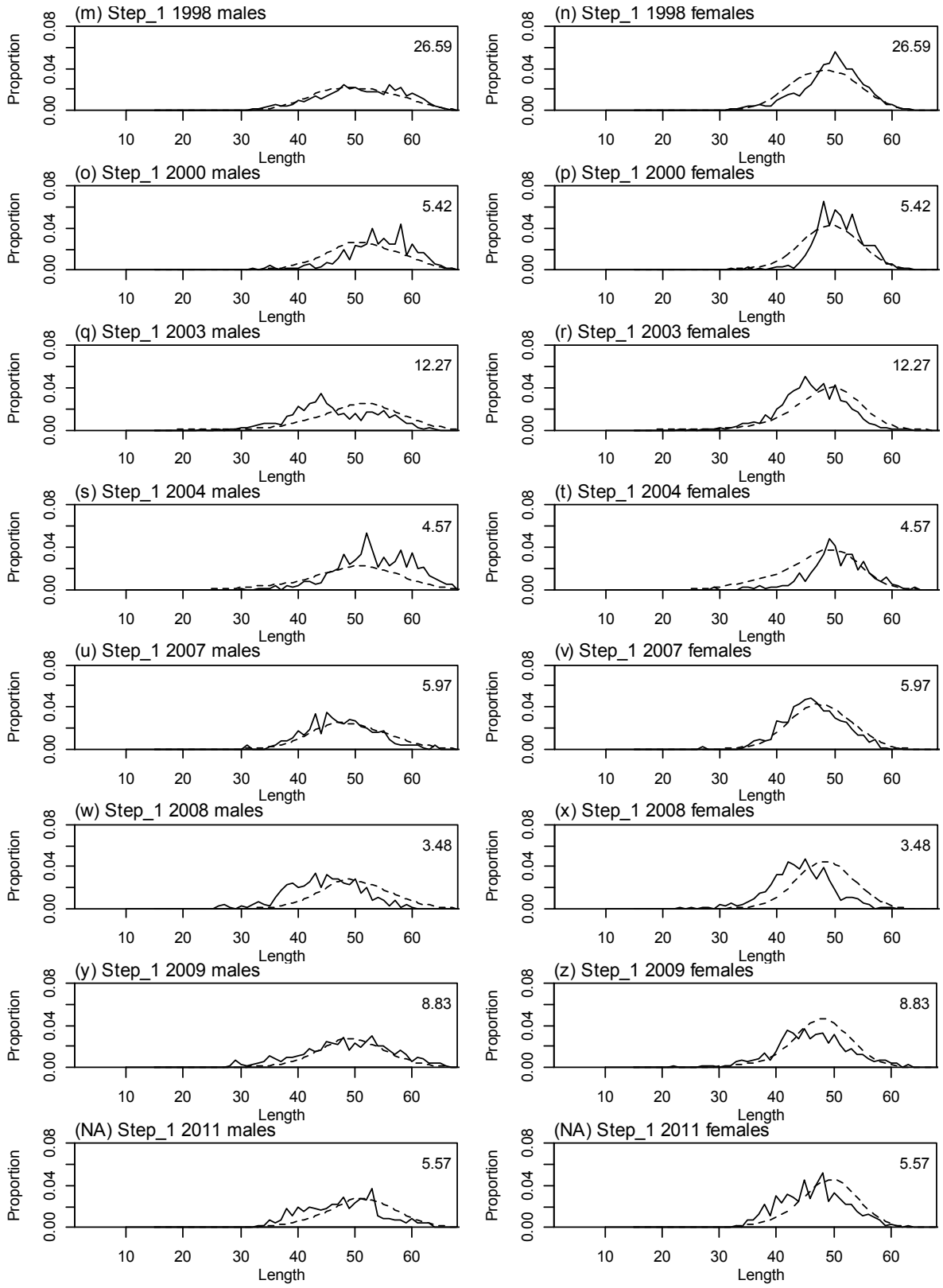

A3.5 ctd.: Observed (solid line) and fitted (dashed line) length frequency distributions for observer samples, time step 1.

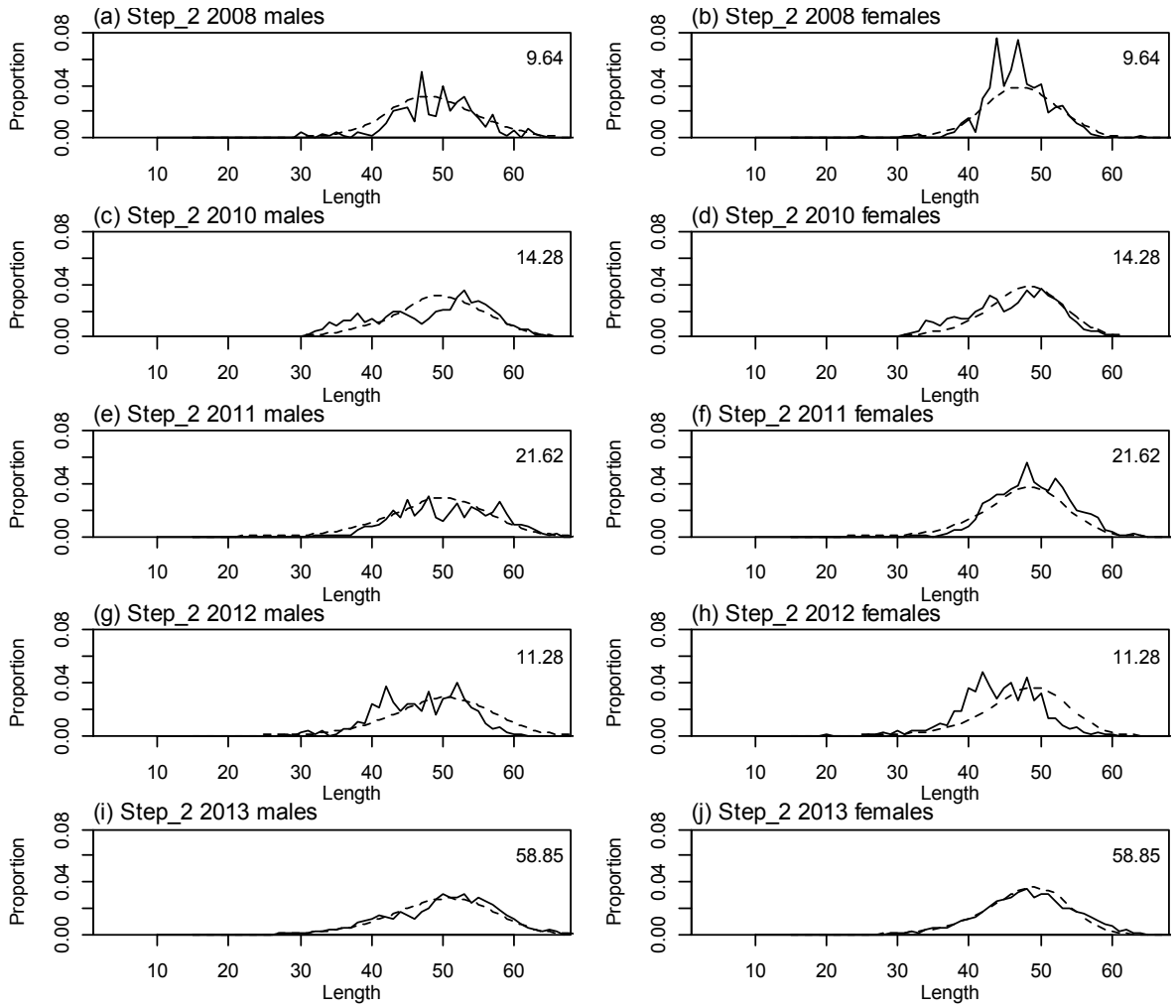

A3. 6: Observed (solid line) and fitted (dashed line) length frequency distributions for observer samples, time step 2.

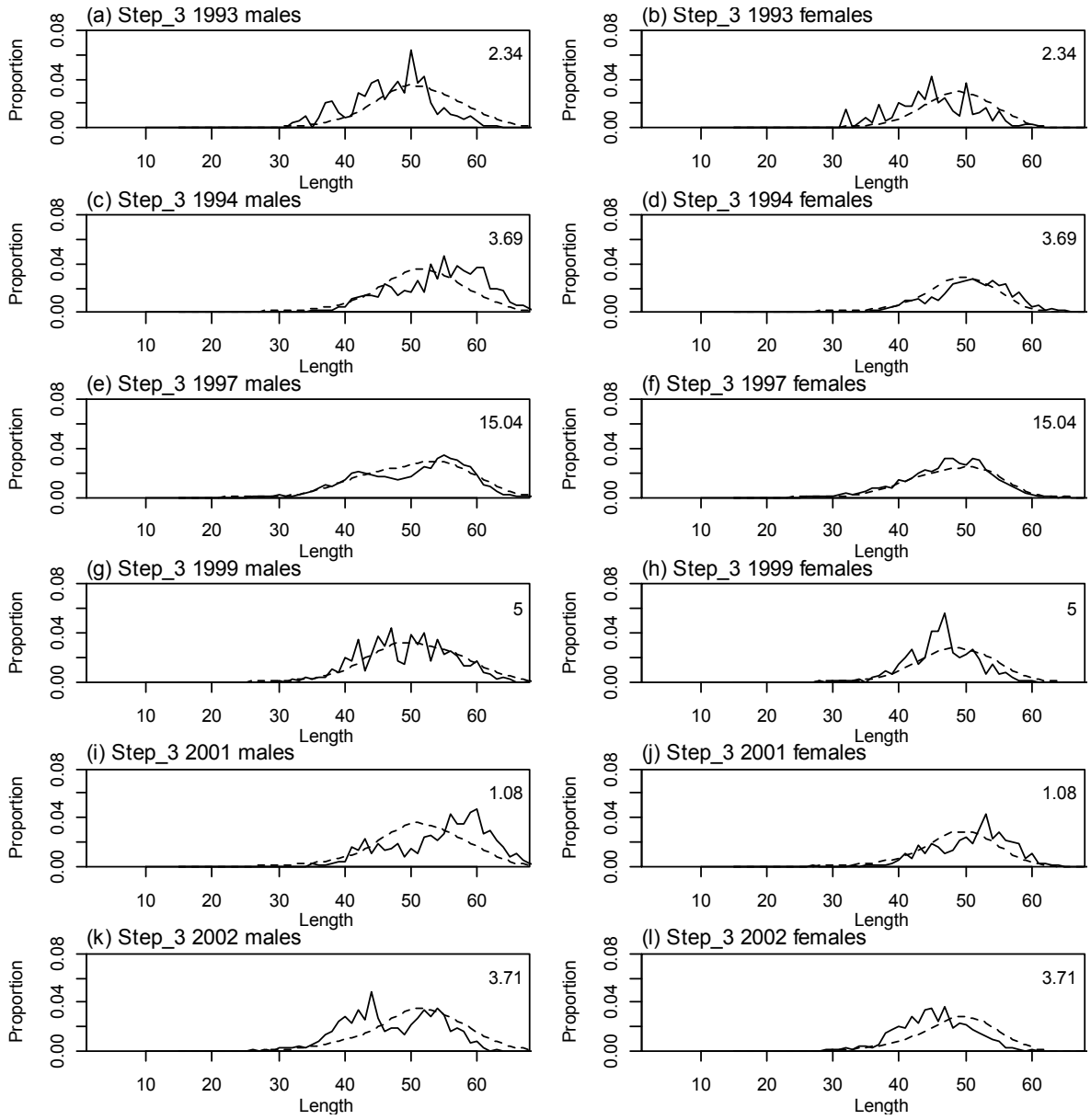

A3. 7: Observed (solid line) and fitted (dashed line) length frequency distributions for observer samples, time step 3.

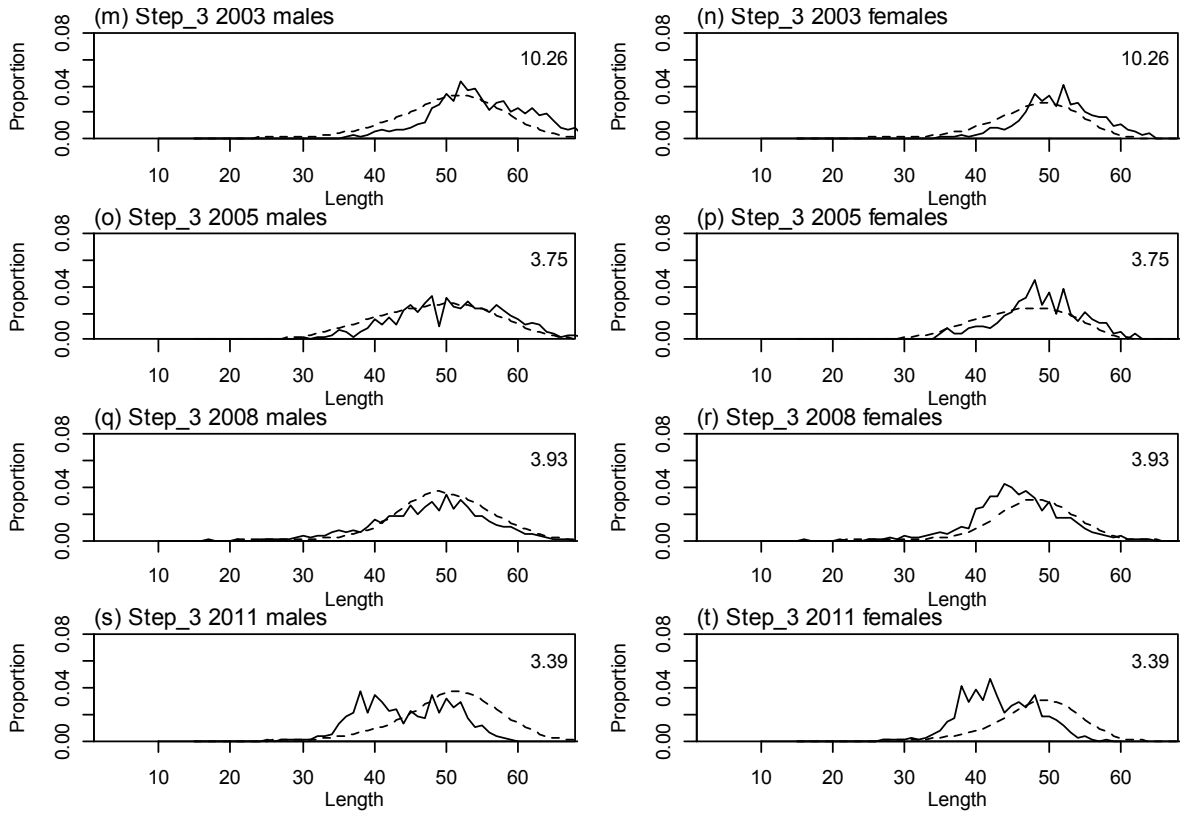

A3.7 ctd.: Observed (solid line) and fitted (dashed line) length frequency distributions for observer samples, time step 3.

A3. 8: Numbers of scampi measured, estimated multinomial N sample size, and effective sample size used within the model for length frequency distributions for observer samples, time step 1.

	Measured	Multinomial N	Effective sample size
N_1992	9250	3276	19.27
N_1993	2641	1334	7.84
N_1994	9300	3813	22.43
N_1995	2600	1357	7.98
N_1996	3200	1704	10.02
N_1997	2794	1129	6.64
N_1998	11964	4520	26.59
N_2000	2449	921	5.42
N_2002	1975	434	2.55
N_2003	4965	2085	12.27
N_2004	1214	777	4.57
N_2007	3235	1014	5.97
N_2008	1269	591	3.48
N_2009	2959	1500	8.82
N_2011	4035	946	5.57

A3. 9: Numbers of scampi measured, estimated multinomial N sample size, and effective sample size used within the model for length frequency distributions for observer samples, time step 2.

	Measured	Multinomial N	Effective sample size
N_1997	3287	1505	19.60
N_1998	703	475	6.19
N_2001	4782	2479	32.29
N_2008	1035	740	9.64
N_2010	4194	1096	14.27
N_2011	2725	1660	21.62
N_2012	2370	866	11.28
N_2013	10883	4518	58.85

A3. 10: Numbers of scampi measured, estimated multinomial N sample size, and effective sample size used within the model for length frequency distributions for observer samples, time step 3.

	Measured	Multinomial N	Effective sample size
N_1993	1264	745	2.34
N_1994	1960	1174	3.69
N_1996	2035	686	2.15
N_1997	8816	4791	15.04
N_1998	172	157	0.49
N_1999	2707	1593	5.00
N_2001	1650	345	1.08
N_2002	5663	1181	3.71
N_2003	8746	3268	10.26
N_2005	1600	1195	3.75
N_2007	1238	342	1.07
N_2008	4435	1250	3.92
N_2011	5214	1078	3.38

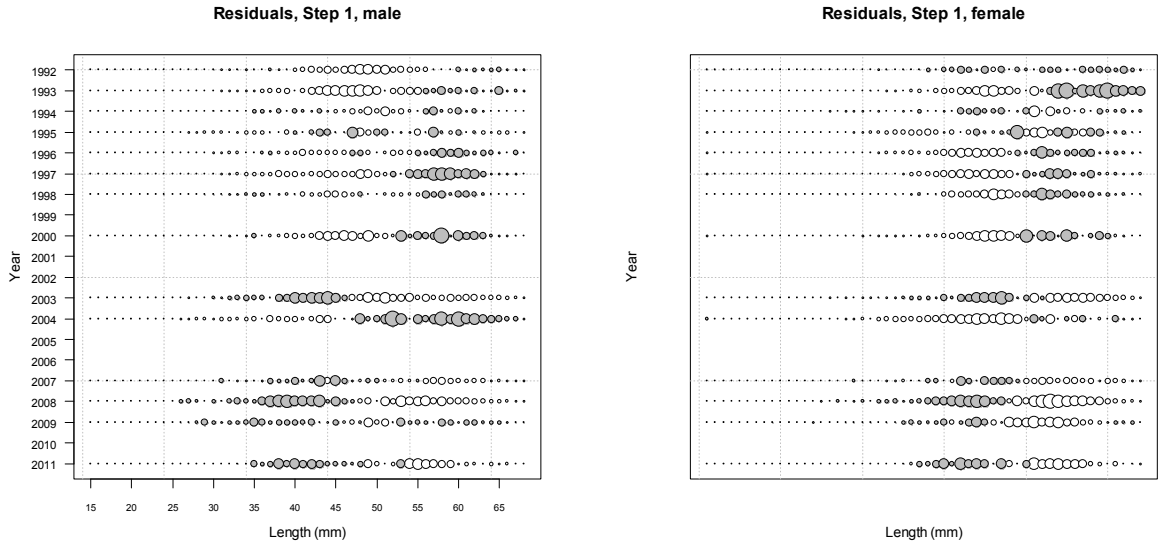

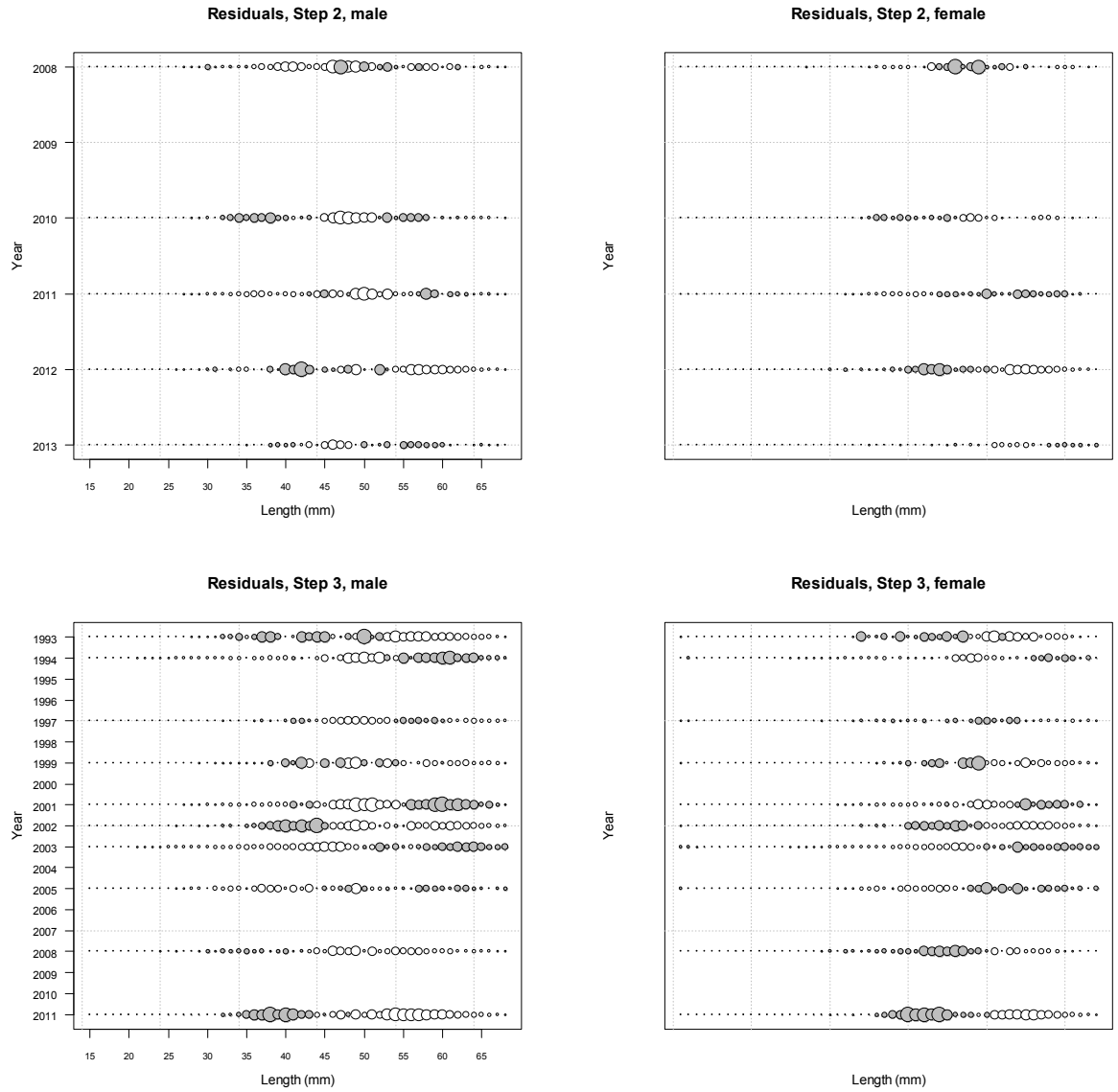

A3. 11: Bubble plots of residuals for fits to length frequency distributions for observer sampling.

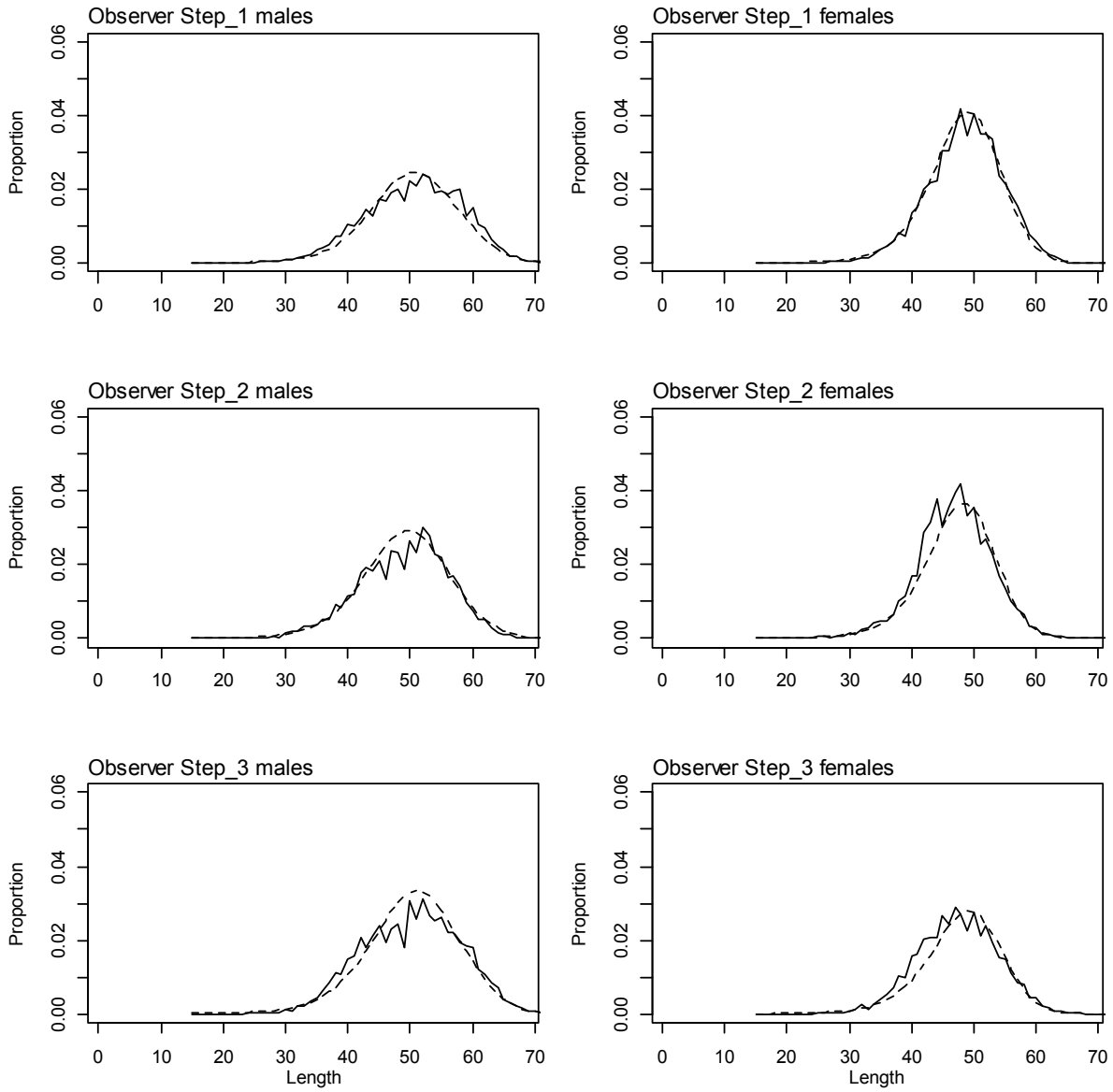

A3. 12: Average observed (solid line) and fitted (dashed line) length frequency distributions for observer samples.

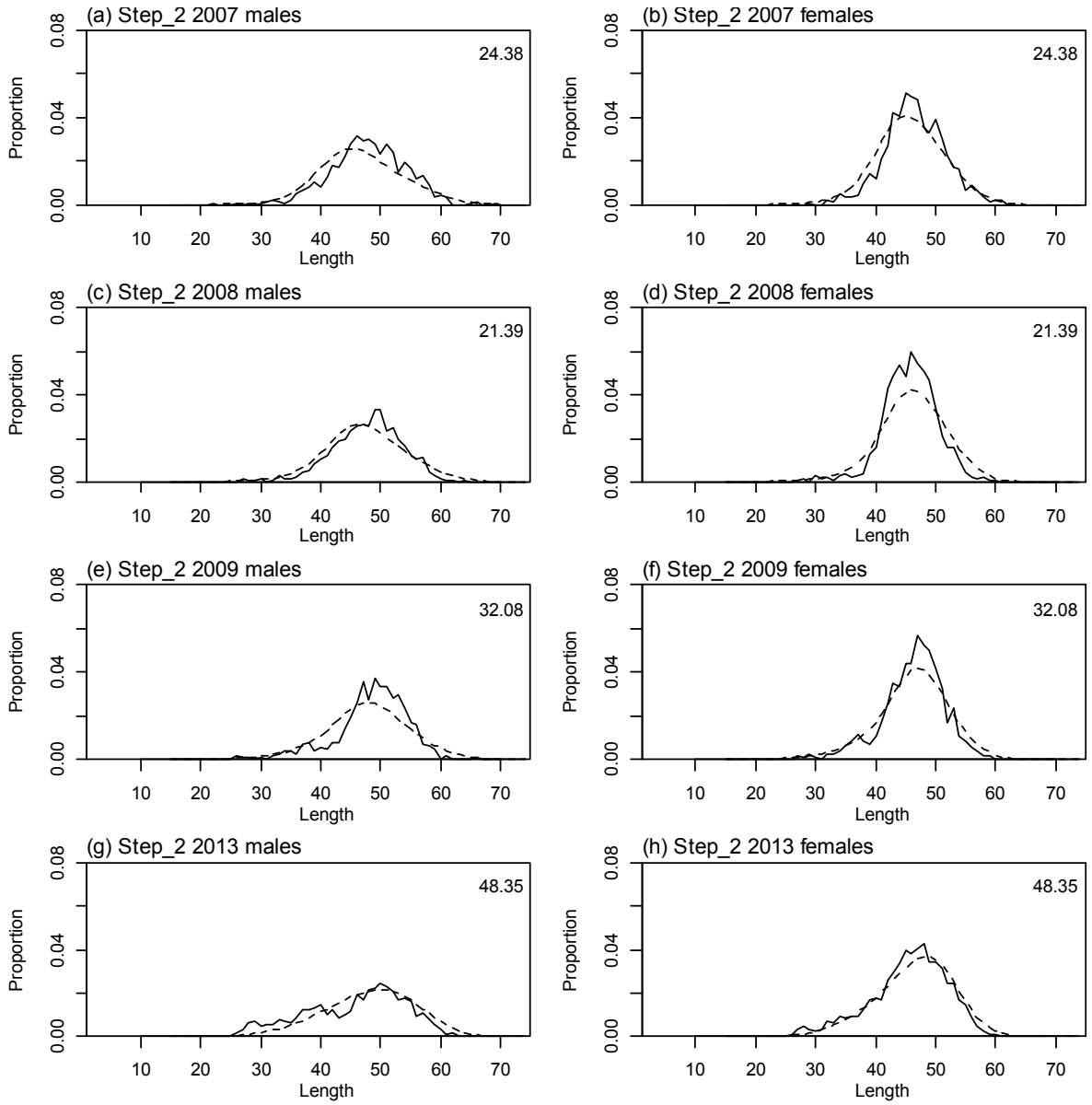

A3. 13: Observed (solid line) and fitted (dashed line) length frequency distributions for research survey samples.

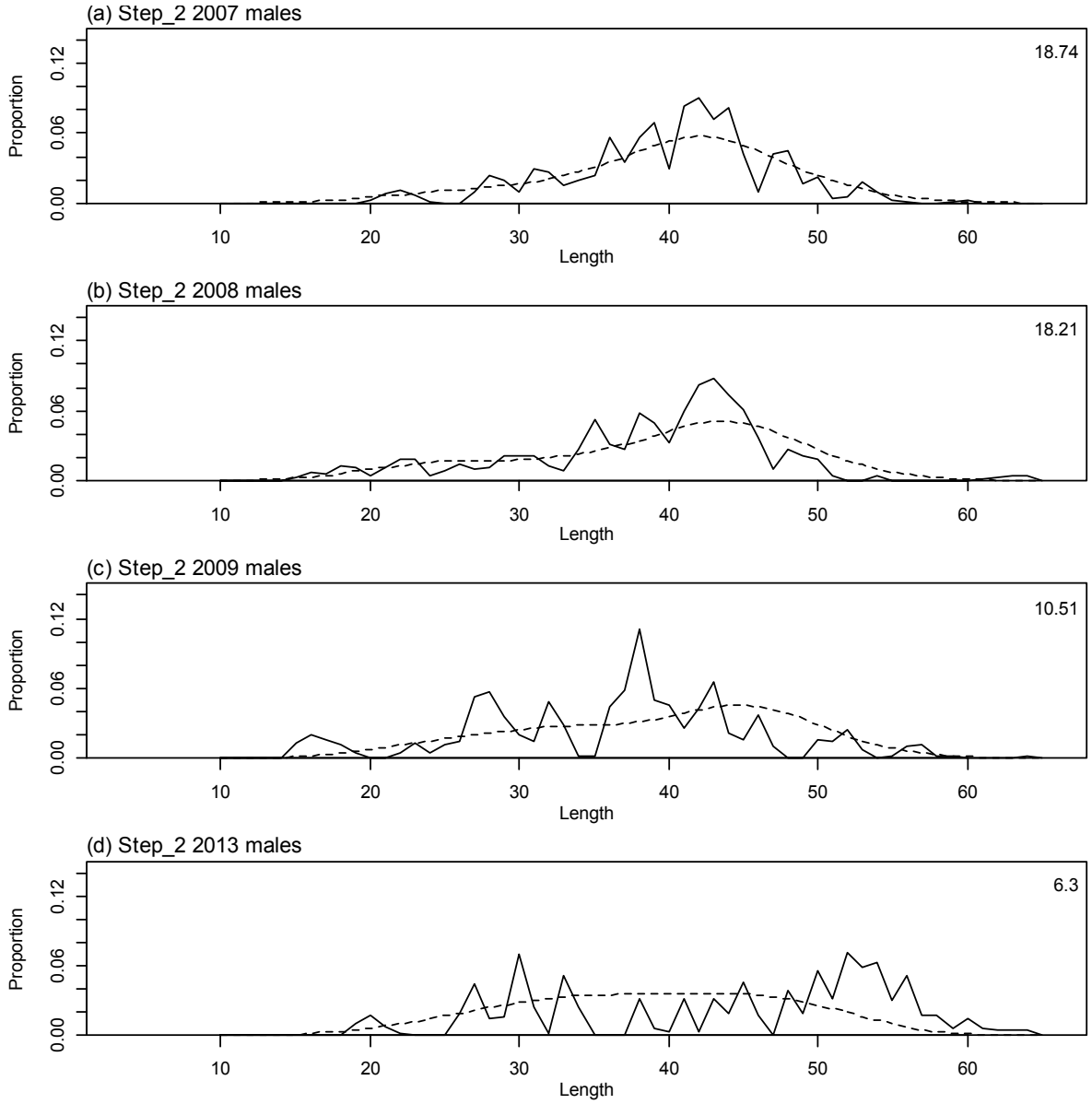

A3. 14: Observed (solid line) and fitted (dashed line) length frequency distributions for photographic survey scampi size estimation.

A3. 15: Numbers of scampi measured, estimated multinomial N sample size, and effective sample size used within the model for length frequency distributions for research survey samples.

	Measured	Multinomial N	Effective sample size
N_2007	1981	2127	24.38
N_2008	2291	1866	21.39
N_2009	4054	2798	32.08
N_2013	4808	4218	48.35

A3. 16: Numbers of scampi measured, estimated multinomial N sample size, and effective sample size used within the model for length frequency distributions for photographic survey samples.

	Measured	Multinomial N	Effective sample size
N_2007	70	107	18.74
N_2008	73	104	18.21
N_2009	45	60	10.51
N_2013	26	36	6.30

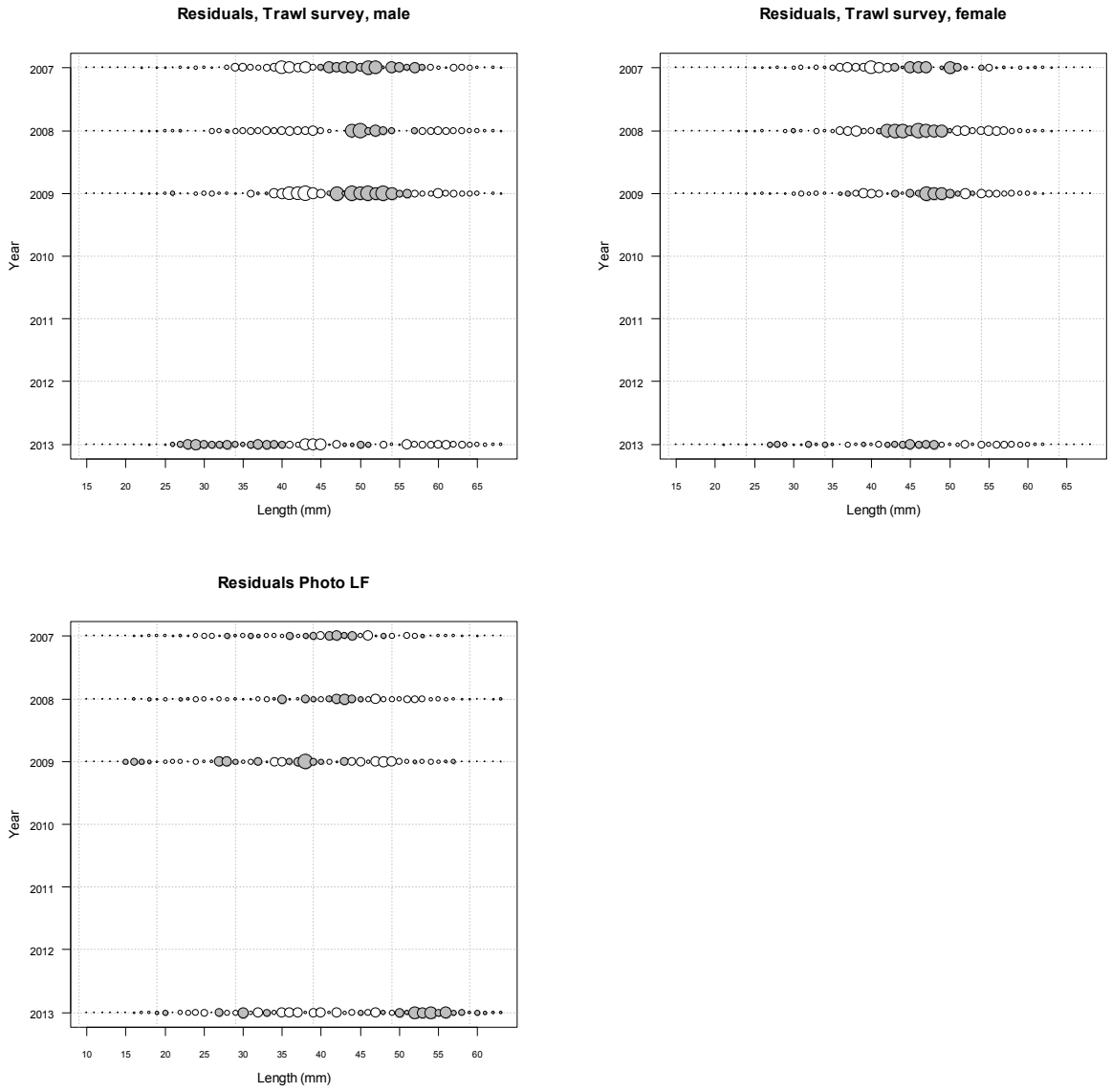

A3. 17: Bubble plots of residuals for fits to length frequency distributions for trawl survey sampling and photographic survey scampi size estimation.

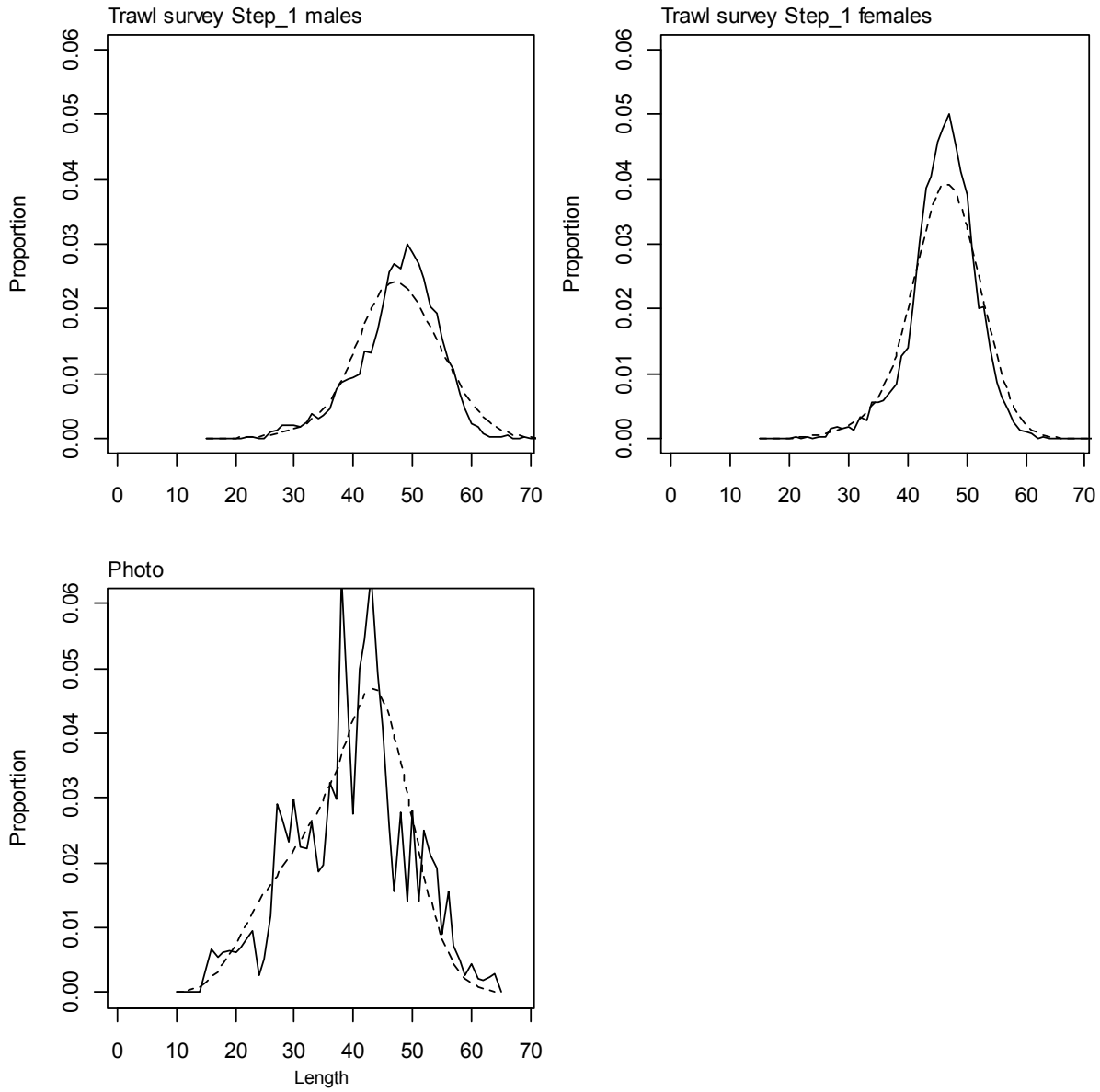

A3. 18: Average observed (solid line) and fitted (dashed line) length frequency distributions for trawl survey sampling and photographic survey scampi size estimation.

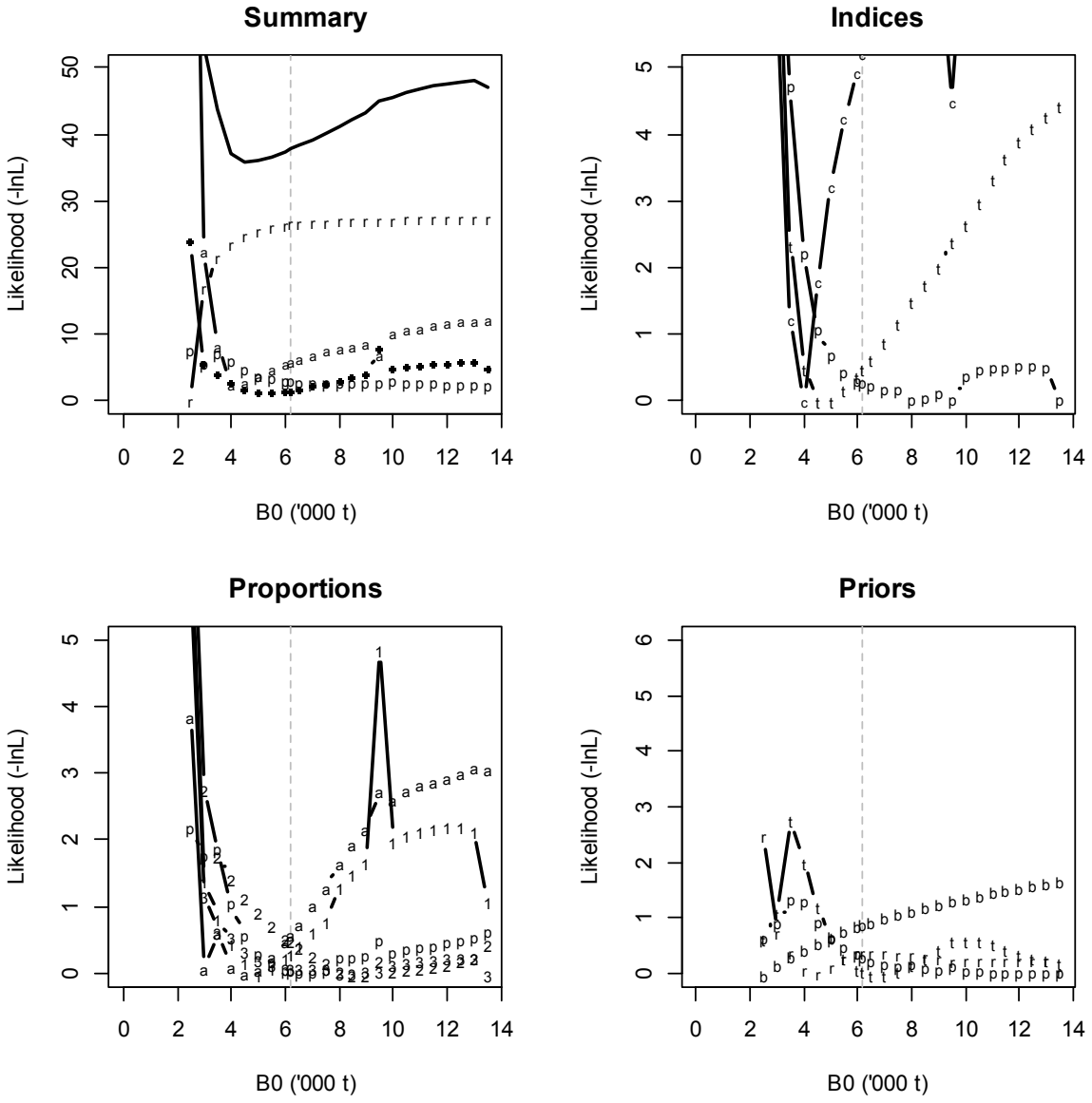

A3. 19: Likelihood profiles for the F_0.25 model for SCI 6A when B_0 is fixed in the model. Figures show profiles for main priors (top left, p – priors, a - abundance indices, • – proportions at length, r – recapture data), abundance indices (top right, t - trawl survey, c - CPUE, p – photo survey), proportion at length data (bottom left, a-trawl, 1 – observer time step 1, 2 – observer time step 2, 3 – observer time step 3, p - photo) and priors (bottom right, b- B_0, YCS - r, p- *q-Photo*, t – *q-Trawl*). Vertical dashed line represents MPD.

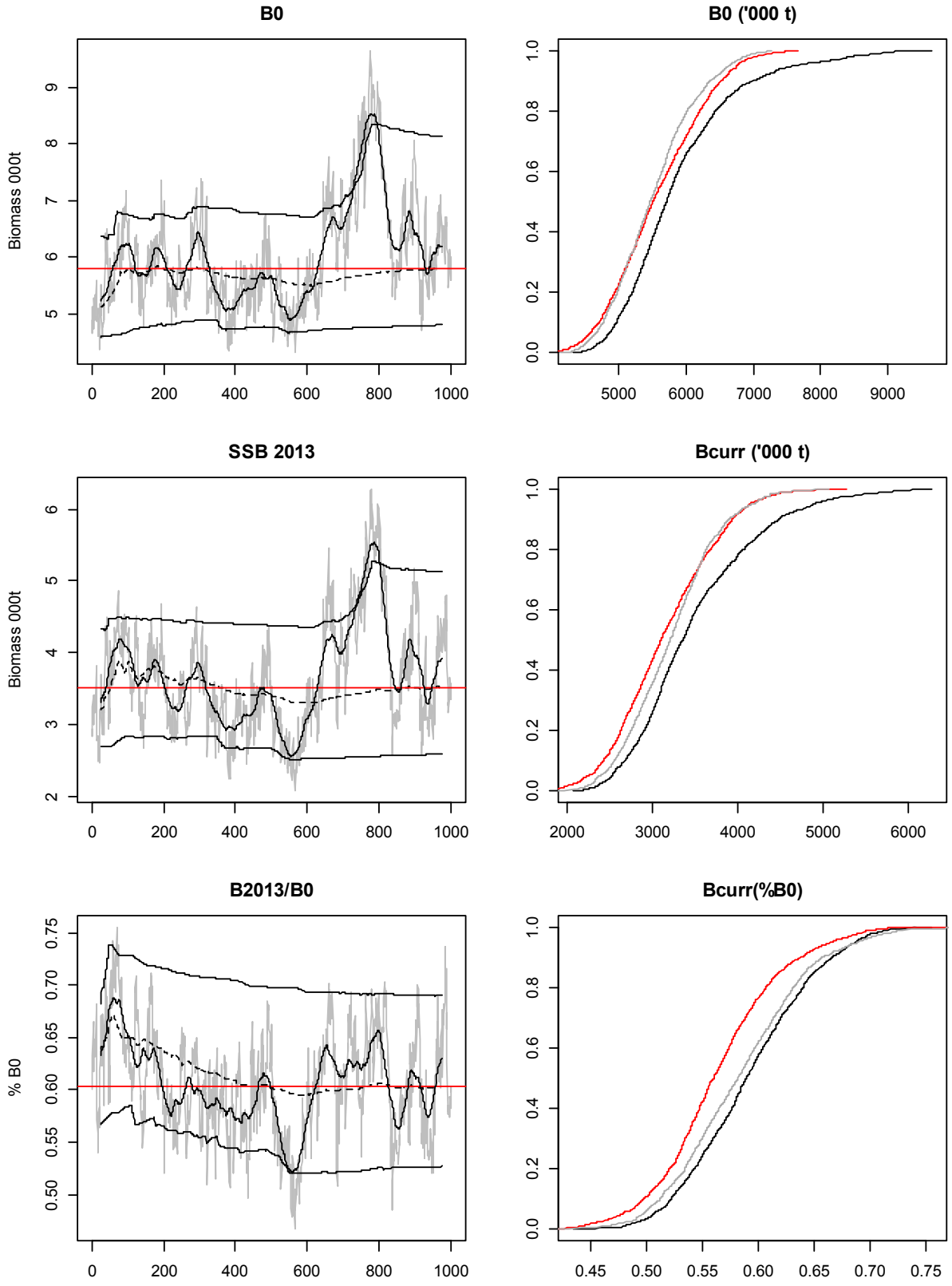

A3. 20: MCMC traces for B_0, SSB_{2013}, and SSB_{2013}/B_0 terms for the F_0.2 model for SCI 6A (trace – grey line, cumulative moving median –dashed black line, moving average and cumulative moving 2.5%, 97.5% quantiles – solid black lines, overall median – solid red line, left plots), along with cumulative frequency distributions for three independent MCMC chains (shown as red, grey and black lines, right plots).

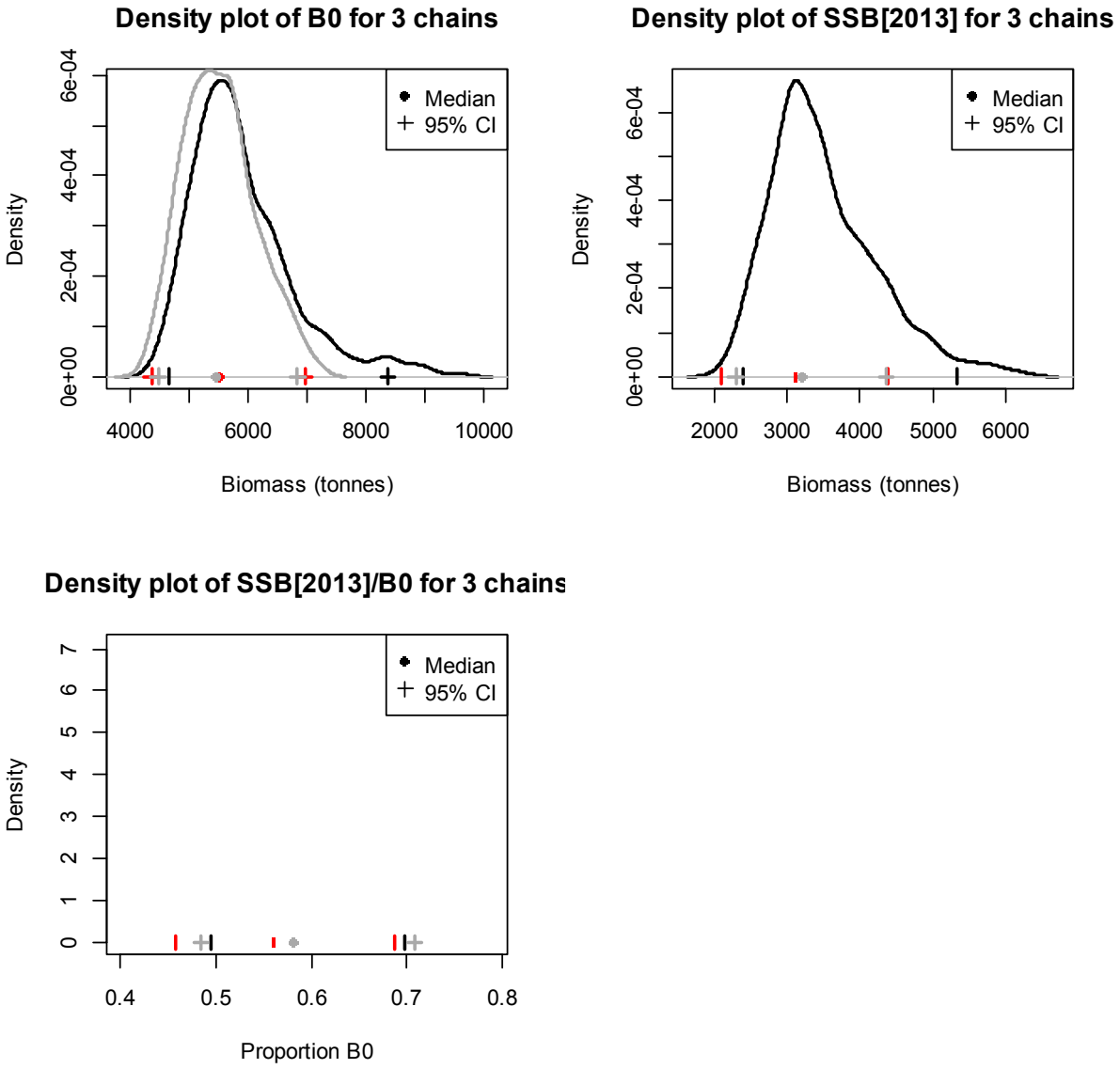

A3. 21: Density plots for B_0, SSB_{2013}, and SSB_{2013}/B_0 terms for the F_0.2 model for SCI 6A for three independent MCMC chains, with median and 95% confidence intervals.

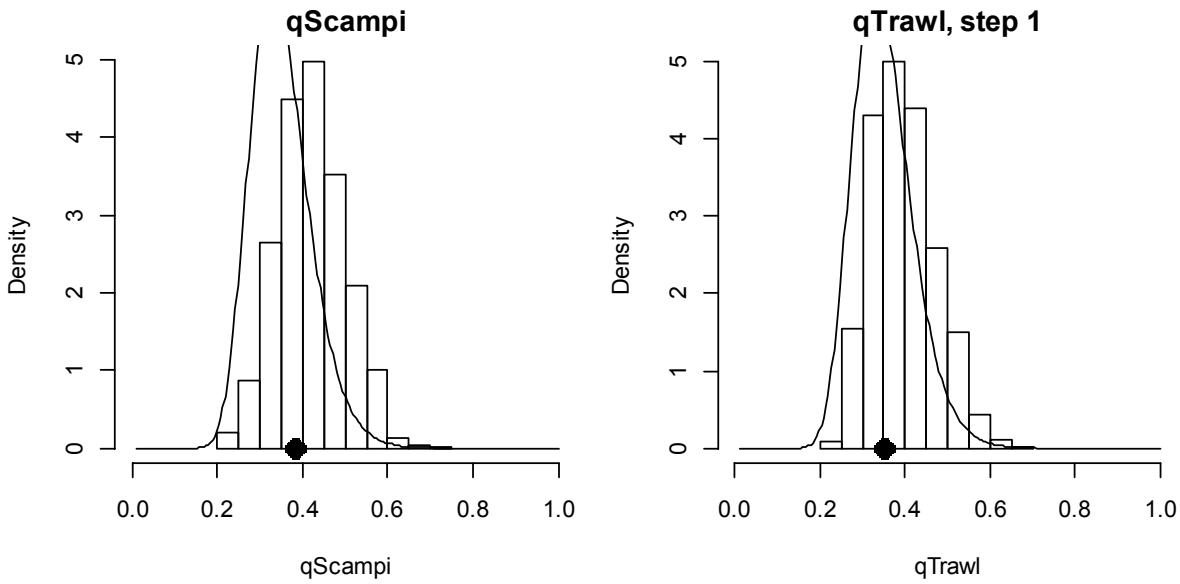

A3. 22: Marginal posterior distributions (histograms), MPD estimates (solid symbols) and distributions of priors (lines) for catchability terms.

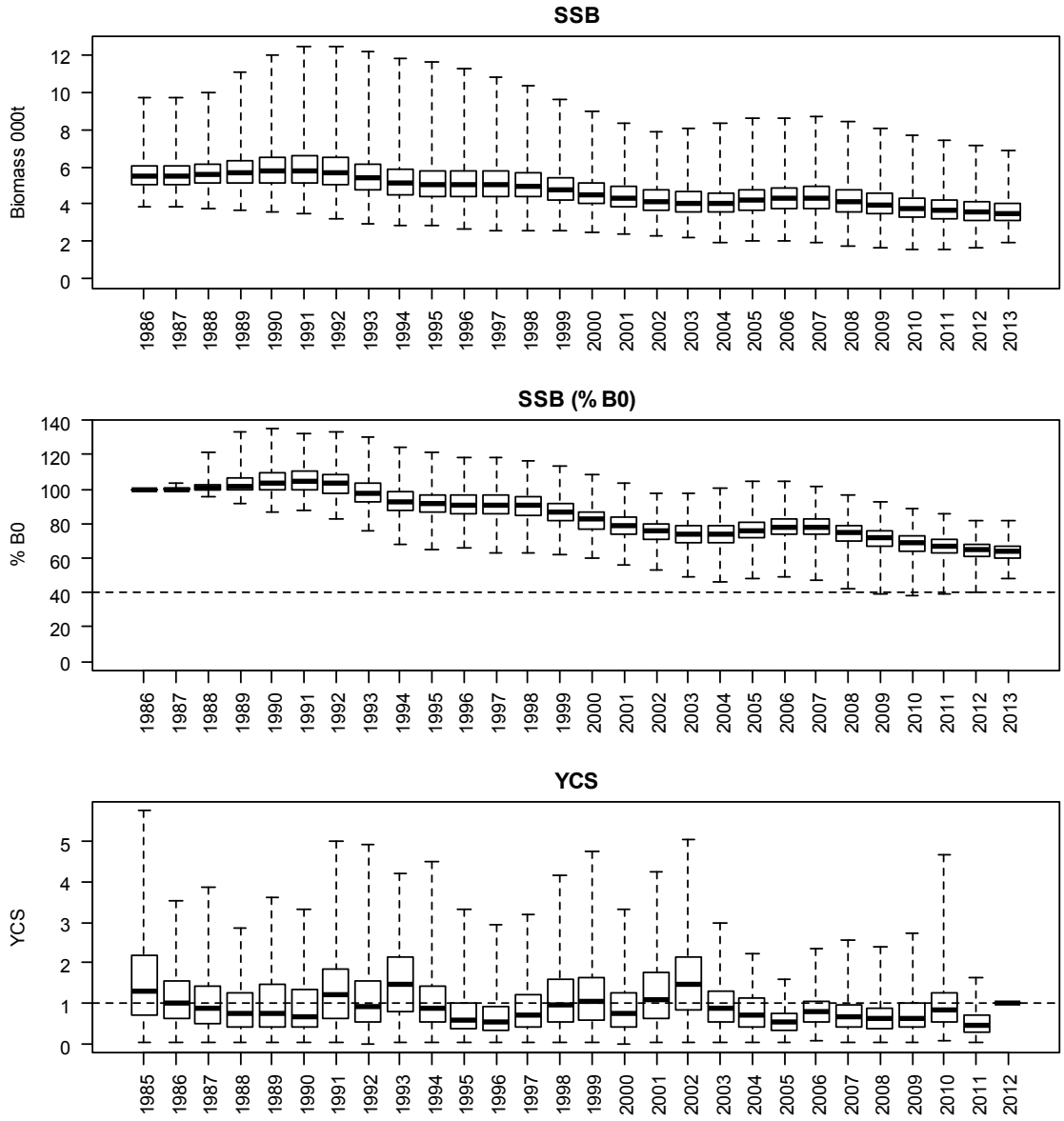

A3. 23: Posterior trajectory of SSB, SSB_{2013}/B_0 and YCS.

APPENDIX 4. MODEL F_0.25

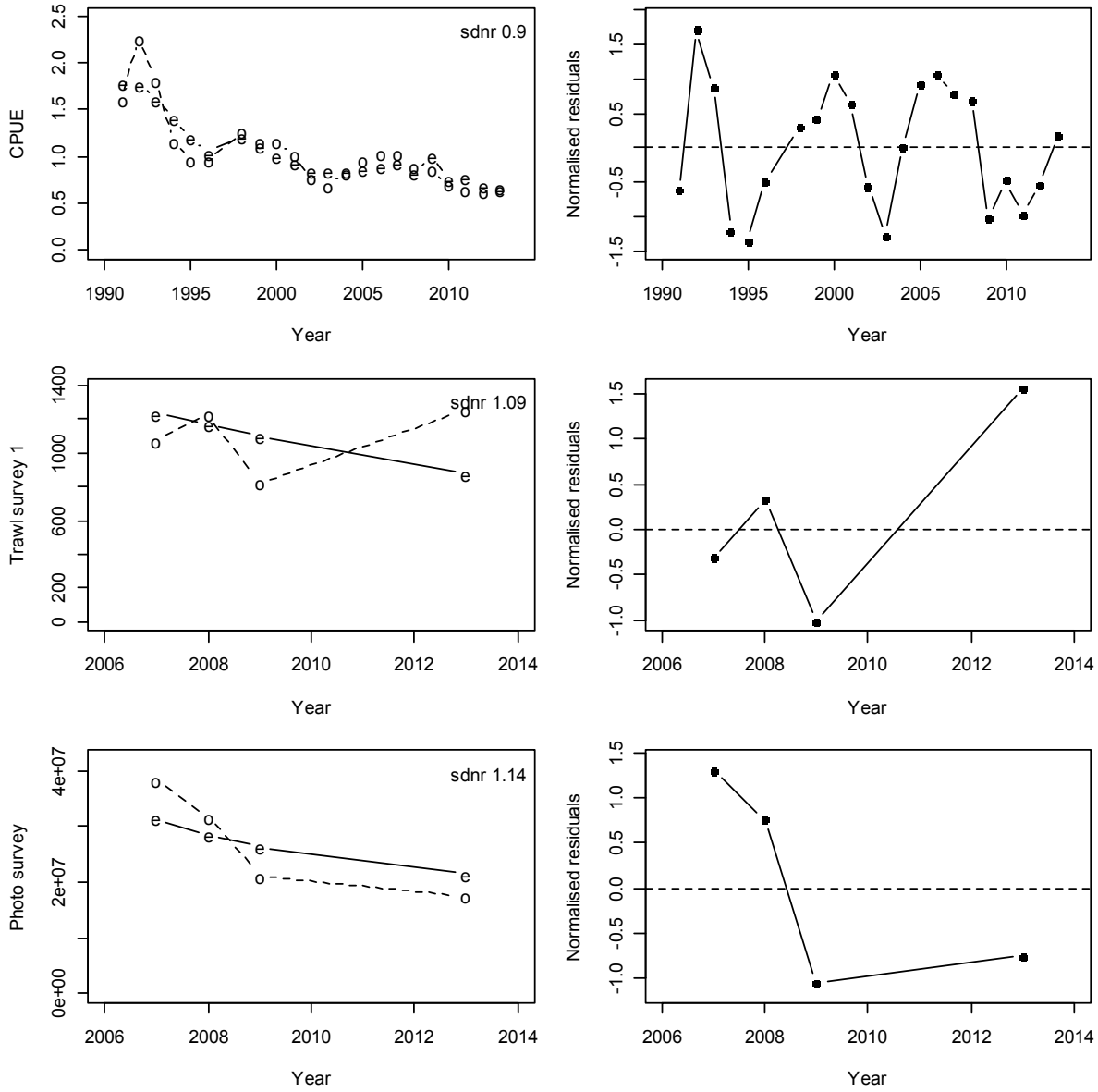

A4. 1: Fits to abundance indices (left column) and normalised residuals (right column) for standardised CPUE index (top row) trawl survey biomass index covering whole area (second row), trawl survey biomass index covering limited area (third row) and photo survey abundance index (fourth row) for SCI 6A F_0.25.

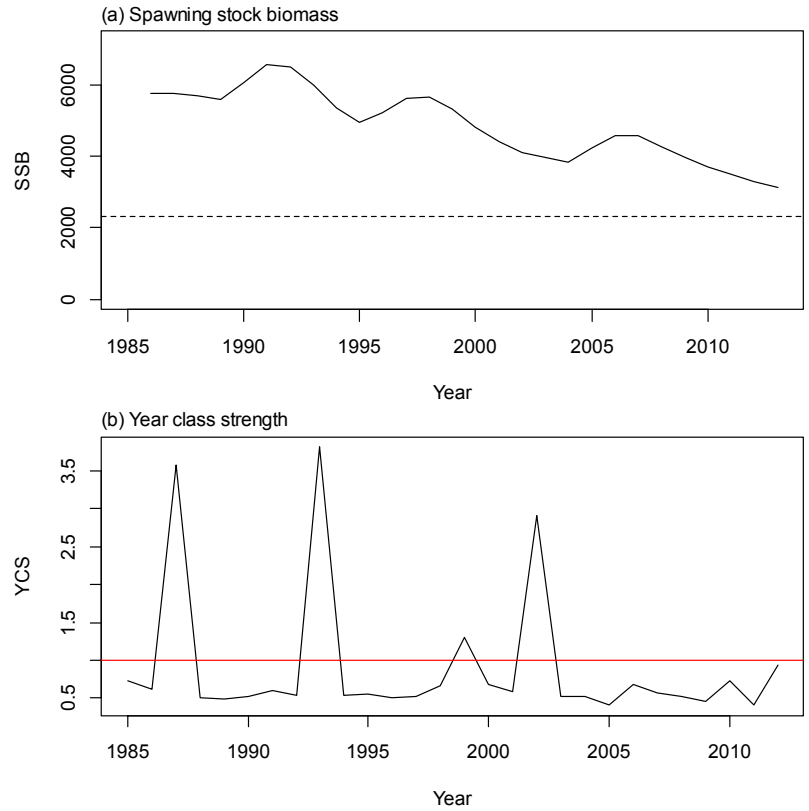

A4. 2: Spawning stock biomass trajectory (upper plot), year class strength (lower plot) for SCI 6A F_0.25.

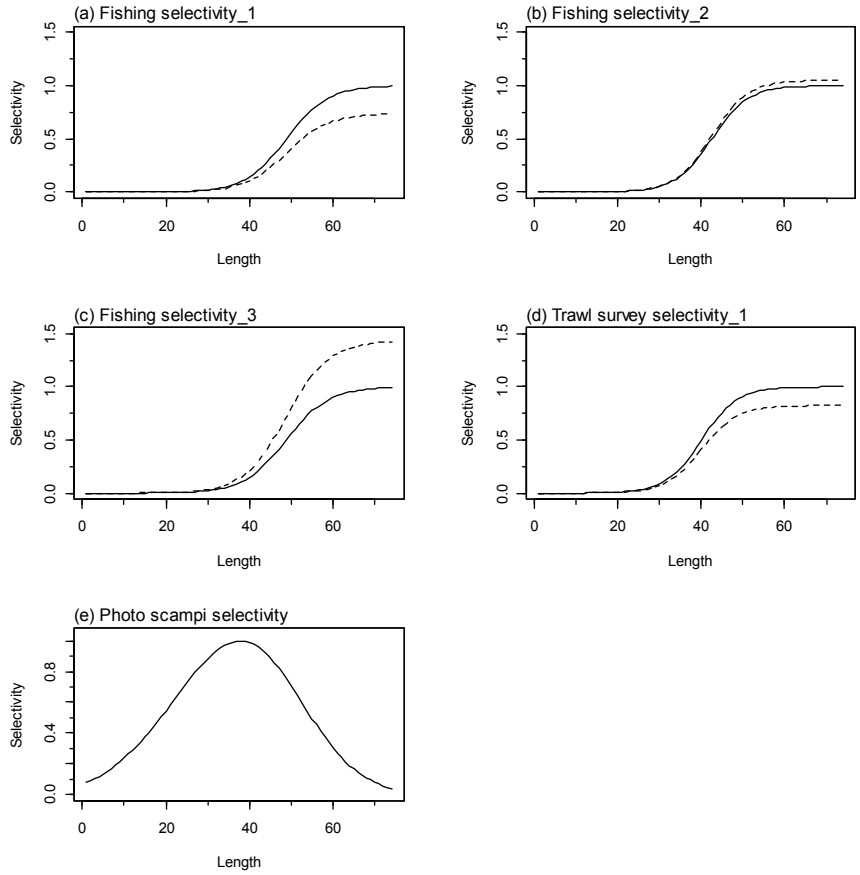

A4. 3: Fishery and survey selectivity curves. Solid line – females, dotted line – males. The scampi photo index is not sexed, and a single selectivity applies.

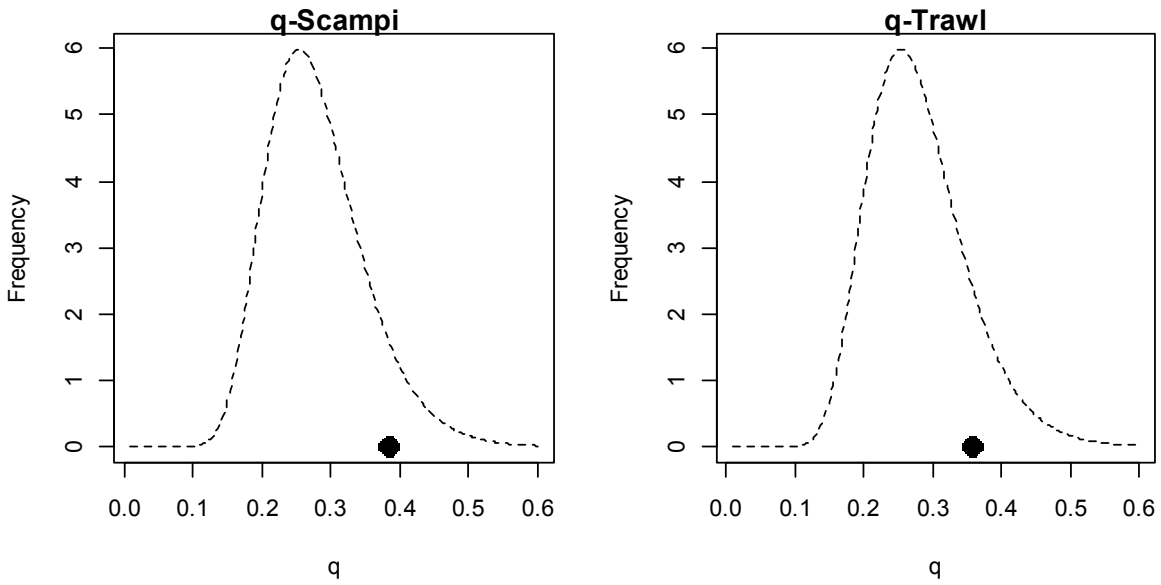

A4. 4: Catchability estimates from MPD model run, plotted in relation to prior distribution.

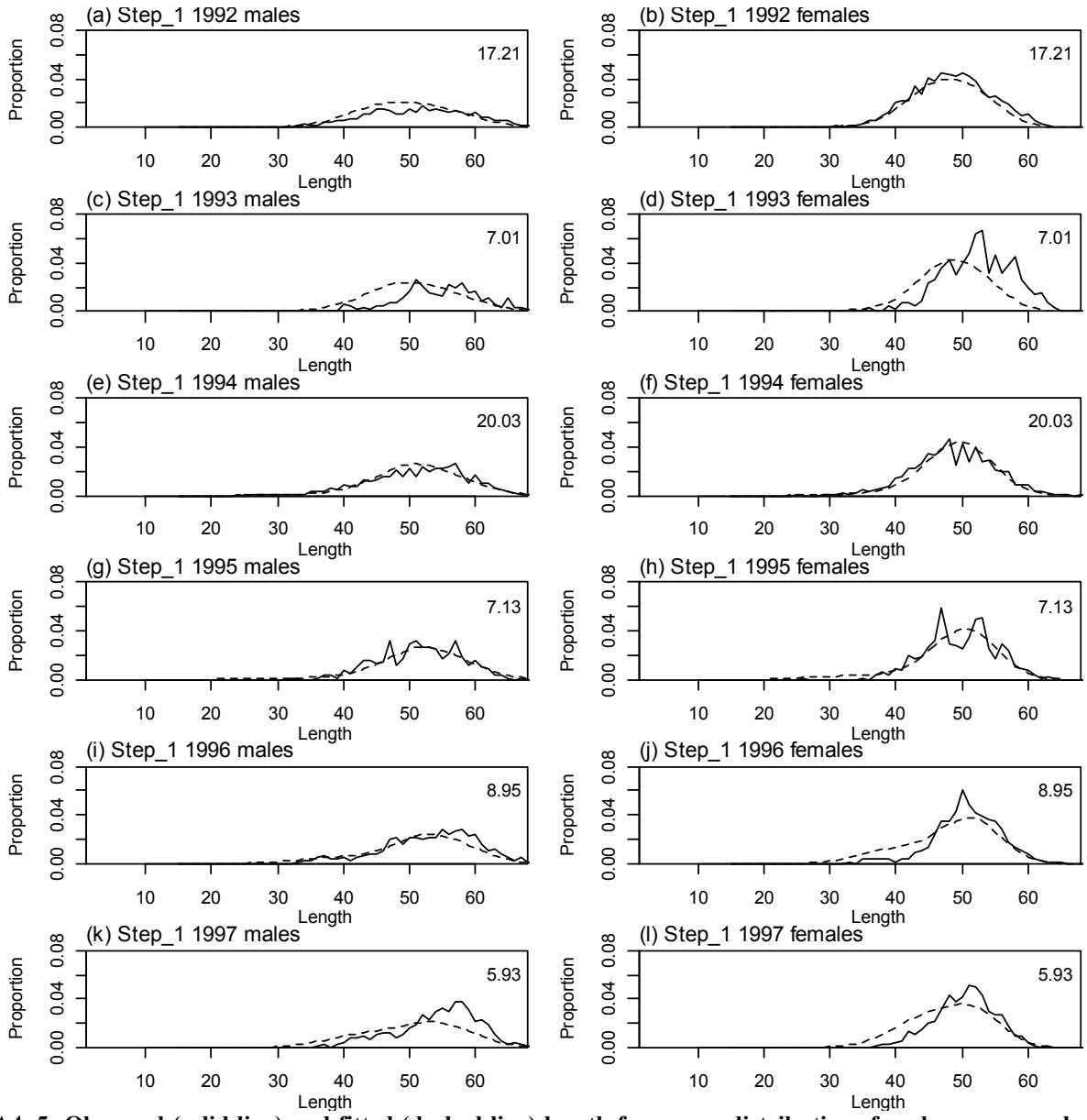

A4. 5: Observed (solid line) and fitted (dashed line) length frequency distributions for observer samples, time step 1.

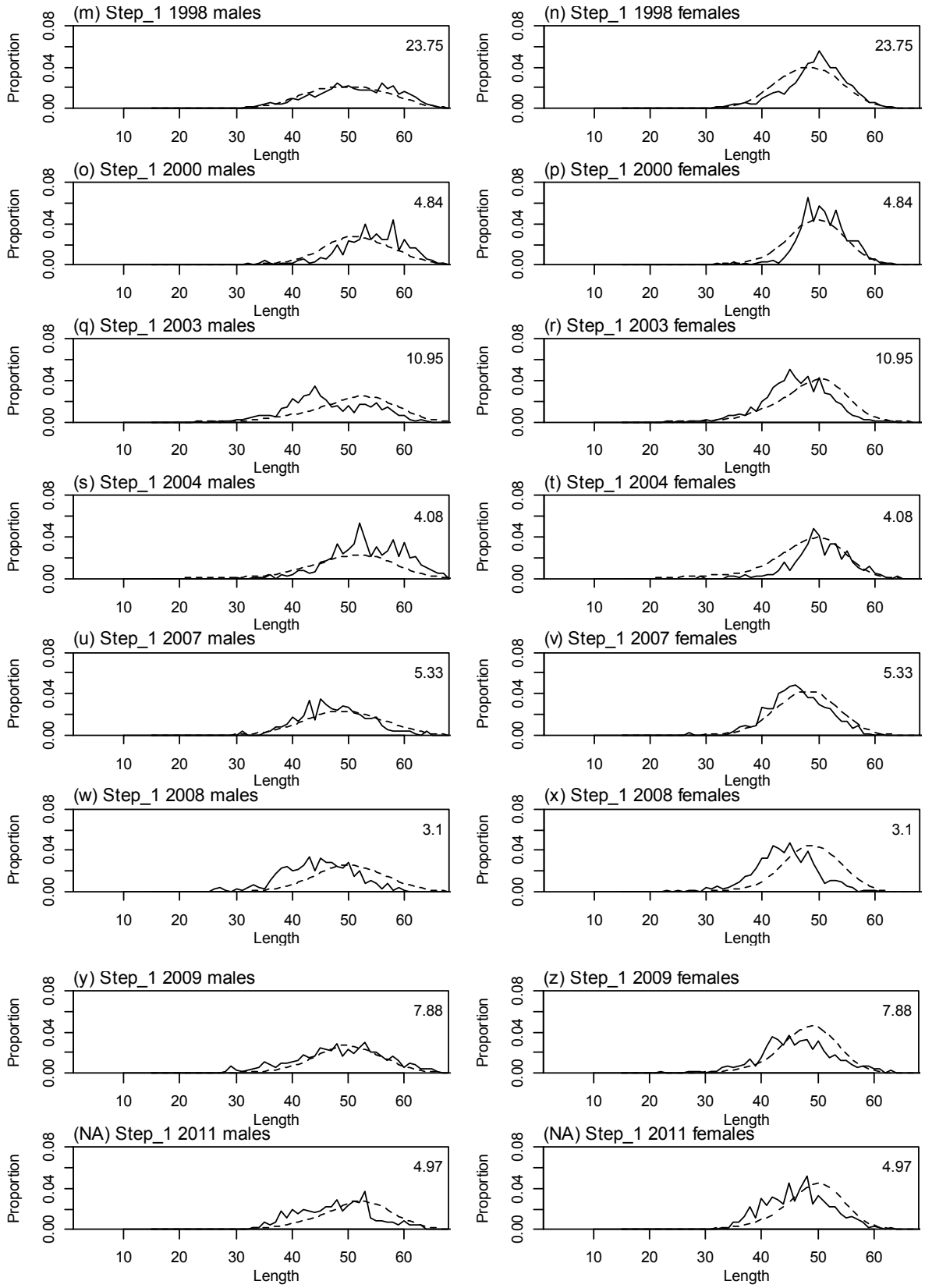

A4. 5 ctd.: Observed (solid line) and fitted (dashed line) length frequency distributions for observer samples, time step 1.

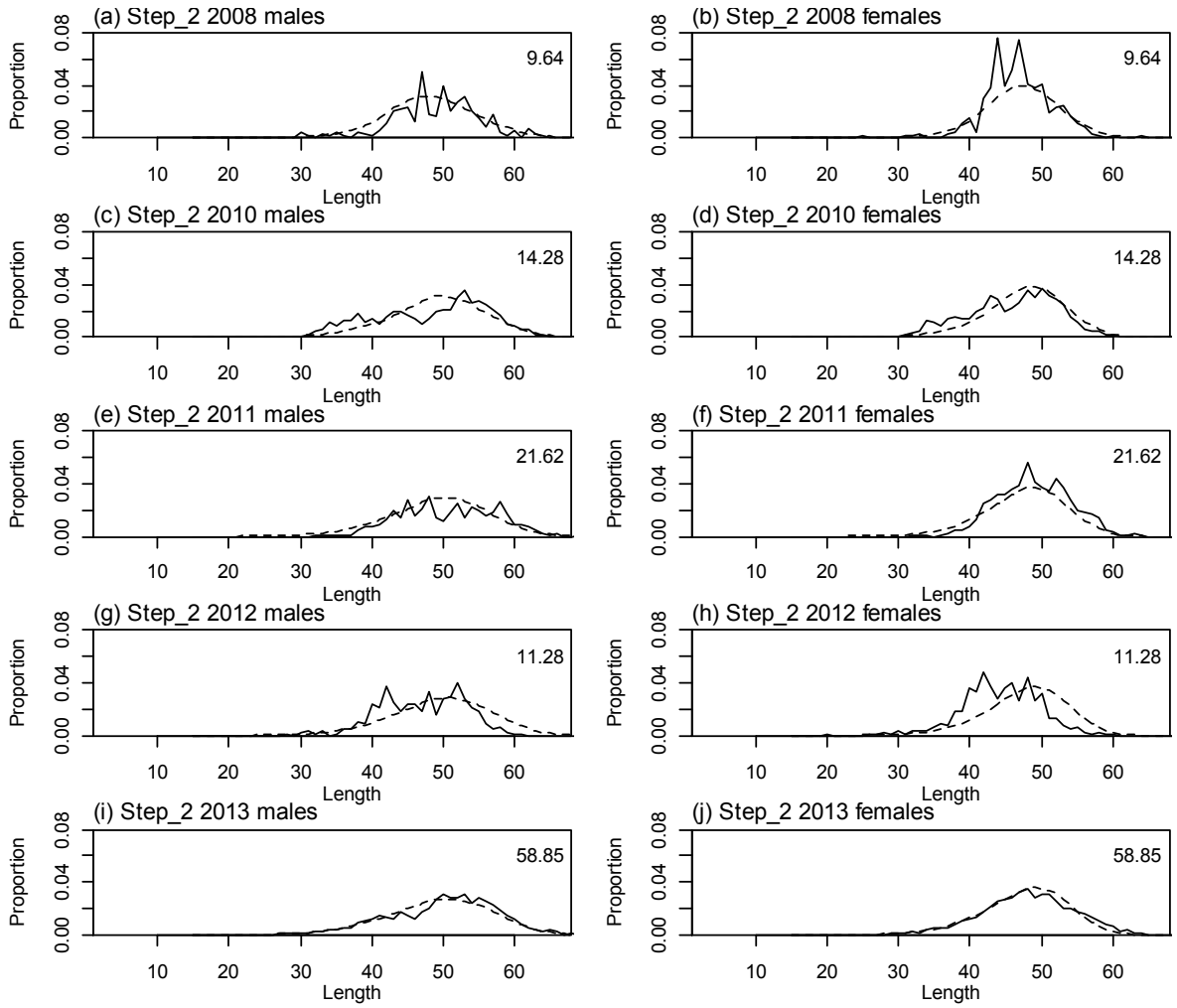

A4. 6: Observed (solid line) and fitted (dashed line) length frequency distributions for observer samples, time step 2.

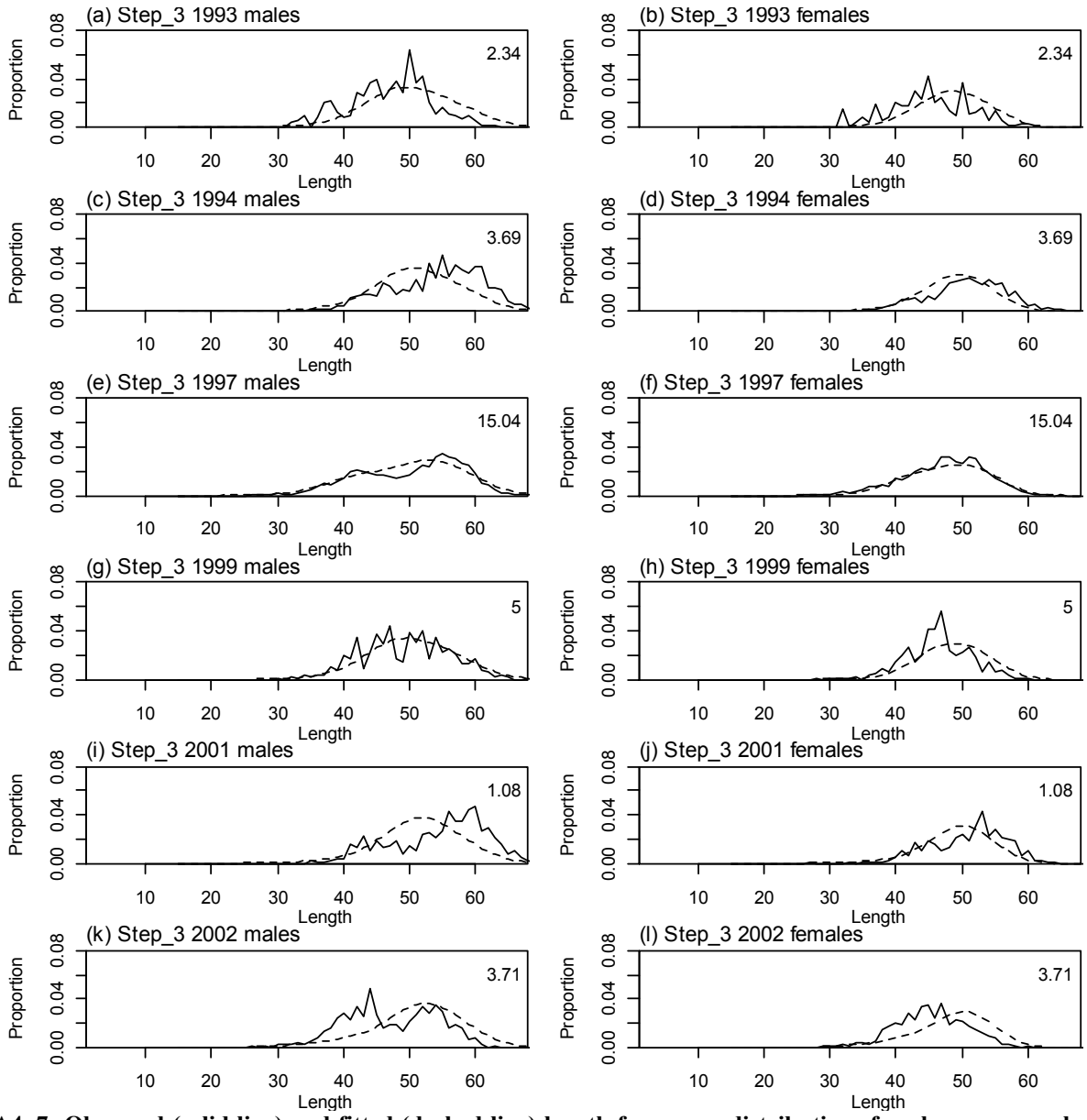

A4. 7: Observed (solid line) and fitted (dashed line) length frequency distributions for observer samples, time step 3.

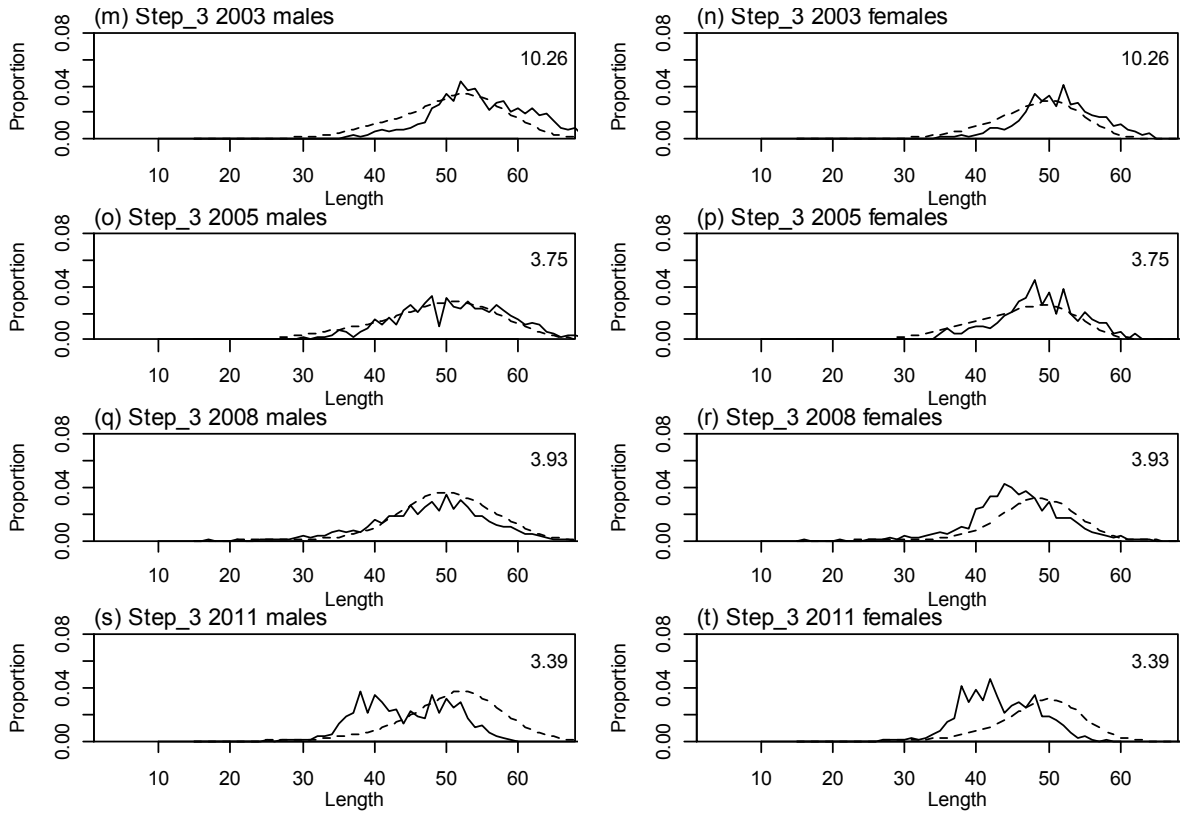

A4. 7 ctd.: Observed (solid line) and fitted (dashed line) length frequency distributions for observer samples, time step 3.

A4. 8: Numbers of scampi measured, estimated multinomial N sample size, and effective sample size used within the model for length frequency distributions for observer samples, time step 1.

	Measured	Multinomial N	Effective sample size
N_1992	9250	3276	17.21
N_1993	2641	1334	7.01
N_1994	9300	3813	20.03
N_1995	2600	1357	7.13
N_1996	3200	1704	8.95
N_1997	2794	1129	5.93
N_1998	11964	4520	23.75
N_2000	2449	921	4.84
N_2002	1975	434	2.28
N_2003	4965	2085	10.95
N_2004	1214	777	4.08
N_2007	3235	1014	5.33
N_2008	1269	591	3.10
N_2009	2959	1500	7.88
N_2011	4035	946	4.97

A4. 9: Numbers of scampi measured, estimated multinomial N sample size, and effective sample size used within the model for length frequency distributions for observer samples, time step 2.

	Measured	Multinomial N	Effective sample size
N_1997	3287	1505	19.60
N_1998	703	475	6.19
N_2001	4782	2479	32.29
N_2008	1035	740	9.64
N_2010	4194	1096	14.28
N_2011	2725	1660	21.62
N_2012	2370	866	11.28
N_2013	10883	4518	58.85

A4. 10: Numbers of scampi measured, estimated multinomial N sample size, and effective sample size used within the model for length frequency distributions for observer samples, time step 3.

	Measured	Multinomial N	Effective sample size
N_1993	1264	745	2.34
N_1994	1960	1174	3.69
N_1996	2035	686	2.15
N_1997	8816	4791	15.04
N_1998	172	157	0.49
N_1999	2707	1593	5.00
N_2001	1650	345	1.08
N_2002	5663	1181	3.71
N_2003	8746	3268	10.26
N_2005	1600	1195	3.75
N_2007	1238	342	1.07
N_2008	4435	1250	3.93
N_2011	5214	1078	3.39

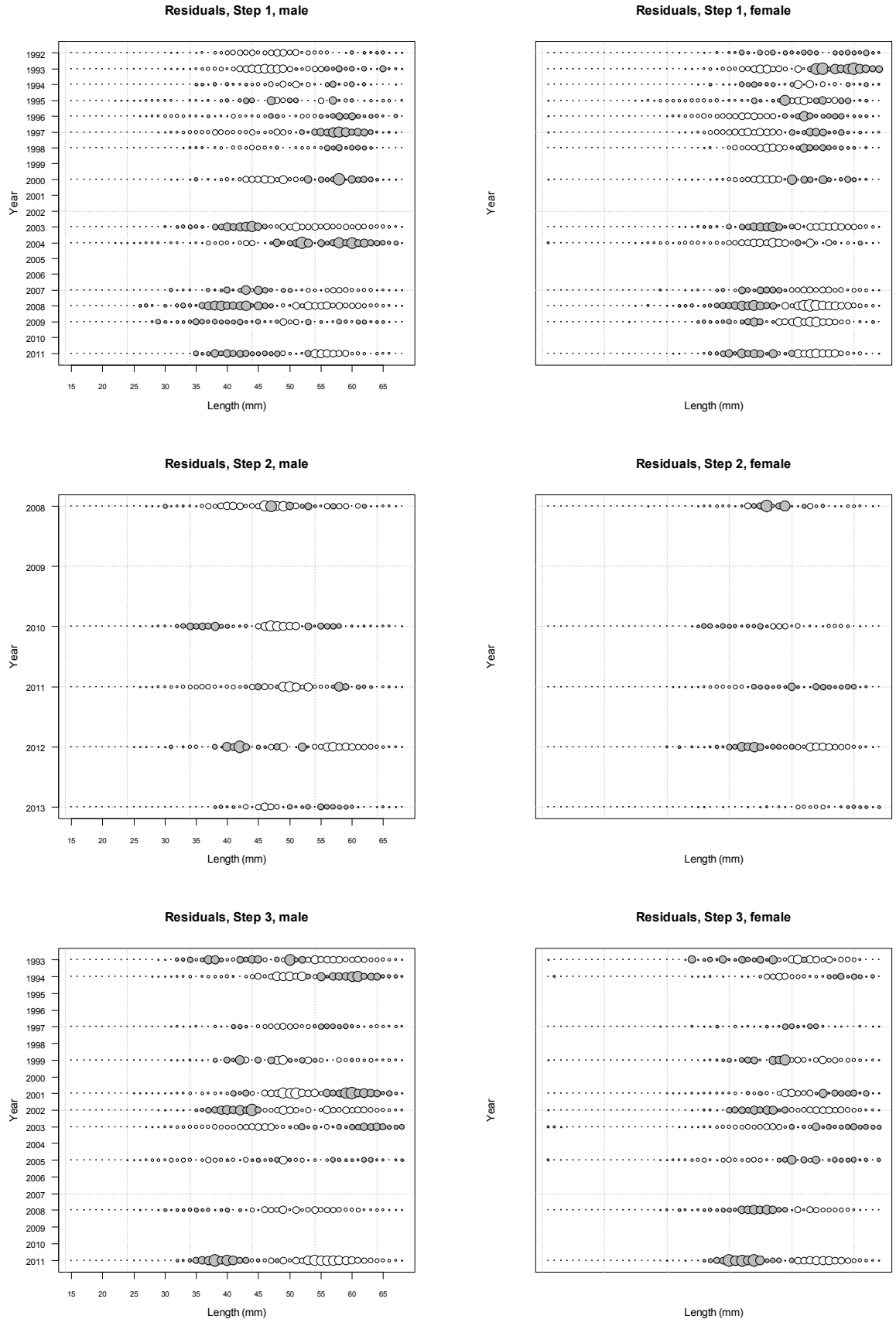

A4. 11: Bubble plots of residuals for fits to length frequency distributions for observer sampling.

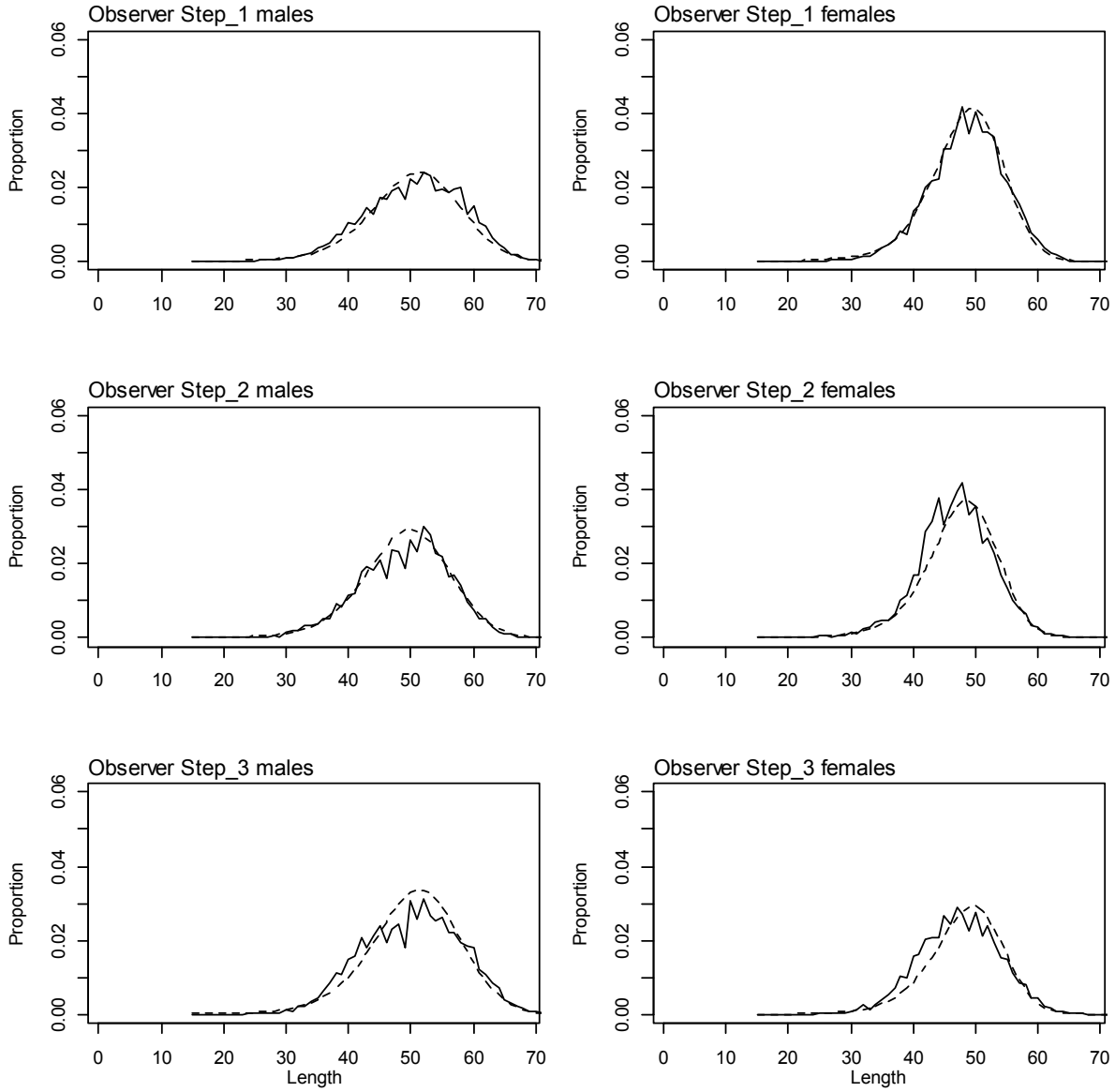

A4. 12: Average observed (solid line) and fitted (dashed line) length frequency distributions for observer samples.

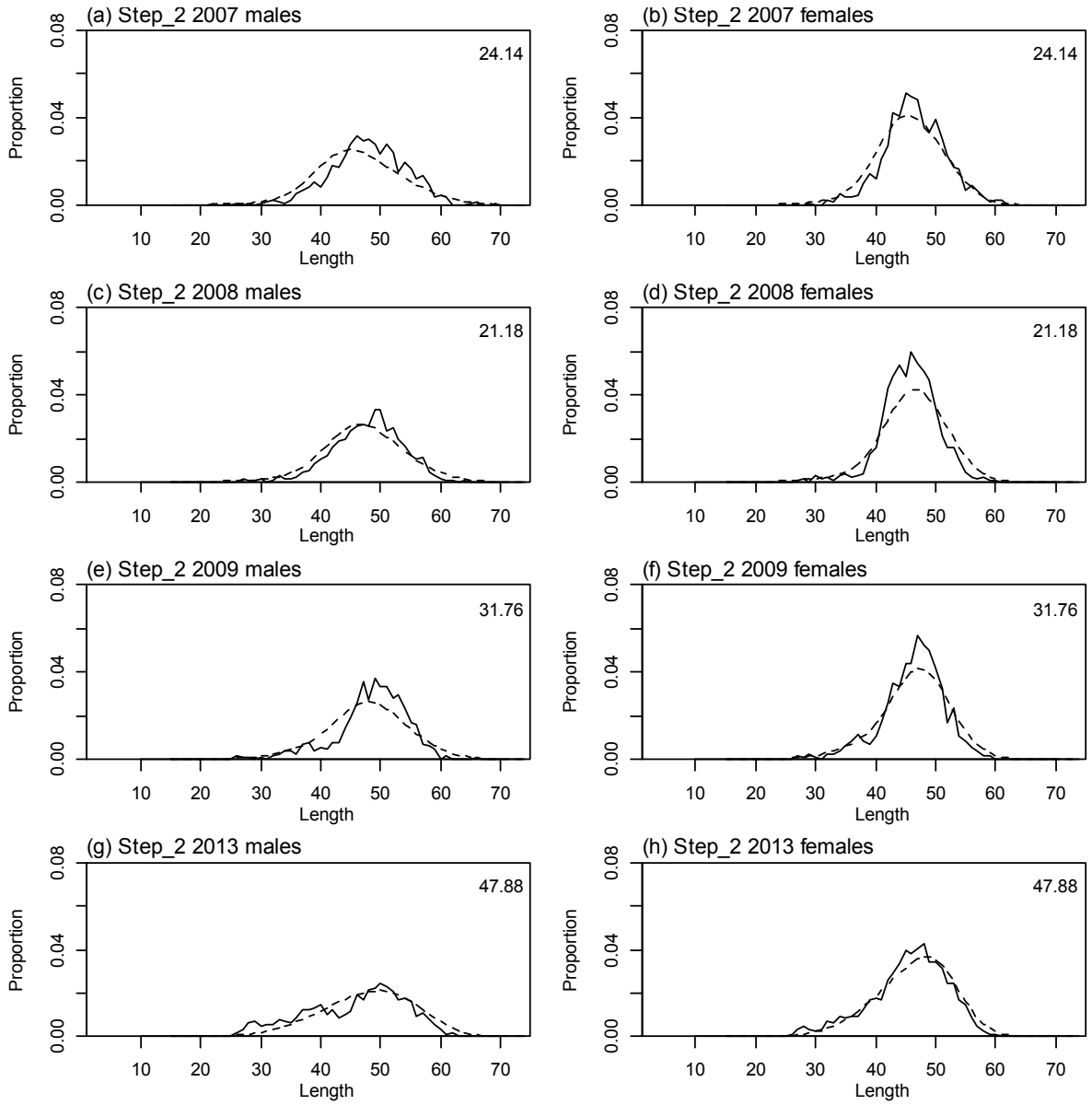

A4. 13: Observed (solid line) and fitted (dashed line) length frequency distributions for research survey samples.

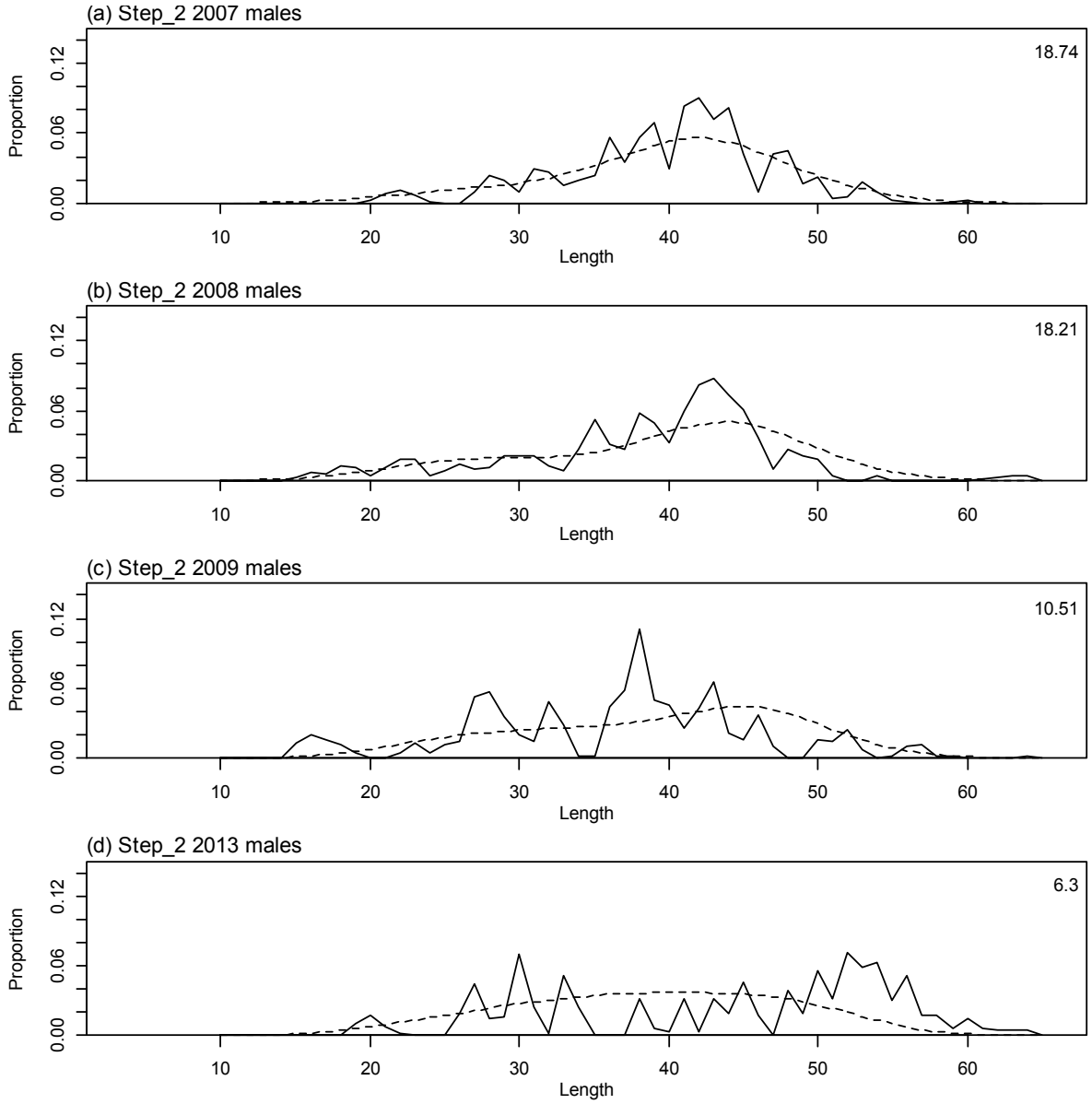

A4. 14: Observed (solid line) and fitted (dashed line) length frequency distributions for photographic survey scampi size estimation.

A4. 15: Numbers of scampi measured, estimated multinomial N sample size, and effective sample size used within the model for length frequency distributions for research survey samples.

	Measured	Multinomial N	Effective sample size
N_2007	1981	2127	24.14
N_2008	2291	1866	21.18
N_2009	4054	2798	31.76
N_2013	4808	4218	47.88

A4. 16: Numbers of scampi measured, estimated multinomial N sample size, and effective sample size used within the model for length frequency distributions for photographic survey samples.

	Measured	Multinomial N	Effective sample size
N_2007	70	107	18.74
N_2008	73	104	18.21
N_2009	45	60	10.51
N_2013	26	36	6.30

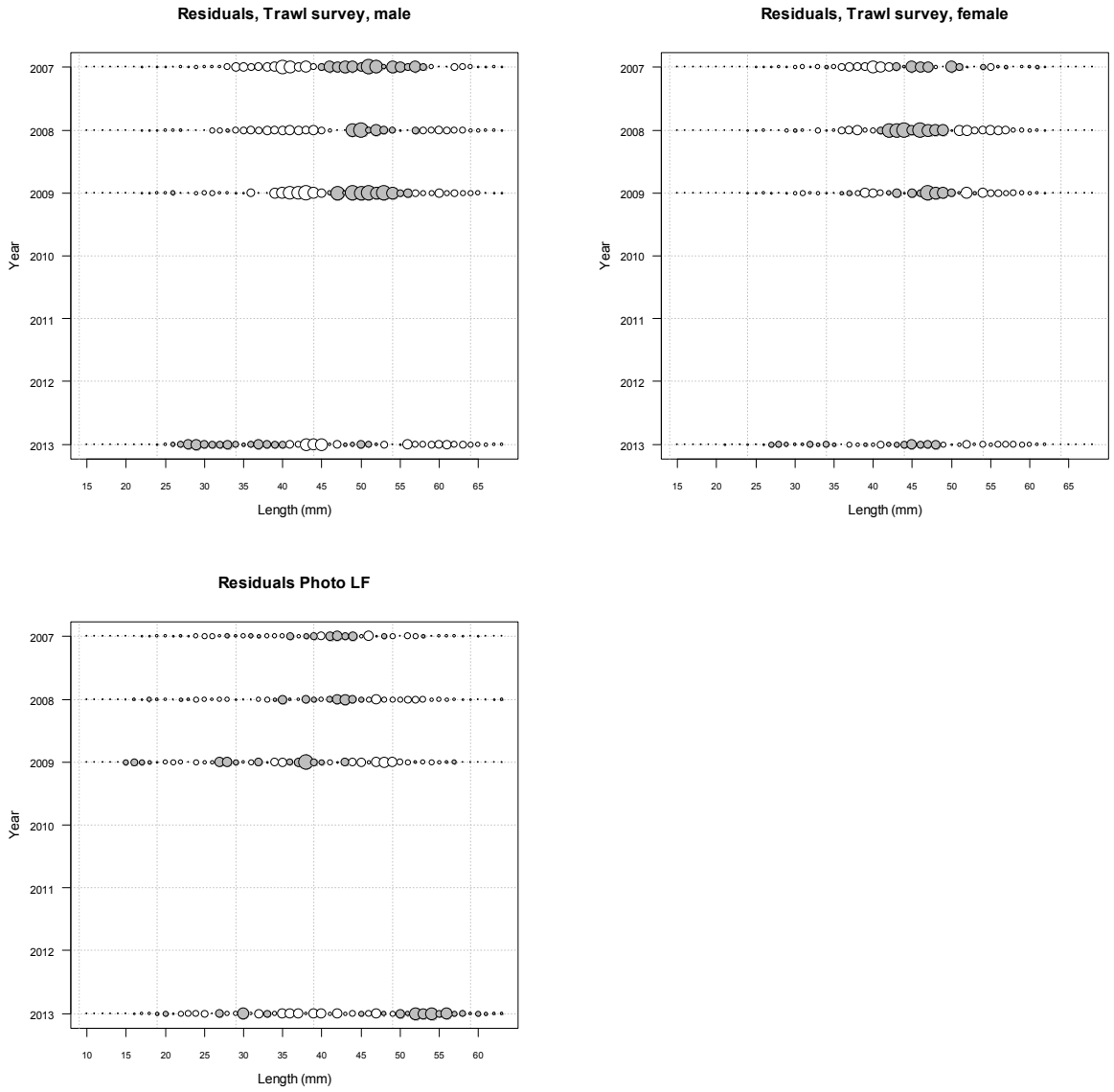

A4. 17: Bubble plots of residuals for fits to length frequency distributions for trawl survey sampling and photographic survey scampi size estimation.

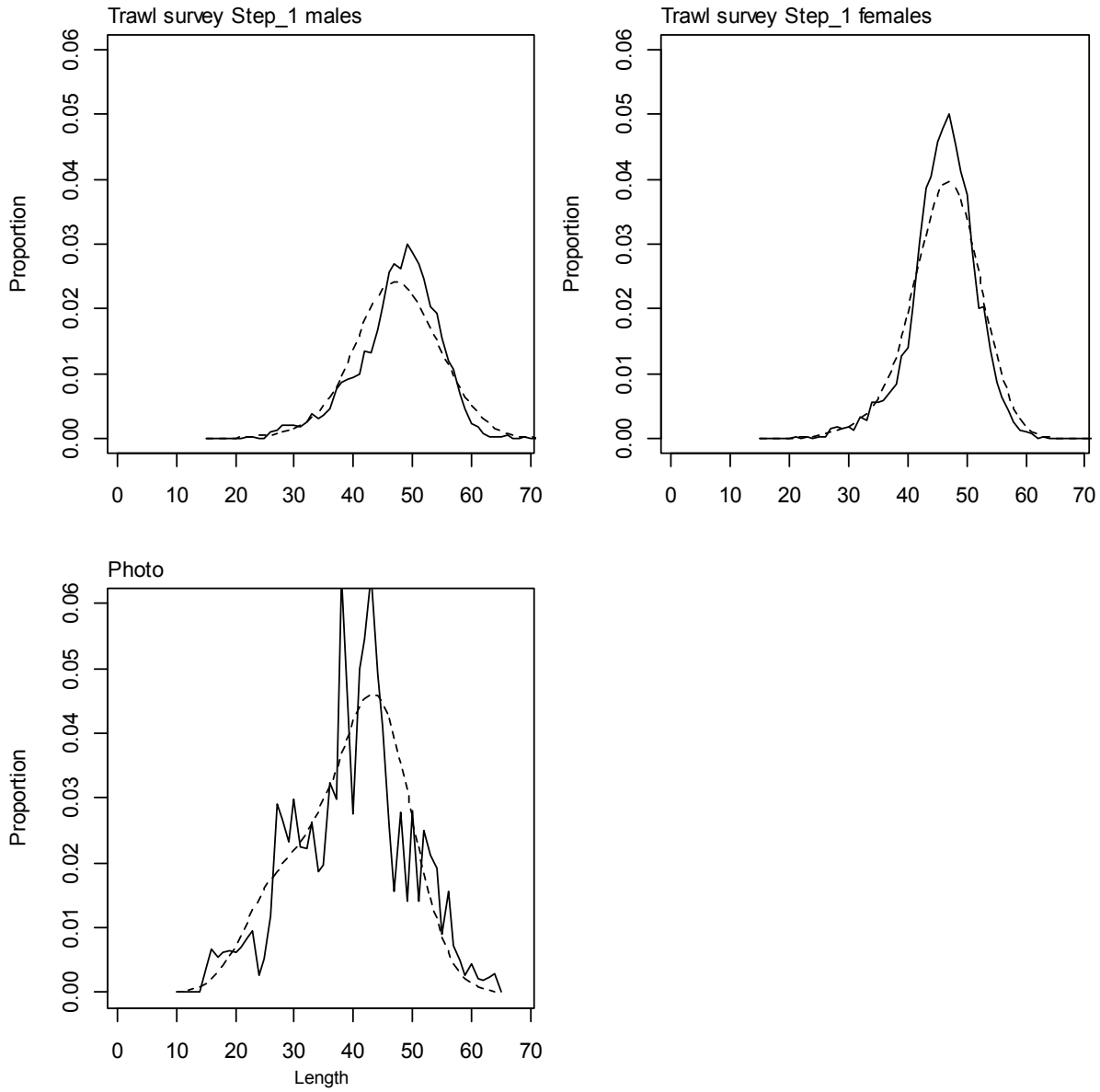

A4. 18: Average observed (solid line) and fitted (dashed line) length frequency distributions for trawl survey sampling and photographic survey scampi size estimation.

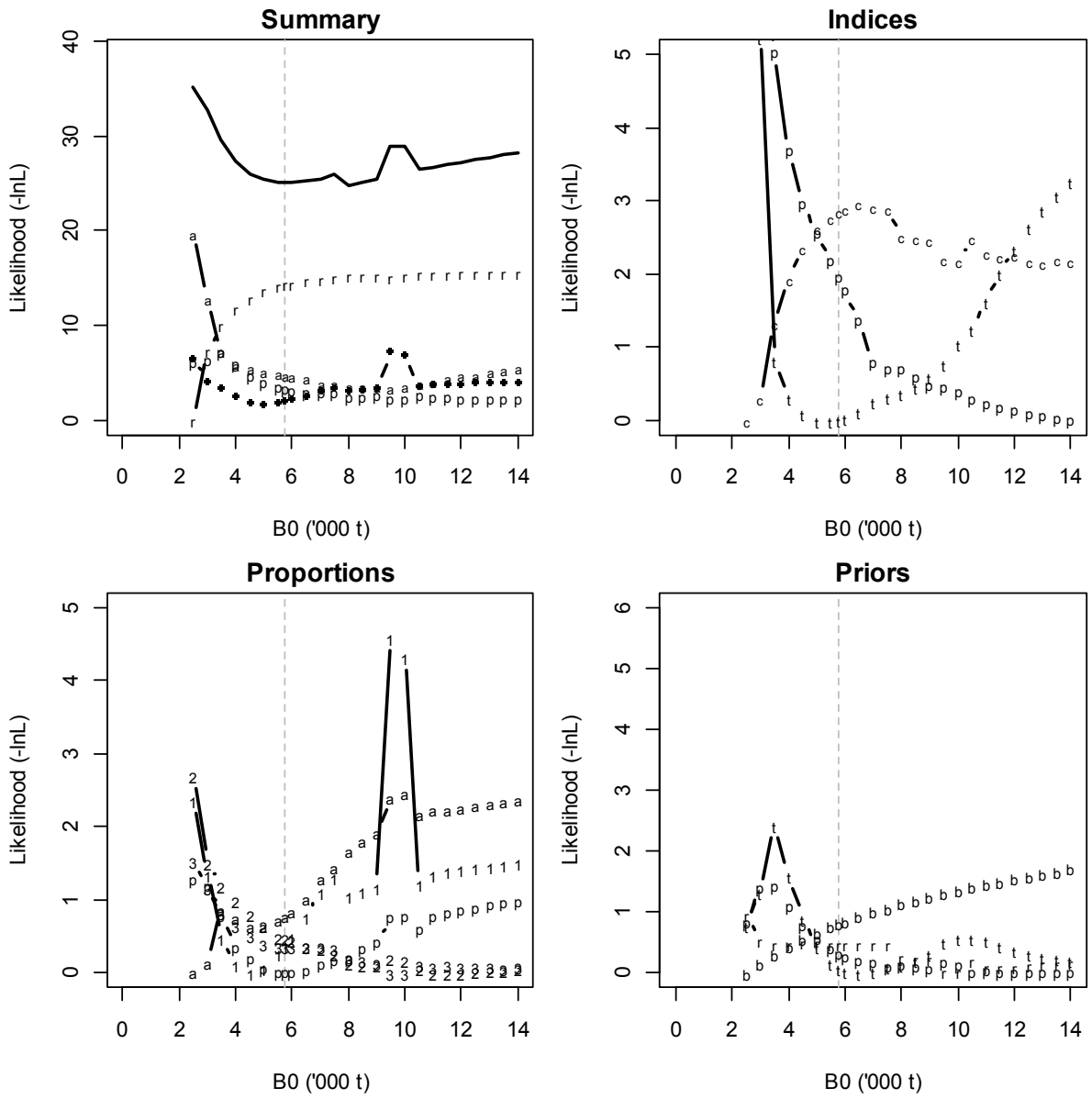

A4. 19: Likelihood profiles for the F_0.25 model for SCI 6A when B_0 is fixed in the model. Figures show profiles for main priors (top left, p – priors, a - abundance indices, • – proportions at length, r – recapture data), abundance indices (top right, t - trawl survey, c - CPUE, p – photo survey), proportion at length data (bottom left, a-trawl, 1 – observer time step 1, 2 – observer time step 2, 3 – observer time step 3, p - photo) and priors (bottom right, b- B_0, YCS - r, p- *q-Photo*, t – *q-Trawl*). Vertical dashed line represents MPD.

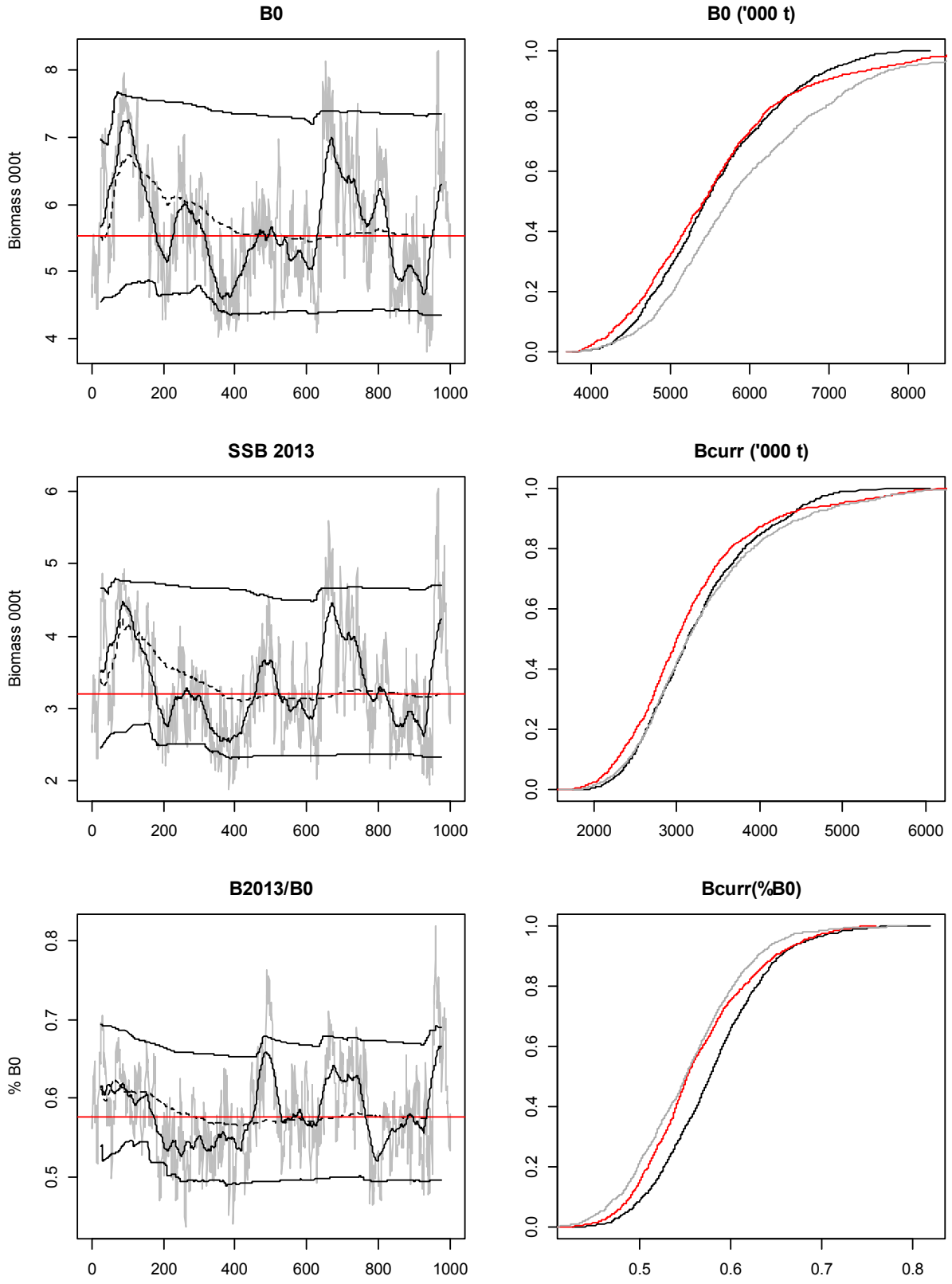

A4. 20: MCMC traces for B_0, SSB_{2013}, and SSB_{2013}/B_0 terms for the F_0.25 model for SCI 6A (trace – grey line, cumulative moving median –dashed black line, moving average and cumulative moving 2.5%, 97.5% quantiles – solid black lines, overall median – solid red line, left plots), along with cumulative frequency distributions for three independent MCMC chains (shown as red, grey and black lines, right plots).

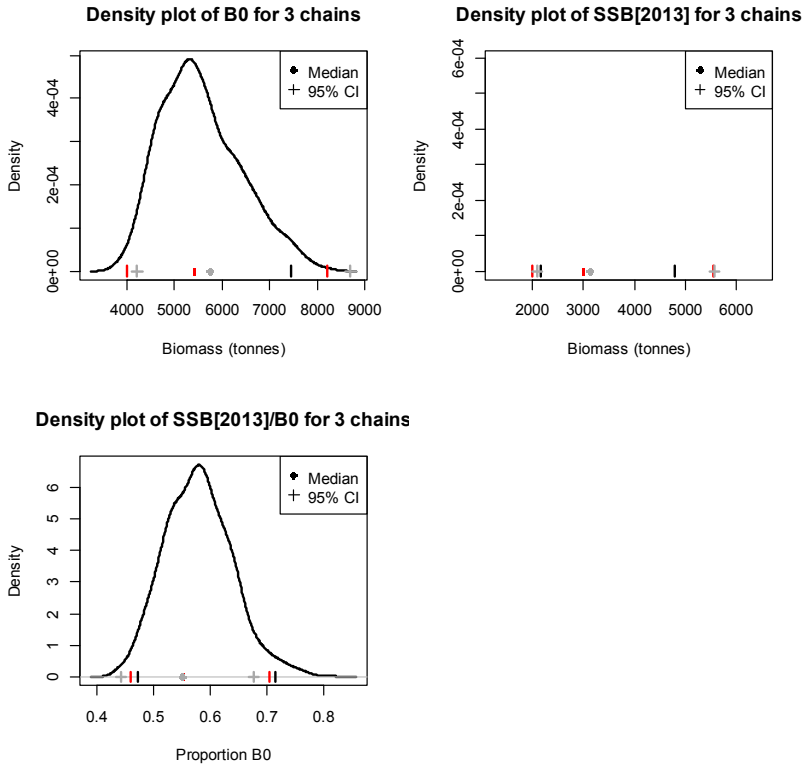

A4. 21: Density plots for B_0, SSB_{2013}, and SSB_{2013}/B_0 terms for the F_0.25 model for SCI 6A for three independent MCMC chains, with median and 95% confidence intervals.

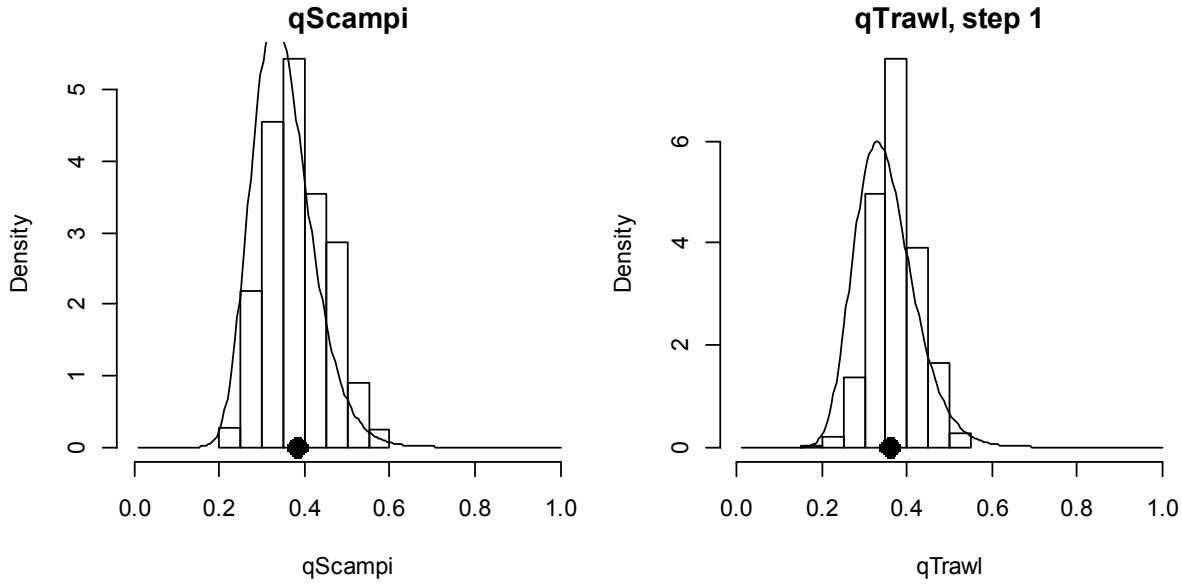

A4. 22: Marginal posterior distributions (histograms), MPD estimates (solid symbols) and distributions of priors (lines) for catchability terms.

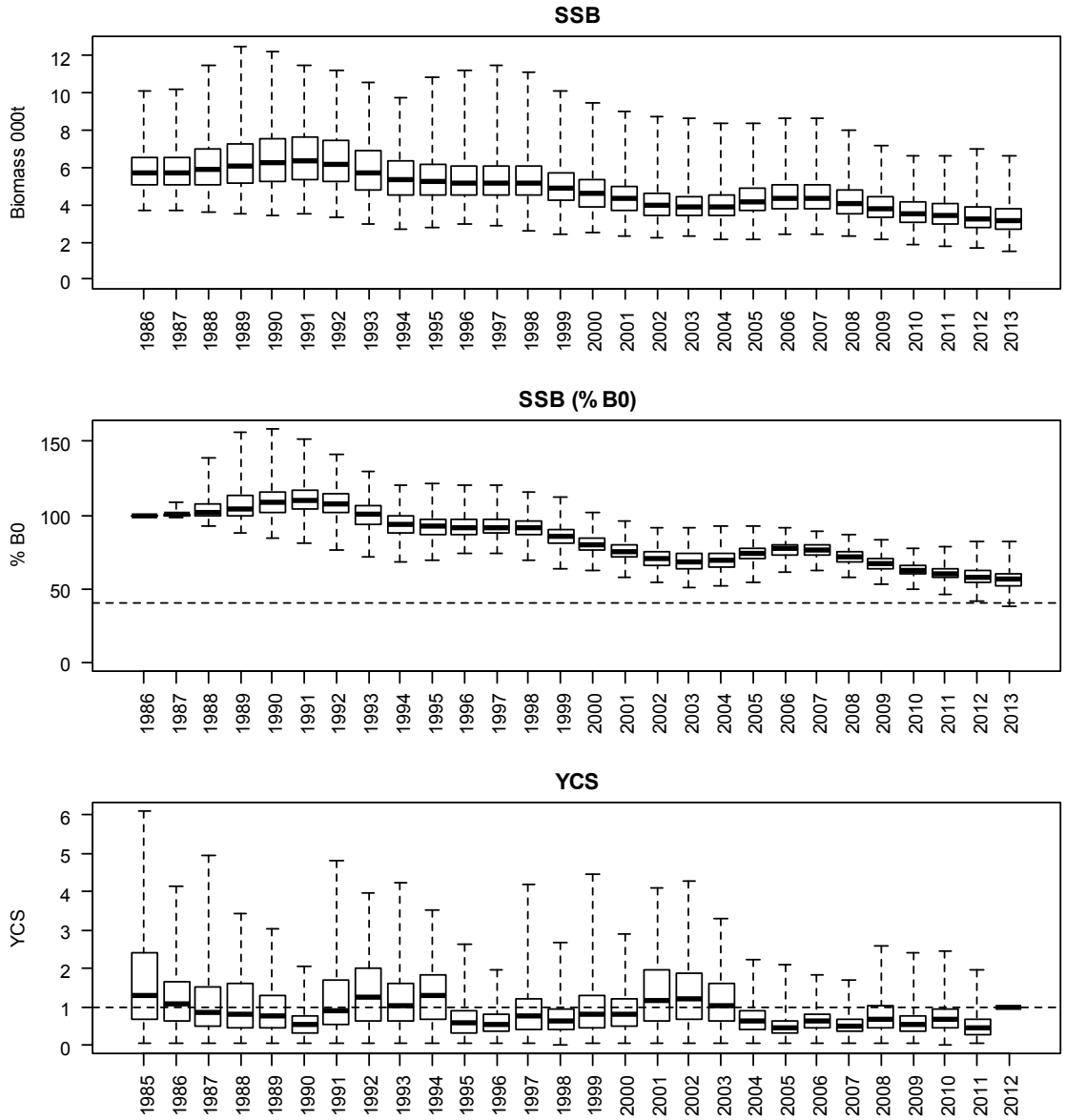

A4. 23: Posterior trajectory of SSB, SSB_{2013}/B_0 and YCS.

APPENDIX 5. MODEL F_0.3

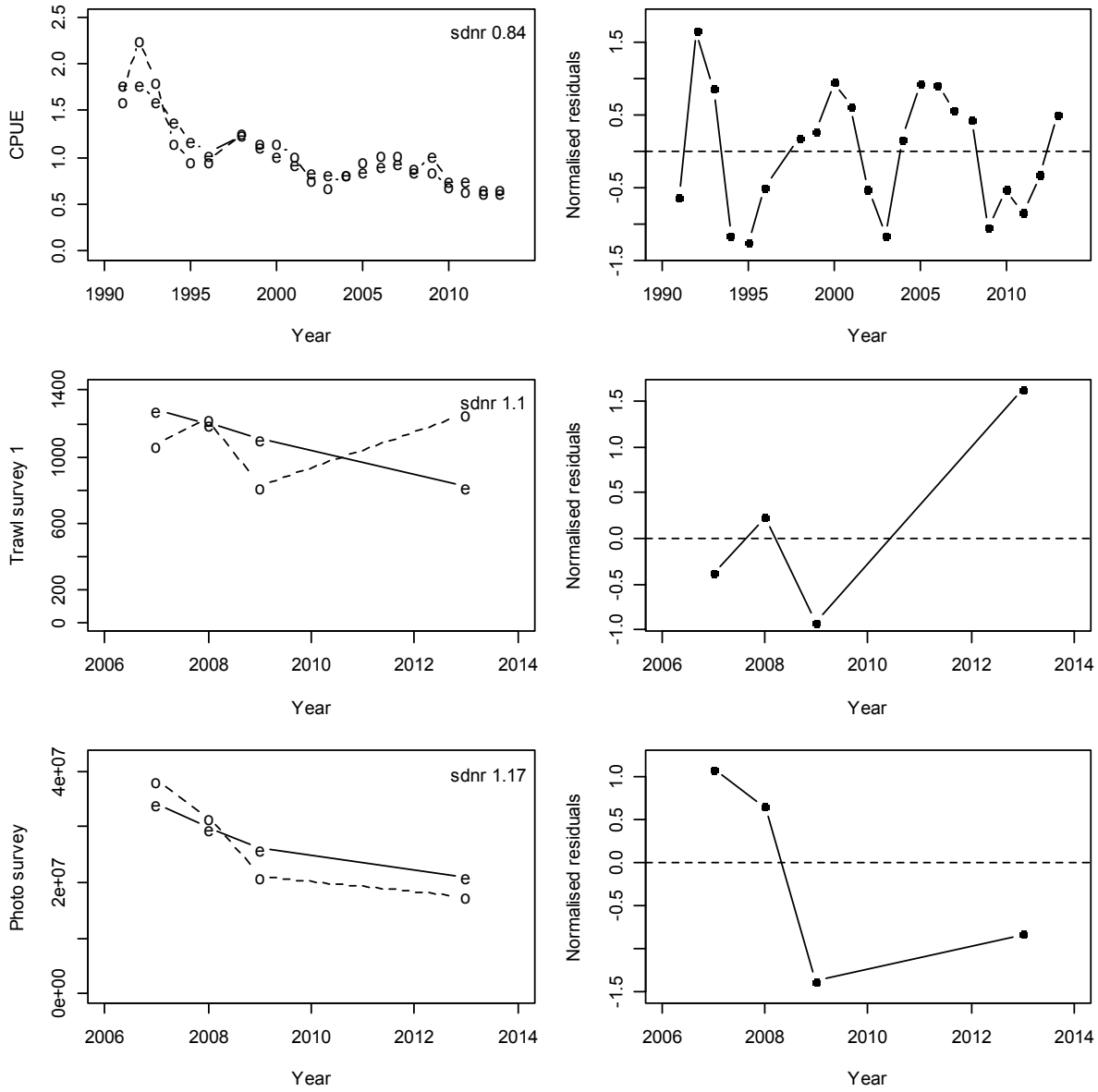

A5. 1: Fits to abundance indices (left column) and normalised residuals (right column) for standardised CPUE index (top row) trawl survey biomass index covering whole area (second row), trawl survey biomass index covering limited area (third row) and photo survey abundance index (fourth row) for SCI 6A F_0.3.

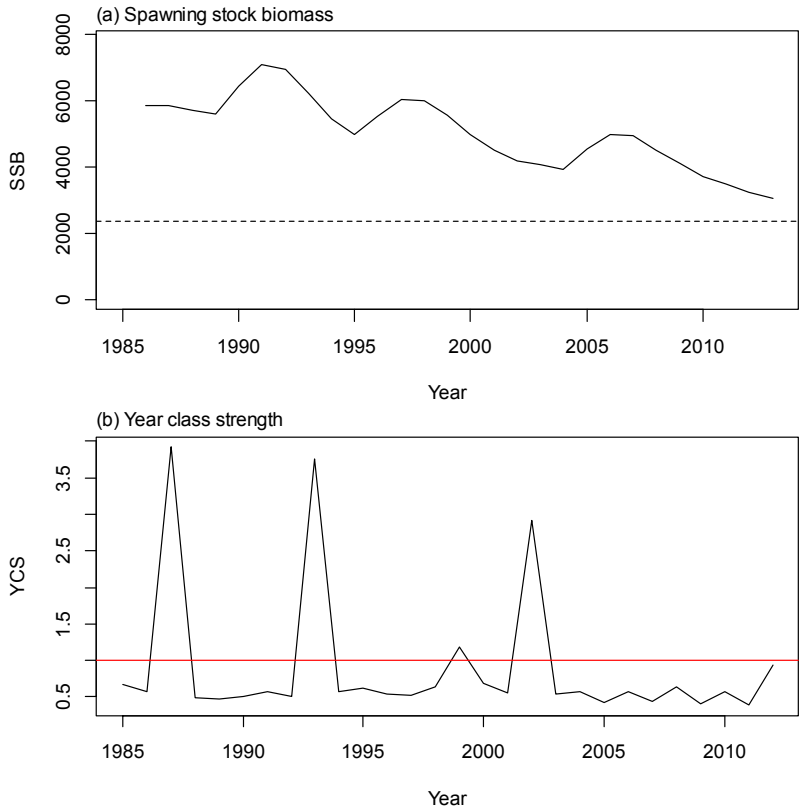

A5. 2: Spawning stock biomass trajectory (upper plot), year class strength (lower plot) for SCI 6A F_0.3.

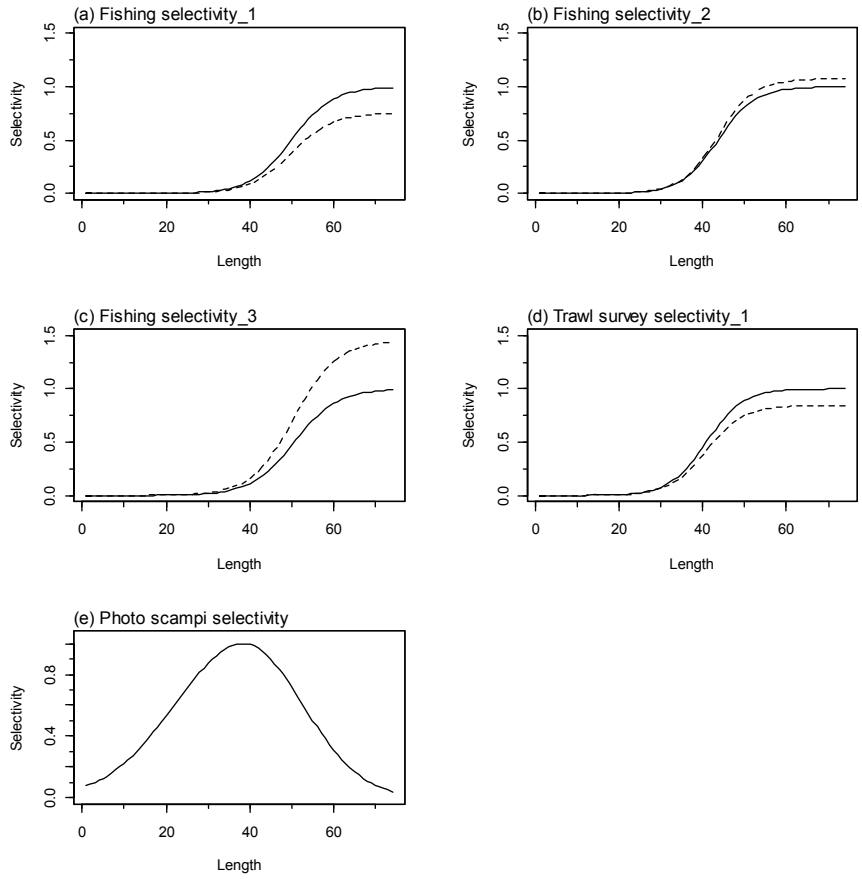

A5. 3: Fishery and survey selectivity curves. Solid line – females, dotted line – males. The scampi photo index is not sexed, and a single selectivity applies.

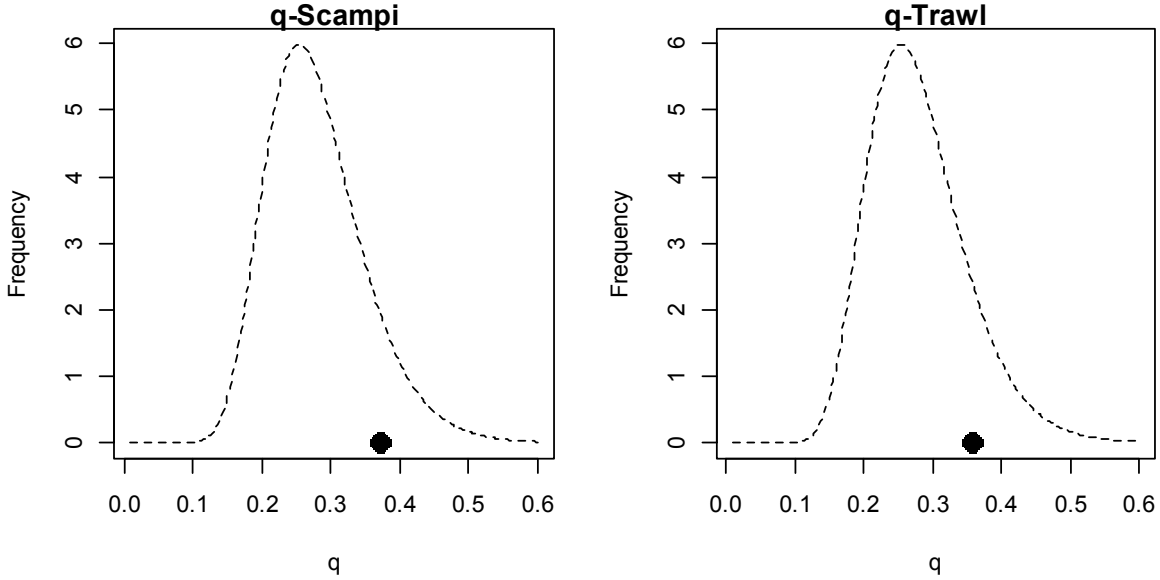

A5. 4: Catchability estimates from MPD model run, plotted in relation to prior distribution.

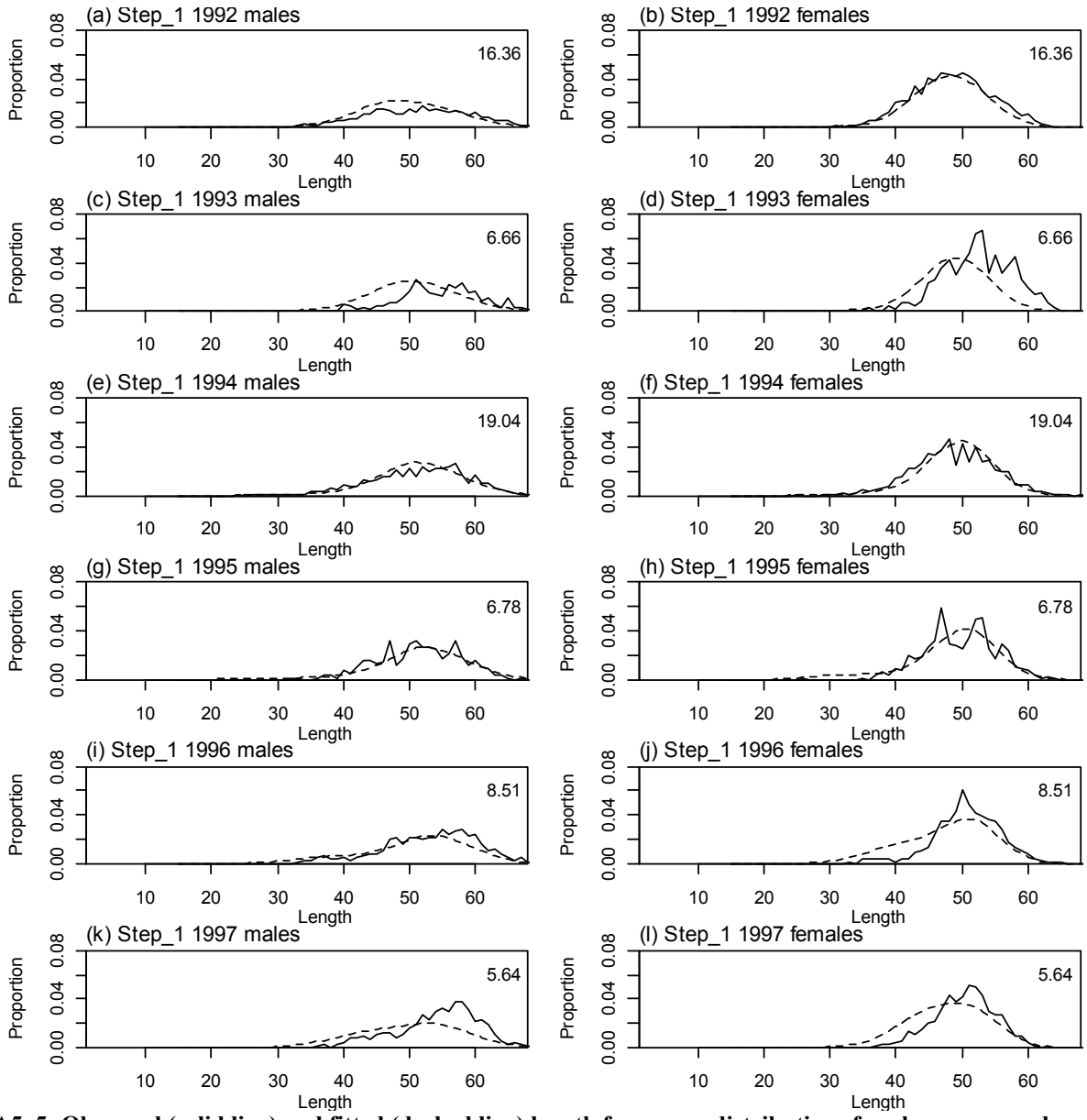

A5. 5: Observed (solid line) and fitted (dashed line) length frequency distributions for observer samples, time step 1.

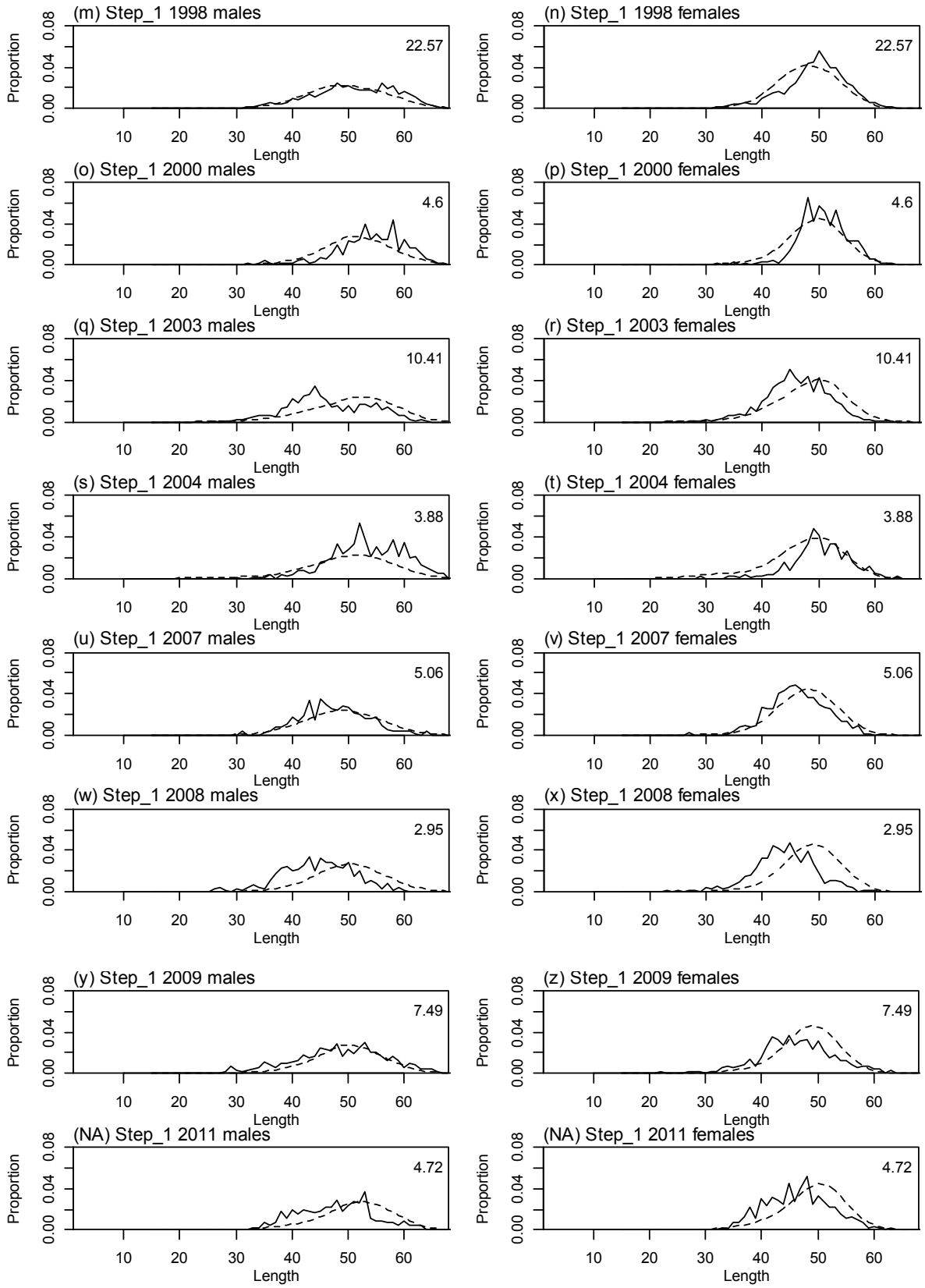

A5. 5 ctd.: Observed (solid line) and fitted (dashed line) length frequency distributions for observer samples, time step 1.

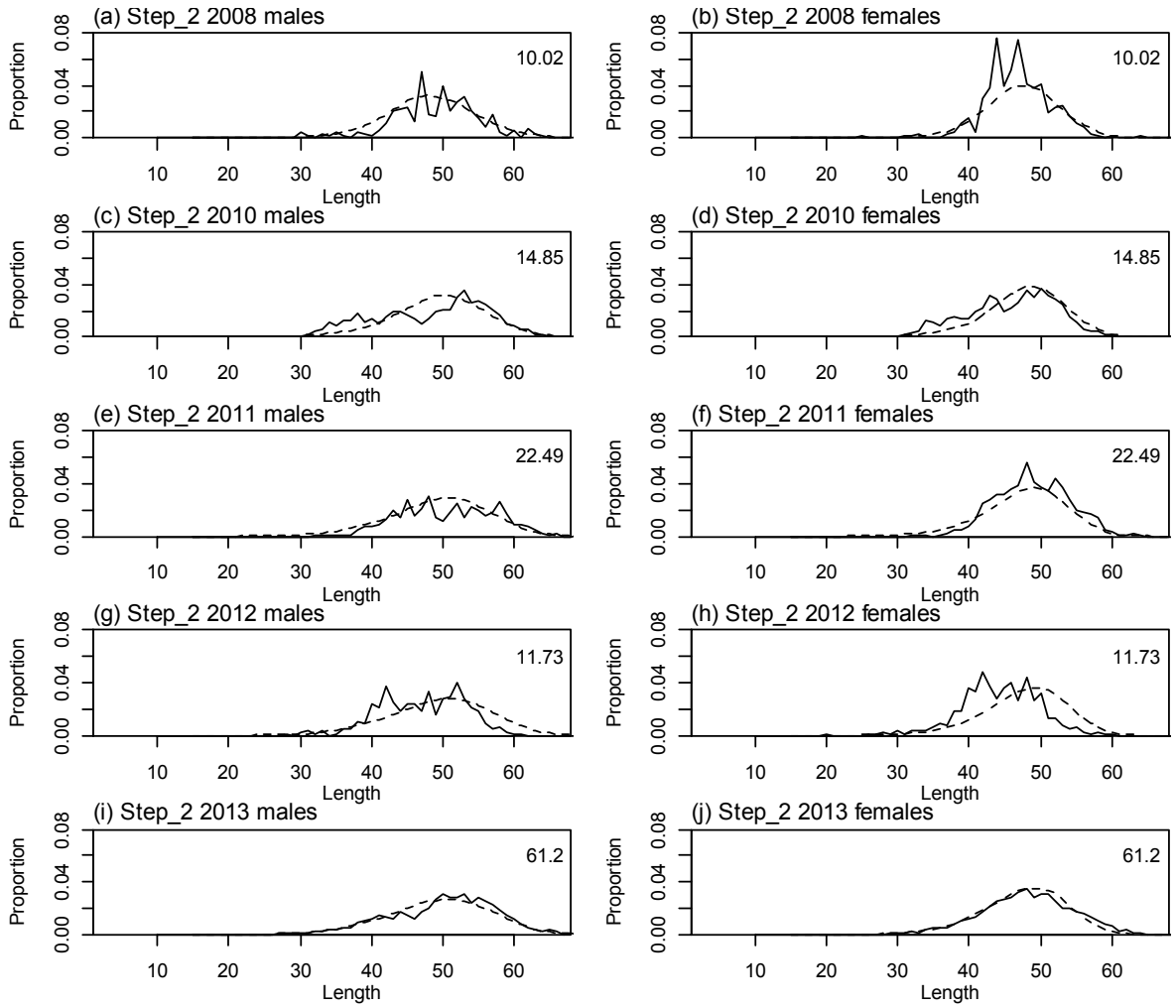

A5. 6: Observed (solid line) and fitted (dashed line) length frequency distributions for observer samples, time step 2.

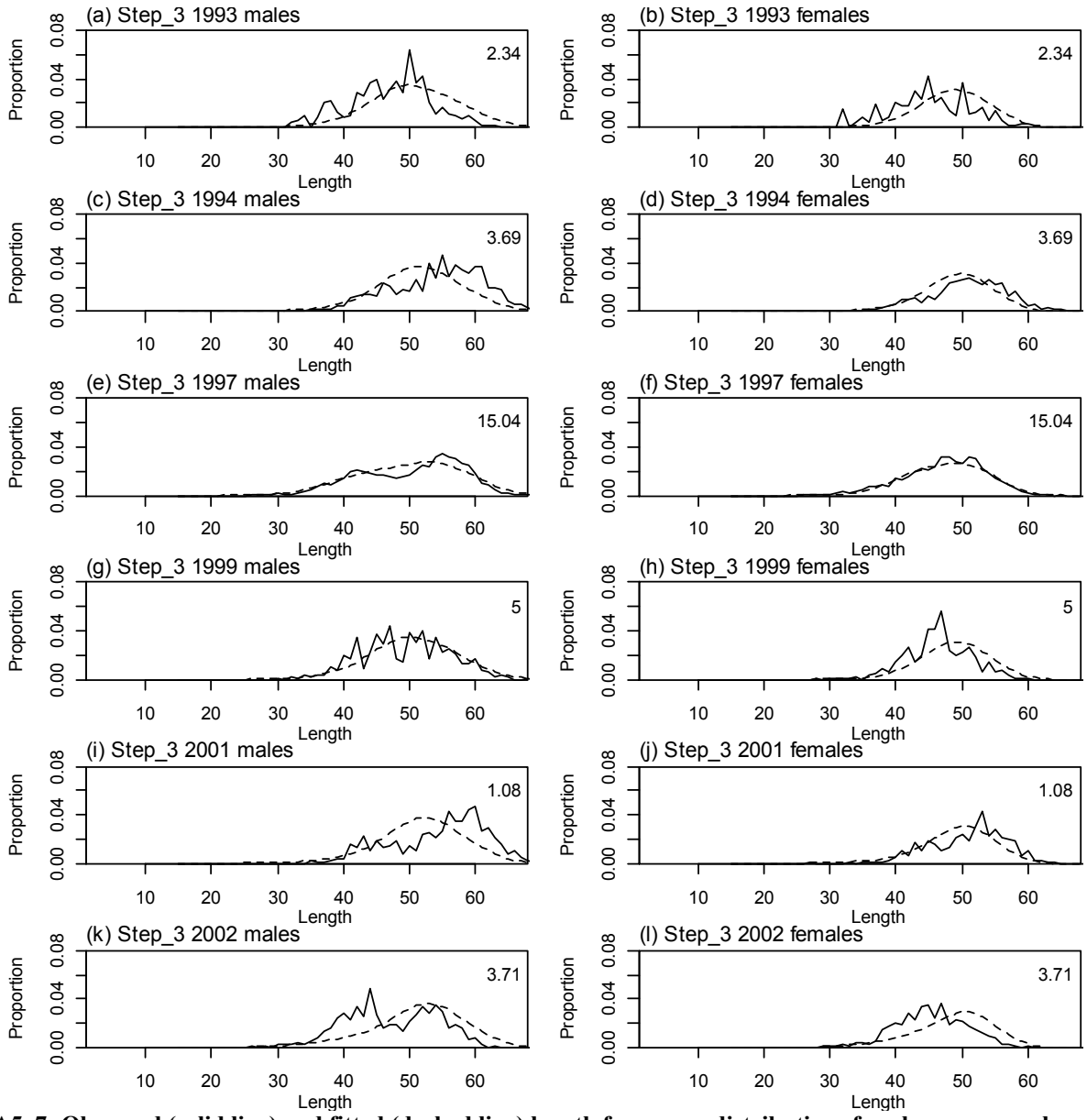

A5. 7: Observed (solid line) and fitted (dashed line) length frequency distributions for observer samples, time step 3.

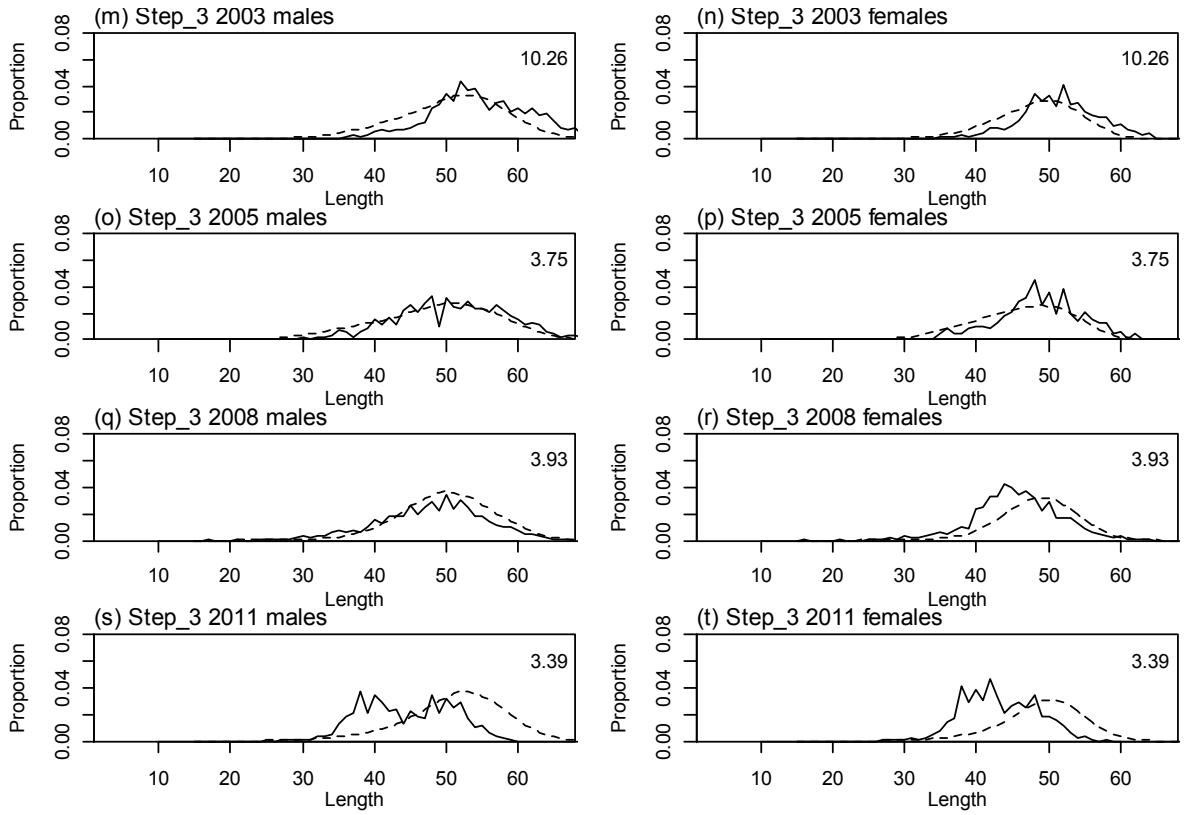

A5. 7 ctd.: Observed (solid line) and fitted (dashed line) length frequency distributions for observer samples, time step 3.

A5. 8: Numbers of scampi measured, estimated multinomial N sample size, and effective sample size used within the model for length frequency distributions for observer samples, time step 1.

	Measured	Multinomial N	Effective sample size
N_1992	9250	3276	16.36
N_1993	2641	1334	6.66
N_1994	9300	3813	19.04
N_1995	2600	1357	6.78
N_1996	3200	1704	8.51
N_1997	2794	1129	5.64
N_1998	11964	4520	22.57
N_2000	2449	921	4.60
N_2002	1975	434	2.17
N_2003	4965	2085	10.41
N_2004	1214	777	3.88
N_2007	3235	1014	5.06
N_2008	1269	591	2.95
N_2009	2959	1500	7.49
N_2011	4035	946	4.72

A5. 9: Numbers of scampi measured, estimated multinomial N sample size, and effective sample size used within the model for length frequency distributions for observer samples, time step 2.

	Measured	Multinomial N	Effective sample size
N_1997	3287	1505	20.39
N_1998	703	475	6.43
N_2001	4782	2479	33.58
N_2008	1035	740	10.02
N_2010	4194	1096	14.85
N_2011	2725	1660	22.49
N_2012	2370	866	11.73
N_2013	10883	4518	61.20

A5. 10: Numbers of scampi measured, estimated multinomial N sample size, and effective sample size used within the model for length frequency distributions for observer samples, time step 3.

	Measured	Multinomial N	Effective sample size
N_1993	1264	745	2.34
N_1994	1960	1174	3.69
N_1996	2035	686	2.15
N_1997	8816	4791	15.04
N_1998	172	157	0.49
N_1999	2707	1593	5.00
N_2001	1650	345	1.08
N_2002	5663	1181	3.71
N_2003	8746	3268	10.26
N_2005	1600	1195	3.75
N_2007	1238	342	1.07
N_2008	4435	1250	3.93
N_2011	5214	1078	3.39

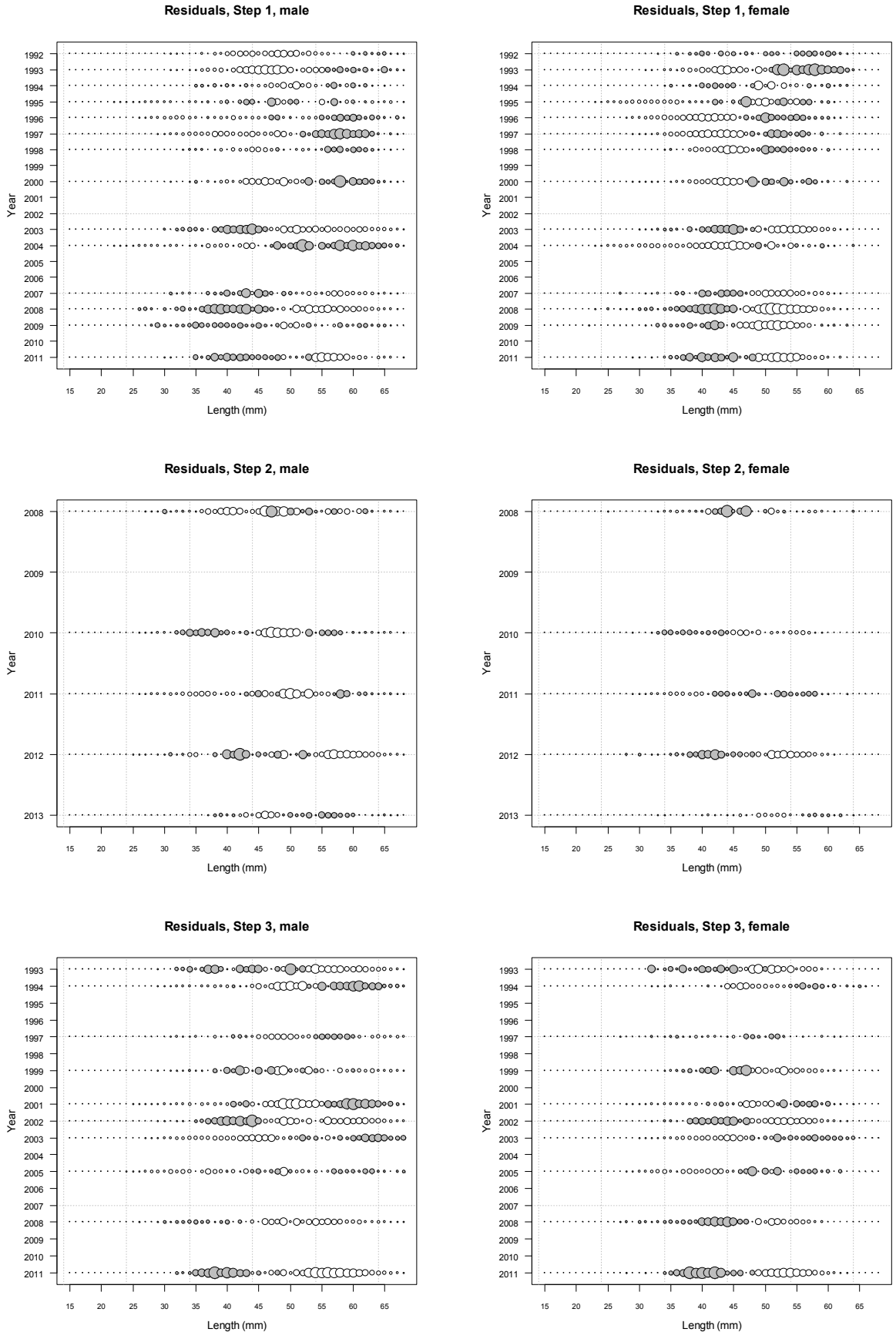

A5. 11: Bubble plots of residuals for fits to length frequency distributions for observer sampling.

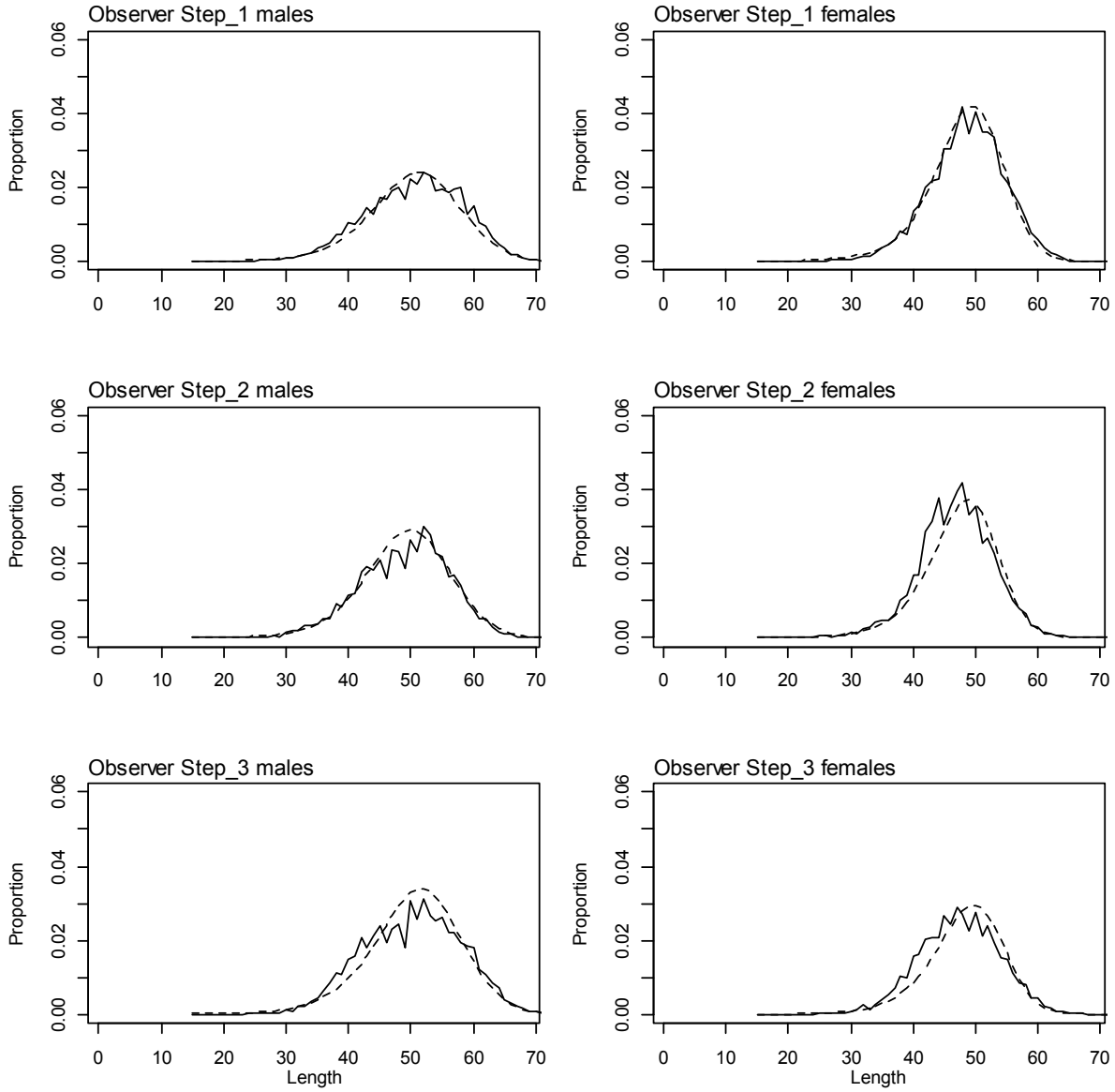

A5. 12: Average observed (solid line) and fitted (dashed line) length frequency distributions for observer samples.

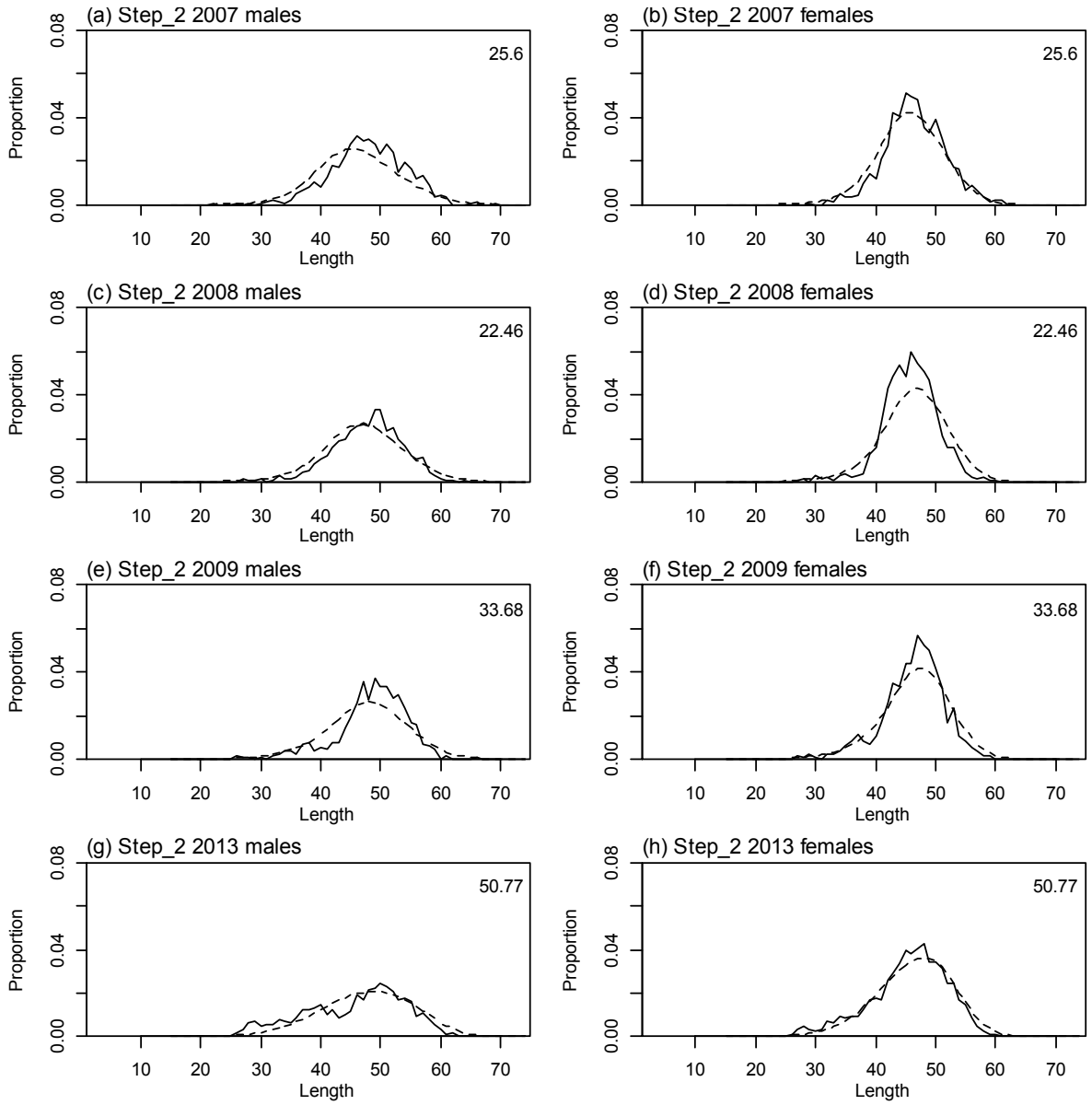

A5. 13: Observed (solid line) and fitted (dashed line) length frequency distributions for research survey samples.

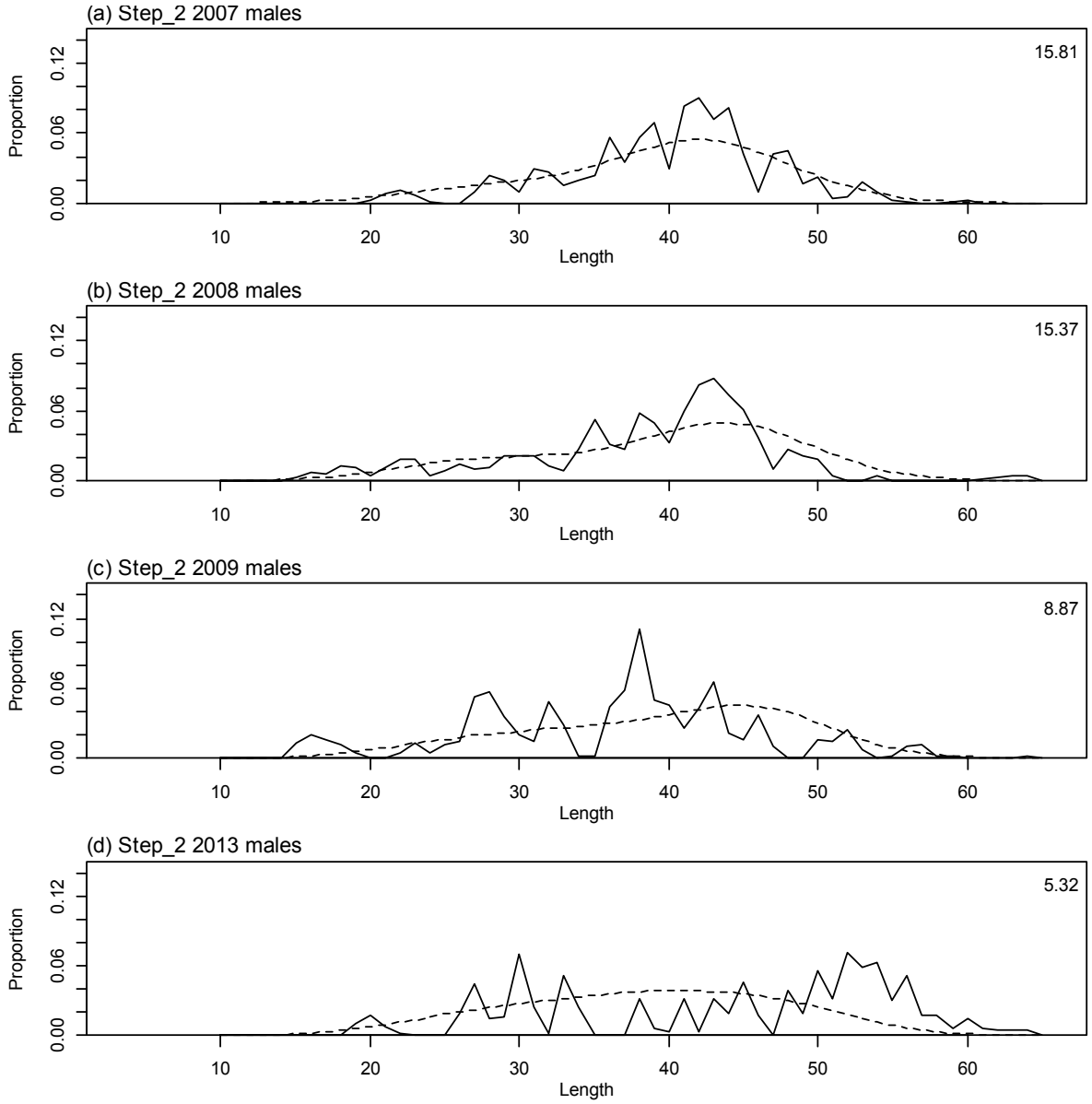

A5. 14: Observed (solid line) and fitted (dashed line) length frequency distributions for photographic survey scampi size estimation.

A5. 15: Numbers of scampi measured, estimated multinomial N sample size, and effective sample size used within the model for length frequency distributions for research survey samples.

	Measured	Multinomial N	Effective sample size
N_2007	1981	2127	25.60
N_2008	2291	1866	22.46
N_2009	4054	2798	33.68
N_2013	4808	4218	50.77

A5. 16: Numbers of scampi measured, estimated multinomial N sample size, and effective sample size used within the model for length frequency distributions for photographic survey samples.

	Measured	Multinomial N	Effective sample size
N_2007	70	107	15.81
N_2008	73	104	15.37
N_2009	45	60	8.87
N_2013	26	36	5.32

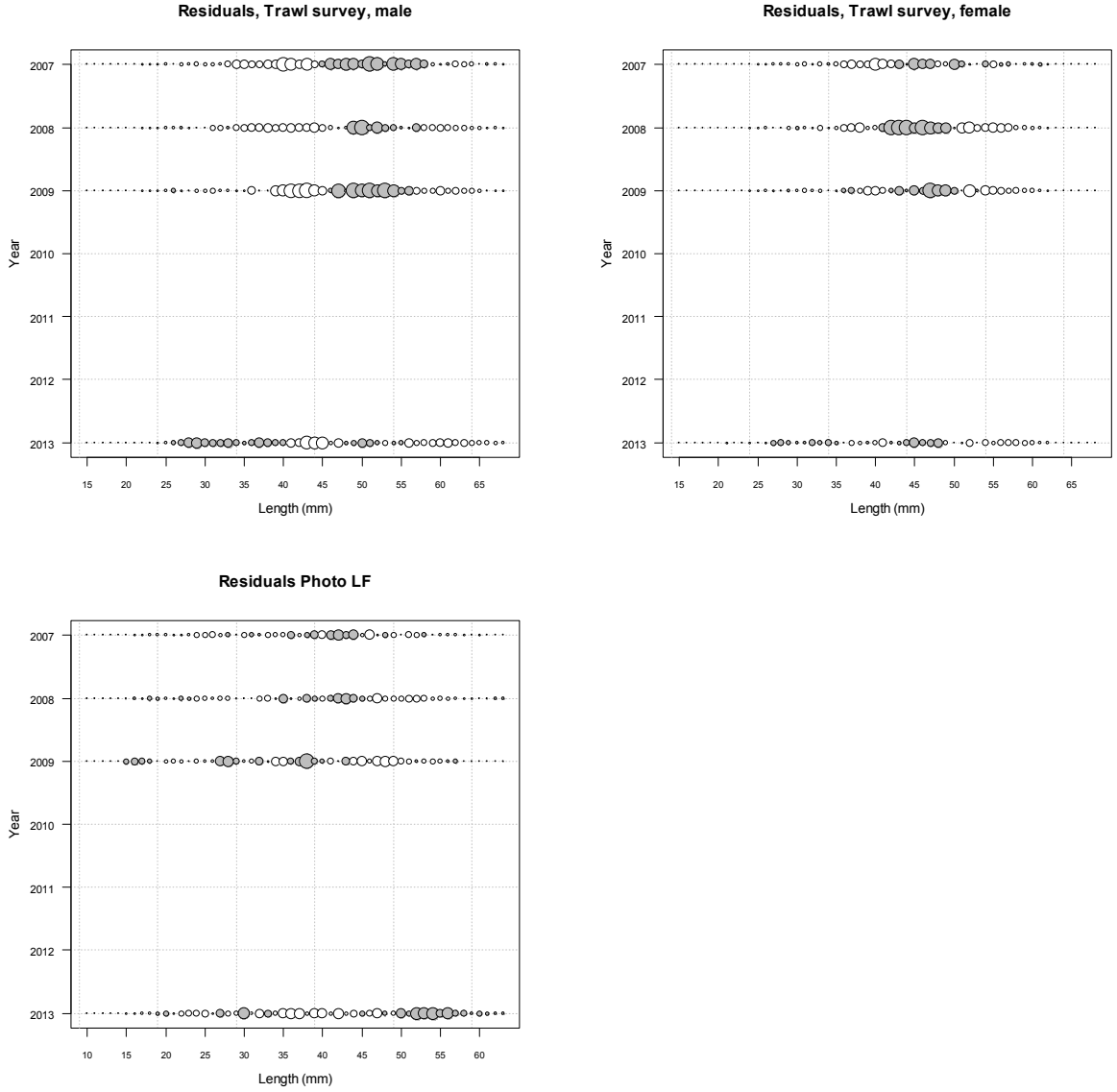

A5. 17: Bubble plots of residuals for fits to length frequency distributions for trawl survey sampling and photographic survey scampi size estimation.

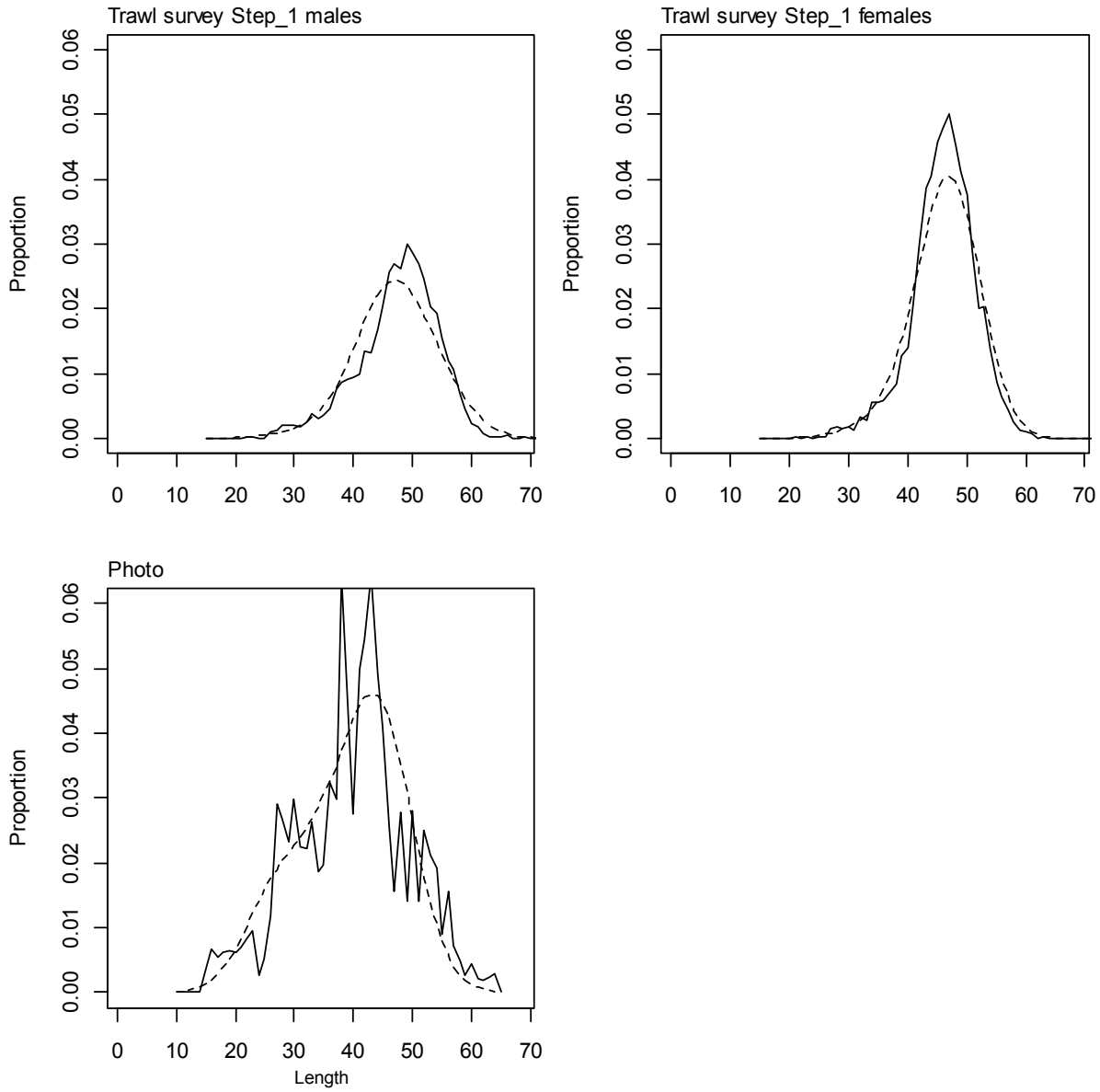

A5. 18: Average observed (solid line) and fitted (dashed line) length frequency distributions for trawl survey sampling and photographic survey scampi size estimation.

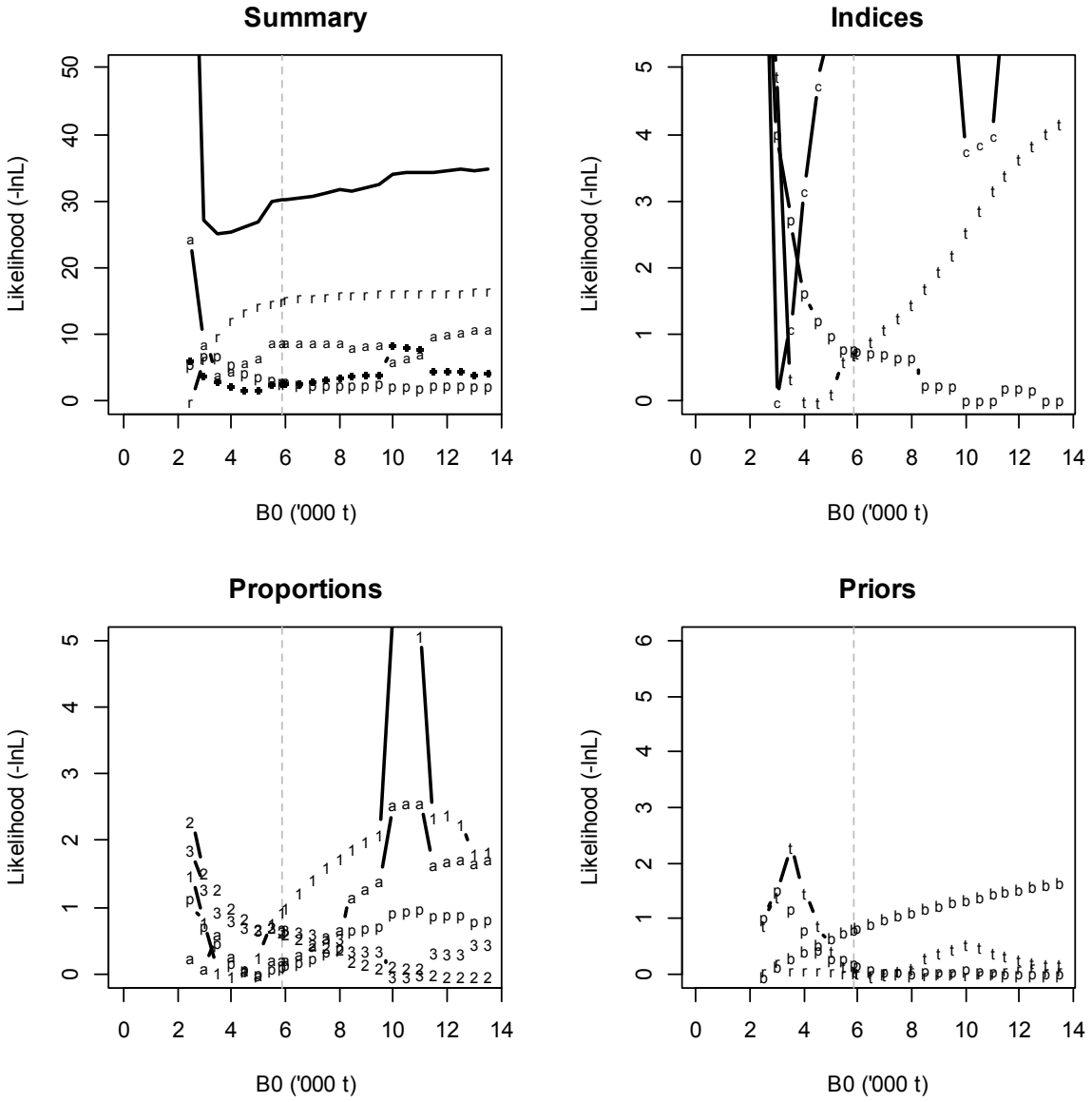

A5. 19: Likelihood profiles for the F_0.25 model for SCI 6A when B_0 is fixed in the model. Figures show profiles for main priors (top left, p – priors, a - abundance indices, • – proportions at length, r – recapture data), abundance indices (top right, t - trawl survey, c - CPUE, p – photo survey), proportion at length data (bottom left, a-trawl, 1 – observer time step 1, 2 – observer time step 2, 3 – observer time step 3, p - photo) and priors (bottom right, b- B_0, YCS - r, p- *q-Photo*, t – *q-Trawl*). Vertical dashed line represents MPD.

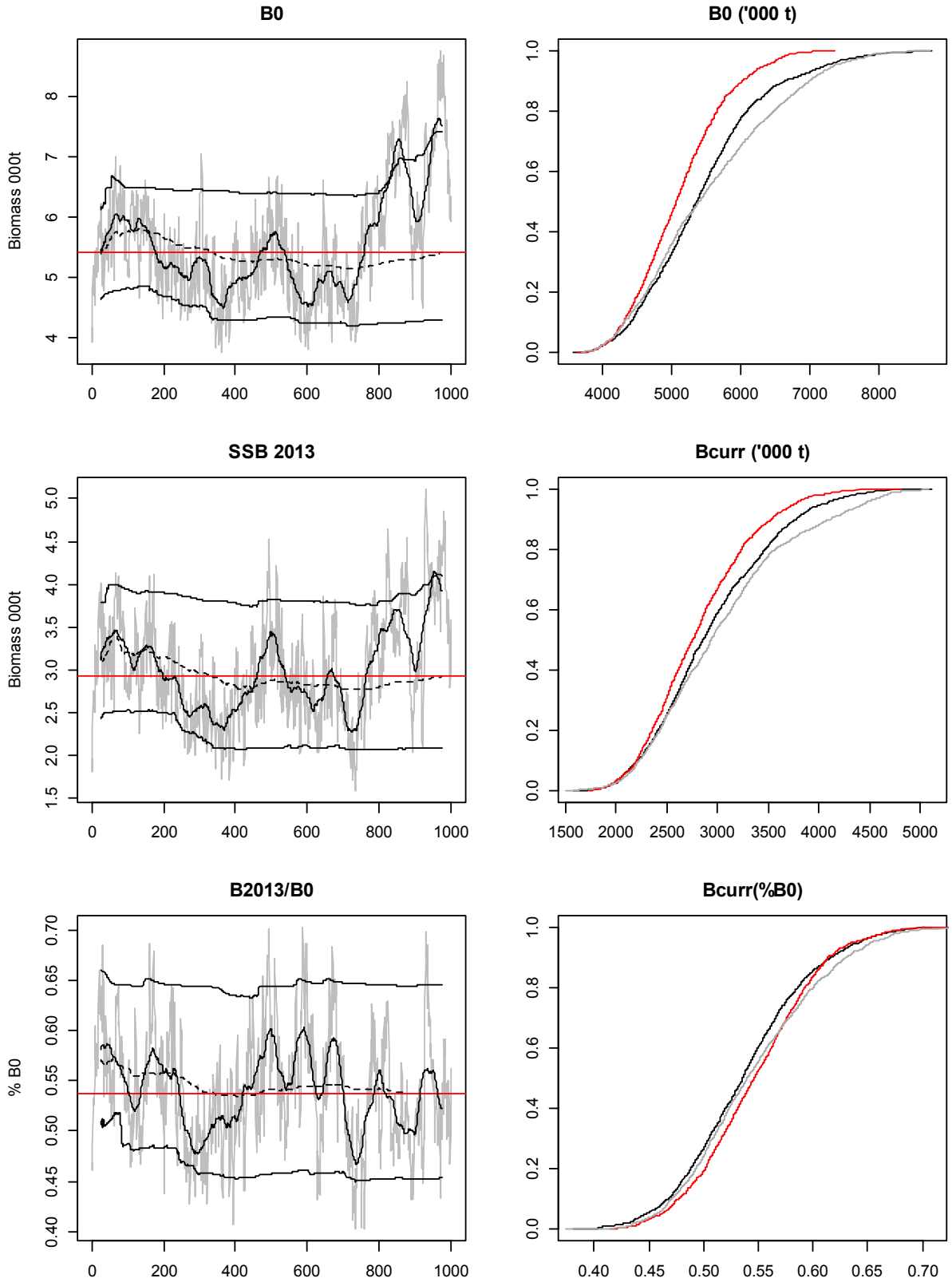

A5. 20: MCMC traces for B_0, SSB_{2013}, and SSB_{2013}/B_0 terms for the F_0.3 model for SCI 6A (trace – grey line, cumulative moving median –dashed black line, moving average and cumulative moving 2.5%, 97.5% quantiles – solid black lines, overall median – solid red line, left plots), along with cumulative frequency distributions for three independent MCMC chains (shown as red, grey and black lines, right plots).

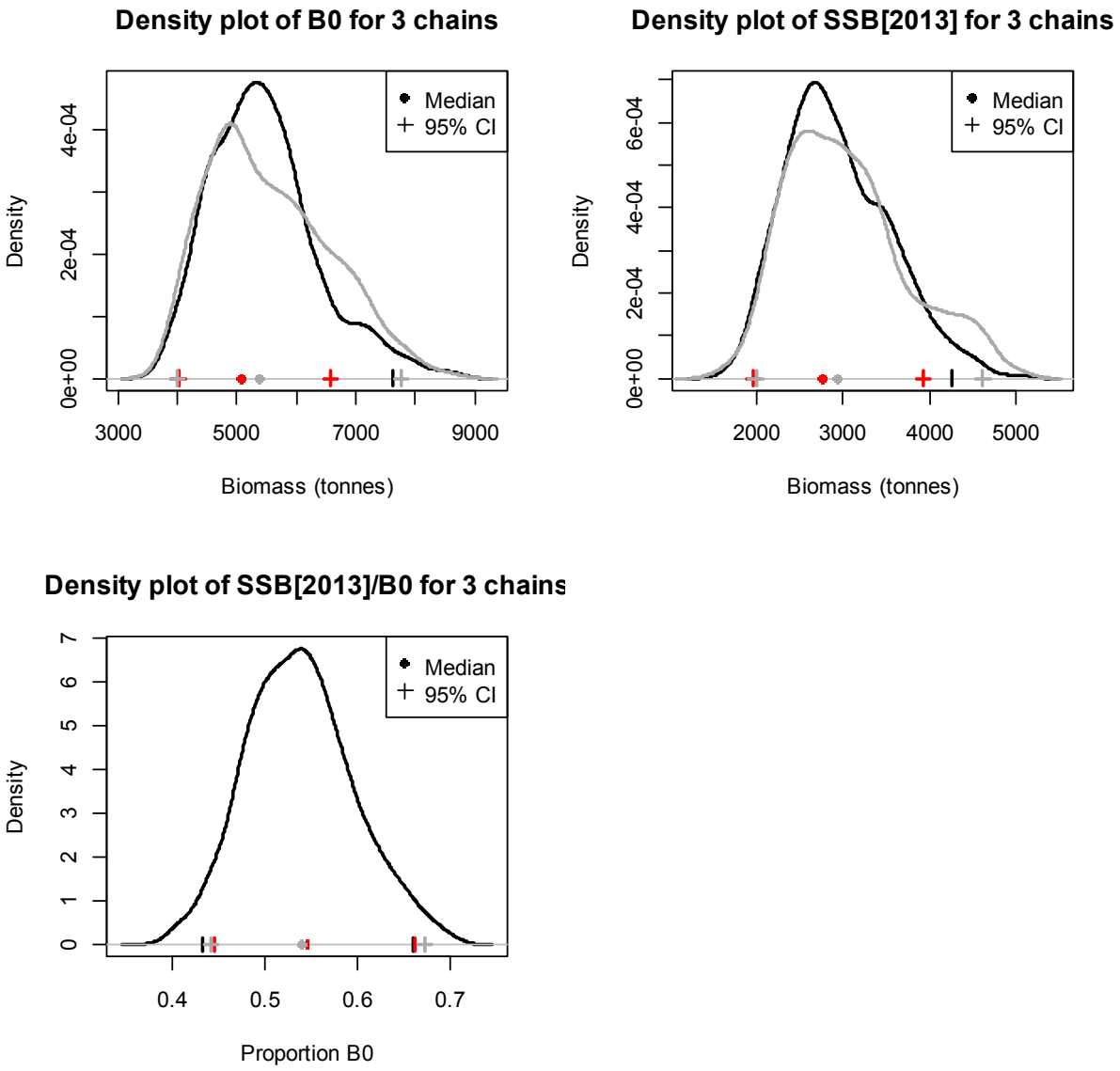

A5. 21: Density plots for B_0, SSB_{2013}, and SSB_{2013}/B_0 terms for the F_0.3 model for SCI 6A for three independent MCMC chains, with median and 95% confidence intervals.

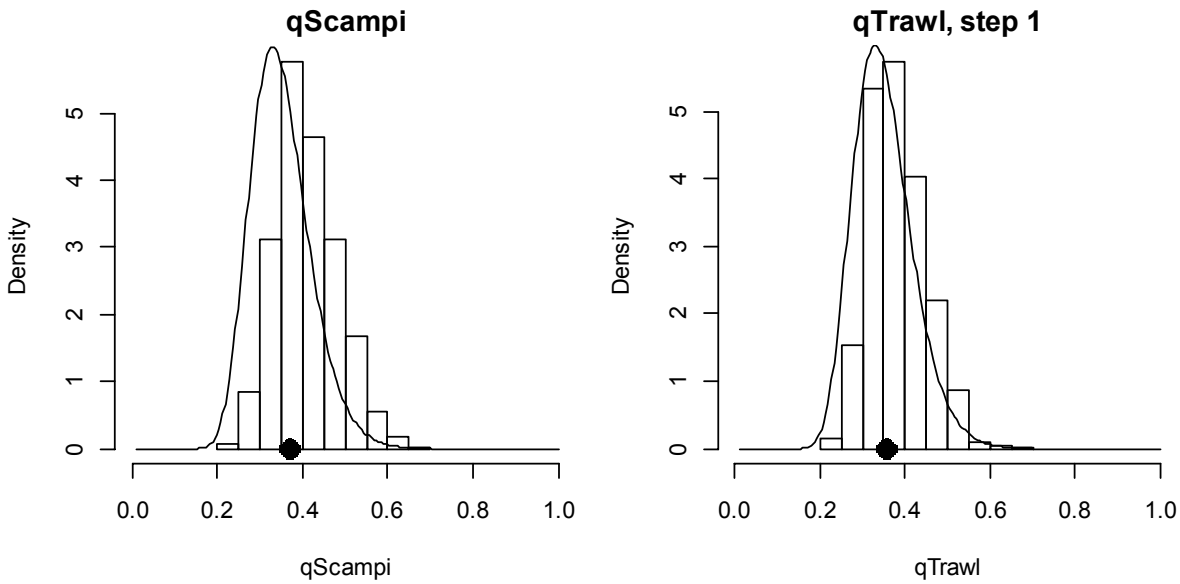

A5. 22: Marginal posterior distributions (histograms), MPD estimates (solid symbols) and distributions of priors (lines) for catchability terms.

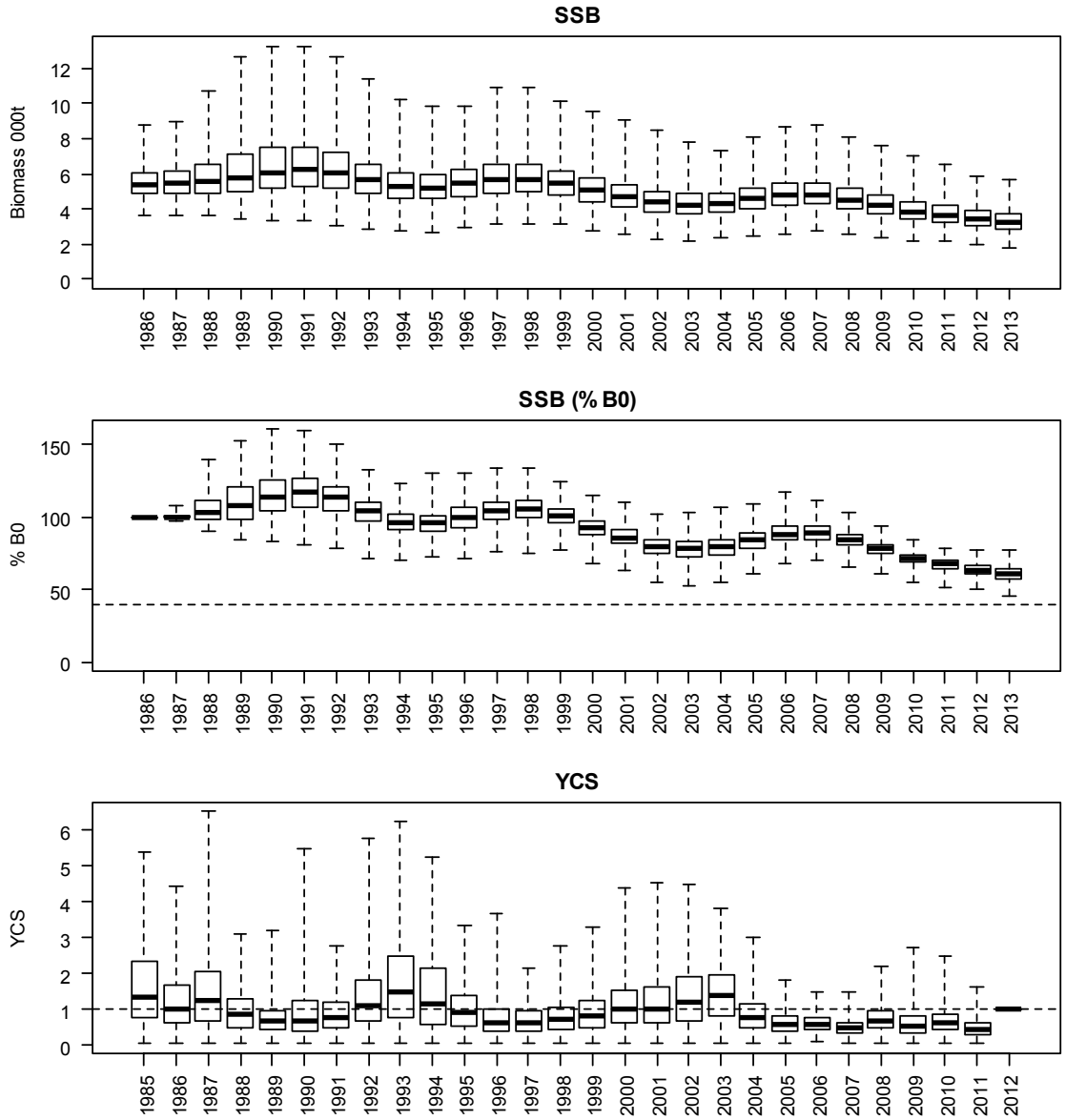

A5. 23: Posterior trajectory of SSB, SSB_{2013}/B_0 and YCS.

APPENDIX 6. MODEL N_0.25

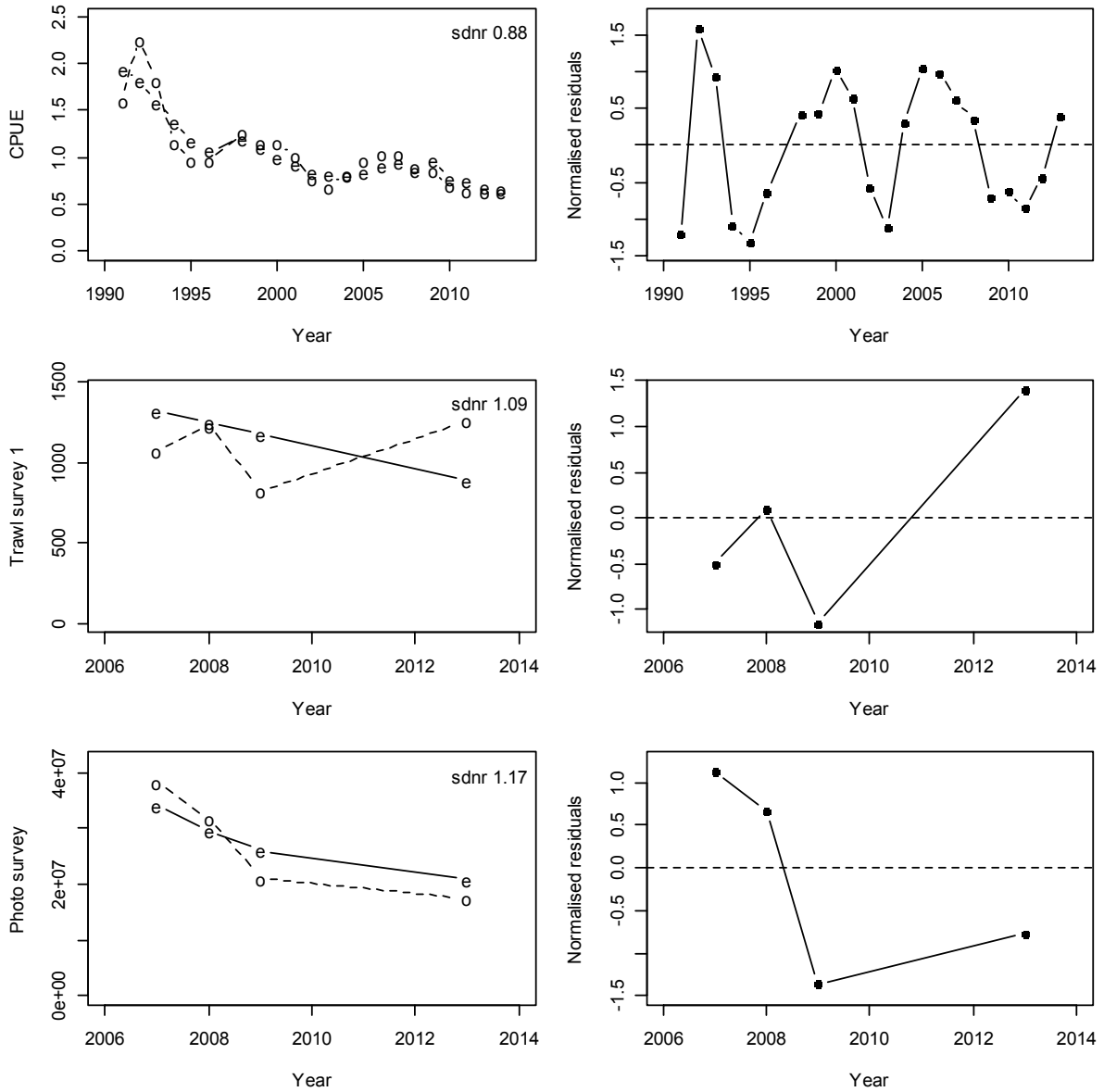

A6. 1: Fits to abundance indices (left column) and normalised residuals (right column) for standardised CPUE index (top row) trawl survey biomass index covering whole area (second row), trawl survey biomass index covering limited area (third row) and photo survey abundance index (fourth row) for SCI 6A N_0.25.

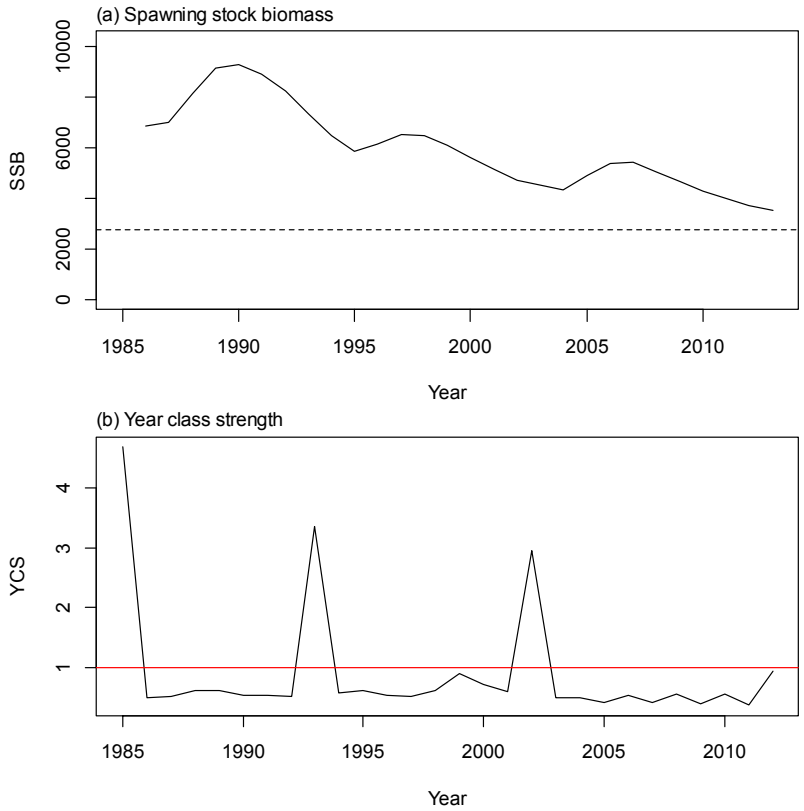

A6. 2: Spawning stock biomass trajectory (upper plot), year class strength (lower plot) for SCI 6A N_0.25.

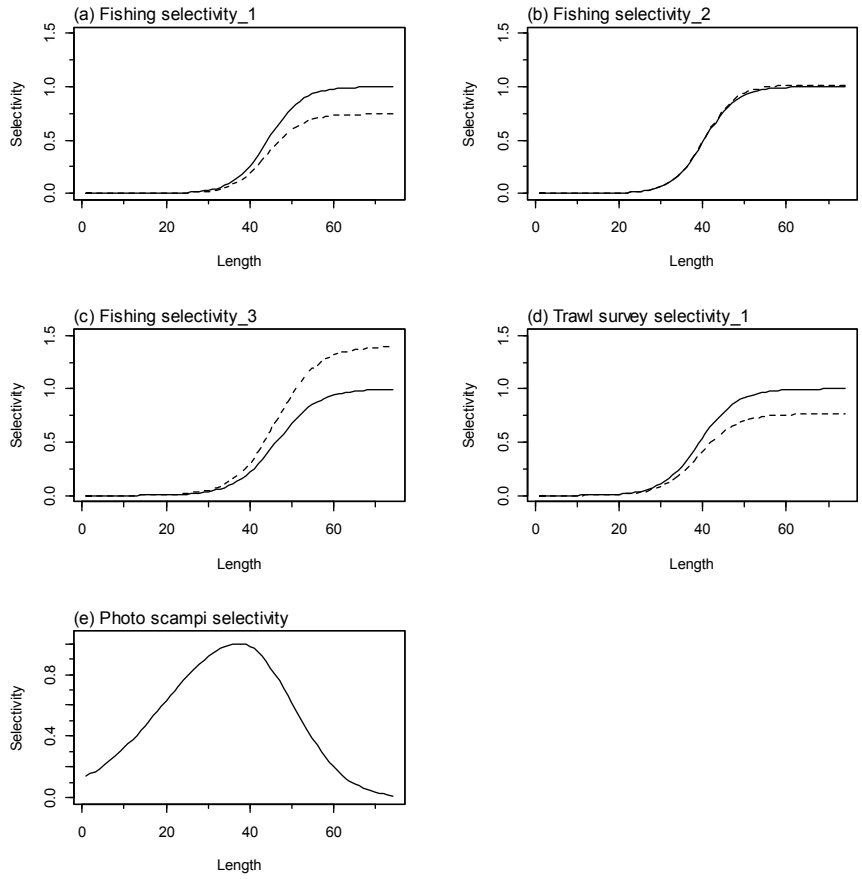

A6. 3: Fishery and survey selectivity curves. Solid line – females, dotted line – males. The scampi photo index is not sexed, and a single selectivity applies.

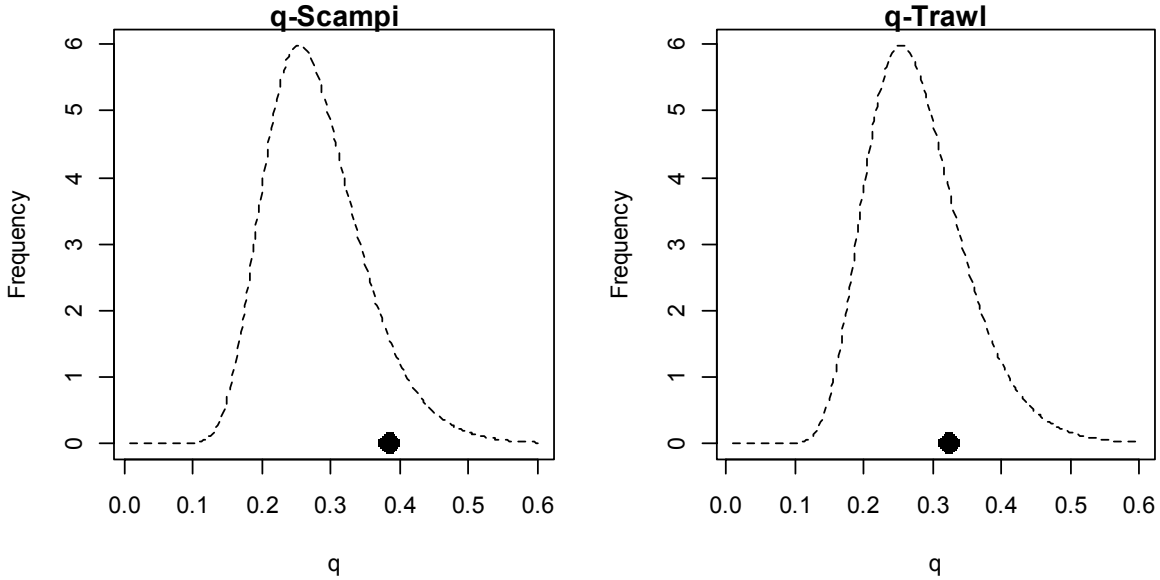

A6. 4: Catchability estimates from MPD model run, plotted in relation to prior distribution.

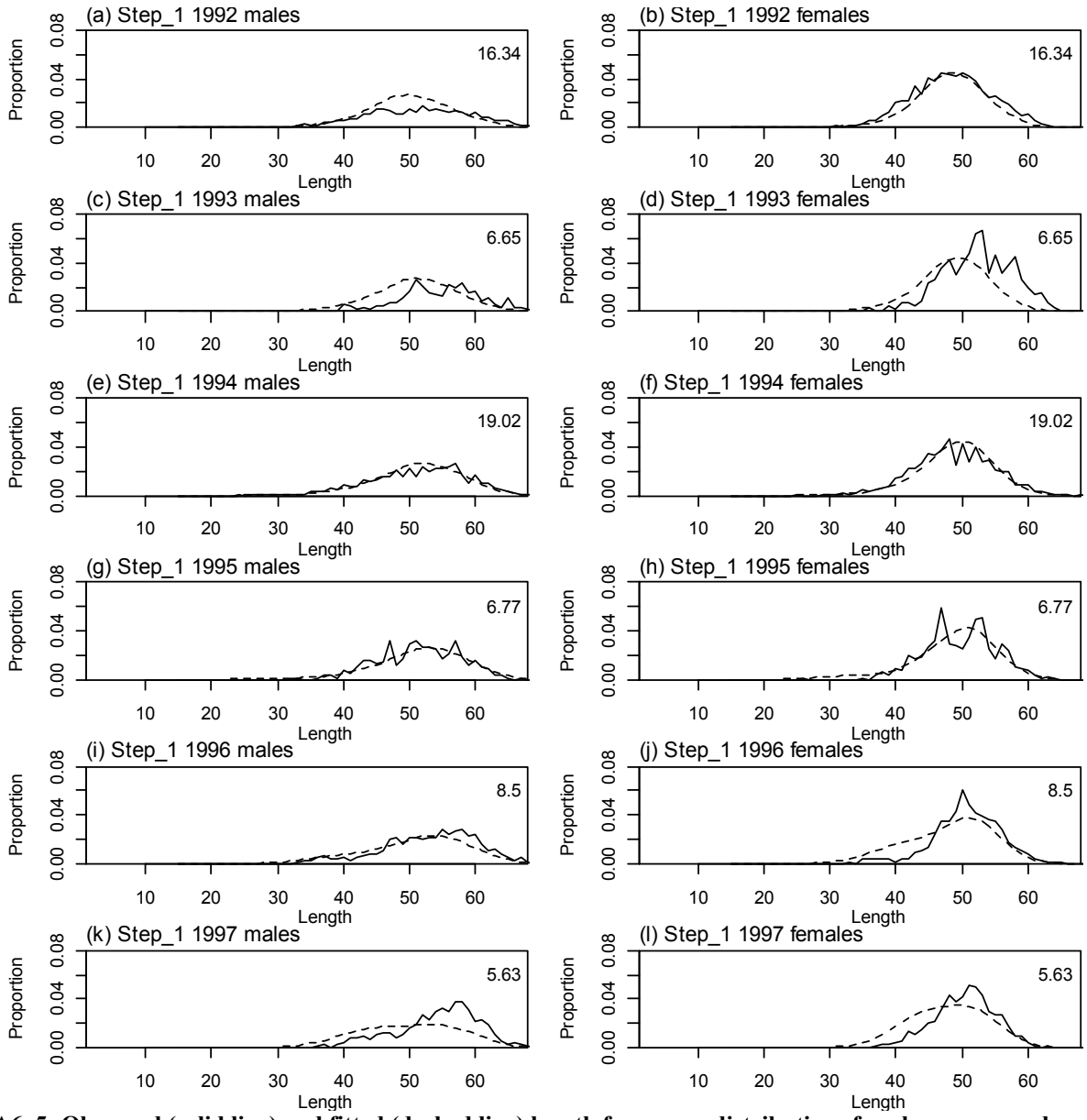

A6. 5: Observed (solid line) and fitted (dashed line) length frequency distributions for observer samples, time step 1.

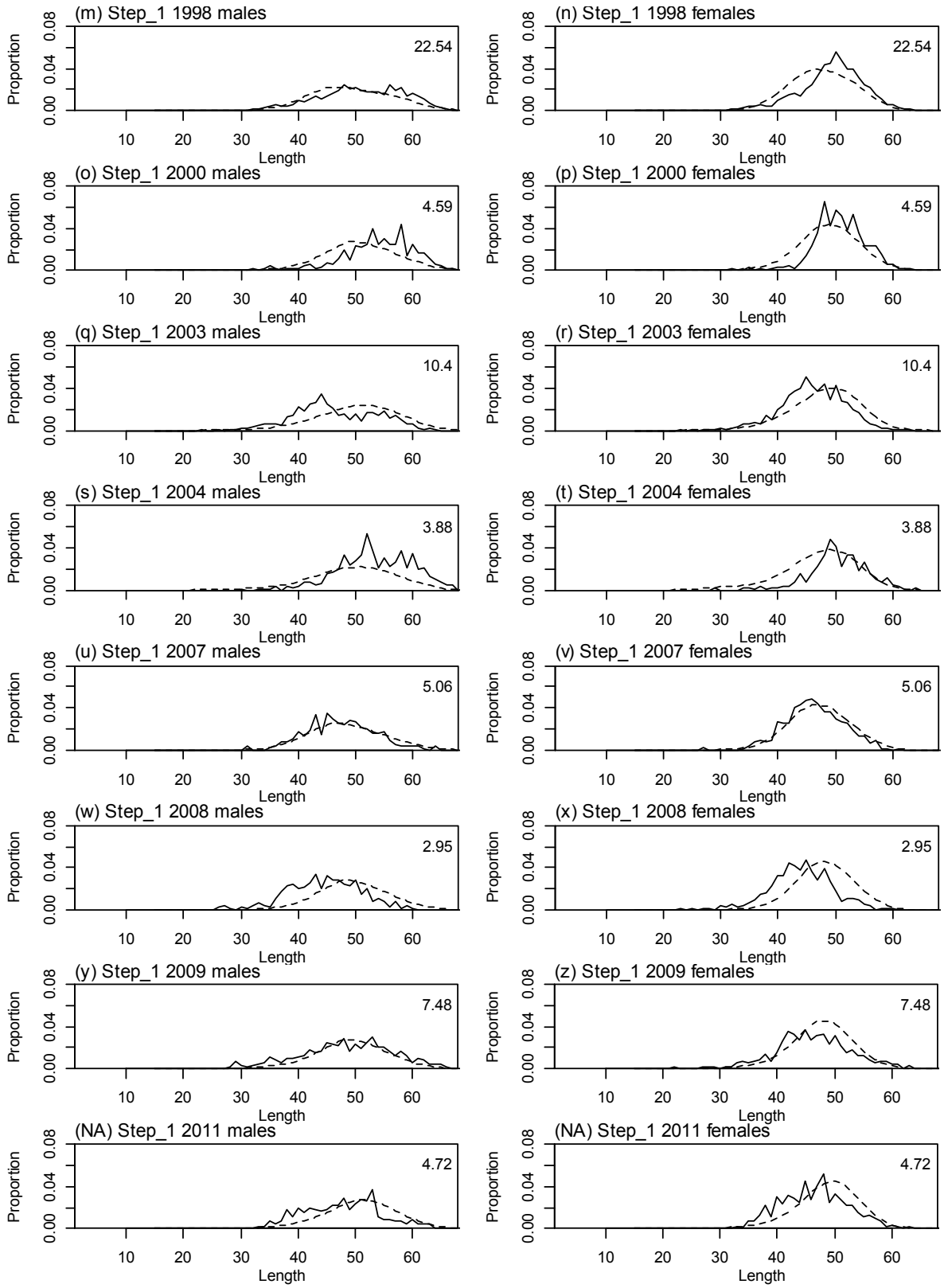

A6. 5 ctd.: Observed (solid line) and fitted (dashed line) length frequency distributions for observer samples, time step 1.

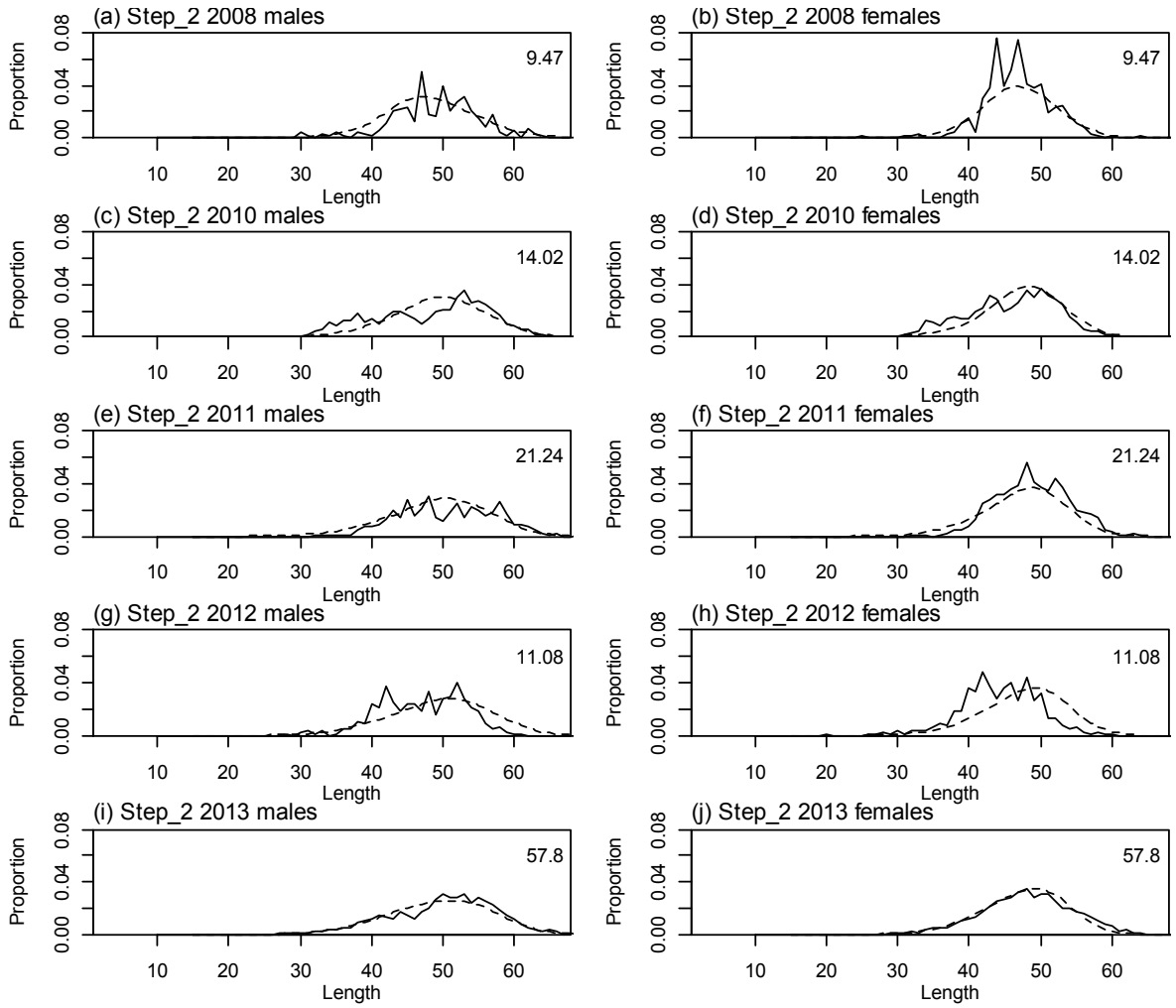

A6. 6: Observed (solid line) and fitted (dashed line) length frequency distributions for observer samples, time step 2.

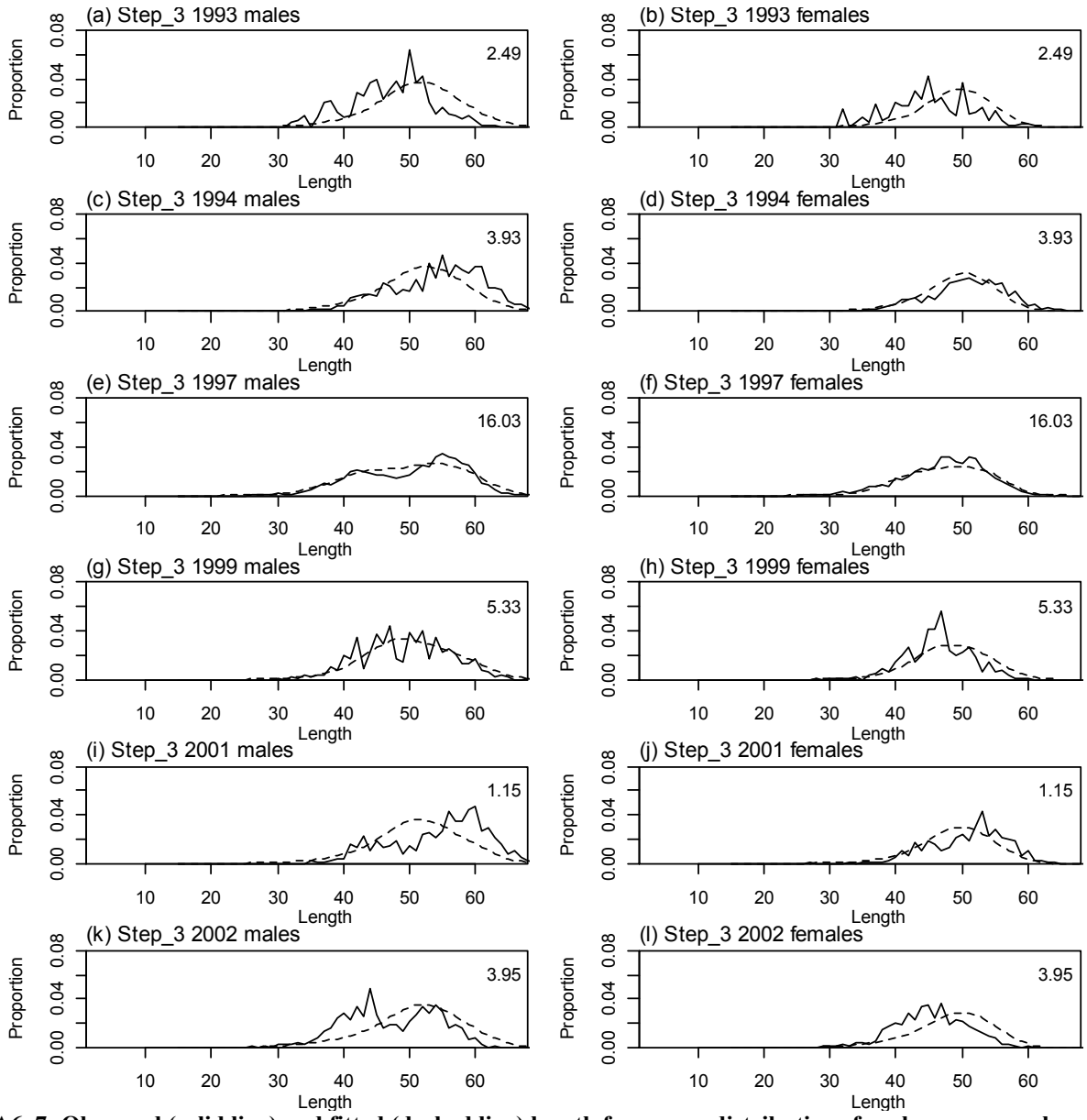

A6. 7: Observed (solid line) and fitted (dashed line) length frequency distributions for observer samples, time step 3.

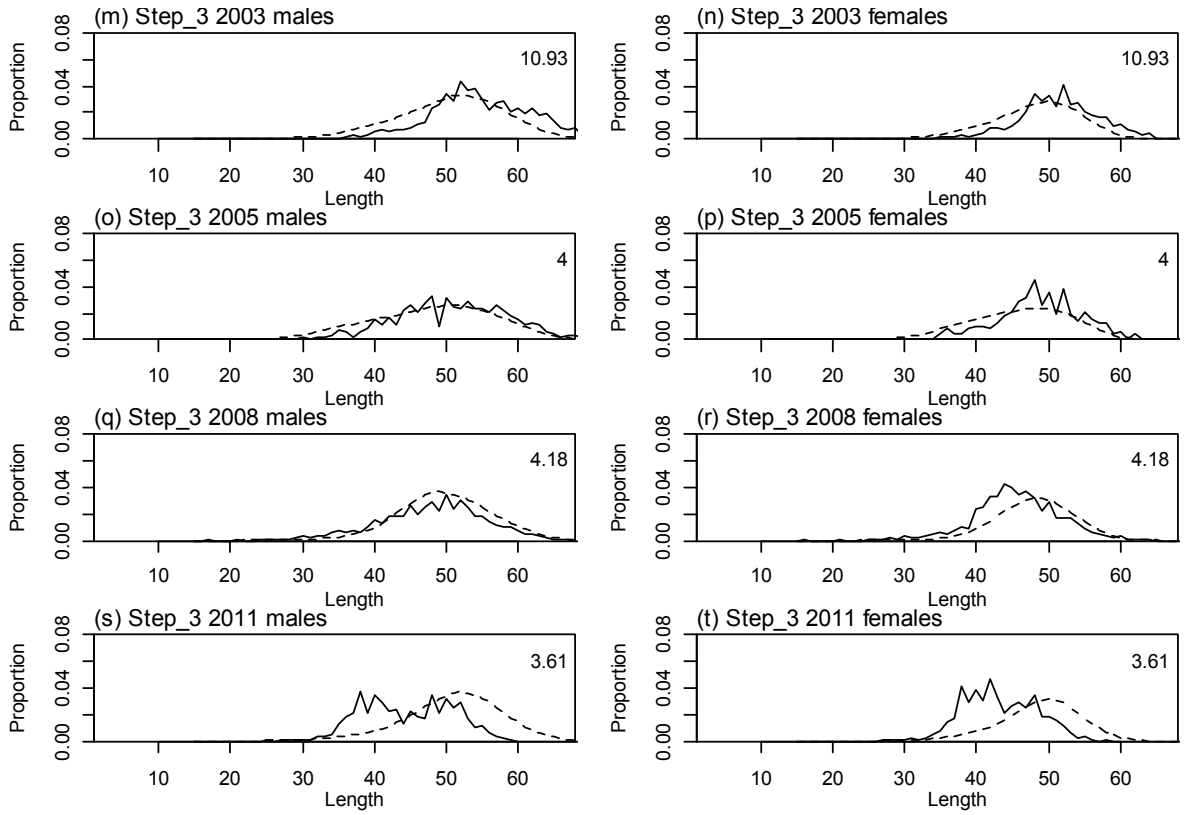

A6. 7 ctd.: Observed (solid line) and fitted (dashed line) length frequency distributions for observer samples, time step 3.

A6. 8: Numbers of scampi measured, estimated multinomial N sample size, and effective sample size used within the model for length frequency distributions for observer samples, time step 1.

	Measured	Multinomial N	Effective sample size
N_1992	9250	3276	16.34
N_1993	2641	1334	6.65
N_1994	9300	3813	19.02
N_1995	2600	1357	6.77
N_1996	3200	1704	8.50
N_1997	2794	1129	5.63
N_1998	11964	4520	22.54
N_2000	2449	921	4.59
N_2002	1975	434	2.16
N_2003	4965	2085	10.40
N_2004	1214	777	3.88
N_2007	3235	1014	5.06
N_2008	1269	591	2.95
N_2009	2959	1500	7.48
N_2011	4035	946	4.72

A6. 9: Numbers of scampi measured, estimated multinomial N sample size, and effective sample size used within the model for length frequency distributions for observer samples, time step 2.

	Measured	Multinomial N	Effective sample size
N_1997	3287	1505	19.25
N_1998	703	475	6.08
N_2001	4782	2479	31.72
N_2008	1035	740	9.47
N_2010	4194	1096	14.02
N_2011	2725	1660	21.24
N_2012	2370	866	11.08
N_2013	10883	4518	57.80

A6. 10: Numbers of scampi measured, estimated multinomial N sample size, and effective sample size used within the model for length frequency distributions for observer samples, time step 3.

	Measured	Multinomial N	Effective sample size
N_1993	1264	745	2.49
N_1994	1960	1174	3.93
N_1996	2035	686	2.30
N_1997	8816	4791	16.03
N_1998	172	157	0.53
N_1999	2707	1593	5.33
N_2001	1650	345	1.15
N_2002	5663	1181	3.95
N_2003	8746	3268	10.93
N_2005	1600	1195	4.00
N_2007	1238	342	1.14
N_2008	4435	1250	4.18
N_2011	5214	1078	3.61

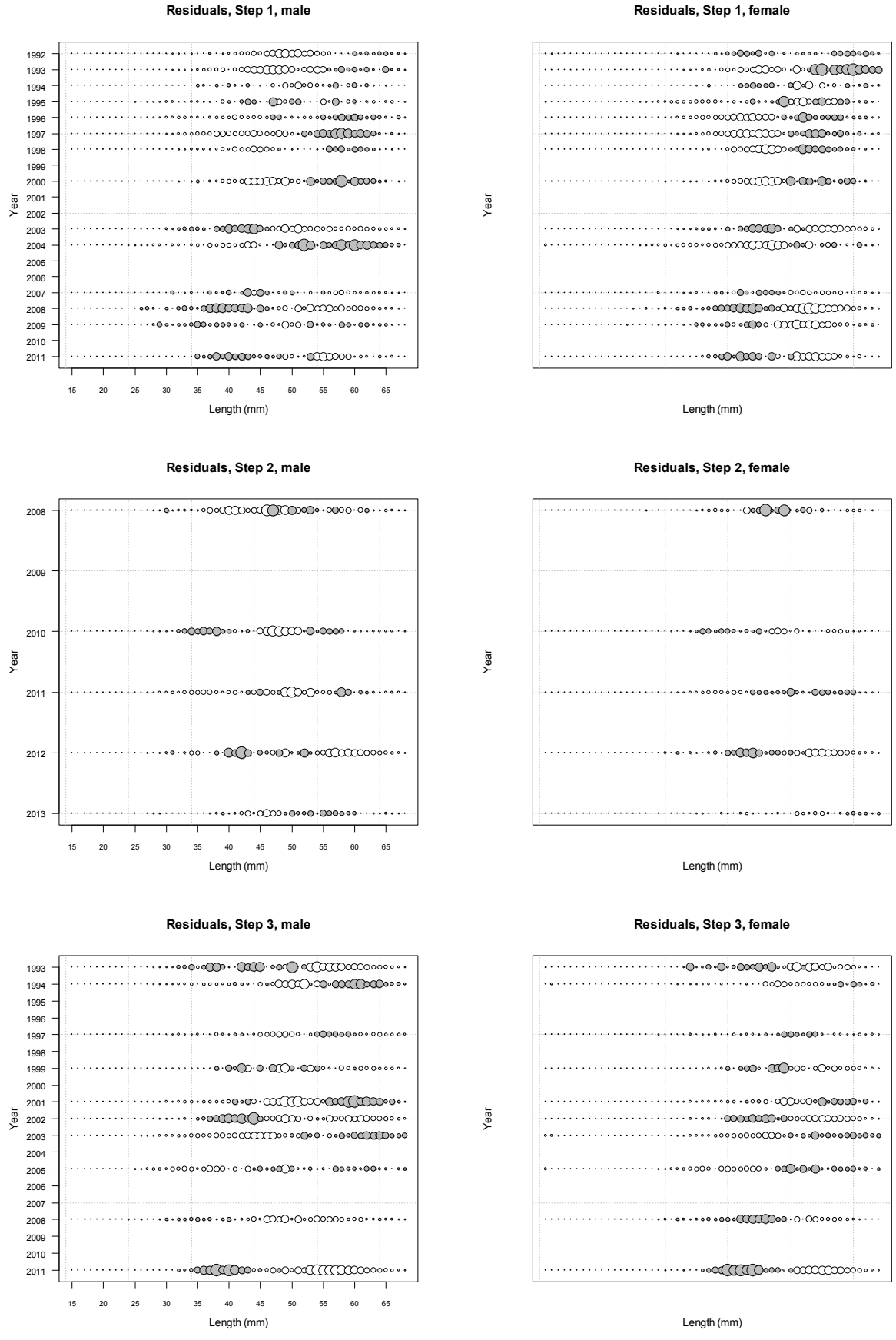

A6. 11: Bubble plots of residuals for fits to length frequency distributions for observer sampling.

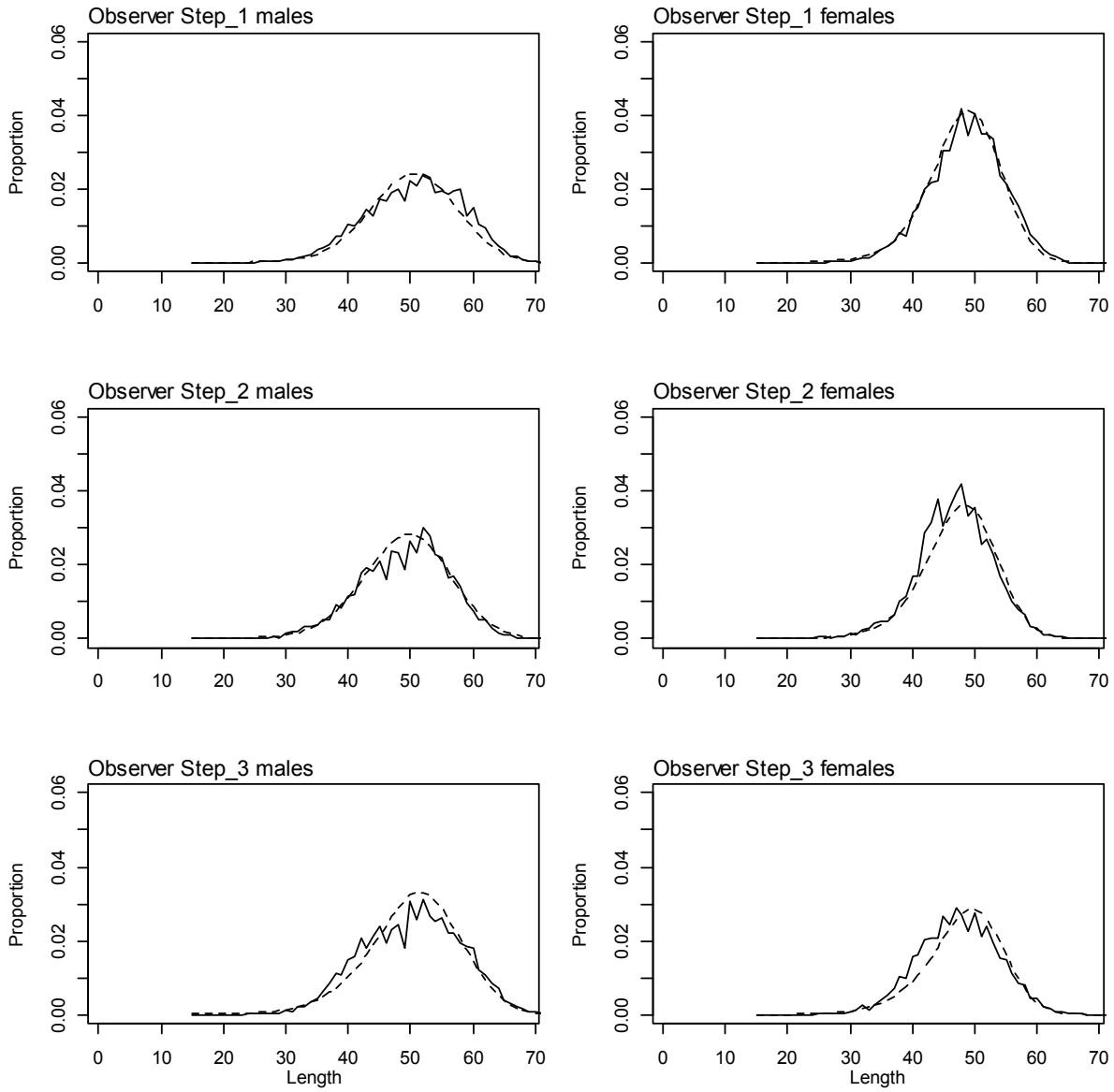

A6. 12: Average observed (solid line) and fitted (dashed line) length frequency distributions for observer samples.

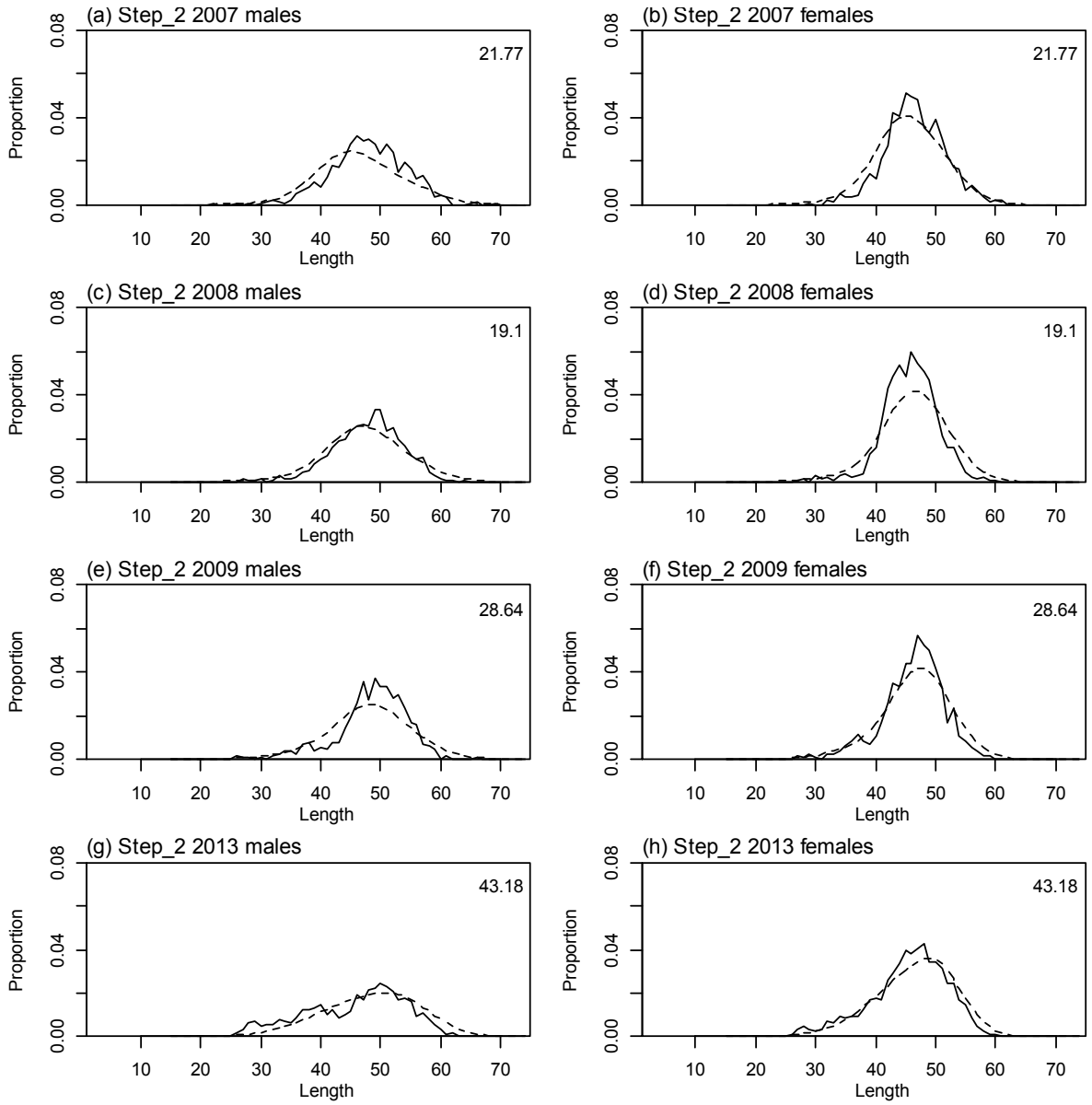

A6. 13: Observed (solid line) and fitted (dashed line) length frequency distributions for research survey samples.

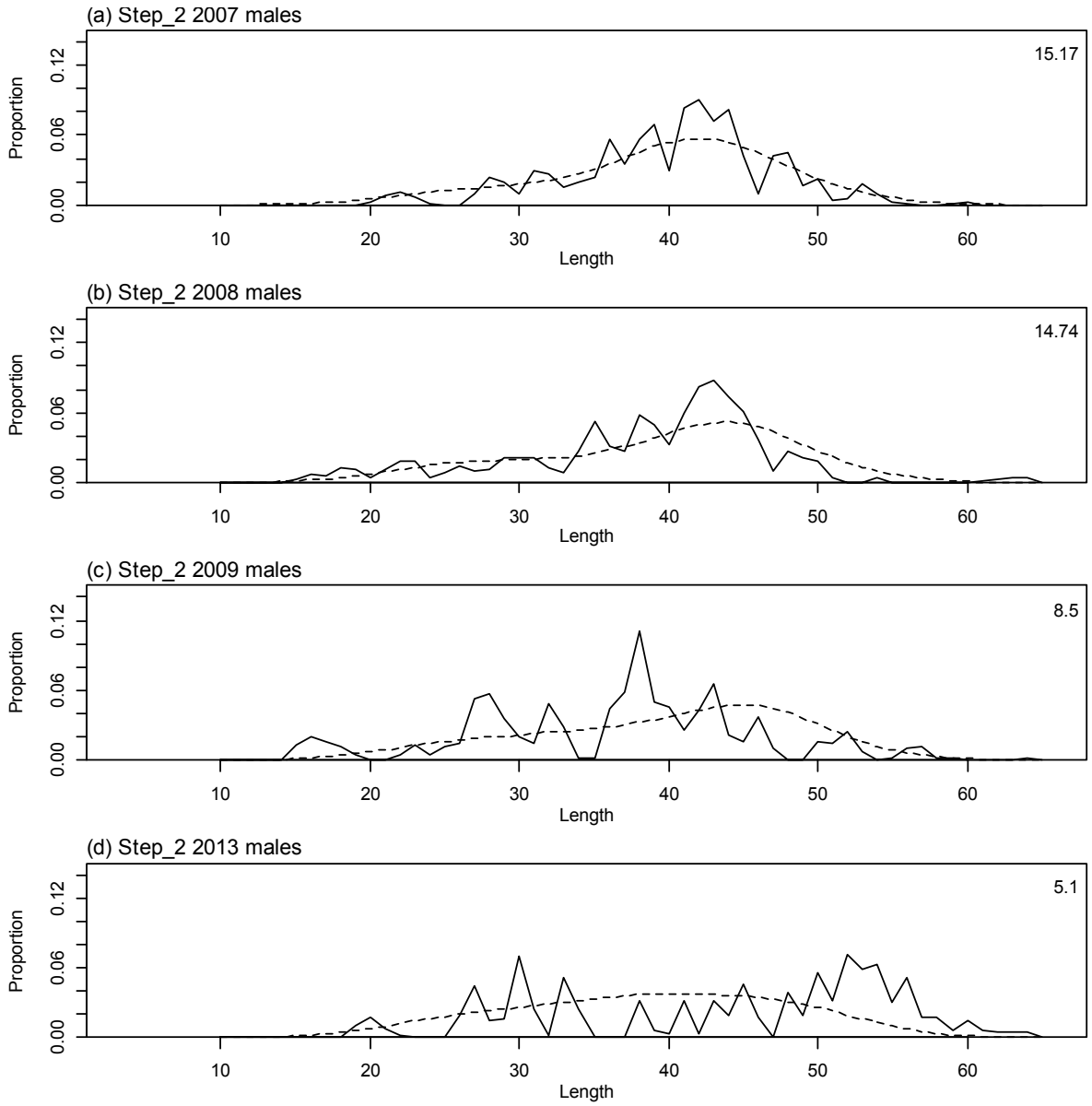

A6. 14: Observed (solid line) and fitted (dashed line) length frequency distributions for photographic survey scampi size estimation.

A6. 15: Numbers of scampi measured, estimated multinomial N sample size, and effective sample size used within the model for length frequency distributions for research survey samples.

	Measured	Multinomial N	Effective sample size
N_2007	1981	2127	21.77
N_2008	2291	1866	19.10
N_2009	4054	2798	28.64
N_2013	4808	4218	43.18

A6. 16: Numbers of scampi measured, estimated multinomial N sample size, and effective sample size used within the model for length frequency distributions for photographic survey samples.

	Measured	Multinomial N	Effective sample size
N_2007	70	107	15.17
N_2008	73	104	14.74
N_2009	45	60	8.50
N_2013	26	36	5.10

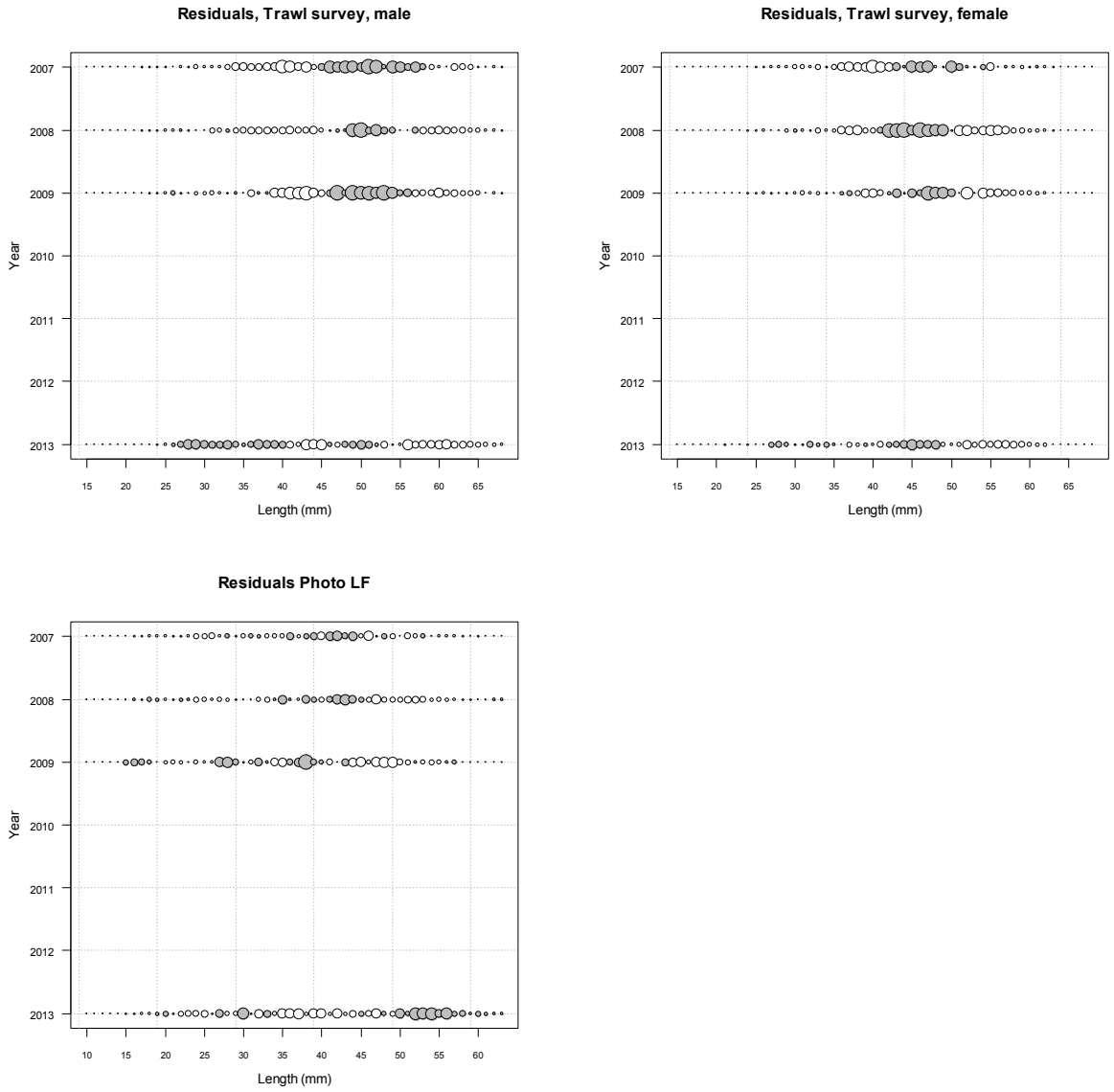

A6. 17: Bubble plots of residuals for fits to length frequency distributions for trawl survey sampling and photographic survey scampi size estimation.

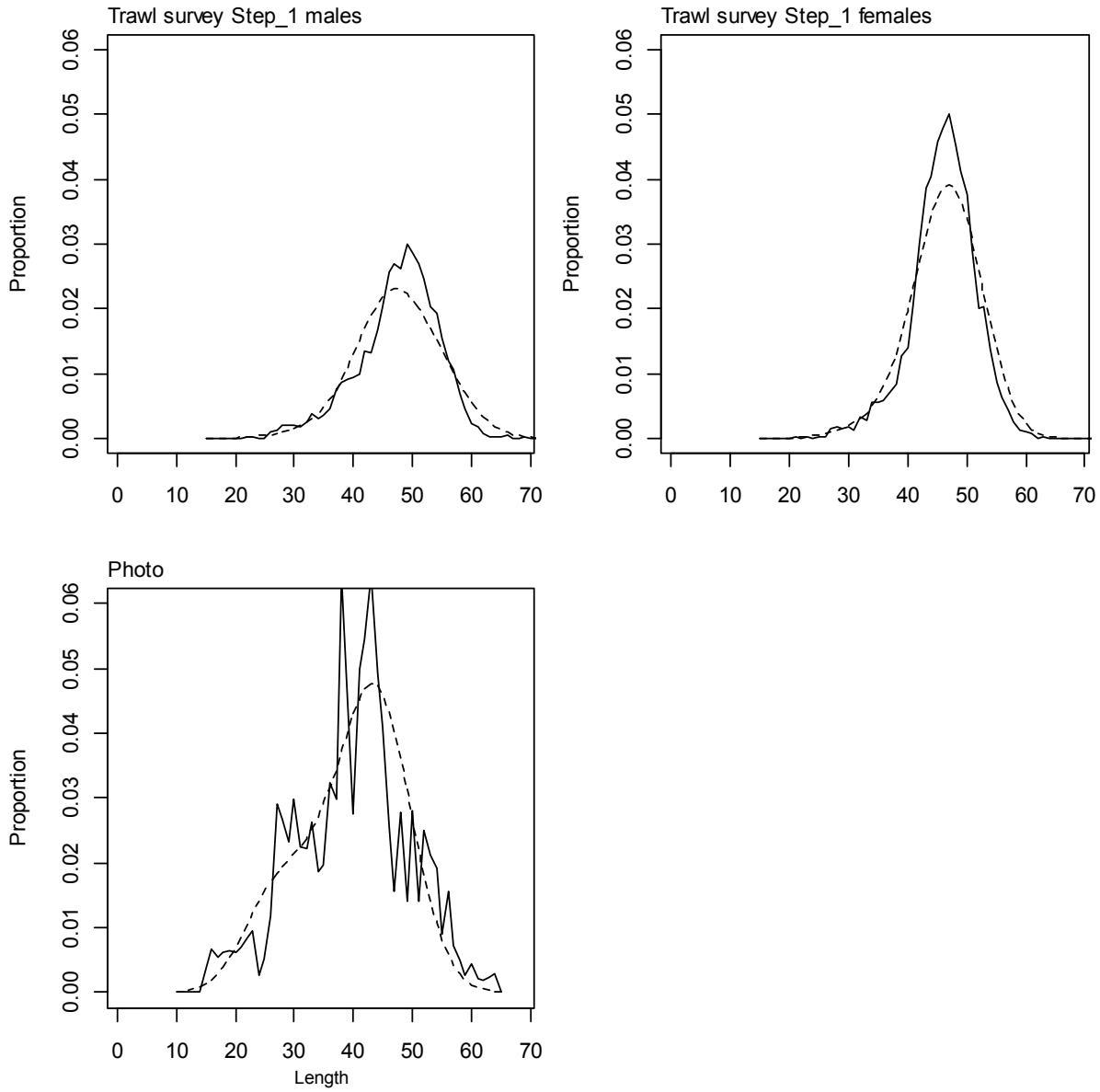

A6. 18: Average observed (solid line) and fitted (dashed line) length frequency distributions for trawl survey sampling and photographic survey scampi size estimation.

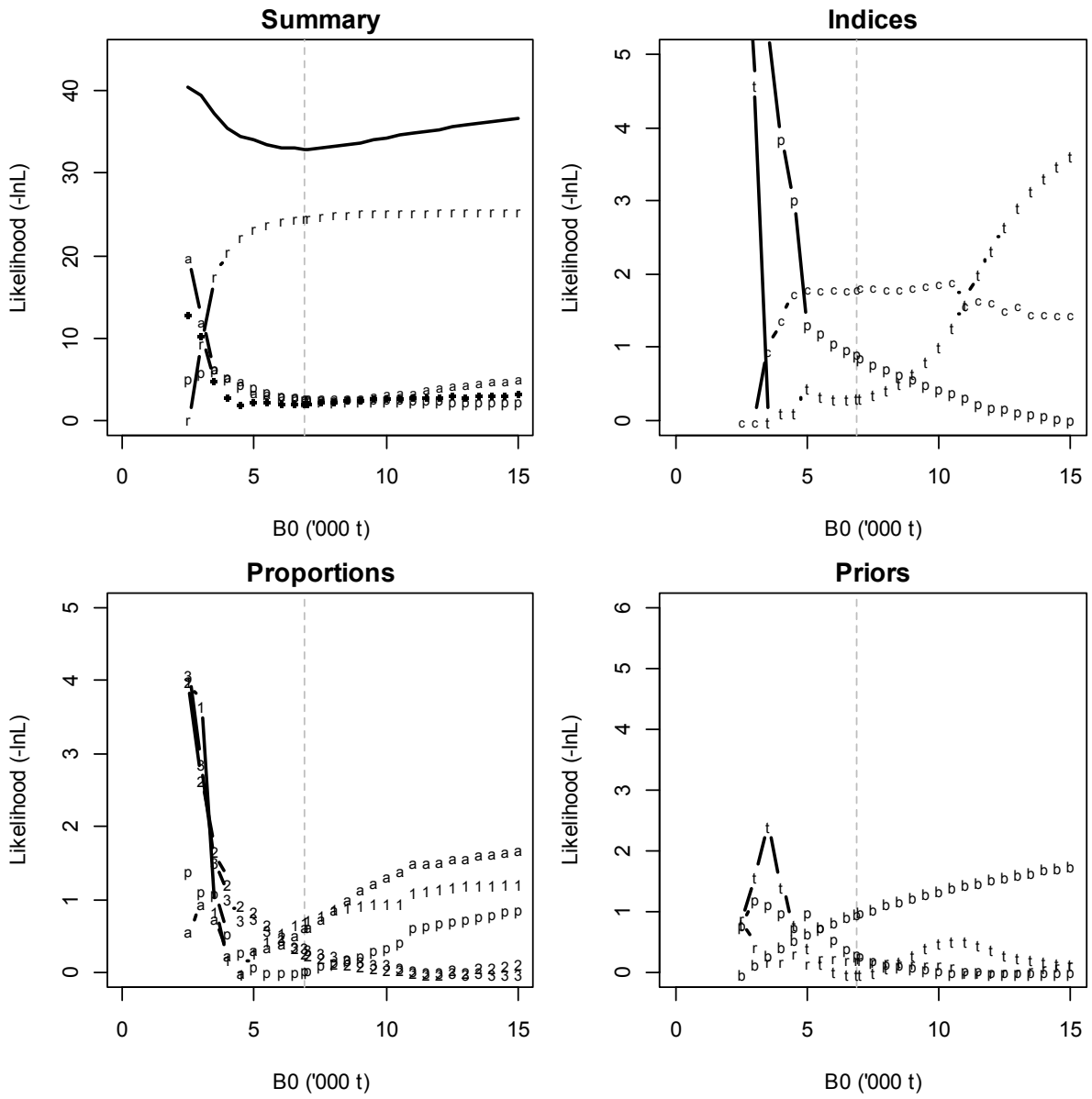

A6. 19: Likelihood profiles for the F_0.25 model for SCI 6A when B_0 is fixed in the model. Figures show profiles for main priors (top left, p – priors, a - abundance indices, • – proportions at length, r – recapture data), abundance indices (top right, t - trawl survey, c - CPUE, p – photo survey), proportion at length data (bottom left, a-trawl, 1 – observer time step 1, 2 – observer time step 2, 3 – observer time step 3, p - photo) and priors (bottom right, b- B_0, YCS - r, p- *q-Photo*, t – *q-Trawl*). Vertical dashed line represents MPD.

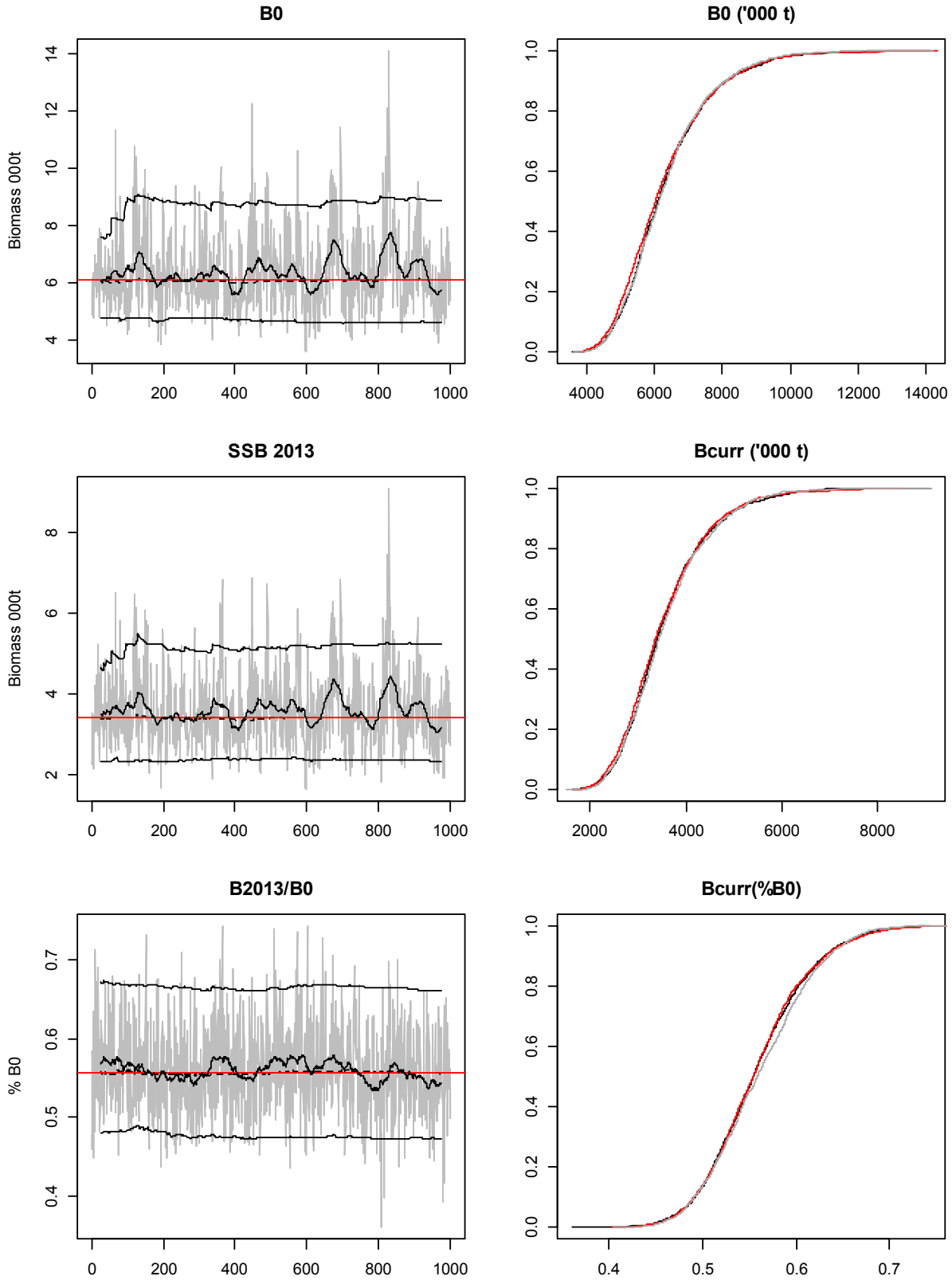

A6. 20: MCMC traces for B_0, SSB_{2013}, and SSB_{2013}/B_0 terms for the N_0.25 model for SCI 6A (trace – grey line, cumulative moving median –dashed black line, moving average and cumulative moving 2.5%, 97.5% quantiles – solid black lines, overall median – solid red line, left plots), along with cumulative frequency distributions for three independent MCMC chains (shown as red, grey and black lines, right plots).

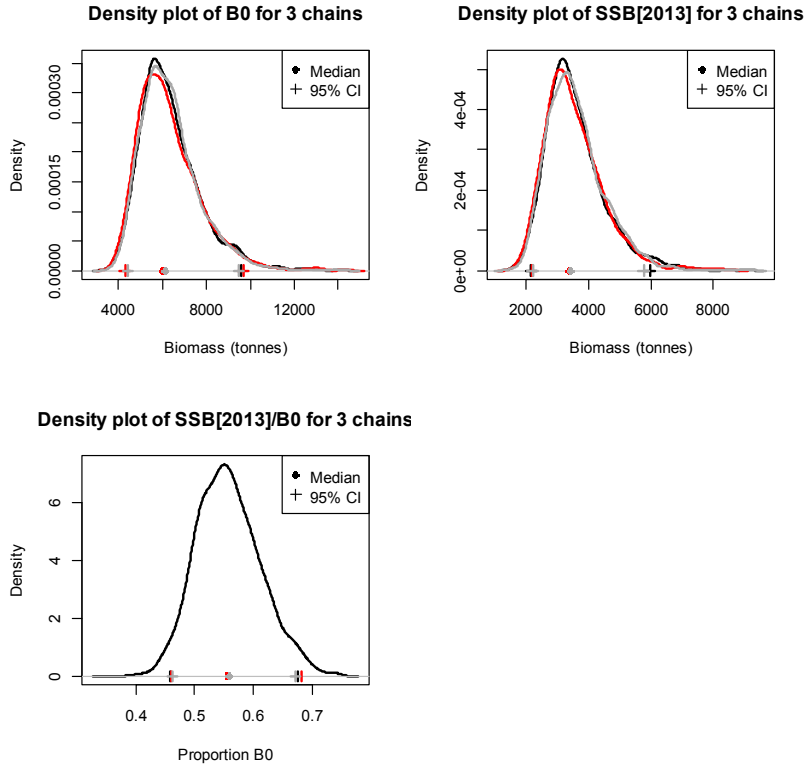

A6. 21: Density plots for B_0, SSB_{2013}, and SSB_{2013}/B_0 terms for the N_0.25 model for SCI 6A for three independent MCMC chains, with median and 95% confidence intervals.

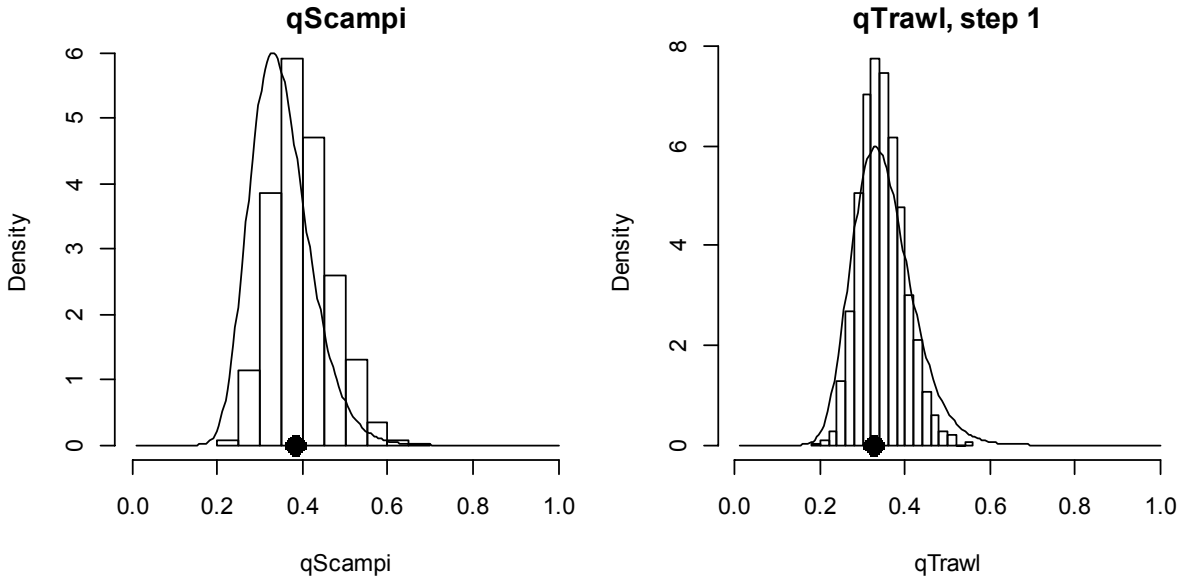

A6. 22: Marginal posterior distributions (histograms), MPD estimates (solid symbols) and distributions of priors (lines) for catchability terms.

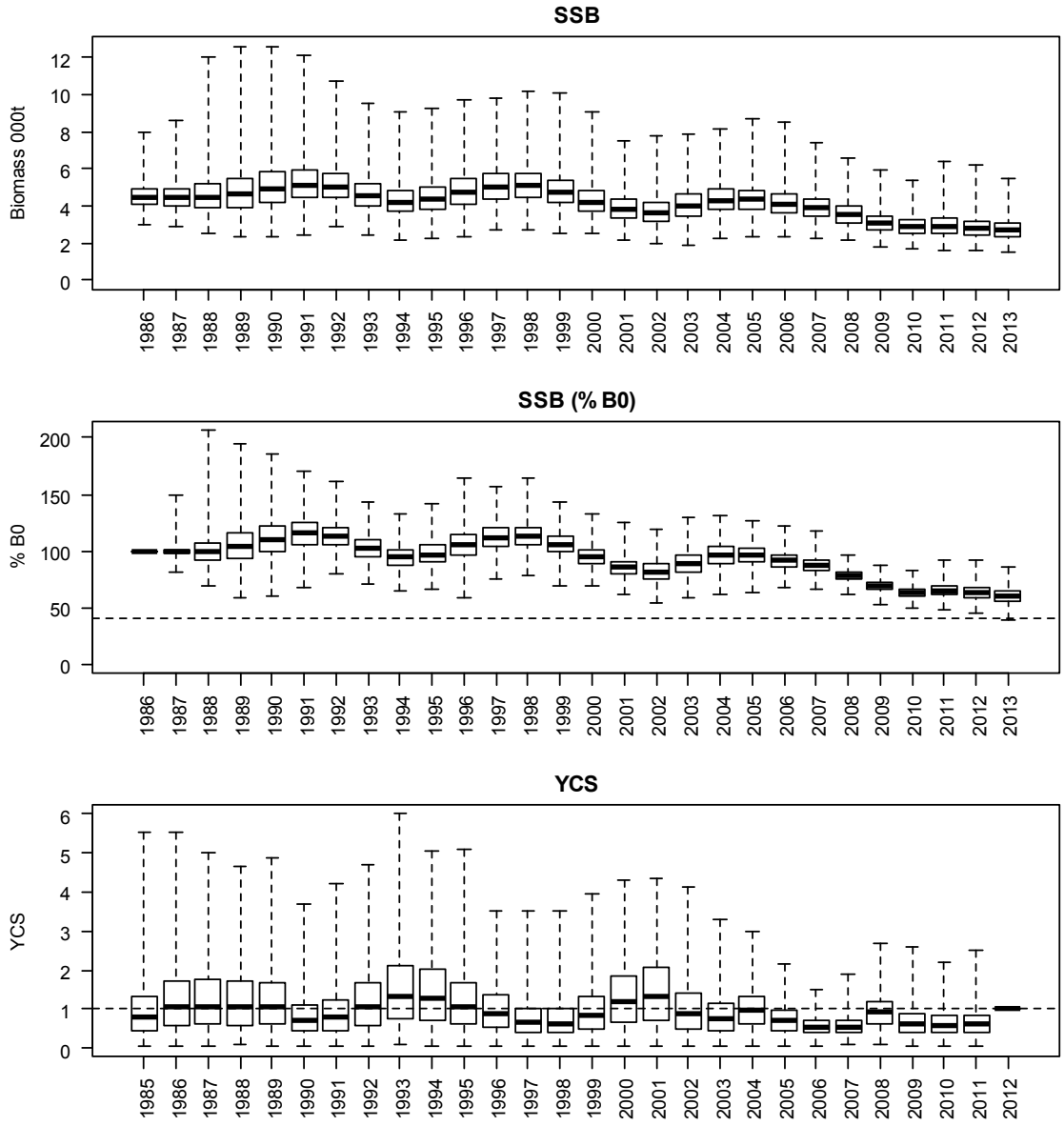

A6. 23: Posterior trajectory of SSB, SSB_{2013}/B_0 and YCS.